UNIVERSITY OF CALIFORNIA
RIVERSIDE

Identification and Synthesis of Semiochemicals for Fireflies, True Bugs, and Longhorn Beetles

A Dissertation submitted in partial satisfaction
of the requirements for the degree of

Doctor of Philosophy

in

Chemistry

by

Kyle B. Arriola

September 2022

Dissertation Committee:
Dr. Jocelyn G. Millar, Chairperson
Dr. Ana Bahamonde
Dr. Michael Pirrung
Dr. Richard Hooley

The Dissertation of Kyle B. Arriola is approved:

_____

_____

_____

_____

Committee Chairperson

University of California, Riverside

ACKNOWLEDGEMENTS

Above all, I would like to extend my gratitude to my advisor Dr. Jocelyn Millar. I will forever remember your patience, empathy, and aptitude. You foster a warm, supportive environment, a truly unique space that I had the immense privilege of developing in as a student and teacher of chemistry. Thank you for your guidance in helping me become a skillful synthetic organic chemist and an effective science communicator. You have kept me motivated and hopeful during every "three steps forward, two steps back" moment, while I worked through problems with the various syntheses. I am committed to bringing the same passion and mentorship into the classrooms ahead of me.

I am also thankful to the professors who have provided their support throughout the years. Thank you to Dr. David Martin for welcoming me into his group, where I had the pleasure of broadening my knowledge of chemistry on the frontiers of discovery, a sense of belonging in the Department of Chemistry, and giving me opportunities to hone my snowboarding skills through many, many mouthfuls of snow. My gratitude to Dr. Michael Pirrung for continually setting high standards to strive for, and providing invaluable assistance which propelled my research forward. My thanks to Dr. Richard Hooley who has inspired me to think carefully and speak thoughtfully, and whose class on spectroscopy in organic chemistry assisted me in obtaining my first publication. I am grateful to Dr. Ana Bahamonde, who adopted me into her research group for many months, and encouraged me to become a well-rounded chemist. I am sure your charismatic leadership, command of chemistry, and motivating presence will spearhead many successes in the future.

I would like to acknowledge the friends and family who have supported me throughout this journey. Aaron Jensen, for your eternal support and keeping me steady. Cheryl Hoffman, for being a lifeline and always reminding me of my worth, your friendship is a true gift. Ryan Barela and dearest Russet, for helping me realize what I find most fulfilling in life. Nicholas Raheja, for memories of recent past and in the distant future, I thank you for your presence. Christopher Jones, for an unexpected fellowship lush with gold that I am only grateful started later than never. Finally, a thank you to my mother, father, grandmother, and aunt for your persistent love and support over these past years that I have spent as an egg, larva, and pupa.

I wish to acknowledge the co-authors that have brought the research in this dissertation to fruition:

Chapter 2 was previously published as and reprinted from Kyle Arriola, Salvatore Guarino, Christian Schlawis, Mokhtar Abdulsattar Arif, Stefano Colazza, Ezio Peri, Stefan Schulz, and Jocelyn G. Millar. Identification of Brassicadiene, a Diterpene Hydrocarbon Attractive to the Invasive Stink Bug *Bagrada hilaris*, from Volatiles of Cauliflower Seedlings, *Brassica oleracea* var. *botrytis. Organic Letters,* **2020**, 22 (8), 2972-2975. Copyright 2020 American Chemical Society. Co-authors Dr. Salvatore Guarino, Dr. Mokhtar Abdulsattar Arif, Dr. Stefano Colazza, and Dr. Ezio Peri conducted bioassays and sample collection. Dr. Christian Schlawis and Dr. Stefan Schulz helped to determine the absolute configuration of brassicadiene. Dr. Jocelyn G. Millar provided supervision over the project and helped determine the structure of brassicadiene. I would also like to thank Dr. Dan Borchardt for his assistance with NMR instrumentation. This project would not

have been possible without funding from: Project “High Studies Programme (Master and Ph.D.) for Iraqi officials at Italian Academic Institutions (HiSPro)” cofinanced by the Iraqi Government and the Italian Ministry of Foreign Affairs (MAE) secured by Drs. Guarino, Abdulsattar Arif, Colazza, and Peri; and Hatch project CA-R*ENT-5181-H secured by Dr. Millar.

The content within Chapter 3 is currently being prepared for publication. Dr. Sarah Lower was responsible for project supervision, collection of insect specimens, and preparation of extracts. Dr. Sean Halloran conducted GC-EAD analyses. Both Dr. Sarah Lower and Dr. Gregory Pask performed bioassays and field experiments with the synthetic standards. Dr. Douglas Collins assisted with project conception and grant proposal preparation. Dr. Jocelyn G. Millar helped with structural identifications of the insect pheromone and project supervision. This project would not have been possible without funding from NSF IOS award number 2035286, secured by Drs. Lower, Pask, and Collins.

For Chapter 4, collaborators Dr. Linnea R. Meier, Dr. Judith A. Mongold-Dyers, and Dr. Lawrence M. Hanks within the Hanks Group at University of Illinois, Urbana-Champaign collected the insects and prepared crude extracts for us to analyze. This work was funded by the United States Department of Agriculture - Animal and Plant Health Inspection Service (grant #s 15, 16, 17, 18, 19, 20, 21, and 22-8130-1422-CA to Jocelyn Millar and Lawrence Hanks.

The content within Chapter 5 has been accepted for publication as Mikael A. Molander, Björn Eriksson, Kyle Arriola, Austin B. Richards, Lawrence M. Hanks, Mattias C. Larsson, Jocelyn G. Millar. *p*-Mentha-1,3-dien-9-ol: A novel aggregation-sex

pheromone for monitoring longhorn beetles (Cerambycidae) in Eurasia and North America. *Journal of Applied Entomology,* **2022**. Drs. Mikael A. Molander, Lawrence M. Hanks, Mattias C. Larsson, and Jocelyn G. Millar conceived and funded the research. Dr. Mikael A. Molander, Björn Eriksson, and Austin B. Richards conducted field experiments. Dr. Jocelyn G. Millar helped identify the pheromone component. Dr. Lawrence M. Hanks performed data and statistical analyses. This work was funded by the United States Department of Agriculture - Animal and Plant Health Inspection Service (grant #s 15, 16, 17, 18, 19, 20, 21, and 22-8130-1422-CA to Jocelyn Millar and Lawrence Hanks.

I am also grateful for two quarters of support from the UCR Agricultural Experiment Station Research and GSR Funding Support Program.

ABSTRACT OF THE DISSERTATION

Identification and Synthesis of Semiochemicals for Fireflies, True Bugs, and Longhorn Beetles

by

Kyle B. Arriola

Doctor of Philosophy, Graduate Program in Chemistry
University of California, Riverside, September 2022
Dr. Jocelyn Millar, Chairperson

The study of insect semiochemistry has vast implications for pest management, conservation efforts, and the evolution of insects. Insect semiochemicals, or chemicals emitted by insects to communicate with conspecific individuals or other organisms, are increasingly used for integrated pest management, have been instrumental in eradicating economically important pests, can be used to assess the health of ecosystems, and can be a tool in elucidating evolutionary and taxonomic relationships. For these and other reasons, it is important to study the semiochemistry of insects.

Semiochemicals used in long-distance communication are volatile, thus, the headspace odors released by insects or host plants can be collected and analyzed. Using both well-established and recently developed chemistry, my goal was to identify and prepare synthetic standards of new semiochemicals. These chemicals have been/will be used in field experiments to unambiguously verify the structures and elucidate the

functions of these semiochemicals. Insect semiochemicals often contain stereocenters, so in the case that mixtures of stereoisomers are ineffective in field experiments, synthesis of enantioenriched or enantiopure material must be conducted.

The following chapters describe the analysis of several plant- and insect-produced semiochemicals. The introductory chapter reviews the importance of structure and chirality in insect olfaction and provides an overview of the study of semiochemicals, with several interwoven examples from the natural world. In the second chapter, I report the identification of a novel diterpene hydrocarbon that attracts the invasive stink bug *Bagrada hilaris* (Hemiptera: Pentatomidae). This stink bug is an important pest of *Brassica* crops such as broccoli, kale, and cauliflower. With volatile extracts of the headspace odors from cauliflower *Brassica oleracea* var. *botrytis* seedlings, the structure and absolute configuration of the tricyclic diterpene, ultimately named brassicadiene, were determined.

In the remaining chapters, I describe the identification and synthesis of a sex-attractant pheromone ((1*S*,3*S*,4*R*)-3-hydroxy-1,7,7-trimethylbicyclo[2.2.1]heptan-2-one) of the "unlighted" winter firefly *Ellychnia corrusca* (Coleoptera: Lampyridae), and aggregation-sex pheromones for several longhorn beetles (Coleoptera: Cerambycidae). Specifically, the identifications and syntheses of the pheromone (*p*-mentha-1,3-dien-9-ol) shared by the Eurasian longhorn beetle *Aromia moschata* and the North American longhorn beetle *Holopleura marginata*, and the likely pheromone ((4*R*,6*S*,7*E*,9*E*)-4,6,8-trimethylundeca-7,9-dien-3-one) shared by the North American longhorn beetle *Graphisurus fasciatus* and South American longhorn beetle *Eutrypanus dorsalis*, are described.

TABLE OF CONTENTS

LIST OF FIGURES

LIST OF TABLES

LIST OF SCHEMES

Chapter 1 – Introduction to Insect Chemical Ecology

1.1 Introduction

Chemical ecology is defined as the study of how chemical signals and cues mediate interactions between organisms and their environments. Among the types of semiochemicals, signals are acted on by natural selection to communicate specific messages, such as an advertisement of one's presence to attract suitable mates. However, these messages may also be exploited by predators as cues to the location of their next meal. Under these pressures, semiochemical signals may change and evolve, and studying this dynamic process can provide insight into the evolution of chemical communication.

Plants belonging to the genus *Capsicum* have evolved to bear fruit that selectively deter mammalian predators, because they are not as effective at seed dispersal as avian predators of *Capsicum* fruit.[1] That is, the seeds of *Capsicum* species are destroyed in the mammalian gut but pass safely through avian guts. To deter these ineffective seed dispersers, the seeds of these plants evolved to produce capsaicin, a chemical that has been found to repel or poison mammals but not birds. In other cases, chemical defenses are not manifested directly, like a feeding deterrent, but rather indirectly by attracting species for damage control. Specifically, feeding damage caused by caterpillars (e.g. the corn earworm *Heliothis zea*) releases so-called "green-leaf volatiles" which attract parasitoids of the caterpillars (e.g. the parasitoid wasp *Microplitis croceipes*).[2] Subsequently, short range chemical cues in the frass of these caterpillars aid the wasp in accurately locating the caterpillar.[3]

1.2 Insect Olfaction

Insects are an especially interesting system for the study of chemical ecology, because much of their life history is mediated by chemical signals and cues, and their chemical communication systems have been shaped by evolution to be chemoselective.[4] According to our current understanding of insect olfaction, insect olfactory receptors are typically tuned to ecologically relevant chemicals.[5] General odors may be processed by combinatorial codes, such that changes in behavior are mediated by a combination of receptor activations. For instance, a combination of green-leaf volatiles (a suite of compounds released by plants upon tissue damage) elicited strong electrophysiological responses from antennae of the Japanese scarab beetle *Phyllopertha diversa*, but far weaker responses were recorded when the antennae were exposed to a single constituent.[6] This combinatorial code for processing odors is also prevalent in mammalian olfaction. Alternatively, insect olfactory receptors may be selectively tuned to a single compound. In one such case, the odor receptor Or56a of the common fruit fly *Drosophila melanogaster* is activated solely by geosmin, an odor produced by toxin-producing molds, and immediately triggers an avoidance response.[7]

Detection of odors may be mediated by odorant binding proteins (OBP). These are thought to transfer hydrophobic odorants through the antennal sensillum lymph to the odorant receptors. While this has been shown *in vitro*, it remains to be conclusively shown *in vivo*.[8] Several studies suggest that these odorant binding proteins could contribute to odorant discrimination,[8] chiefly through ligand-induced conformational changes of the OBPs which then activate odorant receptors as an OBP-ligand complex.[9] In *D.*

melanogaster, the pheromone binding protein (PBP, a type of OBP) LUSH binds to (*Z*)-11-vaccenyl acetate (cVA). Exposure to cVA mediates several behaviors including mate recognition and sexual behavior, by activation of odorant receptor Or67d.[10] Amino acid substitution of LUSH resulted in a protein that could activate Or67d without the presence of cVA.[9] Structural analysis of this protein showed that it resembled the structure of cVA-bound LUSH.

1.3 Importance of Structure in Insect Semiochemistry

Through these biomolecular systems, insects are also able to discriminate between enantiomers of pheromones.[11] Enantioselective odorant receptors have been demonstrated in a variety of insects, including the mosquito *Aedes aegypti*[12] and other mosquito species,[13,14] the bark beetle *Ips typographus*,[15] and the longhorn beetle *Megacyllene caryae*.[16] In fact, use of enantioselective OBPs allows two unique signals to be generated from the same gross structure, and it is not uncommon for insect species to be stimulated by one enantiomer of a signal molecule, and repelled or deterred by the other enantiomer. For example, two sympatric beetles (*Anomola osakana* and *Popillia japonica*) use different enantiomers of the same compound as sex pheromones, mediated by enantioselective odorant binding proteins. Each beetle has two types of receptors, one for each of the two enantiomers. Stimulation of one receptor elicits an attractive response, whereas stimulation of the other strongly inhibits the response, preventing cross attraction to heterospecifics. In the case of these two beetles, a 99% ee sample of the pheromone (*R*)-japonilure was only two-thirds as active as the enantiomerically pure compound to *P. japonica*, whereas a 60%

ee sample was completely inactive. Similarly, for *A. osakana* which produces and responds to (*S*)-japonilure, a 90% ee sample was inactive.

Thus, chirality of insect semiochemicals must be taken into account when elucidating the structure and function of pheromone candidates.[17] Because the presence of other stereoisomers of a pheromone can have unpredictable effects on the response to the pheromone, it is important to exercise caution in the selection of chemicals used to elucidate bioactivity. Thus, careful synthetic planning and purification steps are often required to minimize these unpredictable effects.

Determining the chemical or chemicals that make up a pheromone for an insect is usually a multistep process. For the work discussed in this dissertation, the general order of events leading to the discovery and identification of a bioactive compound is as follows: (1) insects are collected from the wild or reared in the laboratory; (2) volatiles produced by the insect are captured via collection of headspace volatiles above live insects, (3) the extract of volatiles is fractionated; (4) the fractions are assessed for bioactivity; (5) the bioactive fractions are analyzed by several analytical techniques, including coupled gas chromatography-electroantennographic detection (GC-EAD), coupled GC-MS, and if amounts permit, by NMR, to identify the bioactive constituents; (6) identified constituents are synthesized; (7) bioactivity of key constituents is verified with synthetic standards and bioassays/field trials.

GC-EAD is a very valuable tool which is essentially uniquely applicable to insects because insects' sensory receptors are externally located on the antennae and other body parts, rendering them readily accessible for electrode placement for measuring action

potentials as receptor neurons are stimulated by test chemicals. Because the receptors are tuned to biologically relevant compounds, GC-EAD allows one to rapidly locate possible pheromones and other semiochemicals in complex extracts, by measuring the antennal responses to individual compounds as they elute off the GC. The GC effluent is split between the GC detector (typically a flame ionization detector) and an airflow directed over the live antennal preparation. The GC and EAD signals are then plotted simultaneously to indicate exactly which chemicals in the extract elicit responses from the antennae, i.e., compounds which are likely candidates for chemical signals or cues. Having located these compounds, they can then be identified by standard spectrometric methods, in combination with microchemical tests for specific functional groups.

1.4 Insect Semiochemistry as a Tool for Pest Control

Discovery and identification of semiochemicals that mediate insect behaviors have major implications for control of pest insects, in part because they often are species-specific, do not persist for long periods in the environment, and have minimal environmental impact on nontarget organisms.[18] Several landmark successes have arisen from the usage of pheromones with integrated pest management (IPM) tactics, such as detection and monitoring of pests, or population suppression through mating disruption, mass trapping, and attract-and-kill tactics.[19] For example, the boll weevil *Anthonomus grandis* (Coleoptera: Curculionidae) which had caused an estimated $15 billion in damage since its introduction into the United States in the late 19th century, was successfully eradicated from the US with pheromone-based technology, and ongoing pheromone-based monitoring efforts ensure that it is not reintroduced.[20–22] Similarly, the red palm weevil

Rhynchophorus ferrugineus[23] was effectively controlled with pheromone-based methods. Successes also extend to the control of lepidopteran pests,[24] such as the codling moth *Cydia pomonella*[25,26] and spongy moth *Lymantria dispar*.[27] In the case of the codling moth, a six-year long mating disruption program near Sacramento, CA, led to a reduction in fruit damage to as little as 0.1% from initial fluctuations between 20-75%, an 85% reduction of moth trap captures in pheromone-baited traps, and an approximately 75% reduction in pesticide application.[28] This technique is now widely utilized across the western USA, and many other areas of the world where pome fruit are grown. As for the spongy moth, mating disruption has been instrumental in slowing the spread of this invasive, forest defoliator pest of many deciduous tree species. Though not as effective as biological controls (e.g. entomopathogenic fungi) used for mass eradication efforts, a pheromone-based mating disruption strategy implemented across a 3 million hectare zone from midwestern to southeastern USA has been integral in keeping the spongy moth from spreading outside of the more densely infested region.[27] Clearly, pheromone-based methods for pest control can be powerful tools.

1.5 Summary

The primary goal of this dissertation research was to identify and where possible, synthesize several bioactive molecules that mediate insect behavior. With this newly gained knowledge, we have additional insight into how an invasive pest of *Brassica* crops (e.g., cauliflower, broccoli, kale) locates its host, the chemical communication system of an adult firefly (Coleoptera: Lampyridae) that has lost the ability to communicate with the light signals typically associated with fireflies, and the chemical space occupied by and

structural conservation of semiochemicals of longhorn beetle (Coleoptera: Cerambycidae) species across multiple continents. While not all the insect systems whose pheromones were studied are invasive and/or pest species, my research has provided tools that could be used to detect and study the population biology of several species.

Specifically, Chapter 2 focuses on the spectroscopic identification of brassicadiene, a novel diterpene hydrocarbon attractive to the invasive stink bug *Bagrada hilaris*. Volatiles of cauliflower seedlings were collected, fractionated, and spectroscopically analyzed to determine the gross structure and absolute configuration of its tricyclic structure. This work revealed the mechanism by which this pest species locates its host plants at the vulnerable and nutrient-rich seedling stage.

Chapter 3 describes the first identification of a sex attractant pheromone for a firefly species, using a combination of mass spectrometry and microchemical tests. The compound was synthesized, and conditions for the chromatographic separation of the various possible isomers of the pheromone were determined, leading to the identification and synthesis of (1*S*,3*S*,4*R*)-3-hydroxy-1,7,7-trimethylbicyclo[2.2.1]heptan-2-one as the sex-attractant pheromone for the winter firefly *Ellychnia corrusca*, with the bioactivity corroborated through both GC-EAD bioassays and field trials.

Chapter 4 details the identification and efforts to synthesize a male-produced polyketide aggregation-sex pheromone candidate for *Graphisurus fasciatus*, a longhorn beetle (Coleoptera: Cerambycidae) native to northeastern North America. I was able to identify the specific stereoisomer that the beetle produces, from a total of 16 possible stereoisomers. Intriguingly, we also found the same stereoisomer in headspace volatiles of

males of the South American longhorn beetle *Eutrypanus dorsalis*. Both species belong to the same tribe (Acanthocinini), but it is remarkable that the pheromone chemistry is apparently conserved across continents.

Lastly, Chapter 5 describes the identification, synthesis, and field trials of the monoterpene alcohol *p*-mentha-1,3-dien-9-ol, a male-produced aggregation-sex pheromone of the longhorn beetles *Aromia moschata* ssp. *moschata* native to Europe and Central Asia, and *Holopleura marginata* native to western North America. These species belong to different tribes (Callichromatini and Holopleurini, respectively), providing another example of conservation of pheromone structures across two continents, and consequently millions of years.

1.6 References

(1) Tewksbury, J. J.; Nabhan, G. P. Directed Deterrence by Capsaicin in Chillies. *Nature* **2001**, *412* (6845), 403–404. https://doi.org/10.1038/35086653.

(2) Whitman, D. W.; Eller, F. J. Parasitic Wasps Orient to Green Leaf Volatiles. *Chemoecology* **1990**, *1* (2), 69–76. https://doi.org/10.1007/BF01325231.

(3) Jones, R. L.; Lewis, W. J.; Bowman, M. C.; Beroza, M.; Bierl, B. A. Host-Seeking Stimulant for Parasite of Corn Earworm: Isolation, Identification, and Synthesis. *Science* **1971**, *173* (3999), 842–843. https://doi.org/10.1126/SCIENCE.173.3999.842.

(4) Wicher, D.; Miazzi, F. Functional Properties of Insect Olfactory Receptors: Ionotropic Receptors and Odorant Receptors. *Cell Tissue Res* **2021**, *383* (1), 7–19. https://doi.org/10.1007/S00441-020-03363-X/FIGURES/5.

(5) Hansson, B. S.; Stensmyr, M. C. Evolution of Insect Olfaction. *Neuron* **2011**, *72* (5), 698–711. https://doi.org/10.1016/J.NEURON.2011.11.003.

(6) Hansson, B. S.; Larsson, M. C.; Leal, W. S. Green Leaf Volatile-Detecting Olfactory Receptor Neurones Display Very High Sensitivity and Specificity in a Scarab Beetle. *Physiol Entomol* **1999**, *24* (2), 121–126. https://doi.org/10.1046/J.1365-3032.1999.00121.X.

(7) Stensmyr, M. C.; Dweck, H. K. M.; Farhan, A.; Ibba, I.; Strutz, A.; Mukunda, L.; Linz, J.; Grabe, V.; Steck, K.; Lavista-Llanos, S.; Wicher, D.; Sachse, S.; Knaden, M.; Becher, P. G.; Seki, Y.; Hansson, B. S. A Conserved Dedicated Olfactory Circuit for Detecting Harmful Microbes in *Drosophila*. *Cell* **2012**, *151* (6), 1345–1357. https://doi.org/10.1016/J.CELL.2012.09.046.

(8) Zhou, J.-J.; Robertson, G.; He, X.; Dufour, S.; Hooper, A. M.; Pickett, J. A.; Keep, N. H.; Field, L. M. Characterisation of *Bombyx Mori* Odorant-Binding Proteins Reveals That a General Odorant-Binding Protein Discriminates Between Sex Pheromone Components. *J Mol Biol* **2009**, *389* (3), 529–545. https://doi.org/10.1016/j.jmb.2009.04.015.

(9) Laughlin, J. D.; Ha, T. S.; Jones, D. N. M.; Smith, D. P. Activation of Pheromone-Sensitive Neurons Is Mediated by Conformational Activation of Pheromone-Binding Protein. *Cell* **2008**, *133* (7), 1255–1265. https://doi.org/10.1016/J.CELL.2008.04.046.

(10) Kurtovic, A.; Widmer, A.; Dickson, B. J. A Single Class of Olfactory Neurons Mediates Behavioural Responses to a *Drosophila* Sex Pheromone. *Nature* **2007**, *446* (7135), 542–546. https://doi.org/10.1038/nature05672.

(11) Sims, C.; Birkett, M. A.; Withall, D. M. Enantiomeric Discrimination in Insects: The Role of OBPs and ORs. *Insects* **2022**, *13* (4), 368. https://doi.org/10.3390/INSECTS13040368.

(12) Dickens, J. C.; Bohbot, J. D. Mini Review: Mode of Action of Mosquito Repellents. *Pestic Biochem Phys* **2013**, *106* (3), 149–155. https://doi.org/10.1016/J.PESTBP.2013.02.006.

(13) Hill, C. A.; Fox, A. N.; Pitts, R. J.; Kent, L. B.; Tan, P. L.; Chrystal, M. A.; Cravchik, A.; Collins, F. H.; Robertson, H. M.; Zwiebel, L. J. G Protein-Coupled Receptors in *Anopheles Gambiae*. *Science* **2002**, *298* (5591), 176–178. https://doi.org/10.1126/SCIENCE.1076196.

(14) Hill, S. R.; Majeed, S.; Ignell, R. Molecular Basis for Odorant Receptor Tuning: A Short C-Terminal Sequence Is Necessary and Sufficient for Selectivity of Mosquito Or8. *Insect Mol Biol* **2015**, *24* (4), 491–501. https://doi.org/10.1111/IMB.12176.

(15) Yuvaraj, J. K.; Roberts, R. E.; Sonntag, Y.; Hou, X. Q.; Grosse-Wilde, E.; Machara, A.; Zhang, D. D.; Hansson, B. S.; Johanson, U.; Löfstedt, C.; Andersson, M. N. Putative Ligand Binding Sites of Two Functionally Characterized Bark Beetle Odorant Receptors. *BMC Biol* **2021**, *19* (1). https://doi.org/10.1186/S12915-020-00946-6.

(16) Mitchell, R. F.; Hughes, D. T.; Luetje, C. W.; Millar, J. G.; Soriano-Agatón, F.; Hanks, L. M.; Robertson, H. M. Sequencing and Characterizing Odorant Receptors of the Cerambycid Beetle *Megacyllene Caryae*. *Insect Biochem Molec* **2012**, *42* (7), 499–505. https://doi.org/10.1016/J.IBMB.2012.03.007.

(17) Mori, K. Significance of Chirality in Pheromone Science. *Bioorgan Med Chem* **2007**, *15* (24), 7505–7523. https://doi.org/10.1016/J.BMC.2007.08.040.

(18) *Integrated Pest Management (IPM) Principles | US EPA*. https://www.epa.gov/safepestcontrol/integrated-pest-management-ipm-principles (accessed 2022-06-26).

(19) Tewari, S.; Leskey, T. C.; Nielsen, A. L.; Piñero, J. C.; Rodriguez-Saona, C. R. Use of Pheromones in Insect Pest Management, with Special Attention to Weevil Pheromones. *Integrated Pest Management: Current Concepts and Ecological Perspective* **2014**, 141–168. https://doi.org/10.1016/B978-0-12-398529-3.00010-5.

(20) Tumlinson, J. H.; Minyard, J. P.; Gueldner, R. C.; Hardee, D. D.; Thompson, A. C.; Hedin, P. A. Identification and Synthesis of the Four Compounds Comprising the Boll Weevil Sex Attractant. *J Org Chem* **1971**, *36* (18), 2616–2621. https://doi.org/10.1021/JO00817A012/SUPPL_FILE/JO00817A012_SI_001.PDF

(21) Hardee, D. D.; Graves, T. M.; McKibben, G. H.; Johnson, W. L.; Gueldner, R. C.; Olsen, C. M. A Slow-Release Formulation of Grandlure, the Synthetic Pheromone of the Boll Weevil. *J Econ Entomol* **1974**, *67* (1), 44–46. https://doi.org/10.1093/JEE/67.1.44.

(22) Mitchell, E. B.; Hardee, D. D. In-Field Traps: A New Concept in Survey and Suppression of Low Populations of Boll Weevils. *J Econ Entomol* **1974**, *67* (4), 506–508. https://doi.org/10.1093/JEE/67.4.506.

(23) Oehlschlager, A. C. Palm Weevil Pheromones – Discovery and Use. *J Chem Ecol* **2016**, *42* (7), 617–630. https://doi.org/10.1007/S10886-016-0720-0/FIGURES/13.

(24) Cardé, R. T. Utilization of Pheromones in the Population Management of Moth Pests. *Environ Health Persp* **1976**, *14*, 133–144. https://doi.org/10.1289/EHP.14-1475097.

(25) Rizvi, S. A. H.; George, J.; Reddy, G. V. P.; Zeng, X.; Guerrero, A. Latest Developments in Insect Sex Pheromone Research and Its Application in Agricultural Pest Management. *Insects* **2021**, *12* (6). https://doi.org/10.3390/INSECTS12060484.

(26) Witzgall, P.; Stelinski, L.; Gut, L.; Thomson, D. Codling Moth Management and Chemical Ecology *Ann Rev Entomol* **2007**, *53*, 503–522. https://doi.org/10.1146/ANNUREV.ENTO.53.103106.093323.

(27) Lance, D. R.; Leonard, D. S.; Mastro, V. C.; Walters, M. L. Mating Disruption as a Suppression Tactic in Programs Targeting Regulated Lepidopteran Pests in US. *J Chem Ecol* **2016**, *42* (7), 590–605. https://doi.org/10.1007/S10886-016-0732-9/FIGURES/2.

(28) Welter, S. C.; Pickel, C.; Millar, J.; Cave, F.; van Steenwyk, R. A.; Dunley, J. Pheromone Mating Disruption Offers Selective Management Options for Key Pests. *California Agriculture* **2005**, *59* (1), 16–22. https://doi.org/10.3733/CA.V059N01P16.

Chapter 2 – Structural Elucidation of the Diterpene Hydrocarbon Brassicadiene, a Powerful Attractant for the Invasive Stink Bug *Bagrada hilaris*

ABSTRACT

The bagrada bug *Bagrada hilaris* is an invasive stink bug endemic to parts of Asia and Africa. It specializes on cruciferous plants (genus *Brassica*) such as broccoli, kale, and cauliflower, with a preference for the nutrient-rich and vulnerable seedling stage. Feeding damage caused by the bagrada bug leads to crop damage, lower crop yield, and often plant death. Here, I describe the identification of brassicadiene, a novel tricyclic diterpene hydrocarbon that mediates the attraction of *B. hilaris* to *Brassica* plants. Brassicadiene constituted >90% of the volatile organic compounds released by cauliflower seedlings, *Brassica oleracea* var. *botrytis*, and serves as a kairomone by which this pest species locates its host plant.

2.1 Introduction

The stink bug *Bagrada hilaris* Burmeister (Heteroptera: Pentatomidae), endemic to parts of Asia and Africa, attacks a variety of plant species in the genus *Brassica*, including a number of important crops such as broccoli, cauliflower, and kale.[1,2] This pest invaded North America ~10 years ago, spreading rapidly through the southern United States and then further south through Central America and into South America.[2] Wherever it has invaded, it has caused substantial damage to crops. A recent study showed that this bug is particularly attracted to seedlings of cruciferous plants, which are frequently killed by bug feeding activity.[3]

2.1.1 Acquisition of Sample

In preliminary work, crude extracts of the volatile organic compounds (VOCs) released by undamaged seedlings of cauliflower, *Brassica oleracea* var. *botrytis*, and rapeseed, *B. napus*, were found to be highly attractive to *B. hilaris* adults. Bioassay-guided fractionation of the crude extracts revealed that the active compound(s) were contained in the nonpolar hydrocarbons fraction eluted from silica gel with hexane.[3]

A larger sample of the compound was isolated from a composite crude extract, obtained by combining multiple VOC collections from cauliflower seedlings, by liquid chromatography on silica gel, eluting with hexane.

2.1.2 Preliminary Spectral Data

The major component (>90%) of this fraction was tentatively identified as a diterpene on the basis of several pieces of information. First, its molecular formula was confirmed to be $C_{20}H_{32}$, from its high-resolution exact mass measurement (*m/z* 272.2504 [M^+]; calcd for

$C_{20}H_{32}$ 272.2504), which, in turn would require five rings or sites of unsaturation. Second, hydrogenation with palladium on carbon catalyst produced a derivative with a molecular weight of 276 amu, indicating that there were two sites of unsaturation and hence three rings. Third, the electron impact ionization (EI) mass spectra of both the parent compound (**Figure 2.01A**) and the derivative (**Figure 2.01B**) showed fragmentation patterns typical of terpenoids, and both were dominated by a base peak from a loss of 43 mass units, suggestive of an isopropyl group that was readily lost from both structures. These structural features and further fragmentary information obtained from the ^{1}H NMR spectrum did not match any of the ~1000 known diterpene hydrocarbon structures listed in SciFinder.

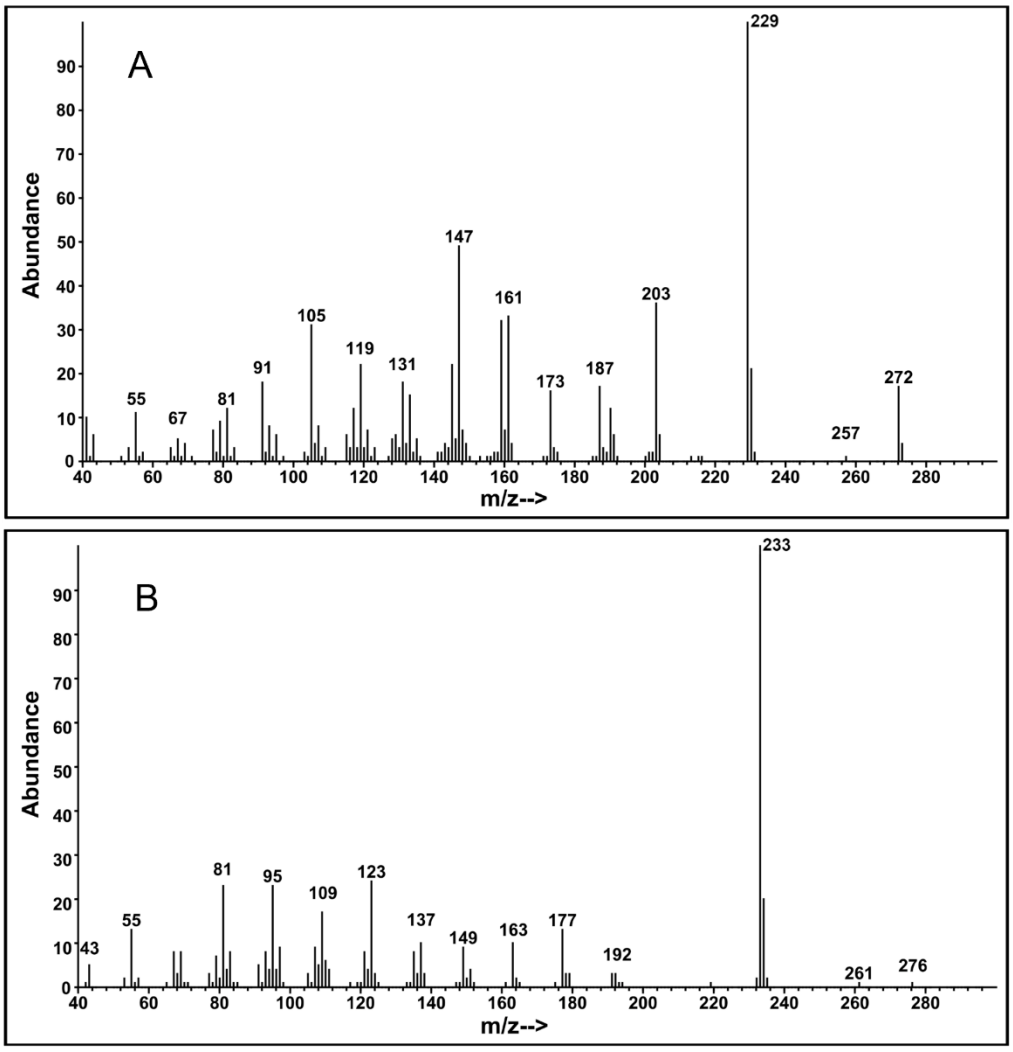

Figure 2.01 *EI GC-MS data for: A) brassicadiene and B) its catalytic hydrogenation derivative.*

2.2 Results and Discussion

A summary of spectroscopic information obtained from the ^{1}H-, ^{13}C-, and ^{1}H-^{13}C HSQC NMR spectra is shown in **Table 2.01**.

Table 2.01 *NMR data of brassicadiene.*

δ ^{13}C	Carbon type	Position	δ ^{1}H, mult.	*J*(H,H) = (Hz)
156.1	>C=	1	-	
136.6	>C=	2	-	
122.2	-CH=	3	5.30 m	
118.3	-CH=	4	5.50 dd	*J* = 8.2, 2.5
55.3	>CH-	5	1.43 td	*J* =~11.5, ~11.5, 2.1
51.8	>C<	6	-	
45.4	>C<	7	-	
43.2	-CH_2-	8a	2.59 dd	*J* = 16.4, 6.9
		8b	1.77 br d	*J* = ~16.4
39.1	>CH-	9	1.70 m	
37.0	-CH_2-	10a	1.99 ddd	*J* = 15.8, 8.2, 3.3
		10b	1.73 ddd	*J* = 15.8, 10.9, 2.5
35.4	-CH_2-	11a	2.28 ddd	*J* = 17.0, ~5.9, ~5.2
		11b	2.10 br ddd	*J* = 17.0, ~7, ~7
33.9	>CH-	12	1.16 m	
32.2	-CH_2-	13a	1.79 dd	*J* = 11.6, 6.9
		13b	1.12 m	
30.8	-CH_3	14	1.15 s	
30.0	-CH_2-	15a	1.66 dd	*J* = 13.6, 8.0
		15b	1.29 m	
28.8	-CH_3	16	1.75 br	
25.7	-CH_2-	17a	1.86 dddd	*J* = 13.7, 7.0, 5.2, 2.4
		17b	1.32 m	
20.0	-CH_3	18	0.92 d	*J* = 6.5
19.2	-CH_3	19	0.73 d	*J* = 6.8
18.7	-CH_3	20	0.89 d	*J* = 6.7

2.2.1 Molecular Fragment Spin Systems

Four spin systems terminating at quaternary carbons were identified with a 2D ^{1}H-^{1}H DQFCOSY spectrum (**Figure 2.02A**).

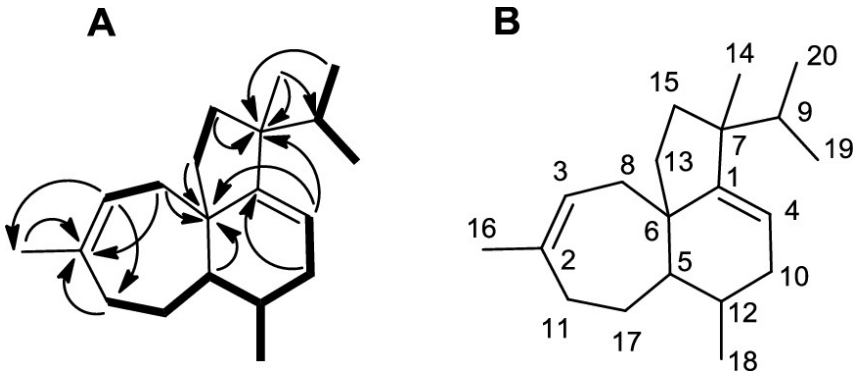

Figure 2.02 *Structural elucidation of the gross structure of brassicadiene: A) four spin systems determined by ^{1}H-^{1}H DQFCOSY (bold) and connections through quaternary carbons determined by ^{1}H-^{13}C HMBC (arrows); B) basic structure assembled with carbons numbered in descending magnitude of chemical shift (see* ***Table 2.01****).*

2.2.2 Fragment Connectivity

Connections of the spin system fragments began with consideration of the two alkenyl protons, which were not coupled to each other, indicating that there were two trisubstituted alkenes. The first of these was substituted with the allylic methyl group CH_3-16 (chemical shift 1.75 ppm) and displayed as a broadened singlet. Data from the ^{1}H-^{13}C HMBC spectrum showed strong correlations between C-2 and H_3-16, C-2 and H_2-11, and C-3 and H_3-16, establishing the C-2 to C-3 alkene fragment. There were additional HMBC correlations between C-2 and allylic H_2-8, supported by $^{3}J_{H-H}$ couplings between H-3 and H-8a in the ^{1}H spectrum, establishing the C3−C8 bond. The fact that there were no obvious additional $^{3}J_{H-H}$ couplings to H-8b or H-8a suggested that C-8 terminated at a quaternary carbon on the other side, providing one end of the spin system. The connection of C-2 to allylic CH_2-11 was verified by the HMBCs of C-11 to H_3-16 and C-3 to H_2-11. $^{3}J_{H-H}$ couplings in the ^{1}H NMR spectrum then established the successive connectivity among C11−C17−C5−C12−C10−C4. The alkenyl unit CH-4, by default, had to be connected to

the remaining quaternary alkenyl carbon C-1. In addition, the ^{1}H and $^{1}H-^{1}H$ COSY spectra showed that H-12 was coupled to H_3-18, and H-5 was only coupled to protons on H_2-17 and H-12, suggesting that the final connection of CH-5 was to a quaternary carbon. The complete spin system is shown in **Figure 2.02A**. The third spin system consisted of an isolated isopropyl group, characterized by the EI mass spectrum and $^{3}J_{H-H}$ couplings between H-9 and H_3-19 and H_3-20, with no other direct couplings to H-9, establishing that the isopropyl group was attached to a quaternary carbon. To establish further connectivity, strong HMBCs were observed between H_3-19, H_3-20, and C-7 in addition to a correlation between C-7 and H-9, producing the connection of C9−C7. The possibility of the sharp methyl singlet H_3-14 being connected to C-7, as opposed to the other quaternary centers C-1 and C-6, was corroborated by HMBCs of H_3-14 to C-15, C-7, and C-9 and its relatively low chemical shift (1.15 ppm). This established the connectivity of C14− C7−C9−C19/20. Additional HMBCs of C-7 to H_2-15 and H-4 and across the quaternary center C-7, such as the correlations C-1 to H_3-14 and C-15 to H_3-14, allowed the identification of the connections C1−C7−C15 and C7−C1−C4. The fourth and final spin system consisted of methylenes C13−C15, which are attached on both ends to quaternary centers, where one had already been previously identified as C7−C15 and the other was to be determined. With four single-bond connections and a lone sp^3 - quaternary carbon (C-6) remaining, HMBCs between C-6 and H_2-8, H-3, H_2-13, H-4, and H-5 gave a strong indication that C-6 was directly connected to carbons 8, 13, 1, and 5. In total, this established the basic structure as the fused 5− 6−7-spirotricyclic skeleton shown in **Figure 2.02B**, with the

unusual moiety of an isopropyl and a methyl group attached to the same sp^3-quaternary center.

2.2.3 Relative and Absolute Stereochemistry

The assignment of the relative stereochemistry was facilitated by using a digital molecular modeling program (ChemSketch) to simulate the shape and orientation of the molecule and its atoms (**Figure 2.03**).

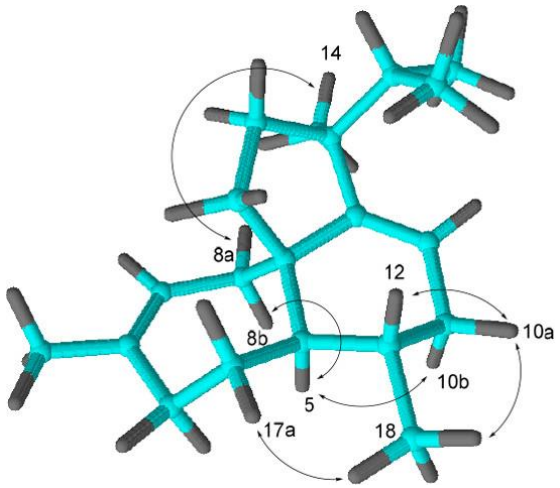

Figure 2.03 *Model of brassicadiene showing key NOE enhancements.*

From the simulated structures, the relative stereochemistry was elucidated beginning with the four diastereoisomeric forms **2.01**-**2.04**, which varied in the relative configurations of the three contiguous stereocenters on carbons 6, 5, and 12 (**Figure 2.04A**), using data from the $^3J_{H-H}$ coupling constants and a NOESY spectrum. A strong NOE enhancement was observed between H-5 and H-8b, eliminating possibilities **2.03** and **2.04**, where the C6−C13 bond is *syn* with respect to the CH-5 bond. Next, the spatial relationships between H-5 and the flanking H-12, H-17b, and H-17a were established from the magnitudes of the respective coupling constants. In particular, the pseudotriplet of

doublets of H-5 corresponded to two large couplings of approximately equal value ($J \simeq$ 11.5 Hz) to H-12 and H-17b, indicating that they were approximately parallel or antiparallel to the CH-5 bond, whereas the remaining small coupling ($J \simeq 2.1$ Hz) between H-5 and H-17a indicated a roughly orthogonal relationship between the CH-5 and the CH-17a bonds. For simulated structure **2.01** with an *anti*-relationship between H-5 and C-18 (**Figure 2.04B**), the expected splitting pattern of H-5 would best be described as a ddd, owing to the approximate dihedral angles of 180, 55, and 90° relative to the flanking protons H_2-17 and H-12. This would not support the two large coupling constants of ~11.5 Hz. Conversely, structure **2.02** with a *syn* relationship between H-5 and C-18 (**Figure 2.04C**) exhibits two pseudoantiperiplanar relationships, specifically between CH-5 and CH-12 as well as CH-5 and CH-17b, and a ~90° dihedral angle between CH-5 and CH-17a, which would accommodate the pseudotriplet of doublets with observed coupling constants of ~11.5, ~11.5, and 2.1 Hz. Taken together, these data established the relative stereochemistry of the three contiguous stereocenters as that shown in structure **2.02** in **Figure 2.04C**.

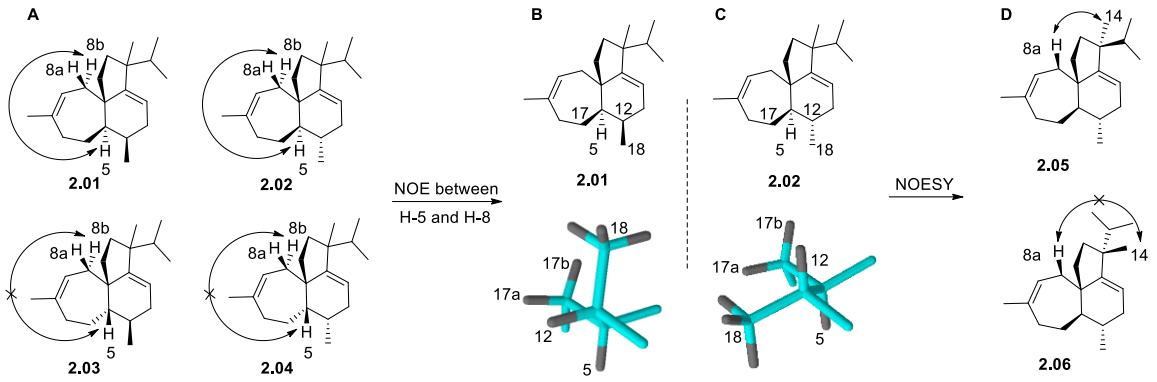

Figure 2.04 *Elucidation of the relative stereochemistry: A) Four diastereomers selected to begin elucidation of the relative stereochemistry; B) Simulated anti-diastereomer and; C) simulated syn-diastereomer in regard to the relative stereochemical relationship between H-5 and C-18, showing key dihedral angles among protons adjacent to H-5; D) Elucidation of the relative stereochemistry of the final stereocenter, showing an NOE between H-8a and H3-14.*

The relative stereochemistry of the fourth and final stereocenter was determined to be as shown in **2.05** in **Figure 2.04D**, from the strong NOE enhancement observed between H_3-14 and H-8a, with a separation estimated from the model of 1.8 Å. Such an enhancement would be improbable in the alternative stereoisomer **2.06**, where the methyl group and H-8a are much farther apart (estimated 4.9 Å). Furthermore, there was no NOE between either H_2-8 and H_3-19 or H_3-20, as would be expected for the alternative stereoisomer **2.06**. Thus the data best supported the structure represented by **2.05**, to which we assign the common name brassicadiene.

In addition to the unusual feature of methyl and isopropyl groups being attached to the same quaternary center in a terpenoid, the connectivity of the 5,6,7-tricyclic ring structure of brassicadiene also appears to be rare. A search of the literature revealed only one other known terpenoid with this particular pattern of fused rings, the sesterterpenoid gascardic acid (**2.07**, **Scheme 2.01**), produced by the scale insect *Gascardia*

madagascariensis Targioni Tozzetti.[4,5] Furthermore, the treatment of gascardic acid with acid had been reported to result in, among other rearrangements, a 1,2-shift of the quaternary methyl group to the ternary carbon bearing the side chain while simultaneously introducing a new double bond, creating a core structure (**2.08**) analogous to that in brassicadiene.[4,5]

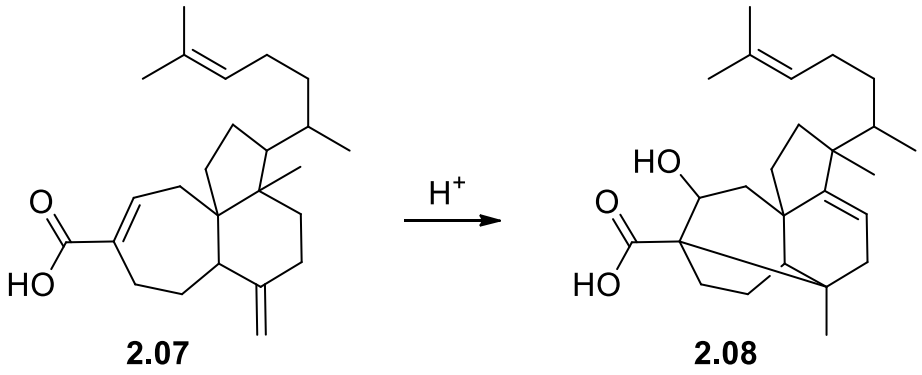

2.07 **2.08**

Scheme 2.01 *Treatment of gascardic acid **2.07** with acid was reported to result in a 1,2 methyl shift and the introduction of a double bond, producing a core structure **2.08** analogous to that in brassicadiene.*

Brassicadiene exhibited a specific rotation of approximately $[\alpha]_D^{20}$ + 41° (c 0.17, CH_2Cl_2). DFT calculations based on the absolute configuration of structure **2.05** shown in **Figure 2.04D** returned a positive value for the calculated specific rotation, suggesting that the absolute configuration of naturally occurring brassicadiene is as shown in **2.05**.

2.3 Conclusions

Plants in the family Brassicaceae are known for being chemically defended from generalist herbivores by glucosinolates.[6] Tissue damage from herbivore feeding releases myrosinases, which cleave the glucosinolates into smaller, strongly irritating isothiocyanates and related chemicals, the odorous compounds typically associated with mustards, cabbage, cauliflower, and other cruciferous plants. Thus, it was unexpected to

find that the headspace odors of undamaged cauliflower seedlings consisted largely of a novel diterpene hydrocarbon, along with trace amounts of several isomers.[3] The stink bug *B. hilaris*, a specialist herbivore that exhibits a strong preference for newly emerged seedlings of crucifers,[1,7] has apparently evolved to use brassicadiene as a host location cue. In previously reported bioassays, the hexane fraction of the plant VOCs consisting of >90% brassicadiene was highly attractive to adult bugs,[3] and this attraction was confirmed with Y-olfactometer bioassays with the purified compound (**Figure 2.05**). The fact that *B. hilaris* exploits this compound for host location is intriguing given that diterpene hydrocarbons are generally thought to contribute to plant defenses against herbivores,[8–10] phytopathogenic fungi,[11–14] and nematodes.[15,16] The possible functions of brassicadiene within the plants that produce it remain to be determined.

The use of Brassicaceae seedlings of *Brassica oleracea* var. *botrytis* (cauliflower) and *Eruca sativa* (arugula) as trap plants for *B. hilaris* has been evaluated to be an effective tool in diverting *B. hilaris* individuals from nearby infested caper bushes[17]. Similarly, use of Brassicaceae seedlings could also be an especially valuable tool for monitoring the presence of *B. hilaris* as opposed to using a synthetic standard of brassicadiene. Given the complexity of the structure, large-scale syntheses of brassicadiene would likely be very expensive relative to the cost of growing cotyledon-stage seedlings. Alternatively, through traditional breeding or genetic engineering, varieties of brassicaceous plants could be developed to not produce brassicadiene, potentially rendering the crop chemically invisible to *B. hilaris*.

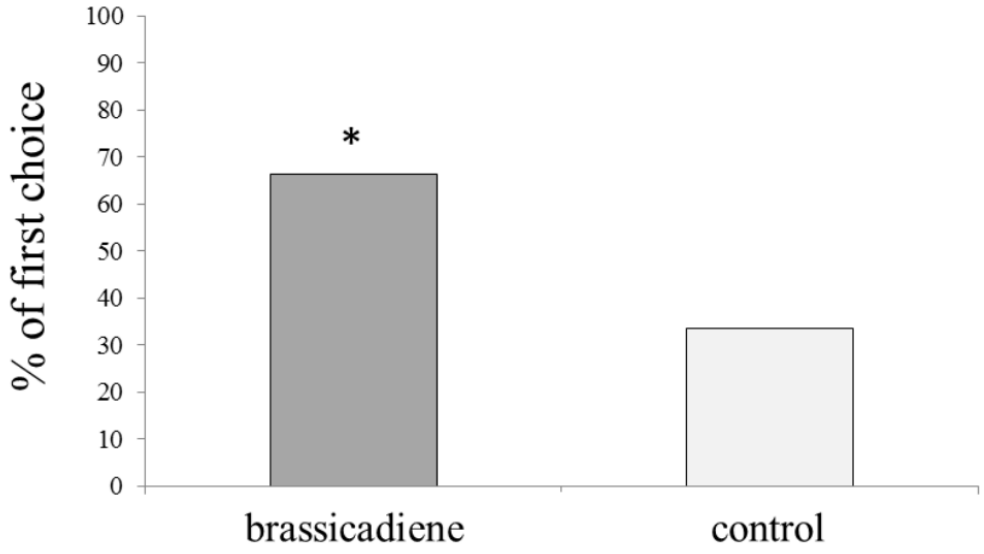

Figure 2.05 *Responses of adult Bagrada hilaris to brassicadiene (200 µg) versus a solvent control in open vertical y-olfactometer bioassays. Bugs selected the treatment arm significantly more than the control arm (Chi square analysis, P < 0.05).*

2.4 Methods

The accurate mass measurement was run by Dr. Felix Grun, Mass Spectrometry Facility, Dept. of Chemistry, University of California, Irvine, using a Waters (Micromass) GCT GC-MS with chemical ionization (ammonia), in positive ion mode. Found: *m/z* 272.2504; calcd for $C_{20}H_{32}$: 272.2504.

Optical rotation measurements were made with an Autopol IV digital polarimeter (Rudolph Research Analytical), and a T32 microsample cell (2.5 mm i.d.× 50 mm length; 250 µL volume; Rudolph Research Analytical). The sample was run in CH_2Cl_2 at a concentration of 1.7 mg/ml at 589 nm and 21.6 ºC, giving an average observed rotation of +0.035 ± 0.001º (n = 20 replicated measurements), equal to a specific rotation of +41º.

2.4.1 Isolation of brassicadiene from *Brassica oleracea* var. *botrytis*

Brassica oleracea var. *botrytis* (cauliflower) seeds were sprouted on cotton wool soaked in water, in covered Petri dishes held in a growth chamber at 25 ± 1 °C, 70 ± 10% RH, photoperiod 16L:8D, under lights with a photosynthetic flux density (PPFD) of 600 mol photons m^{-2} s^{-1}. Once the seeds had sprouted (~3 d), the cover was removed, and after 7 d, the base of each cluster of ~500 seedlings was wrapped with aluminum foil in preparation for collection of headspace volatiles[3]. Briefly, 7-d-old seedling clusters were placed in a 3 L cylindrical glass chamber flushed at 400 ml/min with activated charcoal-scrubbed air. Volatiles were trapped on 100 mg of Porapak Q adsorbent (80–100 mesh; Sigma-Aldrich) for 20 h, then eluted with 1 ml hexane, and the resulting extracts were concentrated to ~100 µl under a nitrogen stream. Collections were carried out at 25 ± 3°C, 60 ± 5% RH, and photoperiod 16L: 8D. After each collection, the chamber was washed, rinsed with acetone, and baked overnight at 150 °C. Blank aerations were carried out as controls to identify system contaminants.

To isolate the diterpene, a composite sample from ~200 aerations was concentrated to ~0.2 ml under a stream of nitrogen. A 12 mm diam sintered glass funnel was loaded with 3 g of 230-400 mesh silica gel, oven dried at 120ºC overnight and cooled in a sealed tube. The silica gel was wetted with pentane, and the concentrated composite headspace sample in ~0.2 ml hexane was loaded onto the column, rinsing 3 times with 0.2 ml pentane. The column was then eluted with eighteen 1 ml aliquots of pentane, pulling the solvent through the bed with mild suction. The diterpene began eluting in the 8th fraction, with fractions 9-14 being >90% pure, and residual amounts eluting in fractions 15 and 16. Fractions 9-13

were combined, yielding a sample (estimated ~20 micrograms) which was >95% pure brassicadiene by GC-MS analysis. The combined fractions were concentrated just to dryness under a gentle stream of nitrogen, leaving a slight film of colorless oil, to which 0.2 ml of deuterated methylene chloride (99.96% D, Aldrich Chem. Co., Minneapolis WI, USA) was added and blown down just to dryness. The process was repeated, and the residue was then dissolved in 20 µl CD_2Cl_2 and transferred to a 1 mm diam microbore NMR tube (Bruker Biospin Corp., Fallenden, Germany). NMR spectra (^1H, ^{13}C) were taken on a Bruker Avance 600 MHz spectrometer and additional NMR spectra (^1H-^1H gCOSY, ^1H-^1H DQFCOSY, ^1H-^1H gHMBC, ^1H-^{13}C gHSQC, gNOESY, TOCSY) were taken on a Bruker Avance III 700 MHz spectrometer. Mass spectra were taken with a Hewlett-Packard 5890 GC interfaced to a 5973 mass selective detector, with electron impact ionization (70 eV). Samples were run in splitless injection mode.

An aliquot of a concentrated extract of *B. oleracea* var *botrytis* volatiles was analyzed by gas chromatography/Fourier transform-infrared spectroscopy (GC/ FT-IR) with a Shimadzu GC2010 gas chromatograph coupled to a DiscovIR-GC infrared detector (4,000−750 cm^{-1}, resolution of 8 cm^{-1}, Spectra Analysis, Marlborough, MA, USA), by Prof. Paulo H. G. Zarbin, Universidade Federal do Paraná, Curitiba, Brazil. The GC was equipped with a RTX-5® (30 m × 0.25 mm × 0.25 µm film thickness) capillary column, with helium as carrier gas (1 mL/min). Injections were made in splitless mode (250 °C), with an oven temperature program of 50 °C for 1 min, increasing at 7 °C/min to 250 °C, then held for 10 min.

2.4.2 Calculation of the absolute stereochemistry of brassicadiene

To estimate the calculated specific rotation of brassicadiene, structure **2.05**, with the absolute configuration shown in **Figure 2.04D**, was submitted to conformational analysis using Spartan´08 and MMFF94.[18] Three relevant conformers were found in an energy window of 12.5 KJ/mol. The three structures were optimized in Gaussian´09, Revision A.02. using B3LYP-D/6-311G(d,p) and a solvent model (IEFPCM) for dichloromethane.[19] The obtained total energies are: 1) -781,63703768 hartree (+1.8 KJ/mol); 2) -781,63772535 hartree 3); -781,6332785 hartree (+11.7 KJ/mol). At 20 °C this translates to a Boltzmann-population of: 1) 32.10%; 2) 67.34%; 3) 0.56%. The optical rotation values at 589 nm were calculated at the B3LYP/6-311++G(2d,2p) level of theory. The predicted values are: 1) +195.6; 2) +146.2; 3) +228.5. Using the calculated Boltzmann-populations the predicted averaged optical rotation of structure **2.05** is +162.5.

2.5 References

(1) Huang, T. I.; Reed, D. A.; Perring, T. M.; Palumbo, J. C. Feeding Damage by *Bagrada Hilaris* (Hemiptera: Pentatomidae) and Impact on Growth and Chlorophyll Content of Brassicaceous Plant Species. *Arthropod-Plant Inte* **2014**, *8* (2), 89–100. https://doi.org/10.1007/S11829-014-9289-0.

(2) Bundy, C. S.; Perring, T. M.; Reed, D. A.; Palumbo, J. C.; Grasswitz, T. R.; Jones, W. A. *Bagrada Hilaris* (Burmeister). In *Invasive Stink Bugs and Related Species (Pentatomoidea)*; McPherson, J., Ed.; CRC Press: Boca Raton, 2018; pp 205–242. https://doi.org/10.1201/9781315371221-3.

(3) Guarino, S.; Arif, M. A.; Millar, J. G.; Colazza, S.; Peri, E. Volatile Unsaturated Hydrocarbons Emitted by Seedlings of *Brassica* Species Provide Host Location Cues to *Bagrada hilaris*. *PLoS ONE* **2018**, *13* (12). https://doi.org/10.1371/JOURNAL.PONE.0209870.

(4) Scartazzini, R. Gascardinsaure, Ein Sester-Terpen, ETH, Zurich, 1966.

(5) Boeckman, R. K.; Blum, D. M.; Arnold, E. v.; Clardy, J. The Structure of Gascardic Acid from an X-Ray Diffraction Study. *Tetrahedron Lett* **1979**, *20* (48), 4609–4612. https://doi.org/10.1016/S0040-4039(01)86662-4.

(6) Agerbirk, N.; Olsen, C. E. Glucosinolate Structures in Evolution. *Phytochemistry* **2012**, *77*, 16–45. https://doi.org/10.1016/J.PHYTOCHEM.2012.02.005.

(7) Ludwig, S. W.; Kok, L. T. Harlequin Bug, *Murgantia Histrionica* (Hahn) (Heteroptera: Pentatomidae) Development on Three Crucifers and Feeding Damage on Broccoli. *Crop Prot* **2001**, *20* (3), 247–251. https://doi.org/10.1016/S0261-2194(00)00150-2.

(8) Gershenzon, J.; Dudareva, N. The Function of Terpene Natural Products in the Natural World. *Nat Chem Biol* **2007**, *3* (7), 408–414. https://doi.org/10.1038/NCHEMBIO.2007.5.

(9) Chen, X. Q.; Gao, L. H.; Li, Y. P.; Li, H. M.; Liu, D.; Liao, X. L.; Li, R. T. Highly Oxygenated Grayanane Diterpenoids from Flowers of *Pieris japonica* and Structure-Activity Relationships of Antifeedant Activity against *Pieris brassicae*. *J Agr Food Chem* **2017**, *65* (22), 4456–4463. https://doi.org/10.1021/ACS.JAFC.7B01500.

(10) Hua, J.; Luo, S. H.; Liu, Y.; Liu, Y. C.; Tan, Y. Y.; Feng, L.; Xiao, C. J.; Zhang, K. Q.; Li, S. H.; Niu, X. M. New Bioactive Macrocyclic Diterpenoids from *Euphorbia helioscopia*. *Chem Biodivers* **2017**, *14* (10). https://doi.org/10.1002/CBDV.201700327.

(11) Rhoades, D. F. Evolution of Plant Chemical Defenses against Herbivores. In *Herbivores, Their Interaction with Secondary Plant Metabolites*; Janzen, D. H., Rhoades, D. F., Eds.; Academic Press, Inc.: New York, 1979; pp 3–54.

(12) Bi, Y.; Yu, Z. Diterpenoids from Streptomyces Sp. SN194 and Their Antifungal Activity against *Botrytis cinerea*. *J Agr Food Chem* **2016**, *64* (45), 8525–8529. https://doi.org/10.1021/ACS.JAFC.6B03645.

(13) Koga, J.; Ogawa, N.; Yamauchi, T.; Klkuchi, M.; Ogasawara, N.; Shimura, M. Functional Moiety for the Antifungal Activity of Phytocassane E, a Diterpene Phytoalexin from Rice. *Phytochemistry* **1997**, *44* (2), 249–253. https://doi.org/10.1016/S0031-9422(96)00534-1.

(14) Salah, M. A.; Bedir, E.; Toyang, N. J.; Khan, I. A.; Harries, M. D.; Wedge, D. E. Antifungal Clerodane Diterpenes from *Macaranga monandra* (L) Muell. et Arg. (Euphorbiaceae). *J Agr Food Chem* **2003**, *51* (26), 7607–7610. https://doi.org/10.1021/JF034682W.

(15) Sun, Y. J.; Gao, M. L.; Zhang, Y. L.; Wang, J. M.; Wu, Y.; Wang, Y.; Liu, T. Labdane Diterpenes from the Fruits of *Sinopodophyllum emodi*. *Molecules* **2016**, *21* (4). https://doi.org/10.3390/MOLECULES21040434.

(16) Liu, T.; Meyer, S. L. F.; Chitwood, D. J.; Chauhan, K. R.; Dong, D.; Zhang, T.; Li, J.; Liu, W. C. New Nematotoxic Indoloditerpenoid Produced by *Gymnoascus reessii* Za-130. *J Agr Food Chem* **2017**, *65* (15), 3127–3132. https://doi.org/10.1021/ACS.JAFC.6B04353.

(17) Arif, M. A.; Guarino, S.; Peri, E.; Colazza, S. Evaluation of Brassicaceae Seedlings as Trap Plants for *Bagrada hilaris* Burmeister in Caper Bush Cultivations. *Sustainability 2020, Vol. 12, Page 6361* **2020**, *12* (16), 6361. https://doi.org/10.3390/SU12166361.

(18) Shao, Y.; Molnar, L. F.; Jung, Y.; Kussmann, J.; Ochsenfeld, C.; Brown, S. T.; Gilbert, A. T. B.; Slipchenko, L. v.; Levchenko, S. v.; O'Neill, D. P.; DiStasio, R. A.; Lochan, R. C.; Wang, T.; Beran, G. J. O.; Besley, N. A.; Herbert, J. M.; Yeh Lin, C.; van Voorhis, T.; Hung Chien, S.; Sodt, A.; Steele, R. P.; Rassolov, V. A.; Maslen, P. E.; Korambath, P. P.; Adamson, R. D.; Austin, B.; Baker, J.; Byrd, E. F. C.; Dachsel, H.; Doerksen, R. J.; Dreuw, A.; Dunietz, B. D.; Dutoi, A. D.; Furlani, T. R.; Gwaltney, S. R.; Heyden, A.; Hirata, S.; Hsu, C. P.; Kedziora, G.; Khalliulin, R. Z.; Klunzinger, P.; Lee, A. M.; Lee, M. S.; Liang, W.; Lotan, I.; Nair, N.; Peters, B.; Proynov, E. I.; Pieniazek, P. A.; Min Rhee, Y.; Ritchie, J.; Rosta, E.; David Sherrill, C.; Simmonett, A. C.; Subotnik, J. E.; Lee Woodcock, H.; Zhang, W.; Bell, A. T.; Chakraborty, A. K.; Chipman, D. M.; Keil, F. J.; Warshel, A.; Hehre, W. J.; Schaefer, H. F.; Kong, J.; Krylov, A. I.; Gill, P. M. W.; Head-Gordon, M. Advances in Methods and Algorithms in a Modern Quantum Chemistry Program Package.

Phys Chem Chem Phys **2006**, *8* (27), 3172–3191. https://doi.org/10.1039/B517914A.

(19) Frisch, M. J.; Trucks, G. W.; Schlegel, H. B.; Scuseria, G. E.; Robb, M. A.; Cheeseman J. R.; Scalmani, G.; Barone, V.; Mennucci, B.; Petersson, G. A.; Nakatsuji, H.; Caricato, M.; Li, X.; Hratchian, H. P.; Izmaylov, A. F.; Bloino, J.; Zheng, G.; Sonnenberg, J. L.; Hada, M.; Ehara, M.; Toyota, K.; Fukuda, R.; Hasegawa, J.; Ishida, M.; Nakajima, T.; Honda, Y.; Kitao, O.; Nakai, H.; Vreven, T.; Montgomery, J. A.; Peralta, J. E.; Ogliaro, F.; Bearpark, M.; Heyd, J. J.; Brothers, E.; Kudin, K. N.; Staroverov, V. N.; Kobayashi, R.; Normand, J.; Raghavachari, K.; Rendell, A.; Burant, J. C.; Iyengar, S. S.; Tomasi, J.; Cossi, J. M.; Rega, N.; Millam, J. M.; Klene, M.; Knox, J. E.; Cross, J. B.; Bakken, V.; Adamo, C.; Jaramillo, J.; Gomperts, R.; Stratmann, R. E.; Yazyev, O.; Austin, A. J.; Cammi, R.; Pomelli, C.; Ochterski, J. W.; Martin, R. L.; Morokuma, K.; Zakrzewski, J. B. V. G.; Voth, G. A.; Salvador, P.; Dannenberg, J. J.; Dapprich, S.; Daniels, A. D.; Farkas, O.; Foresman, J. B. J.; Ortiz, V.; Cioslowski, J.; Fox, D. J. Gaussian 09, Revision A.02. Gaussian, Inc.: Wallingford CT 2009.

2.6 Supporting Information

2.6.1 ^{1}H NMR of brassicadiene (CD_2Cl_2, 600 MHz, 292 K)

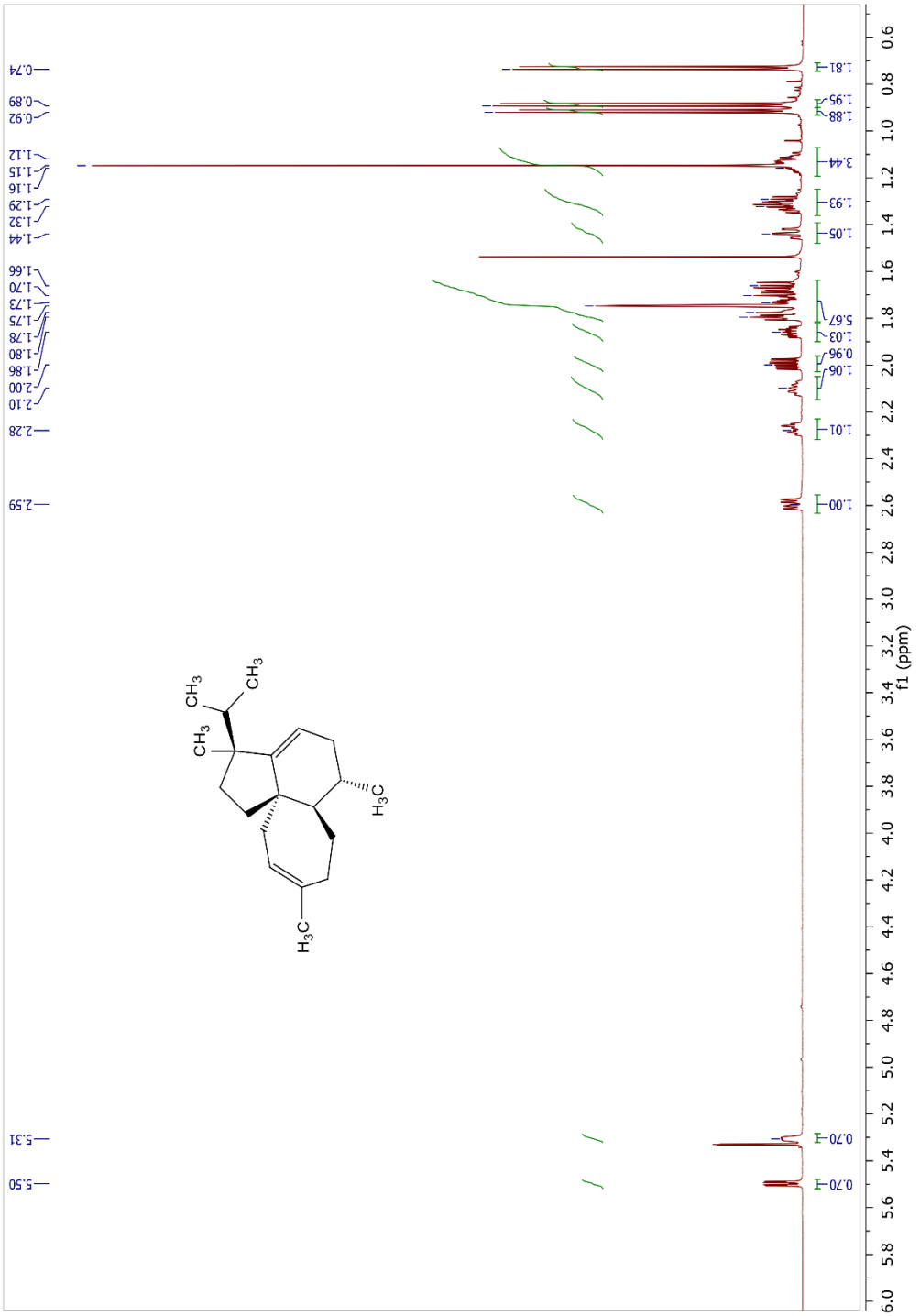

2.6.2 ^{1}H NMR of Brassicadiene (Aliphatic Region, CD_2Cl_2, 600 MHz, 292 K)

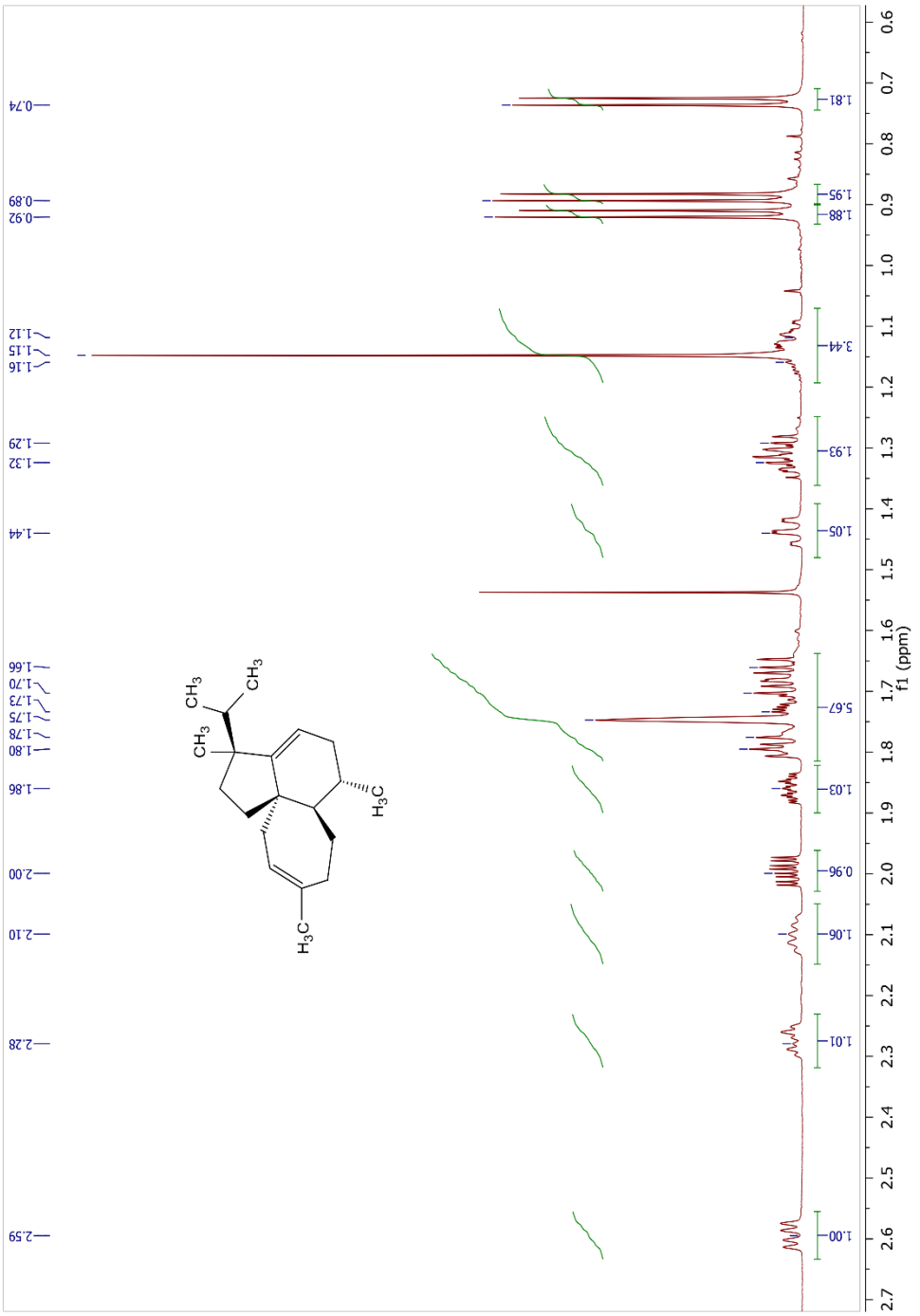

2.6.3 ^{13}C NMR of Brassicadiene (CD_2Cl_2, 176 MHz, 288 K)

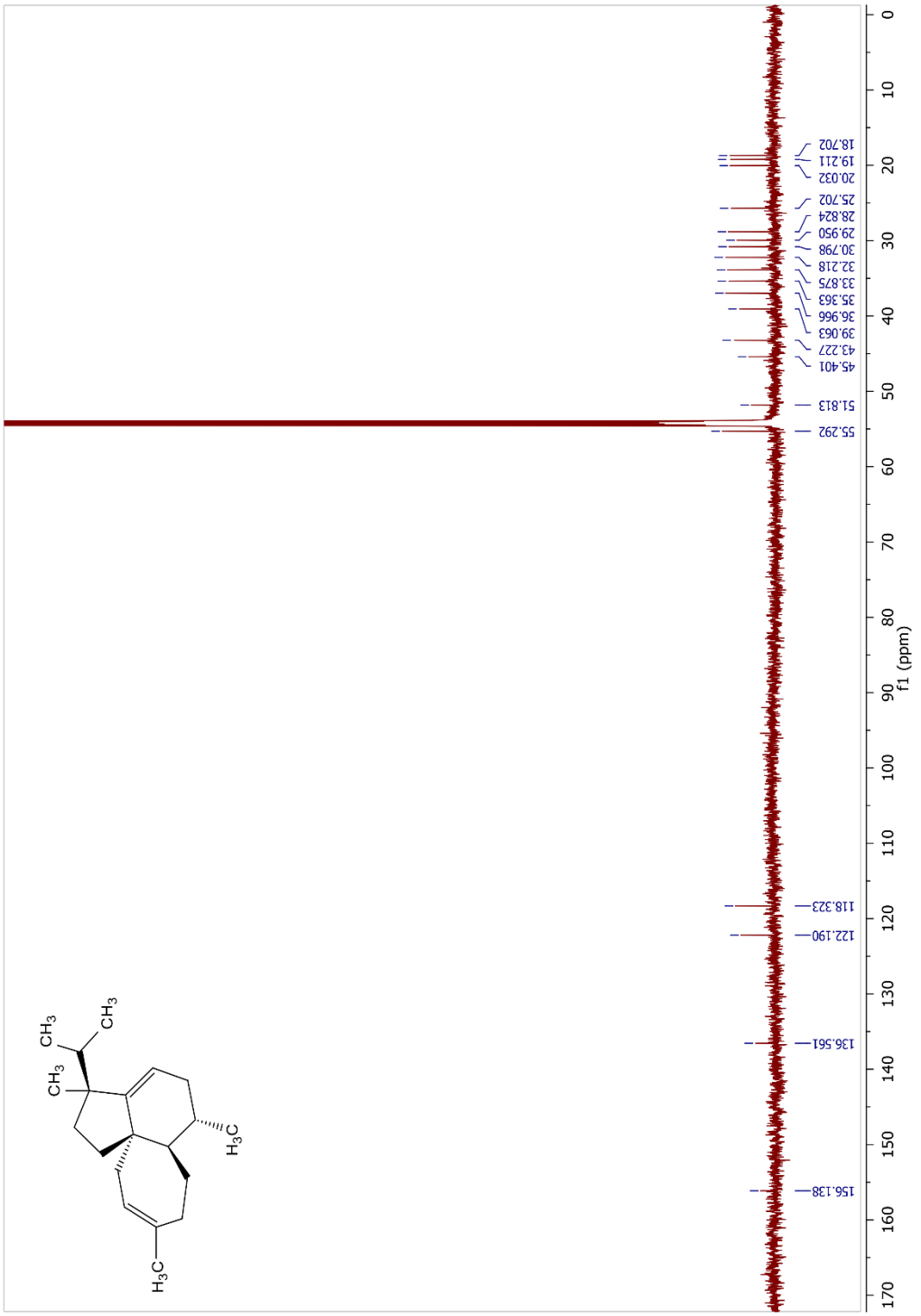

2.6.4 ^{1}H-^{13}C gHSQC NMR of Brassicadiene (CD_2Cl_2; 700, 176 MHz; 288 K)

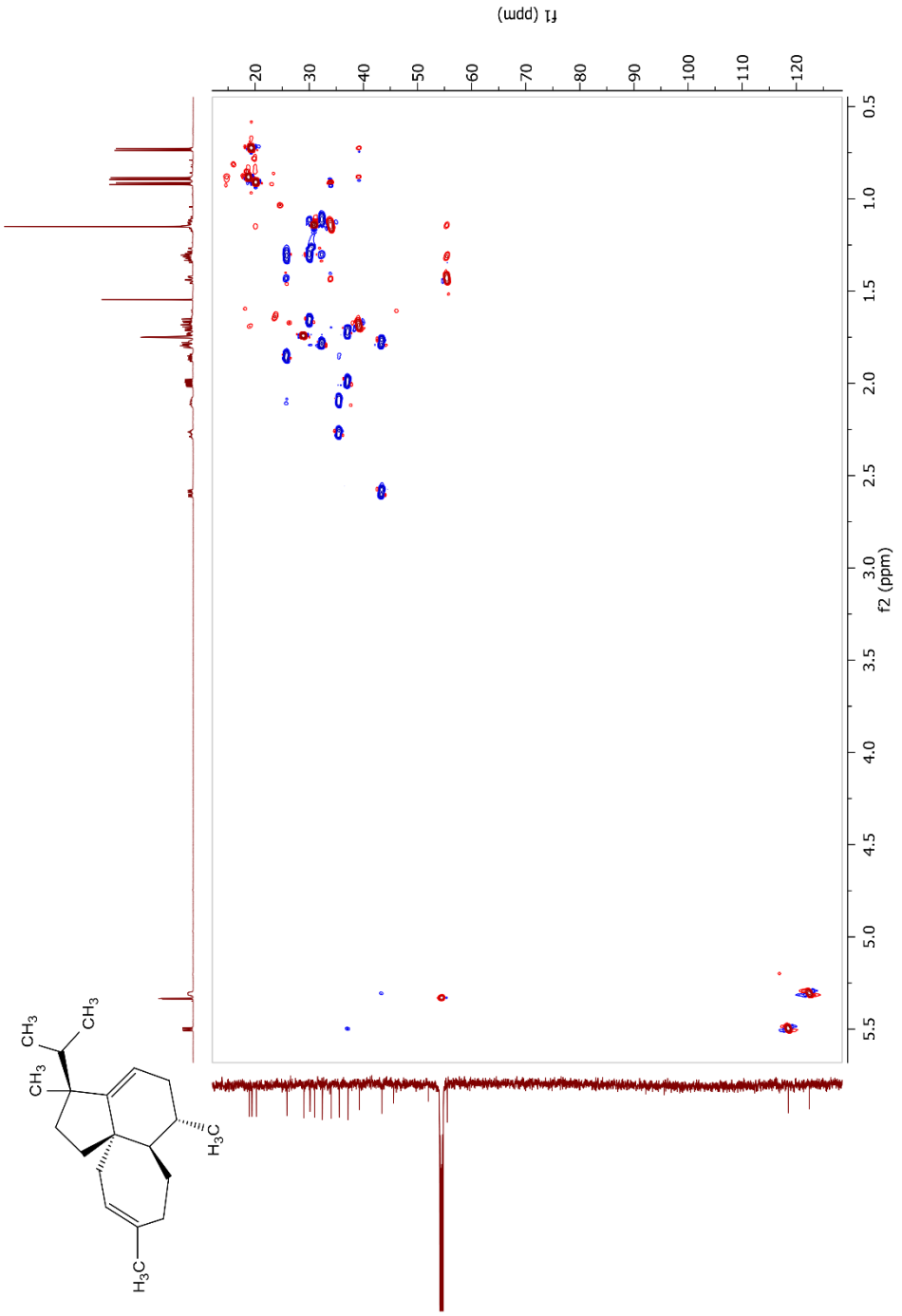

2.6.5 ^{1}H-^{13}C gHSQC NMR of Brassicadiene (Aliphatic Region, (CD_2Cl_2; 700, 176 MHz; 288 K)

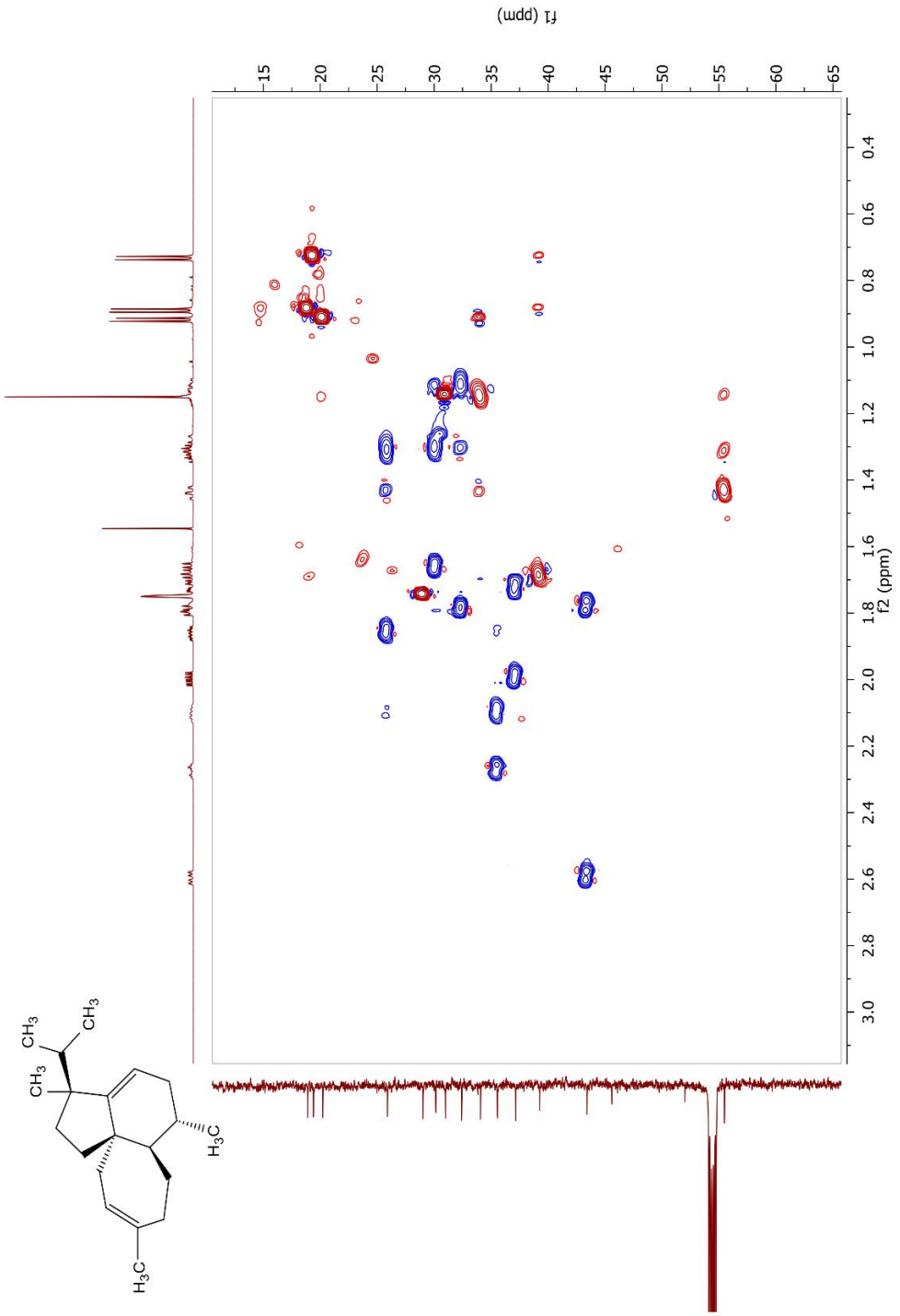

2.6.6 ^{1}H-^{1}H DQFCOSY NMR of Brassicadiene (CD_2Cl_2, 700 MHz, 288 K)

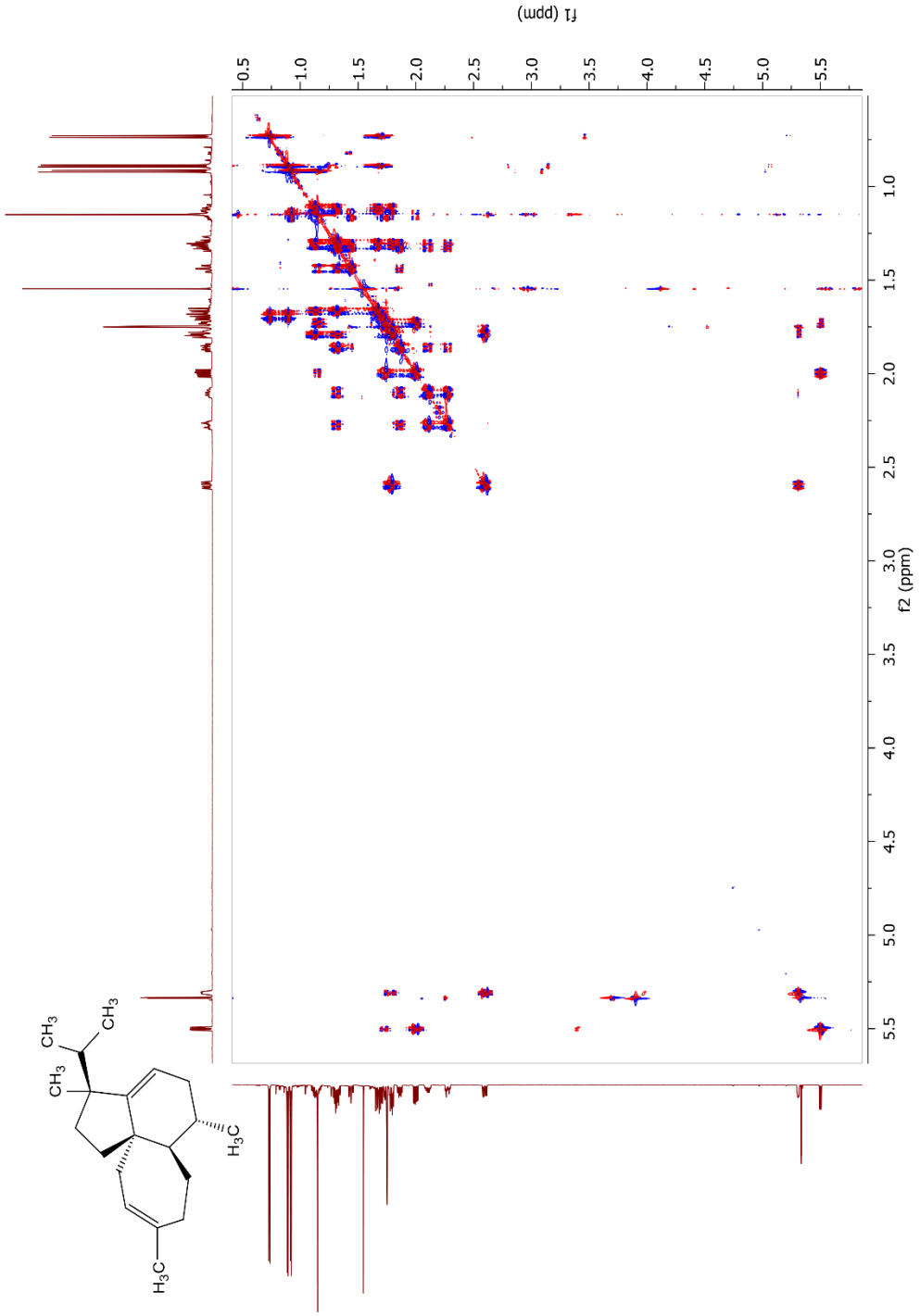

2.6.7 ^{1}H-^{1}H DQFCOSY NMR of Brassicadiene (Aliphatic Region, CD_2Cl_2, 700 MHz, 288 K)

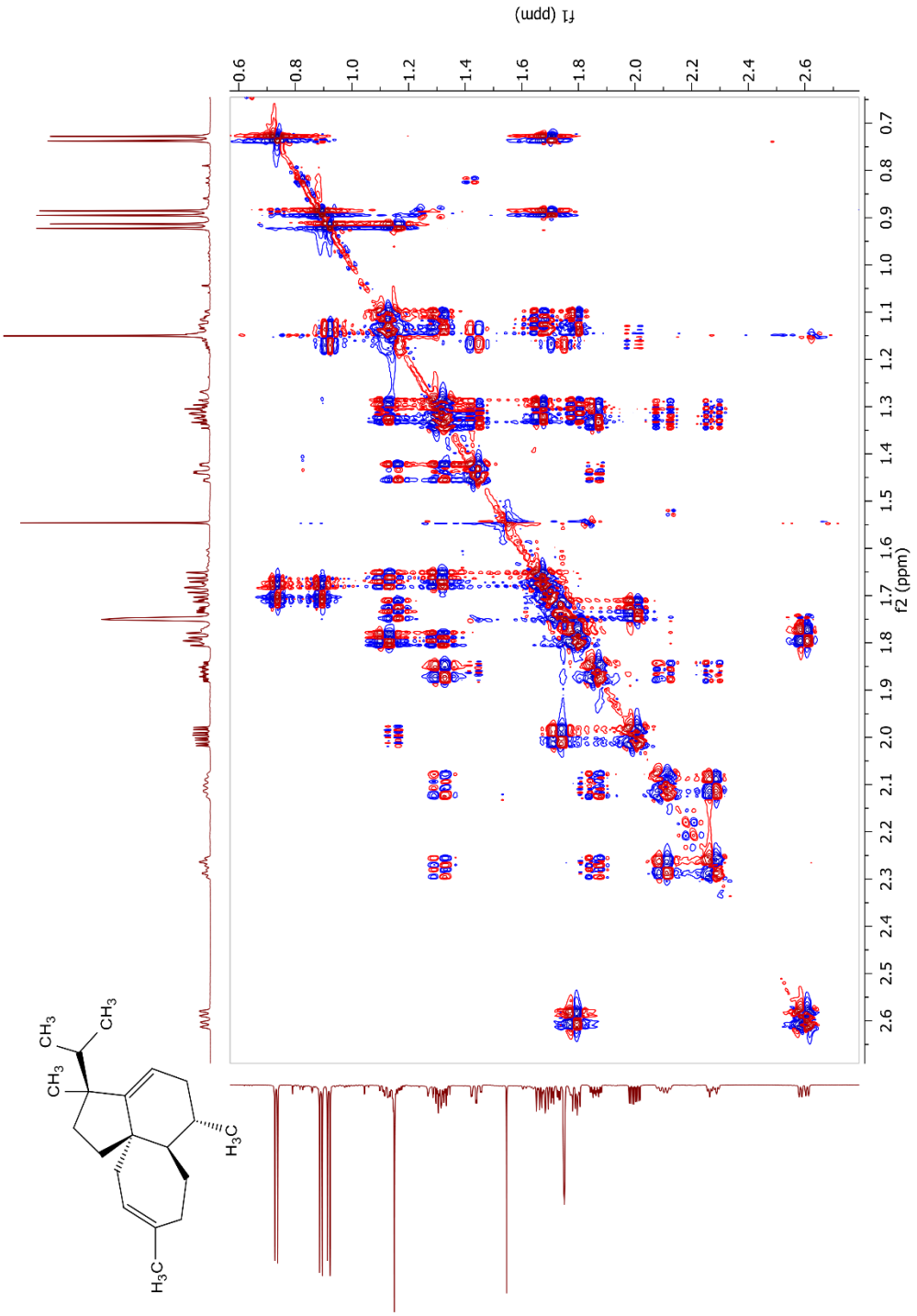

2.6.8 ^{1}H-^{13}C gHMBC NMR of Brassicadiene (CD_2Cl_2; 700, 176 MHz; 288 K)

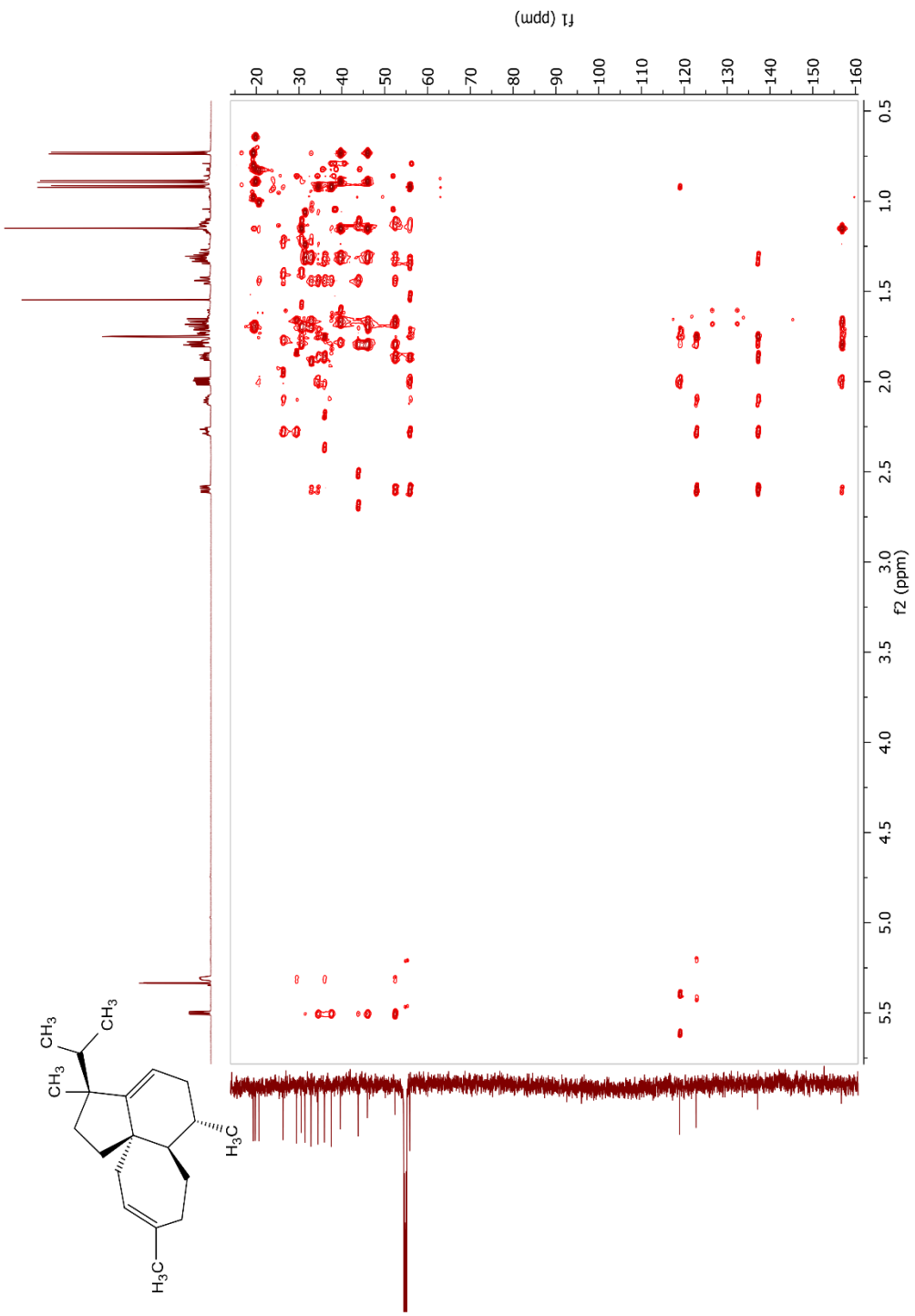

2.6.9 ^{1}H-^{13}C gHMBC NMR of Brassicadiene (Aliphatic Region, CD_2Cl_2; 700, 176 MHz; 288 K)

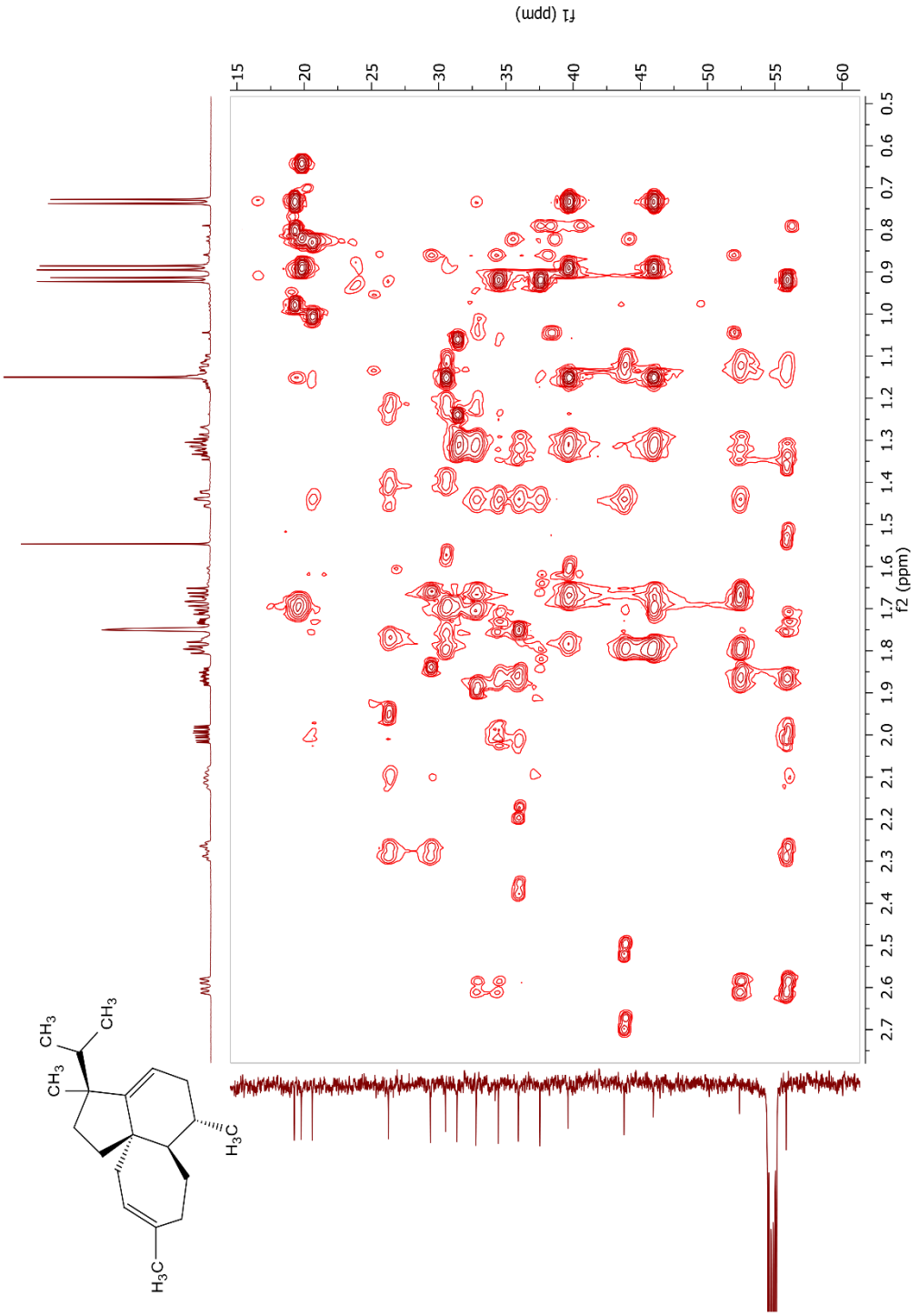

2.6.10 ^{1}H-^{1}H NOESY NMR of Brassicadiene (CD_2Cl_2, 700 MHz, 288 K, mixing time = 0.5 s)

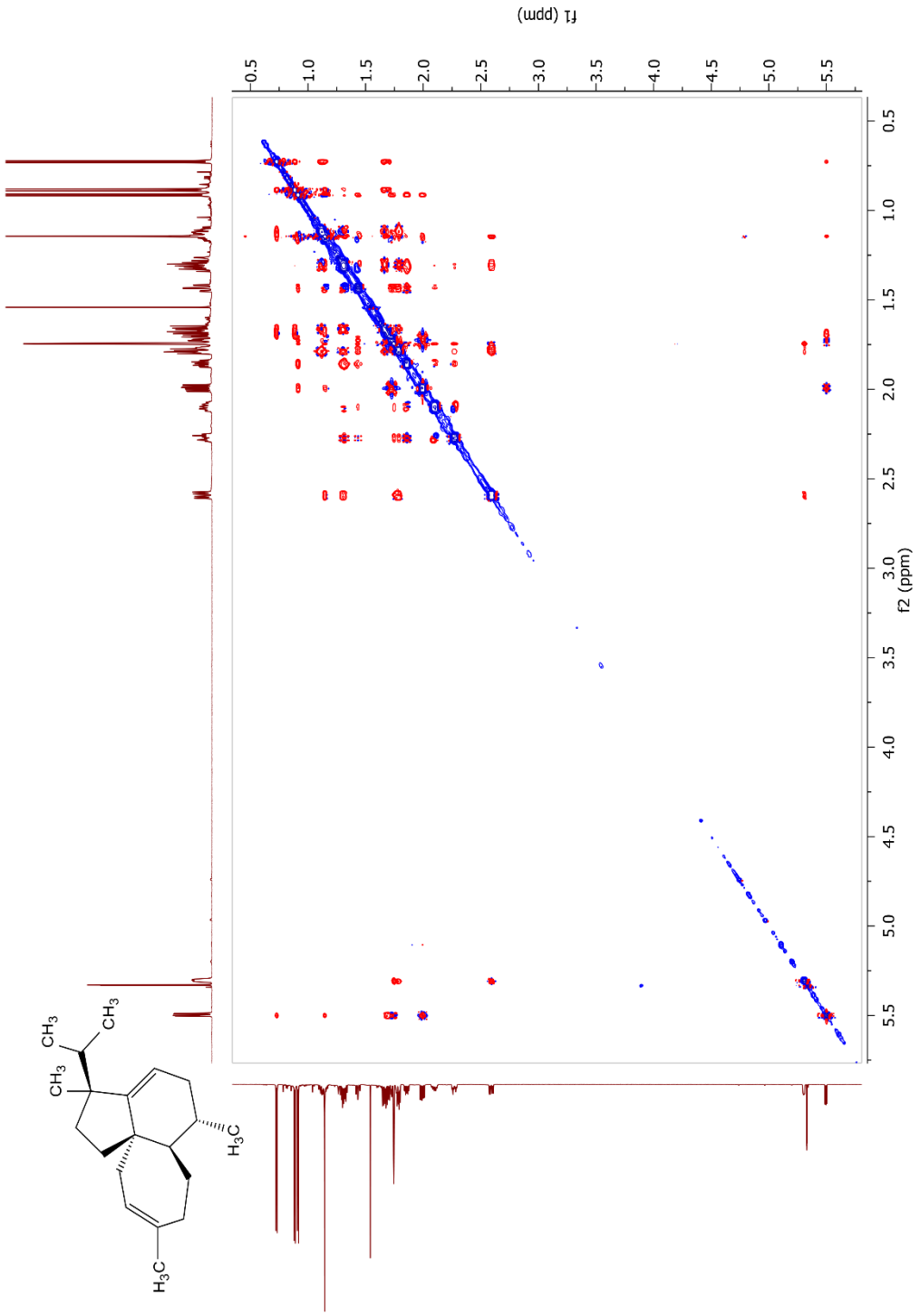

2.6.11 ^{1}H-^{1}H NOESY NMR of Brassicadiene (Aliphatic Region, (CD_2Cl_2, 700 MHz, 288 K, mixing time = 0.5 s)

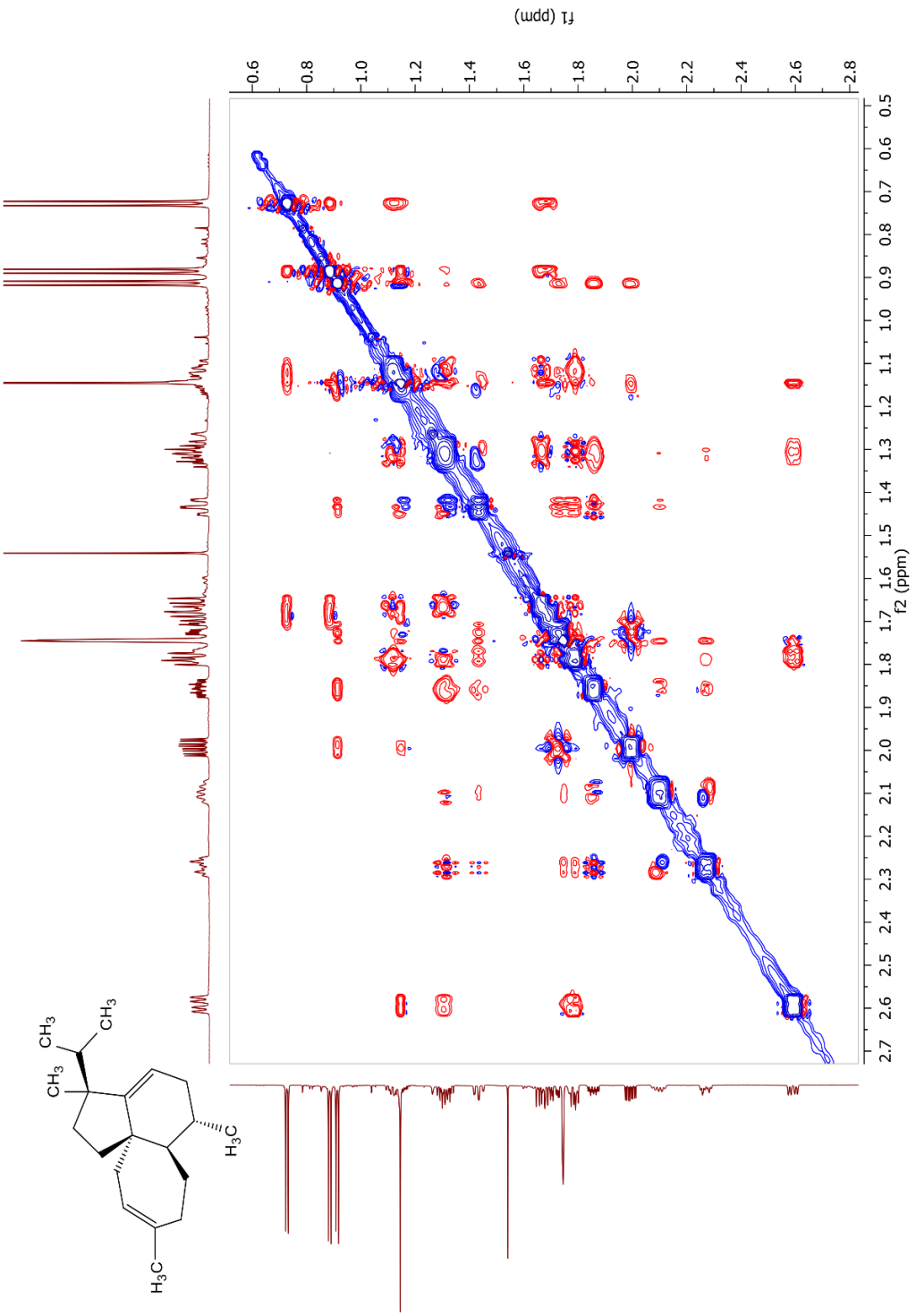

2.6.7 IR spectrum of brassicadiene

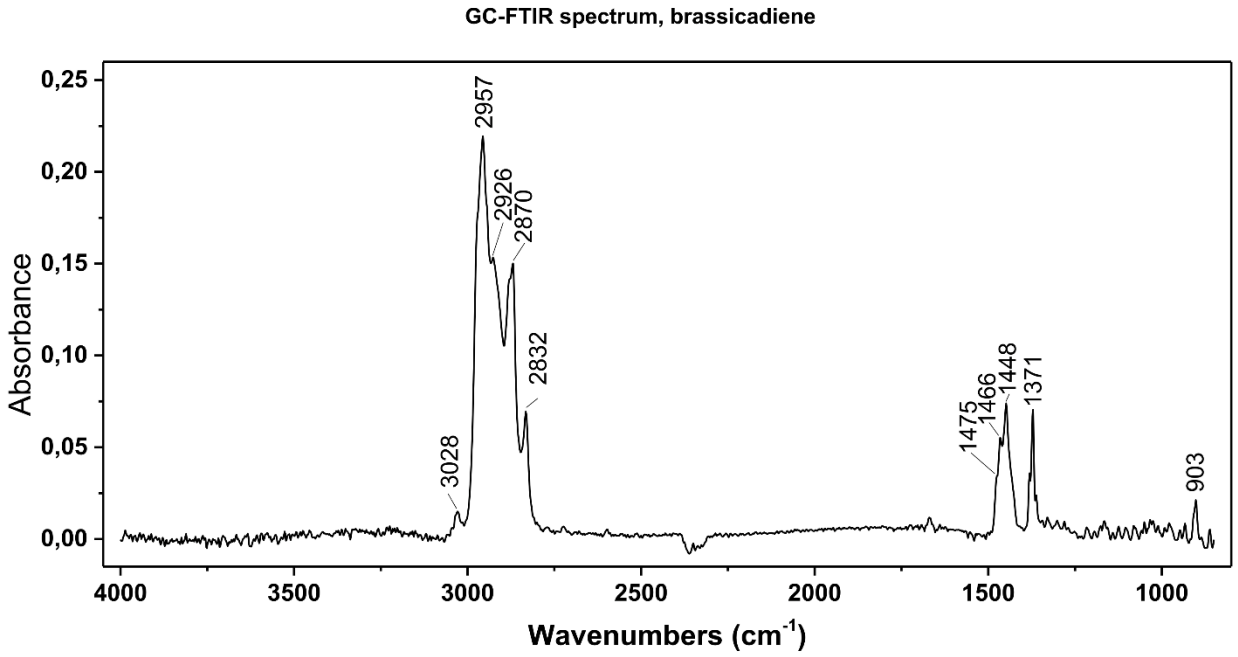

Chapter 3 – Identification and Synthesis of the Sex Attractant Pheromone of the Firefly *Ellychnia corrusca*

ABSTRACT

Fireflies (Coleoptera: Lampyridae) are known for their charismatic and characteristic use of light signaling. However, several genera of the Lampyridae have lost their ability to communicate with light, termed as unlighted fireflies, and there is some indirect evidence that these species have reverted to using chemical communication for mate location and recognition. Here, I describe the first identification of a female-produced sex attractant pheromone for the winter firefly *Ellychnia corrusca* (synonymized with *Photinus corrusca*) as (1*S*,3*S*,4*R*)-3-hydroxy-1,7,7-trimethylbicyclo[2.2.1]heptan-2-one, an isomer of hydroxycamphor. In field trials males were strongly attracted to lures loaded with the synthesized pheromone, verifying the structure and function of the female-produced compound.

3.1 Introduction

Fireflies (Coleoptera: Lampyridae), also known as lightning bugs, are well known for their bioluminescence. Fireflies belong to the superfamily Elateroidea which includes several beetle families capable of bioluminescence. Within this superfamily, bioluminescence has been gained twice and lost once, with glowworm beetles (Phengodidae) regaining bioluminescence after their ancestor had lost it.[1] In the case of Lampyridae, all known firefly larvae emit light, but only some species emit light as adults. Firefly larvae may utilize bioluminescence as an aposematic display to deter predators, whereas in adults, bioluminescence functions primarily as a signal for mate recognition and mate choice. Species that do not emit light as adults are termed "unlighted" fireflies and are diurnally active rather than flying at night.

It has been assumed that unlighted fireflies utilize volatile sex pheromones for long distance attraction based on several observations. First, comparing lighted and unlighted fireflies, unlighted fireflies typically have larger antennae and smaller eyes, presumably as an adaptation to better detect pheromones.[2] Second, caged female unlighted fireflies, vessels which recently contained a female firefly, and recently dead females have been shown to attract males.[3] Third, males situated downwind of unlighted females find them sooner than males situated upwind.[4] In addition, Ohba and coworkers have collected sex-attractant pheromones, confirmed the biological activity of the crude extracts through bioassays,[5] and unsuccessfully attempted to identify the bioactive compound(s) as (*Z*)-9-tricosene and tricosane by coupled gas chromatography-mass spectrometry (GC-MS).[6] In addition, cuticular hydrocarbons of female *Ellychnia corrusca* fireflies have recently been

shown to function as contact pheromones, and mediate mating behavior of conspecific males once they have found females, but these large, nonvolatile compounds play no part in bringing the sexes together from a distance.[7] In the same study, the authors detected a sex-specific compound from female fireflies, tentatively identified as *exo,exo*-2,3-camphanediol, which was suspected to be a volatile attractant, but males were not attracted to the synthetic compound in field tests. Thus, despite there being considerable evidence for female-produced sex attractant pheromones, no pheromones of any type have been unambiguously identified for any member of the Lampyridae. Herein, the identification and synthesis of the female-produced sex attractant pheromone for *Ellychnia corrusca* L. (syn. *Photinus corrusca* L.) are described.

This work forms part of a multidisciplinary study of the evolution of signaling in fireflies, and particularly, the loss of bioluminescence in favor of a return to chemical signaling to bring the sexes together for mating. It appears that this may have happened independently several times within the family, providing an opportunity to examine the repeated, generalizable behavioral and biomolecular changes among lighted and unlighted fireflies, using tools from chemistry, genomics, and neurobiology. One facet of this multidisciplinary study includes identifying volatile pheromones from the lineages which have independently returned to using chemical signals, to assess whether the recovery of pheromone signaling has converged on similar chemistry, or whether the newly evolved pheromones are derived from a variety of biosynthetic pathways. The study reported here represents the first step along that path.

3.2 Results and Discussion

3.2.1 Identification of the Pheromone Candidate

A sex-specific compound was reproducibly observed in extracts of headspace odors collected from live female *Ellychnia corrusca* fireflies. This compound, and no others in the extracts, elicited consistent, strong responses from the antennae of male fireflies by coupled gas chromatography-electroantennogram detection (GC-EAD), suggesting that it was a likely candidate for a sex pheromone component.

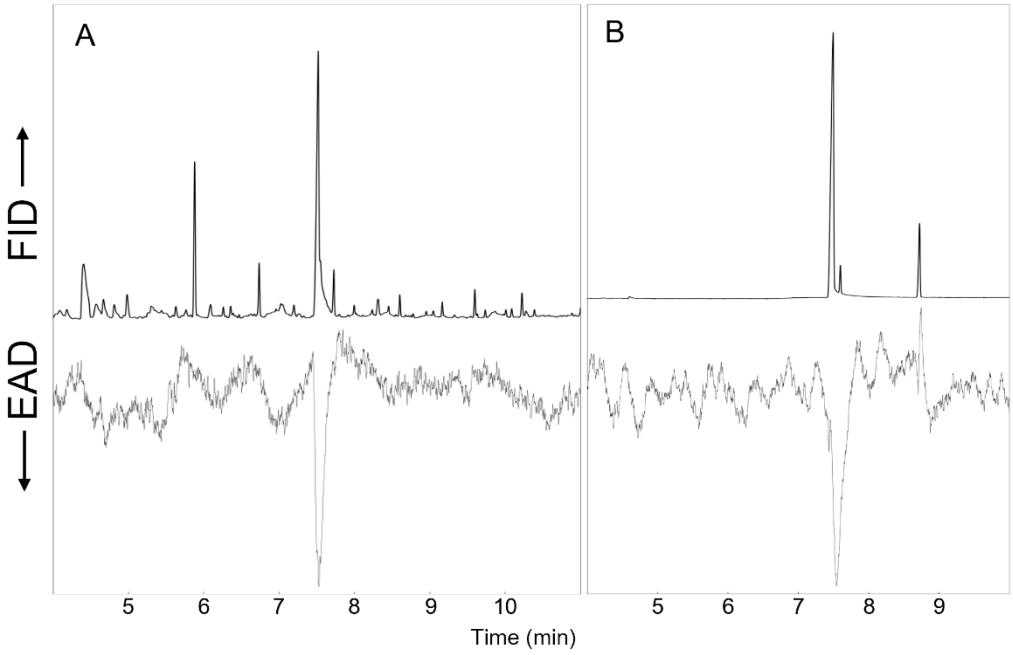

Figure 3.01 *Coupled GC-EAD chromatograms showing: A) the response of an antenna of an E. corrusca male to the extract of the headspace odors collected from live E. corrusca females; and B) the response of an antenna of an E. corrusca male to an isomer from the $LiAlH_4$ reduction of (1S)-camphorquinone.*

When analyzed by EI-GC/MS, the compound had an apparent molecular ion at *m/z* 168 (**Figure 3.02**), for possible molecular formulae of $C_{12}H_{24}$, $C_{11}H_{20}O$, or $C_{10}H_{16}O_2$, with 1, 2, or three rings/sites of unsaturation, respectively.

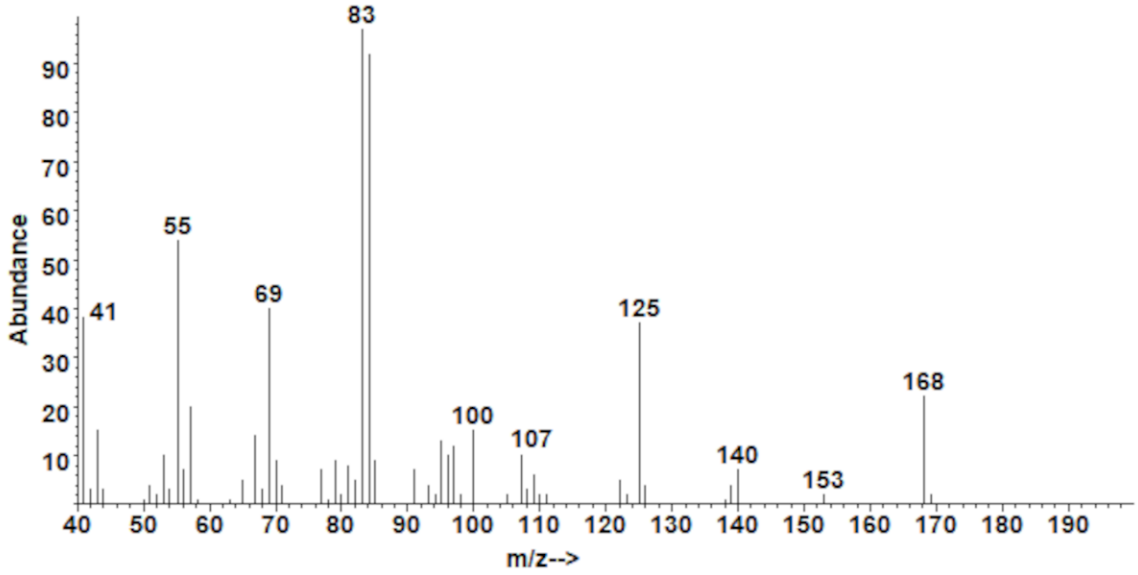

Figure 3.02 *Mass spectrum for the unknown compound produced by Ellychnia corrusca.*

The compound eluted from a silica gel column with 25-100% ether, indicating that it was of medium polarity. This eliminated the possibility of the molecular formula being $C_{12}H_{24}$, i.e., a hydrocarbon with no polar functional groups. Several microderivatization experiments were useful in providing additional information. The unknown was unchanged by catalytic hydrogenation, indicating the absence of carbon-carbon pi bonds. The unknown seemed to be reduced with $LiAlH_4$, such that the unknown peak disappeared from the GC trace, but the product(s) were not found. However, when an aliquot of the insect extract was oxidized with pyridinium dichromate (PDC, **Scheme 3.01)**, the unknown disappeared, and a new peak appeared that was tentatively identified as camphorquinone (*m/z* 166) by a match with the NIST spectral database. The identification was confirmed by matching the retention time and mass spectrum with those of an authentic standard of camphorquinone. The facts that the unknown had a molecular weight that was two mass

units higher than that of camphorquinone, and that PDC oxidation converted the unknown to camphorquinone, suggested that the unknown had to be a hydroxycamphor isomer.

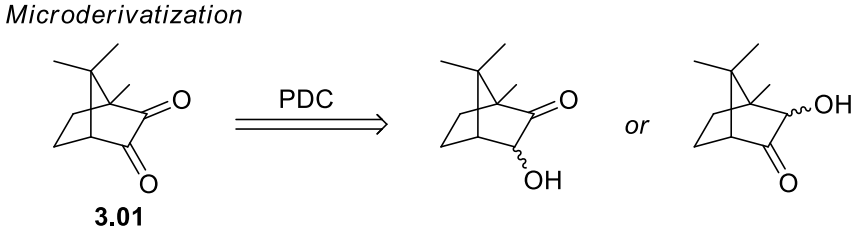

3.01

Scheme 3.01 *Pyridinium dichromate microderivatization of the unknown compound produced by Ellychnia corrusca.*

Thus, in a "quick and dirty" proof of the unknown's structure, partial reduction of (1*S*)-camphorquinone with $LiAlH_4$ yielded a mixture of isomers, one of which matched the retention time of the unknown on achiral and chiral GC stationary phases (DB-5, DB-17, and Cyclodex B), and the mass spectrum of the unknown. Additionally, that isomer elicited a response from the antenna of a male firefly when analyzed by GC-EAD. (**Figure 3.01)**.

In total, the data suggested that the bioactive unknown was an isomer of α-hydroxycamphor, likely with the same stereochemistry at the two stereocenters that it shares with (1*S*)-camphorquinone. The remaining uncertainties were the relative positions of the ketone and hydroxyl groups, and whether the hydroxyl group was on the same face as the geminal dimethyl bridge, or the opposite face, i.e., the four possible isomers shown in **Figure 3.03**. The exact structure, including the confirmation of the absolute stereochemistry, was determined as described below. Ming and Lewis[7] had previously described the presence of *exo,exo*-2,3-camphanediol in whole body extracts of *E. corrusca.* We also detected this compound in trace amounts in two of our extracts, but in much

smaller quantities than the α-hydroxycamphor. Somewhat surprisingly, Ming and Lewis[7] did not report finding an α-hydroxycamphor in their studies.

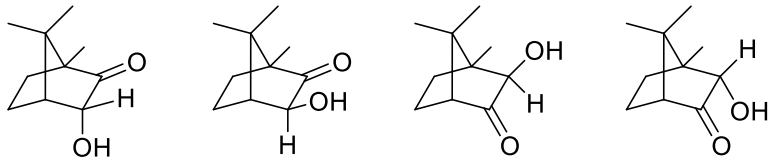

3.02 **3.03** **3.04** **3.05**

Figure 3.03 *Candidate structures for the unknown compound produced by Ellychnia corrusca.*

3.2.2 Methods for the Synthesis and Identification of Each Isomer

We were fortunate to find established methods for the syntheses of the candidate isomers with sufficient spectroscopic information to identify each one by NMR. To determine the placement of the carbonyl and stereochemistry of the hydroxyl group, mixtures of isomers were synthesized and the individual components were isolated and spectroscopically characterized. To confirm the absolute configuration, commercially available sources of each enantiomer of camphor and camphorquinone were used as starting materials to generate products of known absolute configuration. The synthetic standards and the insect-produced compound were then analyzed by GC with chiral and achiral stationary phases because there was not enough of the unknown in the extracts to isolate and obtain NMR spectra. In these GC analyses, a relatively low injector temperature (120 ºC) was used because of the known propensity for a-hydroxyketones to thermally isomerize.[8] Mixtures of isomers were indeed observed to co-elute when high (240 ºC) injector temperatures were used.

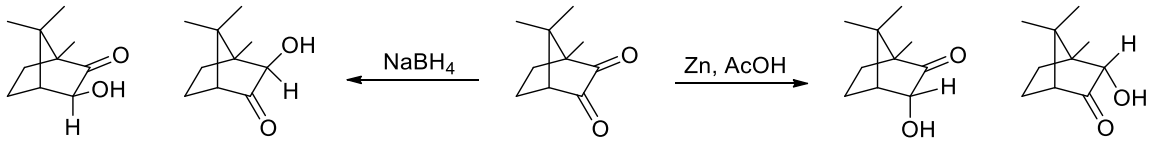

Scheme 3.02 *Access to each candidate isomer from two different reductions of camphorquinone.*

To identify which isomer corresponded with which peak in the chiral GC trace, product ratios from syntheses (in accordance with literature) and NMR of the standards (chemical shift, peak integration) were matched up with the results from analyses of the same samples on a chiral stationary phase Cyclodex B column (retention time, peak integration). Having unambiguously identified each of the synthetic standards, the insect-produced compound was then analyzed under the same conditions, to match it with one of the isomers.

The first candidates synthesized were the *exo*-hydroxycamphor isomers by a reduction of (1*S*)-camphorquinone with $NaBH_4$ (**Scheme 3.02**), producing a 65:35 mixture of **3.03** & **3.04**. This composition is in accord with the literature[9] and allowed for an easy identification of these two regioisomers in the chiral GC chromatogram.

In pursuit of the *endo*-hydroxycamphor isomer **3.02**, a scalemic mixture (33% ee of *R*) of (*R*)- and (*S*)-camphor was oxidized with the Davis reagent[10] (2-(phenylsulfonyl)-3-phenyloxaziridine, **3.06**, **Scheme 3.03**). Two key pieces of information were obtained from this synthesis: (1) the major product formed from the reaction was actually **3.03** (NMR assignment and reaction outcome supported by Piatek et al.[11] and Neisius et al.[12]) and not **3.02** as reported in Davis et al.,[10] and (2) the minor enantiomer of the major product **3.03** (i.e. the oxidized form of (*S*)-camphor, **3.05**, **Scheme 3.03**) co-eluted with the insect

produced compound on the chiral Cyclodex B GC column. Taken together, this indicated that the insect-produced compound was likely to be structure **3.03** (see below).

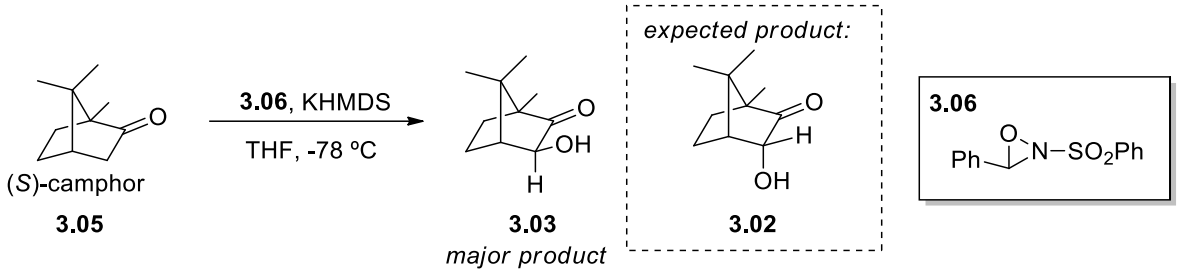

Scheme 3.03 *Davis oxidation of camphor produced exo-hydroxycamphor **3.03** as the major product and the endo-hydroxycamphor as the minor product.*

With the two *endo*-hydroxycamphor candidates remaining to be synthesized, a Zn dust/AcOH reduction of (1*S*)-camphorquinone was performed (**Scheme 3.02**). This straightforward reaction produced a 56:44 mixture of isomers **3.02** and **3.05**. Even though the identification of which isomer was which in the chiral GC chromatogram would be difficult because the product mixture was composed of similar proportions of the two isomers, the two isomers coincidentally co-eluted *and* eluted at a different time relative to the insect-produced compound, eliminating them as possibilities.

The product selectivity obtained in these reductions might arise as follows. With $NaBH_4$, the reductant preferentially approaches and reduces camphorquinone from the most accessible face akin to reductions of cyclohexanones,[13] yielding the *exo*-isomers. Thus, the selectivity is governed primarily by the steric interference posed by the geminal dimethyl bridge, and secondarily by the methyl bridgehead substituent. In contrast, with Zn/AcOH reduction, the reduction may occur by single electron transfer events and protonations[14] (**Scheme 3.04**). Determination of the diastereomeric outcome may occur upon reduction and protonation of the radical intermediate **3.07,** or the products might

tautomerize during the reaction forming enediol **3.08** which, upon workup, equilibrates to the observed mixture of isomers.

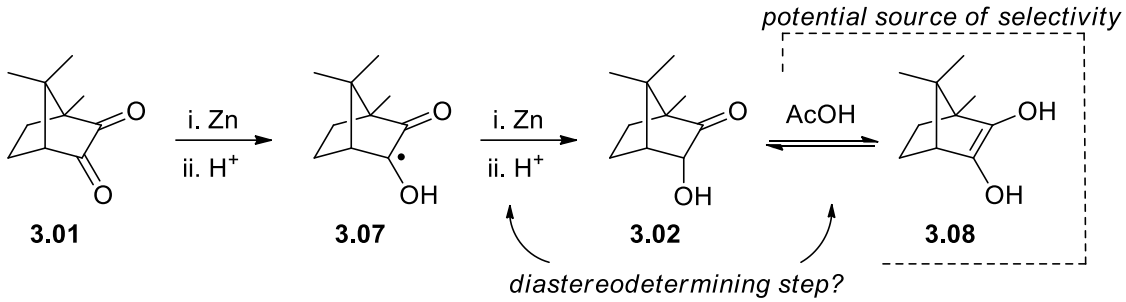

Scheme 3.04 *Proposed mechanism for a representative Zn/AcOH reduction of camphorquinone regarding the origins of stereoselectivity.*

3.2.3 Comparison of Synthetic Hydroxyketones to the Insect-Produced Compound

The chromatograms in **Figure 3.04** illustrate the sequence of injections and co-injections used to identify the gross structure and absolute stereochemistry of the insect-produced compound, and the correct product from the Davis oxidation.

Thus, **Figure 3.04A** shows the single peak in the insect extract. **Figure 3.04B** shows the two *exo*-hydroxycamphor isomers obtained by $NaBH_4$ reduction of (1*S*)-camphorquinone, one of which matched the unknown. In **Figure 3.04C**, the two *exo*-enantiomers from Davis oxidation of the 2:1 mixture of (*R*)- and (*S*)-camphor enantiomers, are well separated, with the minor enantiomer matching the unknown and again confirming that the shared stereocenters in the unknown are the same as those in (*S*)-camphor. **Figures 3.04D** and **3.04E** illustrate injection of the mixture of products shown in panels B and C, and that mixture spiked with the insect extract to show the exact match with the isomer **3.03**. Finally, in **Figure 3.04G** the mixture of *endo* isomers **3.02** and **3.05** eluted as a single peak when injected alone, and when injected with the *exo*-isomers (**Figure 3.04F**) showed

three peaks, verifying that the unknown could not be one of the *endo* isomers. This allowed us to unambiguously identify the unknown as **3.03**, (1*S*,3*S*,4*R*)-3-hydroxy-1,7,7-trimethylbicyclo[2.2.1]heptan-2-one.

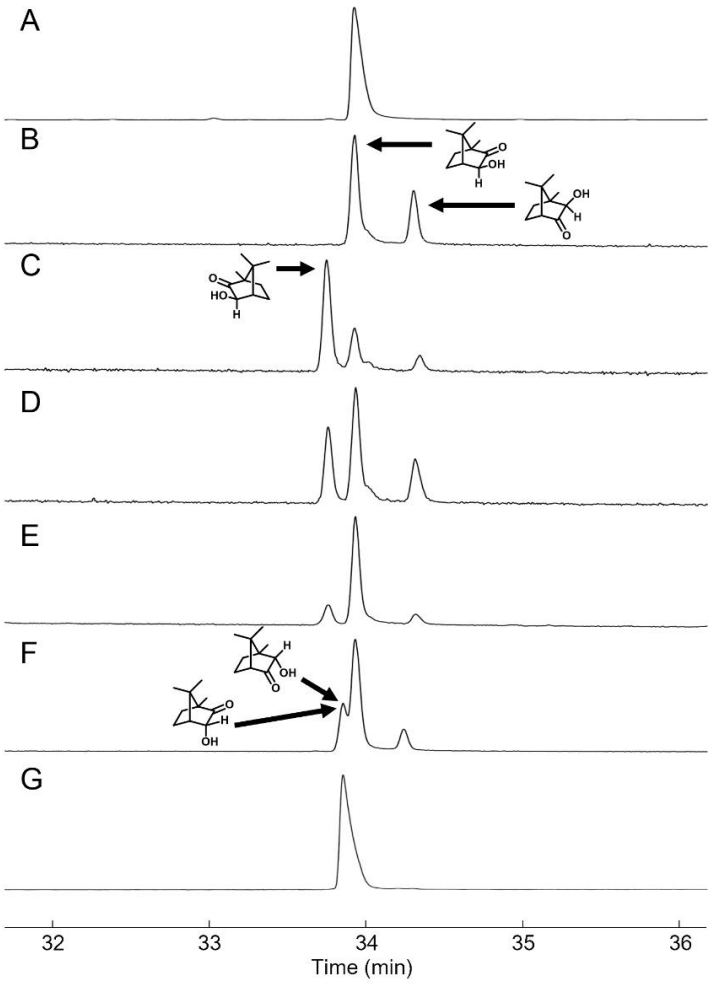

Figure 3.04 *Chiral GC chromatograms depicting the elucidation of the firefly pheromone: A) insect-produced compound; B) $NaBH_4$ reduction affording exo-isomers; C) Davis oxidation of a 2:1 mixture of (1R)- and (1S)-camphor, showing that the enantiomers of the insect produced compound resolve under these conditions; D) co-injection of products from the Davis oxidation with those of $NaBH_4$ reduction; E) co-injection of the sample to produce chromatogram D and the insect-produced compound; F) co-injection of exo-isomers with the co-eluting endo-isomers; G) co-eluting endo-isomers.*

3.2.4 Larger Scale Synthesis of Candidate Firefly Pheromone for Field Trials

A larger scale, stereoselective synthesis of compound **3.03** was effected by reduction of (1*S*)-camphorquinone with *L*-selectride. Unlike syntheses reported in the literature that claimed a completely stereoselective transformation,[9,15,16] an 88:12 mixture of diastereomers (**3.03**:**3.04**, 45% yield, inclusive) was obtained after chromatography. Although literature reports claimed that the isomers are inseparable by column chromatography,[9,17] careful flash chromatography on silica gel (20% EtOAc/Hexanes) provided **3.03** in up to 95% isomeric purity (across multiple experiments), with the remainder being the *endo* isomer **3.04**. Finally, the crystalline material was sublimed and collected with a Kugelrohr distillation apparatus at no detriment to isomeric purity.

3.2.5 Confirmation of Biological Activity

As described above, GC-EAD analysis of a sample of mixed isomers that contained compound **3.03** had shown that antennae of male fireflies responded strongly to the synthetic compound, suggesting that it was indeed the female-produced sex attractant pheromone. This was verified in replicated field trials in Pennsylvania, where large numbers of males (mean 16.8 ± 5.89) were caught in sticky traps (n=5) baited with an 11 mm rubber septum impregnated with 1 mg of synthetic **3.03**, versus zero males caught in any of the unbaited control traps (n=5, Mann-Whitney Wilcoxon test: $p = 0.0037$). Thus, to my knowledge, the work reported here represents the first identification of a long-range sex attractant pheromone for any species in the insect family Lampyridae. It also represents the first crucial step in a much larger project studying the evolution of how signaling with volatile pheromones has been regained in fireflies, rather than the more widely known signaling with bioluminescence.

3.3 Methods

All solvents were Optima grade (Fisher Scientific, Pittsburgh PA, USA) unless otherwise noted. Anhydrous diethyl ether stabilized with BHT was purchased from Fisher Scientific. Vacuum flash chromatography and flash column chromatography were carried out on silica gel (230–400 mesh; Fisher Scientific). TLC analyses were conducted on aluminum-backed sheets of analytical silica gel 60 F_{254} (Merck, Darmstadt, Germany), and compounds were visualized by spraying with 10% phosphomolybdic acid in ethanol and heating. Yields are reported as isolated yields of chromatographically pure products unless otherwise noted. Mass spectra were obtained with an HP 6890 GC (Hewlett-Packard, now Agilent, Santa Clara CA, USA) equipped with a DB-17 column (30 m × 0.25 mm × 0.25 μ film; J&W Scientific, Folsom CA, USA) coupled to an HP 5973 mass selective detector, in EI mode (70 eV) with helium carrier gas. Purity was assessed by gas chromatography (unless otherwise noted) with an HP 5890 GC equipped with a DB-5 column (30 m × 0.25 mm × 0.25 μm film). Isomeric and enantiomeric purity was assessed by gas chromatography with an HP 5890 GC equipped with a chiral stationary phase β-cyclodextrin column (Cyclodex-B, 30 m × 0.25 mm × 0.25 μm film + 2 m × 0.25 mm ID deactivated fused silica; J&W Scientific). NMR spectra were recorded as $CDCl_3$ solutions on either a Bruker Avance 500 or Bruker NEO 400 spectrometer. Chemical shifts are reported in ppm relative to $CDCl_3$ (^1H 7.26 ppm; ^{13}C 77.0 ppm).

3.3.1 Acquisition of Insect-Produced Compound

Male and female fireflies were shipped to UC Riverside by overnight courier service (USDA-APHIS-PPQ permit # P526P-20-02507) and housed in the UCR quarantine facility. Collections of headspace volatiles were conducted using wide-mouth 250 mL Teflon jars (Thermo Scientific, Fisher Scientific; #24030250), with the screw cap lids fitted with Swagelok bulkhead unions (Swagelok, Solon OH, USA) to connect inlet and outlet tubes. Air, purified by passage through granulated activated charcoal (14-16 mesh; Fisher Scientific), was pulled through the system by vacuum at 250 mL/min. Volatiles were adsorbed onto ~50 mg of thermally-desorbed activated charcoal (50-200 mesh; Fisher Scientific) held between glass wool plugs in a short piece of glass tubing. Aerations were conducted under ReptiSun 100 UVB lights (Zoo Med Laboratories Inc., San Luis Obispo CA, USA) with a 16:8 h L:D cycle. Volatiles were eluted from the charcoal with 500 µL of dichloromethane. All fireflies were aerated individually, and given two vials with wicks containing either water or 10% honey solution. Earlier aerations of fireflies were run over 3-5 days and then increased up to 8 days for later aerations. Individuals were aerated repeatedly until death, from May 13 – June 14, 2021. A total of seven females and four males were aerated, yielding 24 extracts of females and 5 of males. Aeration extracts were initially analyzed in splitless mode with an Agilent 7820A GC interfaced to an Agilent 5977E mass selective detector (Agilent Technologies,). A DB-5 column was used (30 m x 0.25 mm ID, J&W Scientific), with a temperature program of 40 °C/1 min, 10 °C /min to 280 °C, hold for 10 min. The injector and transfer line temperatures were 250 °C and

280 °C respectively. Mass spectra were taken in electron impact ionization mode (EI) at 70 eV, with a scan range of 30-500 amu.

Aeration extracts and synthetic standards were analyzed by GC-EAD with an HP 5890 Series II GC equipped with a DB-5MS Column (30m + 10m retention gap x 0.25mm ID x 0.25 micron film; Agilent Technologies). The injector and detector temperatures were 250 °C and 280 °C, respectively, with a column head pressure of 200kPa. The temperature program was 50 °C for 1 min, 20 °C/min to 280 °C, then held for 10 min.

Five aeration extracts from females in CH_2Cl_2 (~2.5 mL) were combined and concentrated to ~0.1 mL under a gentle stream of nitrogen, and 0.5 mL pentane was added. The sample was blown down again, and the procedure was repeated to remove as much of the CH_2Cl_2 as possible. The concentrated sample in ~0.1 mL pentane was then loaded onto a column of silica gel (230-400 mesh, 100 mg), prewetted with pentane. The column was eluted sequentially with 1 mL pentane, 2 x 0.5 mL 25% ether in pentane, and 2 x 1 mL ether, collecting each as a separate fraction. The compound of interest with apparent *m/z* 168 started eluting in the 2nd 25% ether fraction (Frac. 4), with the bulk eluting in the first 100% ether fraction.

An aliquot of the latter was diluted 1:1 with pentane, ~ 1 mg of 10% Pd on carbon was added, and the mixture was stirred under H_2 for 1 h. The mixture was then filtered through a small pad of celite, rinsing with ether, concentrated to ~100 ul, and an aliquot was analyzed by GC-MS. Approximately half of the remaining sample was diluted with 0.5 mL ether, and ~ 2 mg $LiAlH_4$ was added. The mixture was stirred 1 h at room temp, then quenched by careful addition of 0.1 mL aqueous 1 M HCl, followed by 0.5 mL

saturated brine. The mixture was vortexed, and the ether layer was removed and dried over anhydrous Na_2SO_4, and an aliquot was analyzed by GC-MS.

A second aliquot of fraction 4 was concentrated to ~ 10 microliters, then diluted with 0.1 mL CH_2Cl_2, ~2 mg finely powdered pyridinium dichromate was added, and the mixture was stirred for 1 h at room temp. The mixture was then diluted with 0.5 mL ether, and filtered through a plug of celite. An aliquot was analyzed by GC-MS.

3.3.2 Partial reduction of camphorquinone

$LiAlH_4$ (7.5 mg, 0.2 mmol) was added to a solution of (*S*)-(-)-camphorquinone (166 mg, 1 mmol, TCI Americas, Portland OR, USA) in 2.5 mL dry ether. The mixture was stirred 1 h at room temp, then quenched with 1 mL of 1M HCl. The mixture was then diluted with 10 mL brine and extracted with ether. The ether solution was dried and concentrated, and the residue was fractionated by flash chromatography on silica gel, eluting with 25% EtOAc in hexane, achieving a partial separation of the isomers. The fractions were checked by GC on a DB-5 column, matching the retention time of one hydroxycamphor isomer with that of the insect-produced compound. An aliquot was then reanalyzed by GC-MS on a DB-17 column, matching both the retention time and the mass spectrum of one of the isomers with those of the insect-produced compound.

3.3.3 Reduction of camphorquinone with $NaBH_4$

The following procedure was adapted from Xu P. et al.[9] Identities of each product isomer were verified by published ^{1}H-NMR spectral data.[12,15]

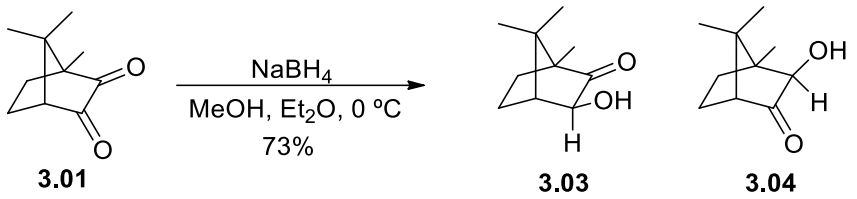

3.01 **3.03** **3.04**

A dry flask flushed with Ar was charged with (1*S*)-camphorquinone (83.1 mg, 0.5 mmol; TCI Americas, Portland OR, USA), diethyl ether (0.5 mL), and methanol (0.5 mL). The flask was cooled to 0 ºC followed by the addition of $NaBH_4$ (5 mg, 0.132 mmol) in one portion. The reaction was stirred at 0 ºC for 30 min, then quenched with water (167 µL) and diluted with brine (300 µL). The mixture was extracted with diethyl ether (3x1 mL), and the organic phases were combined, washed with brine, dried over anhydrous Na_2SO_4, and concentrated under reduced pressure to yield a crude white solid composed of a 65:35 mixture of isomers. This crude material was purified by vacuum flash column chromatography (20% EtOAc/Hex) to yield 59 mg (73%) of a 65:35 mixture of isomers (**3.03**:**3.04**). **3.03** ^{1}H NMR (500 MHz, $CDCl_3$): δ 3.73 (s, 1H), 3.23 (bs, 1H), 2.07 (d, *J* = 4.9 Hz, 1H), 1.97 (dddd, *J* = 12.4, 4.8 Hz, 1H), 1.63 (ddd, *J* = 12.4, 3.7, 1H), 1.47-1.30 (m, 2H), 0.96 (s, 3H), 0.92 (s, 3H), 0.90 (s, 3H). ^{13}C NMR (126 MHz, $CDCl_3$) δ 220.52, 77.26, 57.02, 49.22, 46.72, 28.52, 25.11, 20.95, 20.00, 8.96. **3.04** ^{1}H NMR (500 MHz, $CDCl_3$): δ 3.53 (s, 1H), 3.23 (bs, 1H), 2.14 (d, 1H), 1.89 (m, 1H), 1.82 (m, 1H), 1.47-1.30 (m, 2H), 1.01 (s, 3H), 1.00 (s, 3H), 0.90 (s, 3H). ^{13}C NMR (126 MHz, $CDCl_3$) δ 219.27, 79.35, 58.58, 49.15, 46.51, 33.77, 21.12, 20.28, 18.78, 10.25. **3.03** & **3.04** EI-GC/MS *m/z* (%): 168 (M^+, 36), 153 (6), 140 (9), 125 (41), 107 (11), 100 (13), 84 (92), 83 (100), 71 (22), 70 (33), 69 (42), 57 (20), 55 (53), 43 (22), 41 (46).

3.3.4 Reduction of camphorquinone with Zn and AcOH

The following procedure was adapted from Huckel and Fechtig[18,19] with additional insights from Templeton et al.[19] Identities of each product isomer were verified by comparison with published ^{1}H-NMR spectral data.[17]

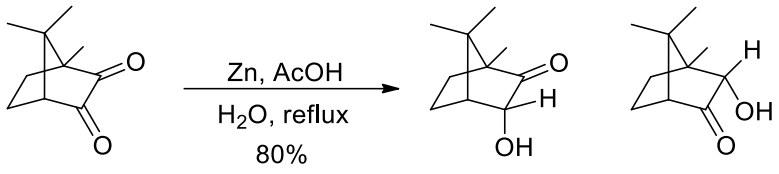

3.01 **3.02** **3.05**

A flask was charged with acetic acid (200 µL, 3.50 mmol, 5.8 eq) and heated to reflux. (1*S*)-camphorquinone (100 mg, 0.602 mmol, 1 eq; TCI Americas, Portland OR, USA) and water (1.8 mL) were added, the heterogenous yellow mixture was briefly stirred, then zinc dust (100 mg, 1.53 mmol, 1.5 eq) was added in portions over 1 min to the reaction. The reaction was stirred for 20 min at 115 ºC, becoming colorless. The reaction was allowed to cool, then diluted with water (2 mL) and extracted with diethyl ether (2.5 mL). The aqueous layer was extracted with additional diethyl ether (2.5 mL), and the combined organic layer was sequentially washed with sat. aq. $NaHCO_3$ (1 mL) and brine (1 mL) before drying over anhydrous Na_2SO_4 and concentration under vacuum. The crude material was purified by vacuum flash chromatography (20% EtOAc/Hex) to yield 81 mg (80%) of a 56:44 mixture of the two endo isomers **3.02** and **3.05**). **3.02** ^{1}H NMR (500 MHz, $CDCl_3$): δ 4.20 (d, 1H), 3.35 (bs, 1H), 2.26 (t, J = 4.0 Hz, 1H), 1.93 (m, 1H), 1.70 (m, 1H), 1.67 (m, 1H), 1.38 (m, 1H), 0.98 (s, 3H), 0.90 (s, 3H), 0.85 (s, 3H). **3.05** ^{1}H NMR (500 MHz, $CDCl_3$): δ 3.84 (s, 1H), 3.35 (bs, 1H), 2.24 (dd, J = 5.4, 1H), 1.96 (m, 2H), 1.38 (m, 2H), 1.03 (s, 3H), 0.95 (s, 3H), 0.90 (s, 3H). **3.02** & **3.05** ^{13}C NMR (126 MHz, $CDCl_3$) δ 220.95,

219.53, 78.73, 74.40, 59.40, 58.41, 50.22, 48.58, 43.08, 43.01, 32.48, 24.99, 24.62, 19.94, 19.32, 18.76, 17.84, 12.91, 9.26. EI-GC/MS *m/z* (%): 168 (M^+, 68), 153 (14), 139 (11), 135 (7), 125 (32), 109 (14), 107 (11), 95 (29), 84 (75), 83 (89), 71 (63), 70 (100), 69 (52), 55 (50), 44 (40), 43 (67).

3.3.5 Reduction of camphorquinone with L-Selectride

The following procedure was adapted from Kouklovsky et al.[16]

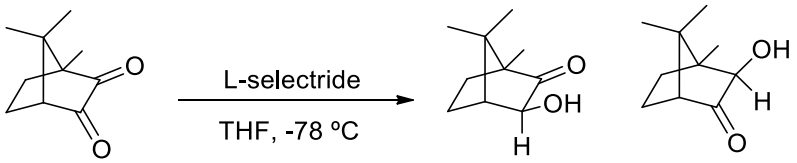

3.01 **3.03** **3.04**

A dry flask flushed with Ar was charged with (1*S*)-camphorquinone (5.83 g, 35.08 mmol, 1 eq; TCI Americas, Portland OR, USA) and dry THF (200 mL), then cooled to -78 ºC. L-Selectride (1 M in THF, 42 mmol, 1.20 eq; MilliporeSigma, St. Louis, Missouri, USA) was added over one hour at this temperature, and the mixture was stirred an additional 5 min. The reaction was quenched by addition of 3 M HCl in methanol (16 mL) over ten min at -78 ºC, then allowed to warm to room temperature. The resulting mixture was diluted with brine (500 mL) and the contents were extracted with dichloromethane (4 x 200 mL). The combined organic layer was dried over anhydrous Na_2SO_4, concentrated under vacuum, then purified by vacuum flash chromatography (5% - 25% EtOAc/Hexanes). The fractions rich in the desired product were concentrated and subjected to flash column chromatography (20% EtOAc/Hexanes) to partially separate the isomers of hydroxycamphor. The resulting material was sublimed with a Kugelrohr distillation apparatus (55 ºC, 0.1 torr), yielding 397 mg (7%) of **3.03**, 92% isomerically pure (NMR).

Impure fractions were consolidated and purified again by flash chromatography to yield an additional 298 mg of **3.03**, ~95% isomerically pure. ^{1}H NMR (500 MHz, $CDCl_3$) δ 3.72 (s, 1H), 3.28 (bs, 1H), 2.06 (d, J = 4.7 Hz, 1H), 2.02 – 1.91 (dddd, 1H), 1.62 (ddd, 1H), 1.46 – 1.29 (m, 2H), 0.96 (s, 3H), 0.91 (s, 3H), 0.89 (s, 3H). ^{13}C NMR (126 MHz, $CDCl_3$) δ 220.51, 77.26, 57.01, 49.22, 46.71, 28.51, 25.10, 20.94, 19.98, 8.95. EI-GC/MS *m/z* (%): 168 (M^+, 32), 153 (2), 140 (9), 125 (42), 107 (10), 100 (14), 84 (92), 83 (100), 69 (38), 57 (19), 55 (51), 43 (14), 41 (37).

3.3.6 Davis oxidation of camphor

The following procedure was adapted from Davis et al.[10] This paper reports the synthesis of an *endo*-hydroxycamphor (**3.02)** as drawn. However in my hands, and based on other published reports[11,12] this reaction yields *exo*-hydroxycamphor (**3.03**) as the major product. This contradiction is corroborated with NMR spectral data.

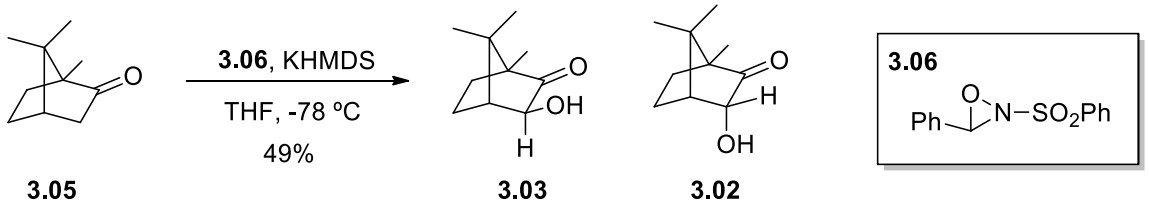

In a preliminary synthesis, a scalemic mixture (33% ee) of (1*R*)-camphor (0.33 mmol) was used in the Davis oxidation with the intention of producing the *endo*-hydroxycamphor isomers (**3.02**). After discovering that the identity of the insect-produced compound and the Davis oxidation product matched, a larger scale reaction from (1*S*)-camphor (>98%) was run as follows:

A dry flask flushed with Ar was charged with THF (40 mL) and potassium hexamethyldisilazane (KHMDS 1 M in THF, 2.22 mL, 2.22 mmol, 1 eq), then cooled to -

78 ºC. (1*S*)-Camphor (338 mg, 2.22 mmol, 1 eq; TCI Americas, Portland OR, USA) was added in portions over 1 min and the mixture was stirred 30 min at -78 ºC. A solution of the Davis reagent, 2-(phenylsulfonyl)-3-phenyloxazaridine (881 mg in 15 mL THF, 3.37 mmol, 1.5 eq; Enamine, Monmouth Junction NJ, USA) was added dropwise over 20 min. The reaction was stirred at -78 ºC for 55 min. Upon completion, the reaction was quenched with sat. aq. NH_4Cl (10 mL) at -78 ºC and allowed to warm to room temperature. Brine (30 mL) and diethyl ether (30 mL) were added to the reaction and the layers were separated. The aqueous layer was extracted with more diethyl ether (30 mL), then the combined organic layer was washed with brine (20 mL), dried over anhydrous Na_2SO_4, and concentrated under vacuum. The resulting cloudy yellow oil was dissolved in 4:1 dichloromethane:hexanes and partially purified by vacuum flash column chromatography (20% EtOAc/hexanes). The fractions enriched in the desired product were concentrated and repurified by flash chromatography (25% EtOAc/hexanes). The product was then purified further by Kugelrohr distillation (80 ºC, 1.85 torr) to yield 182 mg of product (49%), containing ~85% of the desired insect-produced *exo*-hydroxycamphor isomer (**3.03**) and 15% of the *endo*-hydroxycamphor isomer (**3.02**). **3.03** & **3.02** EI-GC/MS *m/z* (%): 169 (4), 168 (M^+, 34), 153 (2), 140 (9), 125 (43), 107 (11), 100 (15), 84 (93), 83 (100), 69 (38), 57 (18), 55 (50), 43 (14), 41 (35).

3.4 References

(1) Branham, M. A.; Wenzel, J. W. The Evolution of Bioluminescence in Cantharoids (Coleoptera: Elateroidea). *Fla Entomol* **2001**, *84* (4), 565–579. https://doi.org/10.2307/3496389.

(2) McDermott, F. A. The Taxonomy of the Lampyridae (Coleoptera). *T Am Entomol Soc* **1964**, *90* (1), 1–72.

(3) Lloyd, J. E. Chemical Communication in Fireflies. *Environ Entomol* **1972**, *1* (2), 265–266. https://doi.org/10.1093/EE/1.2.265.

(4) de Cock, R.; Matthysen, E. Sexual Communication by Pheromones in a Firefly, *Phosphaenus hemipterus* (Coleoptera: Lampyridae). *Anim Behav* **2005**, *70* (4), 807–818. https://doi.org/10.1016/J.ANBEHAV.2005.01.011.

(5) Ohba, N. Flash Communication Systems of Japanese Fireflies. *Integr Comp Biol* **2004**, *44* (3), 225–233. https://doi.org/10.1093/ICB/44.3.225.

(6) Shibue, K.; Goto, Y.; Shibue, T.; Ohba, N. Analysis of Sex-Attractant Pheromones of Firefly *Pyrocoelia oshimana* by Gas Chromatography Mass Spectrometry. *Anal Sci* **2000**, *16* (9), 995–996. https://doi.org/10.2116/ANALSCI.16.995.

(7) Ming, Q. L.; Lewis, S. M. Mate Recognition and Sex Differences in Cuticular Hydrocarbons of the Diurnal Firefly *Ellychnia corrusca* (Coleoptera: Lampyridae). *Ann Entomol Soc Am* **2010**, *103* (1), 128–133. https://doi.org/10.1603/008.103.0116.

(8) Paquette, L. A.; Hofferberth, J. E. The α-Hydroxy Ketone (α-Ketol) and Related Rearrangements. *Org Reactions* **2003**, 477–567. https://doi.org/10.1002/0471264180.OR062.03.

(9) Xu, P. F.; Li, S.; Lu, T. J.; Wu, C. C.; Fan, B.; Golfis, G. Asymmetric Synthesis of α,α-Disubstituted α-Amino Acids by Diastereoselective Alkylation of Camphor-Based Tricyclic Iminolactone. *J Org Chem* **2006**, *71* (12), 4364–4373. https://doi.org/10.1021/JO052435G/SUPPL_FILE/JO052435GSI20060416_063716.PDF.

(10) Davis, F. A.; Vishwakarma, L. C.; Billmers, J. M.; Finn, J. Synthesis of α-Hydroxy Carbonyl Compounds (Acyloins): Direct Oxidation of Enolates Using 2-Sulfonyloxaziridines. *J Org Chem* **1984**, *49* (17), 3241–3243. https://doi.org/10.1021/JO00191A048/SUPPL_FILE/JO00191A048_SI_001.PDF

(11) Piątek, A.; Chapuis, C. Regioselective Short Synthesis of Epiisoborneol Neopentyl Ether as Chiral Auxiliary: An Absolute Configuration Reset. *Helv Chim Acta* **2021**, *104* (11), e2100142. https://doi.org/10.1002/HLCA.202100142.

(12) Neisius, N. M.; Plietker, B. Diastereoselective Ru-Catalyzed Cross-Metathesis-Dihydroxylation Sequence. An Efficient Approach toward Enantiomerically Enriched Syn-Diols. *J Org Chem* **2008**, *73* (8), 3218–3227. https://doi.org/10.1021/JO800145X/SUPPL_FILE/JO800145X-FILE002.PDF.

(13) Gung, B. W. Structure Distortions in Heteroatom-Substituted Cyclohexanones, Adamantanones, and Adamantanes: Origin of Diastereofacial Selectivity. *Cheml Rev* **999**, *99* (5), 1377–1386. https://doi.org/10.1021/CR980365Q/ASSET/IMAGES/LARGE/CR980365QFA07F.JPEG.

(14) Mandal, T.; Jana, S.; Dash, J. Zinc-Mediated Efficient and Selective Reduction of Carbonyl Compounds. *Eur J Org Chem* **2017**, *2017* (33), 4972–4983. https://doi.org/10.1002/EJOC.201700887.

(15) Xu, P. F.; Chen, Y. S.; Lin, S. I.; Lu, T. J. Chiral Tricyclic Iminolactone Derived from (1R)-(+)-Camphor as a Glycine Equivalent for the Asymmetric Synthesis of α-Amino Acids. *J Org Chem* **2002**, *67* (7), 2309–2314. https://doi.org/10.1021/JO011139A/SUPPL_FILE/JO011139A_S.PDF.

(16) Kouklovsky, C.; Pouilhés, A.; Langlois, Y. α,β-Unsaturated Oxazolines, a Powerful Tool in Asymmetric Diels-Alder Cycloadditions. *J Am Chem Soc* **1990**, *112* (18), 6672–6679. https://doi.org/10.1021/JA00174A034.

(17) Tan, Q.; Li, D.; Bao, H.; Wang, Y.; Wen, J.; You, T. A Convenient Preparation of Enantiopure Endo-2-Hydroxyepicamphor and Endo-3-Hydroxycamphor from Camphoric Acid. *Synthetic Comm* **2011**, *34* (16), 2945–2950. https://doi.org/10.1081/SCC-200026645.

(18) Hückel, W.; Fechtig, O. Epicampher, Epiborneol Und Epiisoborneol. *Liebigs Ann Chem* **1962**, *652* (1), 81–95. https://doi.org/10.1002/JLAC.19626520112.

(19) Templeton, J. F.; Majid, S.; Marr, A.; Marat, K. Zinc–Acetic Acid Reduction of the Steroid 4-En-3-One: Novel Conversion of the 4-En-3-One into the 2-En-4-One via a Vinyl Chloride. *J Chem Soc Perk T 1* **1990**, No. 9, 2581–2584. https://doi.org/10.1039/P19900002581.

3.5 Supporting Information

3.5.1 EI mass spectrum for 3.03, the synthetic standard of the insect-produced compound

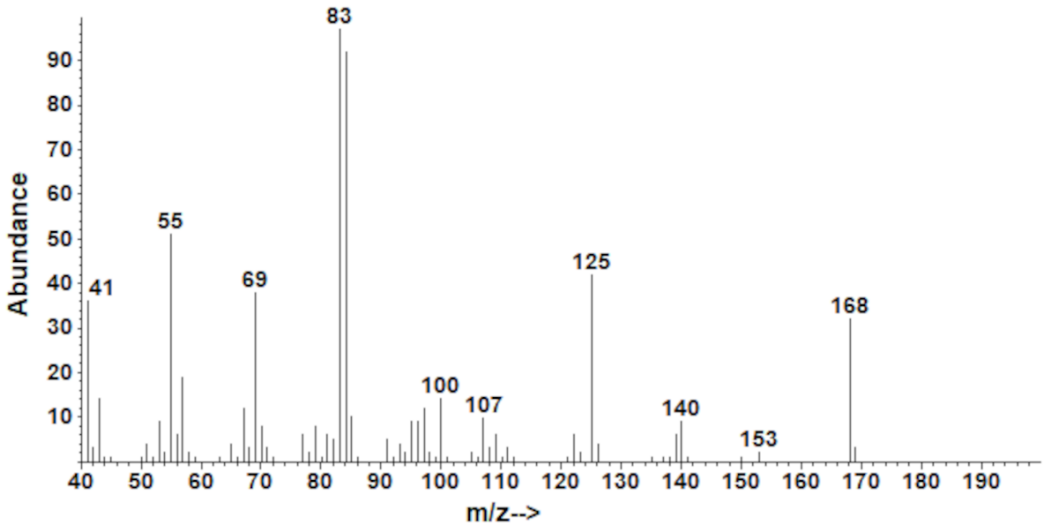

3.5.2 ^{1}H NMR for products of $NaBH_4$ reduction of (1*S*)-camphorquinone ($CDCl_3$, 500 MHz, 294 K)

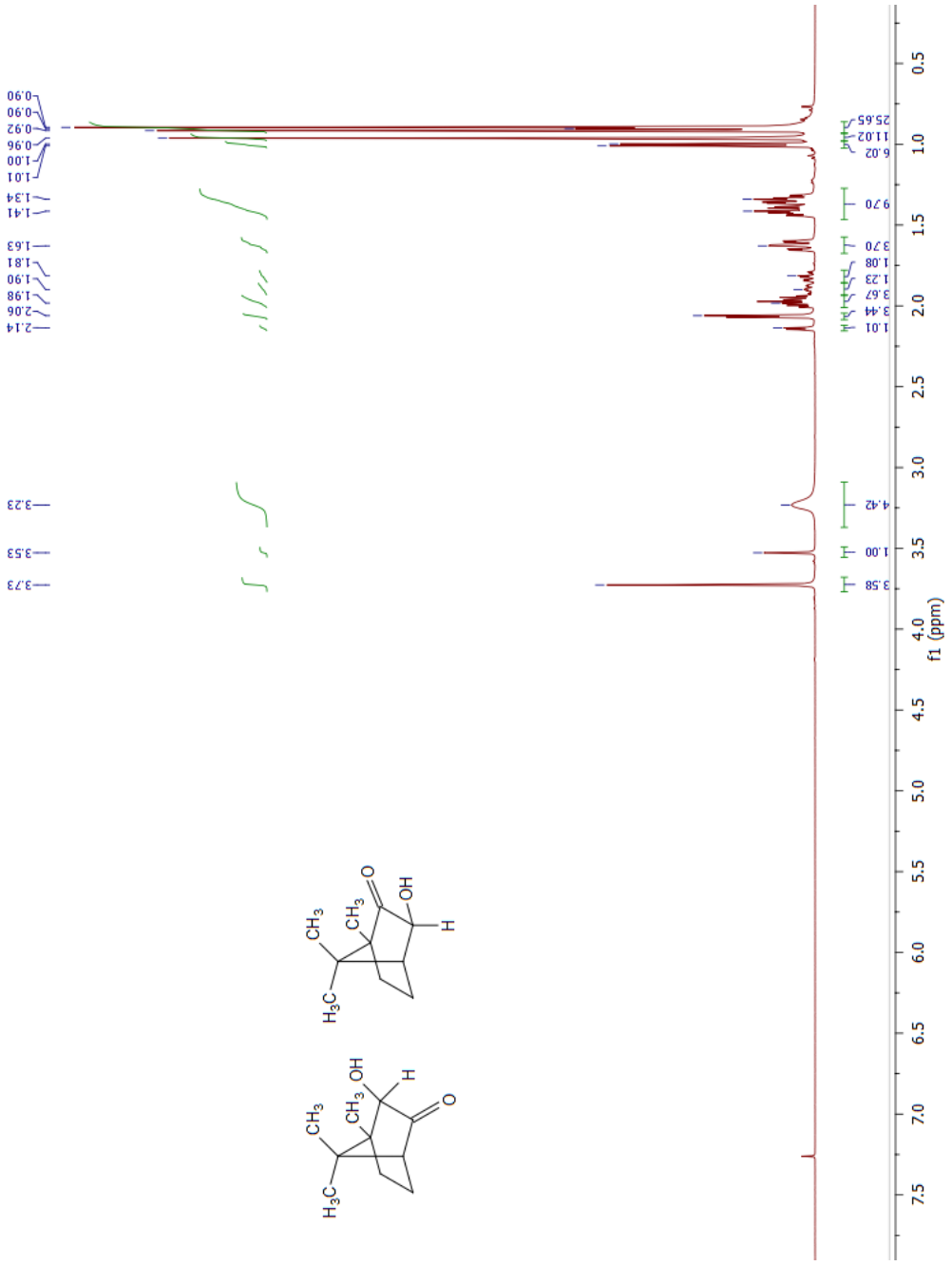

3.5.3 ^{13}C NMR for products of $NaBH_4$ reduction of (1*S*)-camphorquinone ($CDCl_3$, 126 MHz, 294 K)

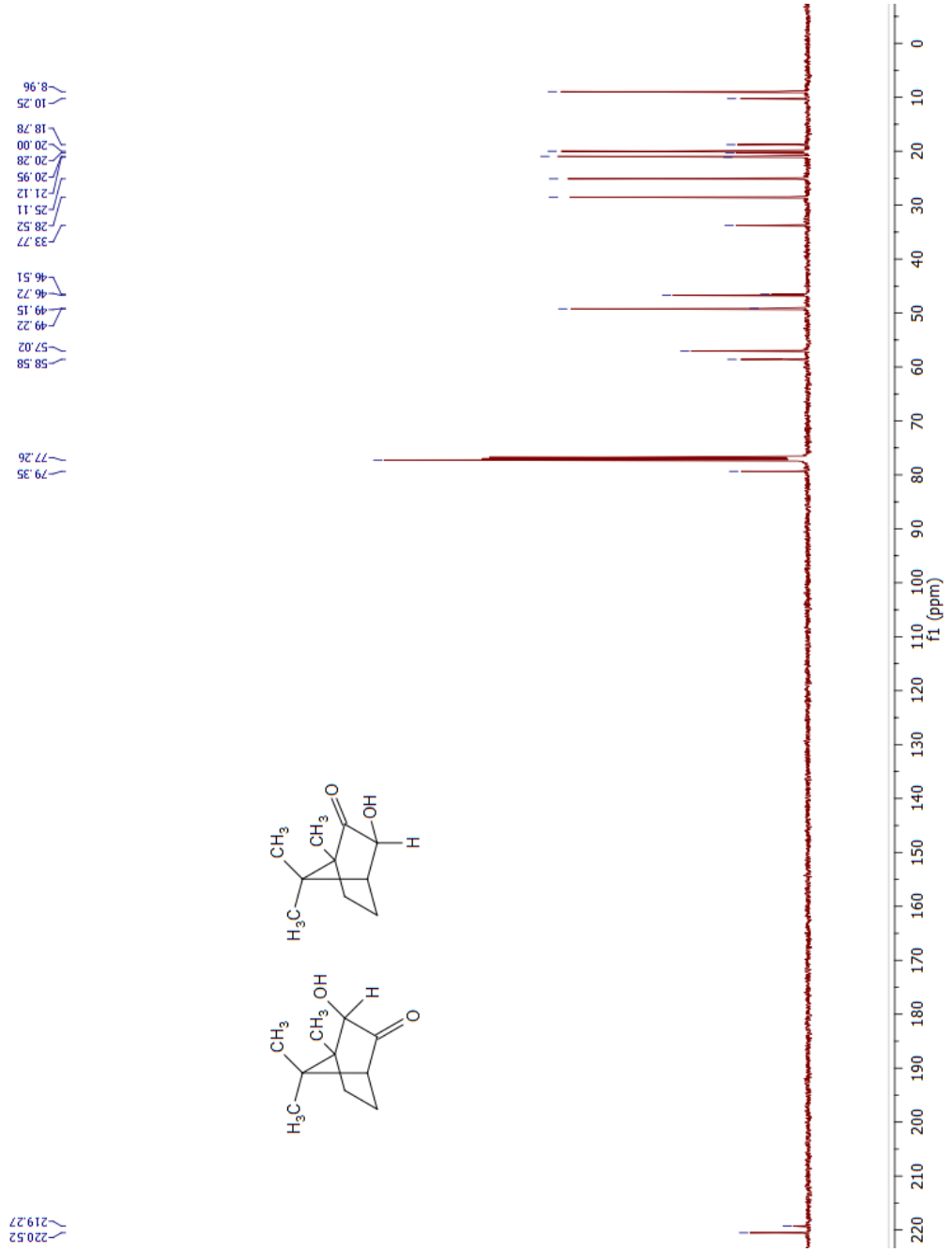

3.5.4 ^{1}H NMR of products from Zn/AcOH reduction of (1*S*)-camphorquinone ($CDCl_3$, 500 MHz, 294 K)

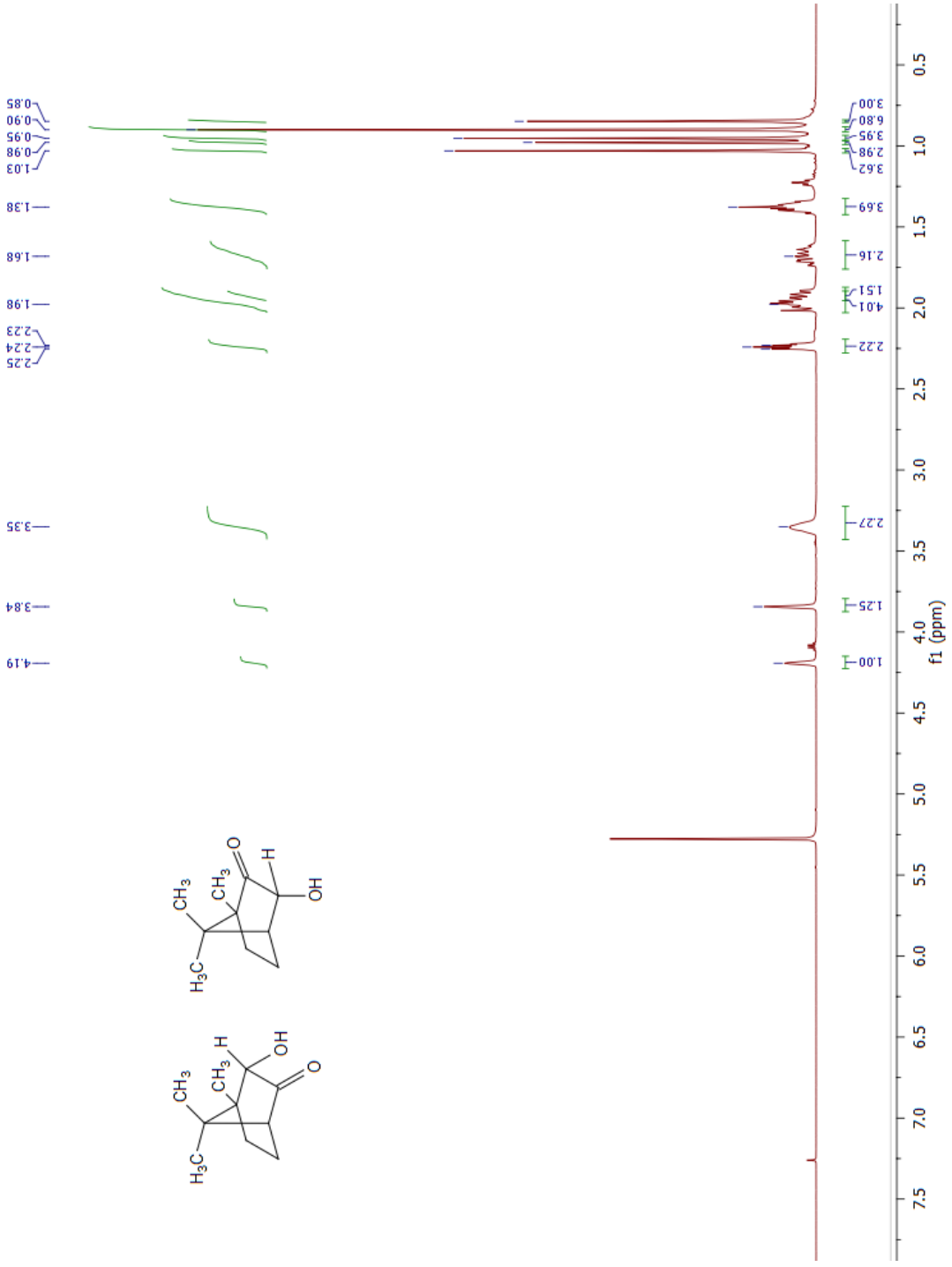

3.5.5 ^{13}C NMR for products of Zn/AcOH reduction of (1*S*)-camphorquinone ($CDCl_3$, 126 MHz, 294 K)

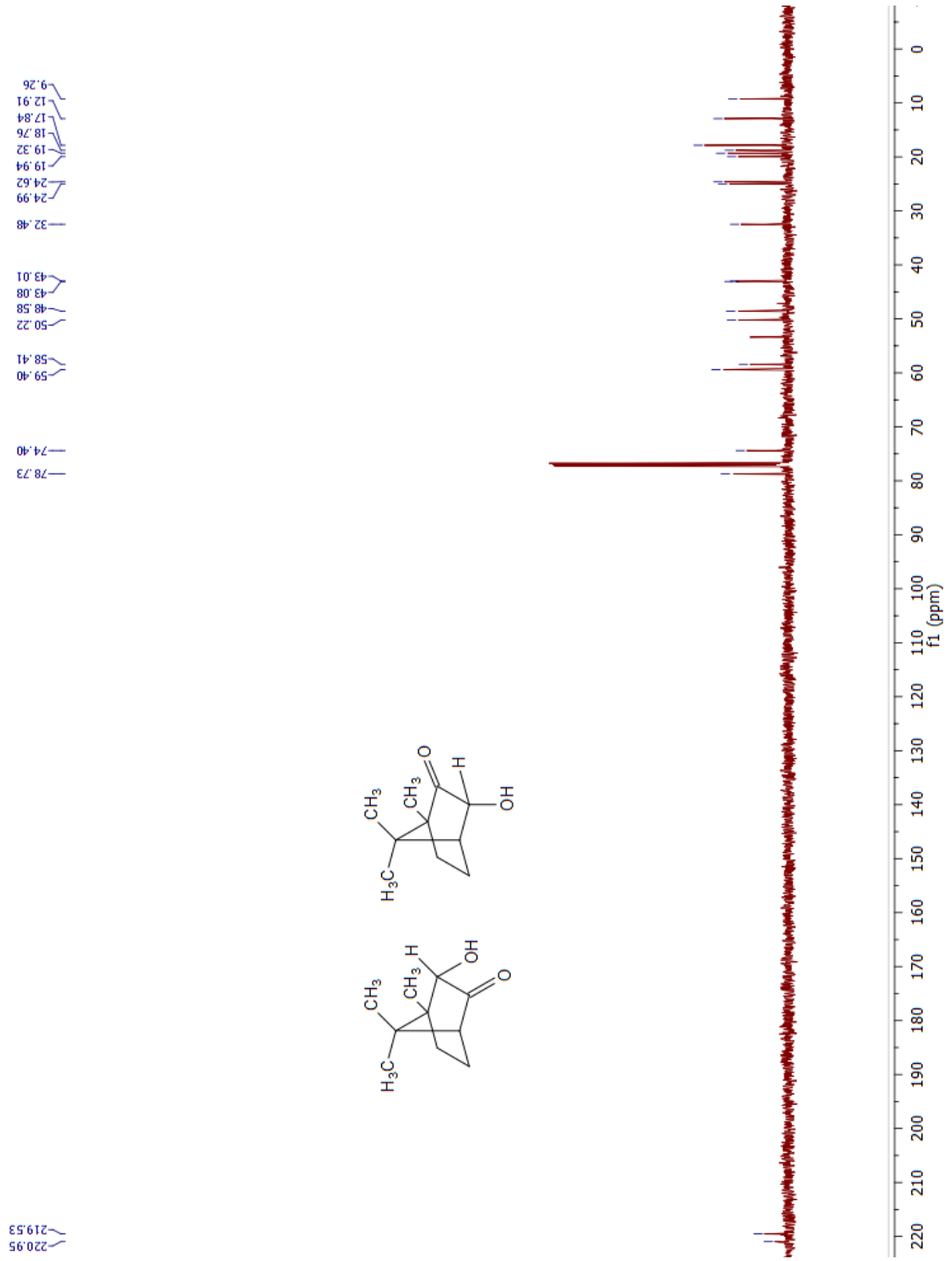

3.5.6 ^{1}H NMR of product from L-Selectride reduction of (1*S*)-camphorquinone ($CDCl_3$, 500 MHz, 293 K)

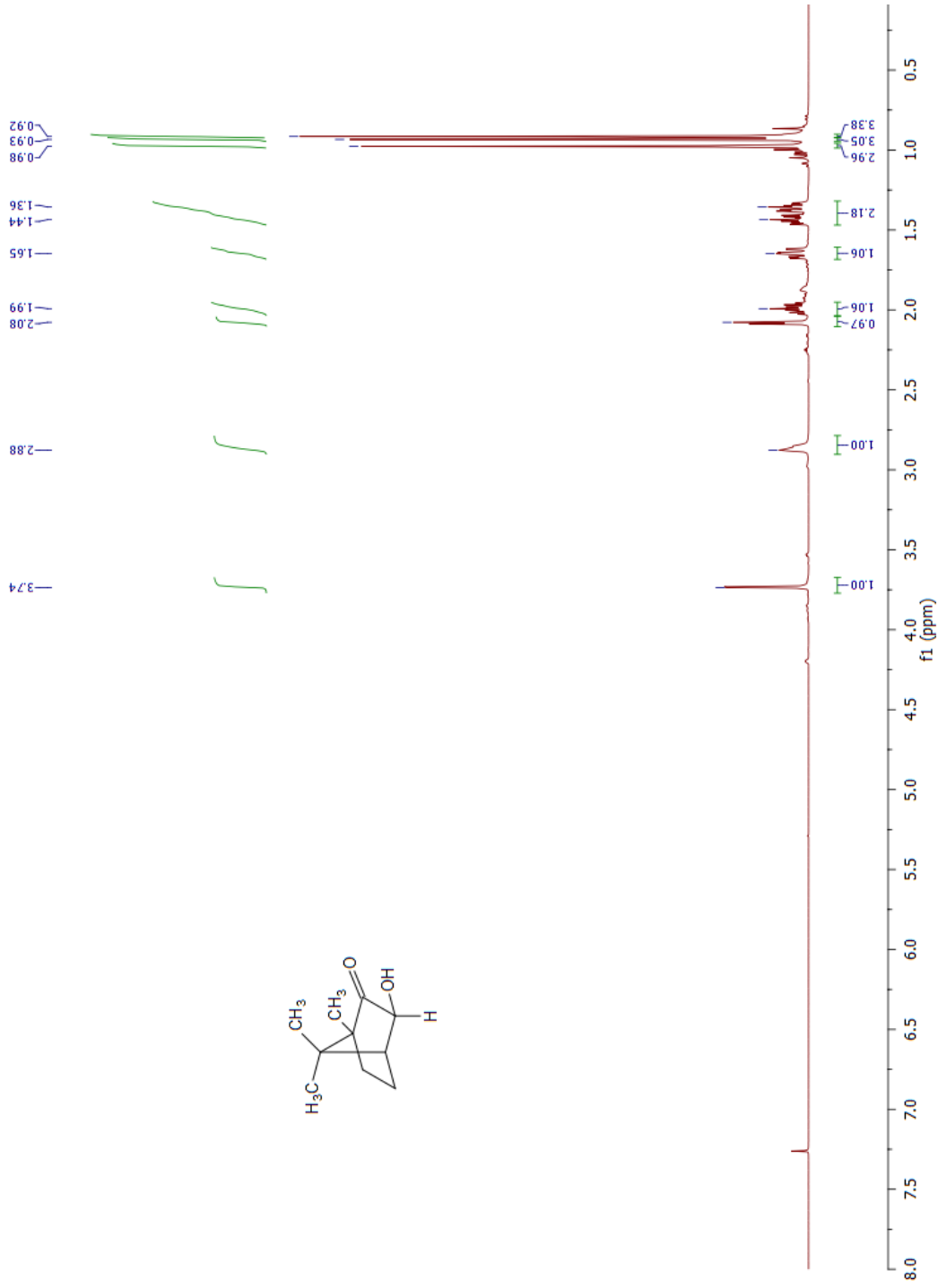

3.5.7 ^{13}C NMR for product from L-Selectride reduction of (1*S*)-camphorquinone ($CDCl_3$, 126 MHz, 293 K)

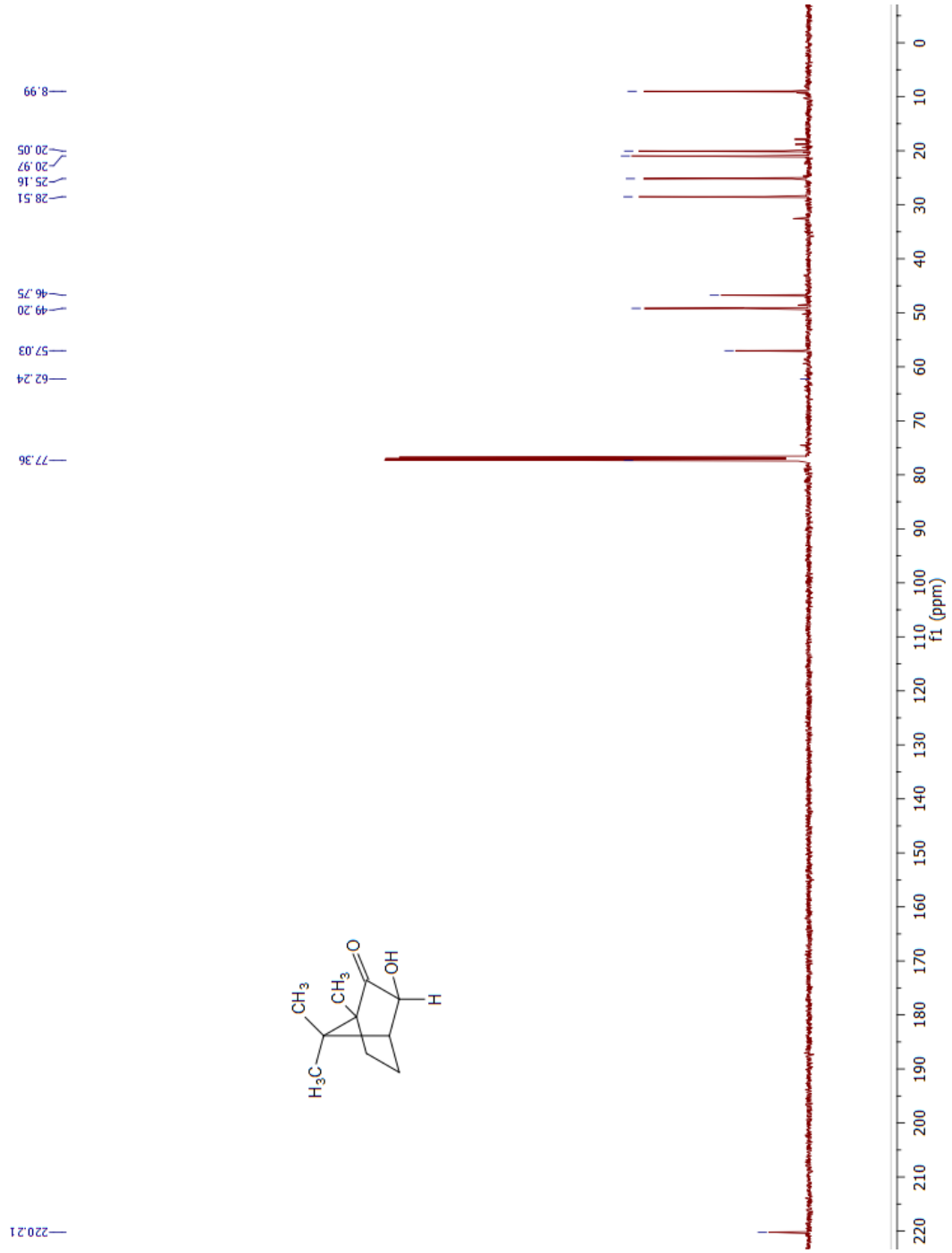

3.5.8 ^{1}H NMR of product from Davis Oxidation of (1*S*)-camphor ($CDCl_3$, 500 MHz, 296 K)

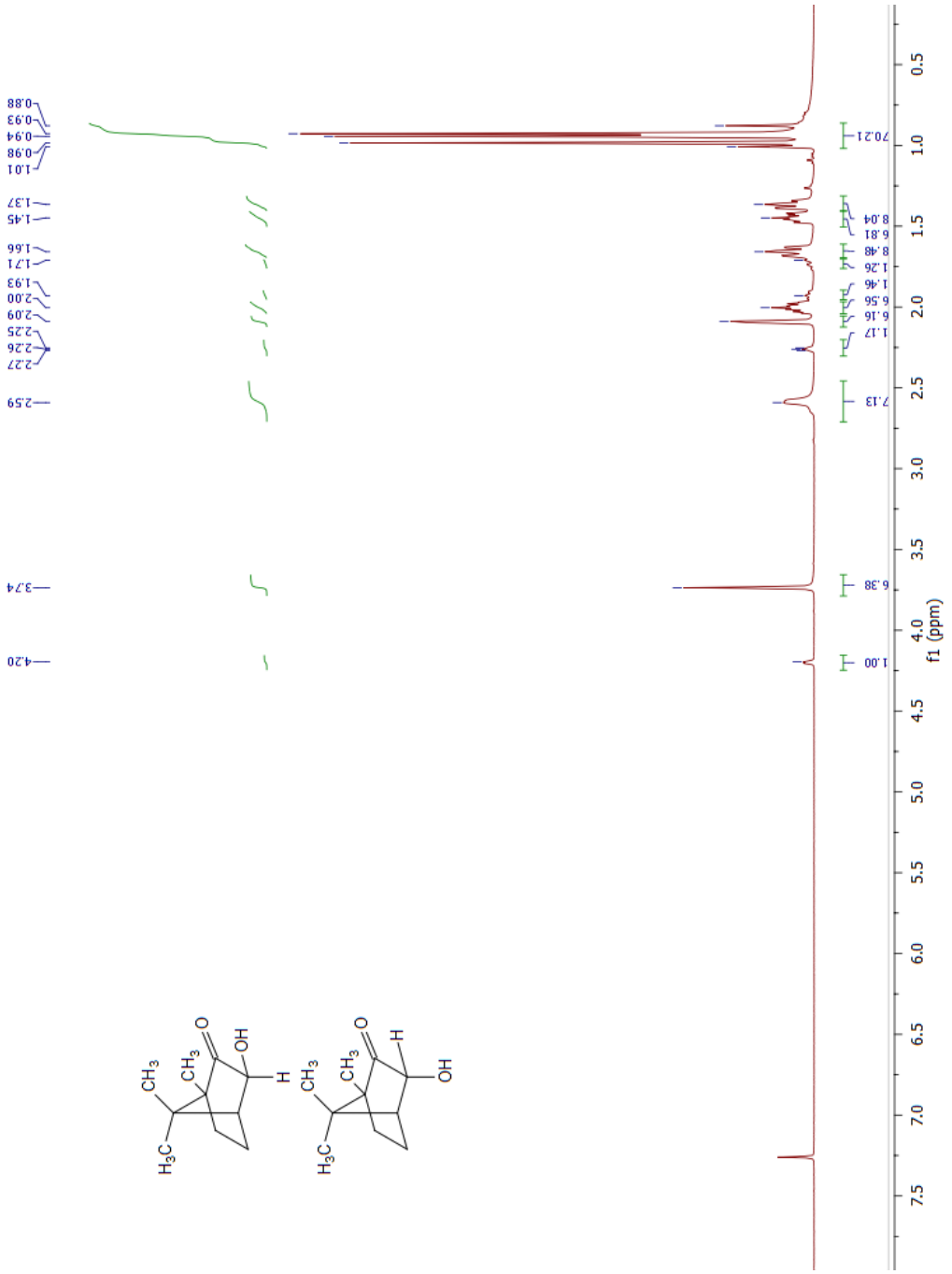

3.5.9 ^{13}C NMR of product from Davis Oxidation of (1*S*)-camphor ($CDCl_3$, 126 MHz, 296 K)

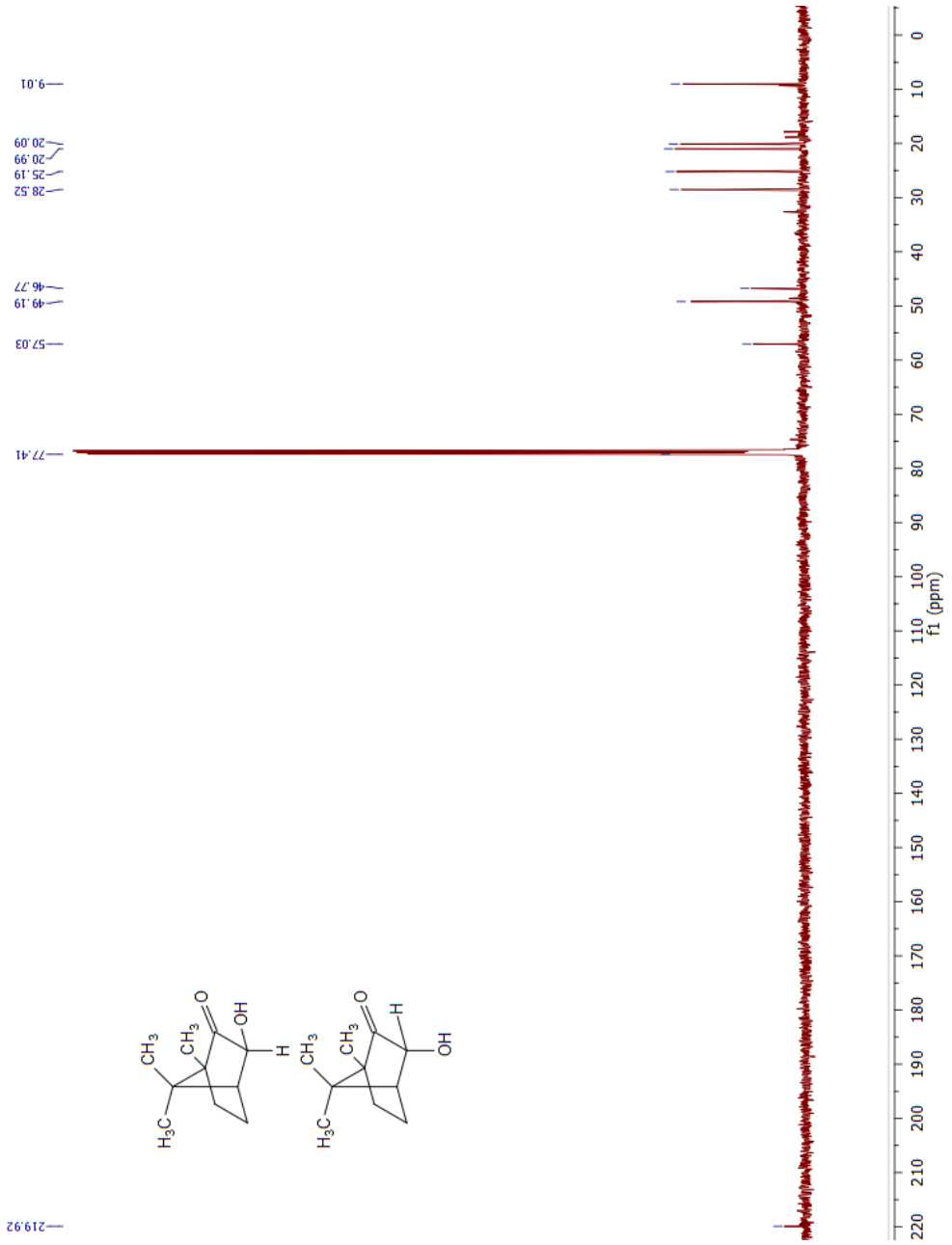

Chapter 4 – Identification and Synthesis of a Likely Aggregation-Sex Pheromone for the Longhorn Beetle *Graphisurus fasciatus* (Cerambycidae)

ABSTRACT

Longhorn beetles (Coleoptera: Cerambycidae) constitute a diverse family of insects with a cosmopolitan distribution. In recent years, the study of cerambycid semiochemistry has revealed widespread use of long-distance attractant pheromones among the major subfamilies, general trends concerning the function of cerambycid pheromones, and both a diversity and conservation of structural motifs within the chemical space occupied by cerambycid semiochemicals. Among the small fraction of cerambycid semiochemicals identified thus far, it is becoming increasingly common to find similarities in pheromone structures between related species, even those in different biogeographic regions and on different continents. Here, I describe the identification and synthesis of graphisurone, (4*R*,6*S*,7*E*,9*E*)-4,6,8-trimethylundeca-7,9-dien-3-one, a compound isolated from males of the North American longhorn beetle *Graphisurus fasciatus* (subfamily Lamiinae; tribe Acanthocinini). During this study, the same compound was isolated from males of the South American longhorn beetle *Eutrypanus dorsalis* (Lamiinae; Acanthocinini). Once the pheromone synthesis is completed, field trials in North and South America will be carried out to verify that the compound functions as a pheromone component for both species. This compound represents another example of the conservation of semiochemical structures within the Cerambycidae.

4.1 Introduction

Cerambycidae, more commonly known as the longhorn beetles, is one of the most diverse families in the Coleoptera and is also one of the most economically important. Invasive cerambycids such as the Asian longhorn borer *Anoplophora glabripennis,*[1] the rednecked longhorn beetle *Aromia bungii,*[2] and several species in the genus *Phoracantha*[3] have the potential to cause major damage to forests, tree crops, and other woody plants. Historically, methods for the detection, surveillance, and control of invasive cerambycids have been limited, particularly as the larvae develop in the woody tissues where insecticide sprays cannot penetrate.

Insect semiochemistry, or chemical communication between insects, has been widely exploited in developing methods for the monitoring and control of pest species.[4–6] To help to address the problems caused by invasive cerambycids and prevent environmental and economic damage, the chemical space occupied by the compounds used by cerambycids for intraspecific signaling should be explored further, so that these chemicals can be developed and exploited in detection, monitoring, and control of pest/invasive species (i.e., integrated pest management). Thus, identification of the specific chemicals that cerambycids use to communicate, and verification of their bioactivity, are the first steps in developing new tools for pest management. Furthermore, identification of the specific stereoisomer(s) produced by a particular species, and development of stereoselective syntheses, is necessary because unnatural stereoisomers may strongly inhibit an insect's response to the natural stereoisomer. For example, contamination of the Japanese beetle pheromone (*R*)-japonilure with only a small percentage of the (*S*)-

enantiomer completely inhibits attraction.[7] In the case of cerambycid semiochemistry, capture rate was shown to decrease when the antipode of the naturally produced pheromone was present in lures for *Neoclytus mucronatus*[8] and *Hylotrupes bajulus.*[9] In other cases, both enantiomers may be required in order to get optimum attraction. For example, capture rate of *Megacyllene caryae*[10] increased with use of a complex blend that included a racemate compared to the blend missing one enantiomer.

Males of species in the cerambycid subfamily Lamiinae produce aggregation-sex pheromones which attract both sexes.[11,12] As part of an ongoing study of the semiochemistry of the Cerambycidae, headspace volatiles were collected from both sexes of the North American species *Graphisurus fasciatus* (subfamily Lamiinae). The volatiles from males were found to contain a sex-specific compound, which I have identified as (4*R*,6*S*,7*E*,9*E*)-4,6,8-trimethylundeca-7,9-dien-3-one (**4.01, Figure 4.01**). Being sex specific, this compound is a likely candidate for an aggregation-sex pheromone component for this species. Here, I describe the complete identification of the compound, given the common name graphisurone, including which of the 16 possible stereoisomers is produced by the beetle, and a stereoselective synthesis of the compound. Based on its structure, the compound is a polyketide, a class of compounds which has only recently been identified in cerambycid pheromones.[13]

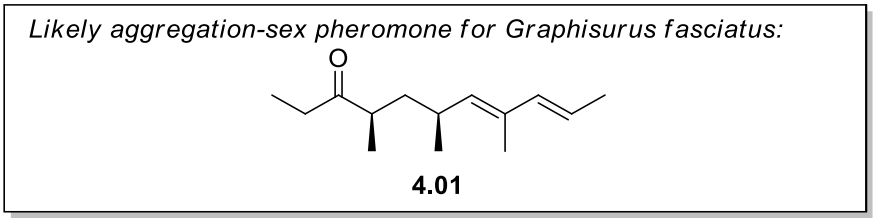

Figure 4.01 *The polyketide structure of the likely aggregation-sex pheromone for Graphisurus fasciatus.*

4.1 Results

4.1.1 Preliminary Spectral Data and Candidate Structures

A sex-specific compound was reproducibly found in headspace extracts of live *G. fasciatus* males. The compound was isolated by preparative GC, and proton NMR spectra of the purified compound were taken with a microbore probe. Tentative structural characterization based on the compound's EI mass spectrum and ^{1}H NMR spectra suggested a polyketide structure.[13] The key spectral information used to identify the gross structure is summarized in **Figure 4.02**.

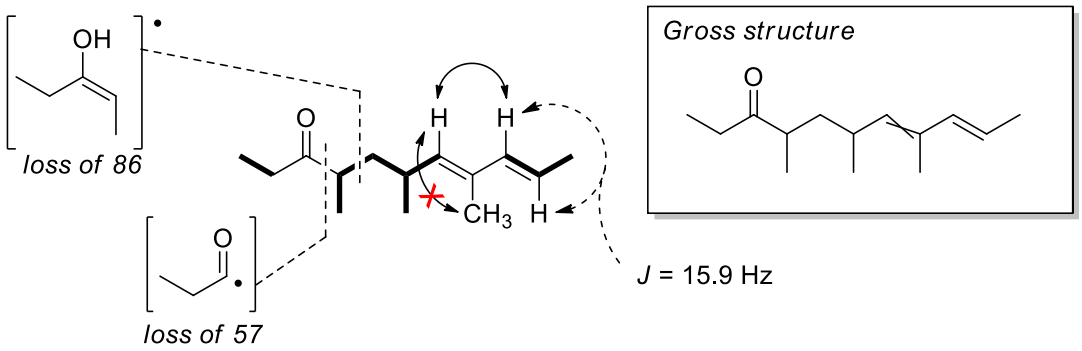

Figure 4.02 *Summary of key information from ^{1}H, ^{1}H-^{1}H COSY, and ^{1}H-^{1}H NOESY NMR, and EI-GC/MS. Spin systems elucidated by coupling constants and ^{1}H-^{1}H COSY NMR are depicted as bold bonds, and a key coupling constant is identified with a dashed double-sided arrow. Key NOE enhancements are denoted by a double-ended arrow, and a red X signifies the absence of an enhancement.*

Specifically, the EI mass spectrum indicated that the pheromone candidate has a molecular ion of *m/z* 208, for possible molecular formulae of $C_{15}H_{28}$, $C_{14}H_{24}O$, or $C_{13}H_{20}O_2$, with 2, 3, or four rings/sites of unsaturation, respectively. Fragments of *m/z* 151 (loss of 57 amu, C_3H_5O) and *m/z* 122 (loss of 86 amu, $C_5H_{10}O$) suggested the presence of a propanoyl moiety and a 3-pentanoyl moiety, respectively (**Figure 4.03**). The even-numbered *m/z* 122 fragment indicated that a rearrangement reaction occurred within the ionized molecule, suggesting that if a ketone were indeed present, a McLafferty rearrangement could have produced the *m/z* 86 fragment. The base peak at *m/z* 107 (loss of 101 amu, 15 greater than 86) suggested a methylene attached to the 3-pentanoyl moiety, but at this stage, no other fragments could be reliably assigned.

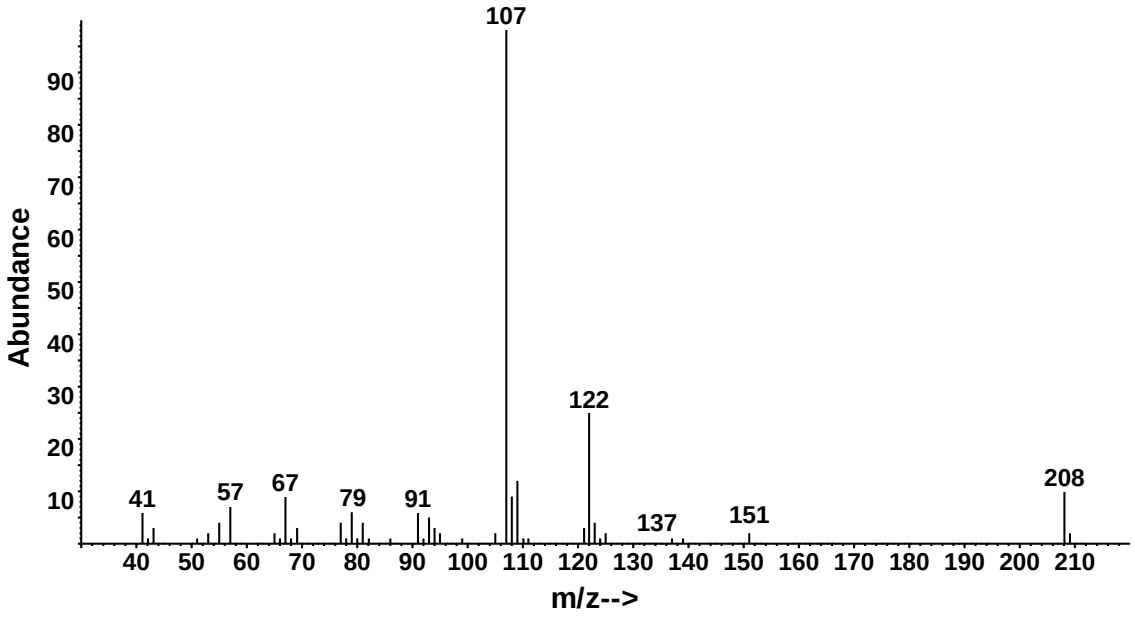

Figure 4.03 *EI GC-MS spectrum of the compound isolated from headspace volatiles of male Graphisurus fasciatus.*

The extract containing the insect-produced compound was subjected to ^{1}H- and ^{1}H-^{1}H COSY NMR spectroscopy using a microbore probe, and a summary of these data is shown in **Table 4.01**. The following spin systems in **Figure 4.04** were identified.

Table 4.01 *NMR data for graphisurone.*

Carbon type	**Position**	**δ ^{1}H, mult.**	***J*(H,H) = (Hz)**
-CH_3	1	0.95 t	*J* = 7.3
-CH_2-	2a	2.38 m	
	2b	2.36 m	
>C=O	3	-	
>CH-	4	2.41 m	
-CH_2-	5a	1.58 ddd	*J* = 13.6, 9.7, 5.6
	5b	1.27 m	
>CH-	6	2.49 m	
-CH=	7	5.01 d	*J* = 10.1
>C=	8	-	
-CH=	9	6.02 d	*J* = 15.9
-CH=	10	5.56 dq	*J* = 15.4, 6.8
-CH_3	11	1.73 d	*J* = 6.6
-CH_3	12	0.98 d	*J* = 6.9
-CH_3	13	0.93 d	*J* = 6.6
-CH_3	14	1.70 d	*J* = 1.0

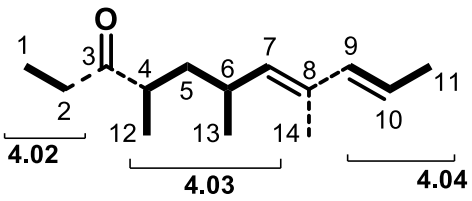

Figure 4.04 *Spin systems (bold) identified by ^{1}H- and ^{1}H-^{1}H COSY NMR spectroscopy for the compound produced by Graphisurus fasciatus.*

The protons on C-1 and C-2 were readily identified as the isolated ethyl spin system **4.02**, likely adjacent to a carbonyl, from their chemical shifts and coupling constants, supporting the hypothesized propanoyl fragment from mass spectrometry. The chemical shift of methinyl H-4 suggested it might be on the other side of the carbonyl, and it was also coupled to the C-12 methyl and the two diastereotopic protons of the C-5 methylene of the extended spin system **4.03**, supporting the 5-carbon 3-pentanone fragment suggested from the mass spectrum. A large coupling (J = 13.6) between protons H-5a and H-5b confirmed that they were diastereotopic geminal methylene protons. This pair exhibited crosspeaks with protons H-4 and H-6 in the ^{1}H-^{1}H COSY NMR, confirming the connections on either side of the C-5 methylene. Analyses of the crosspeaks provided further correlations, showing clear connections of the C-12 methyl group to the C-4 methine, the C-13 methyl to methine C-6, and the C-6 methine to the alkenyl proton of methine C-7 (5.01 ppm, d, J = 10.1 Hz). This completed spin system **4.03**.

Three alkenyl protons were observed, one of which had already been identified at the end of spin system 4.bb (C-7 alkenyl methine). There were two additional alkenyl protons (H-9 & H-10, 6.02 and 5.56 ppm respectively) with a shared coupling constant of ~J = 15.9 Hz, suggesting an (*E*)-1,2-disubstituted alkene. Furthermore, the allylic methyl

group of C-11 (δ = 1.73 ppm) was coupled to the alkenyl proton on C-10 (J = 6.8 Hz), establishing the spin system **4.04**. This was corroborated by crosspeaks in the ^{1}H-^{1}H COSY NMR (**Figure 4.05**).

The remaining connections yet to be assigned in the structure were that of the C-14 methyl, which exhibited as a broadened doublet at 1.70 ppm with a small coupling constant (J = 1.0), and of alkenyl carbons C-8 and CH-9. According to the fragments and spin systems already identified, the only point of connection for the C-14 methyl would be to C-8, the trisubstituted sp^2 carbon connected to the alkenyl methine on C-7. Thus, the remaining connection had to be between C-8 and CH-9, revealing a conjugated diene. A total of 24 protons were observed in the NMR spectrum and together with the purported carbonyl group, confirmed the candidate molecular formula of $C_{14}H_{24}O$.

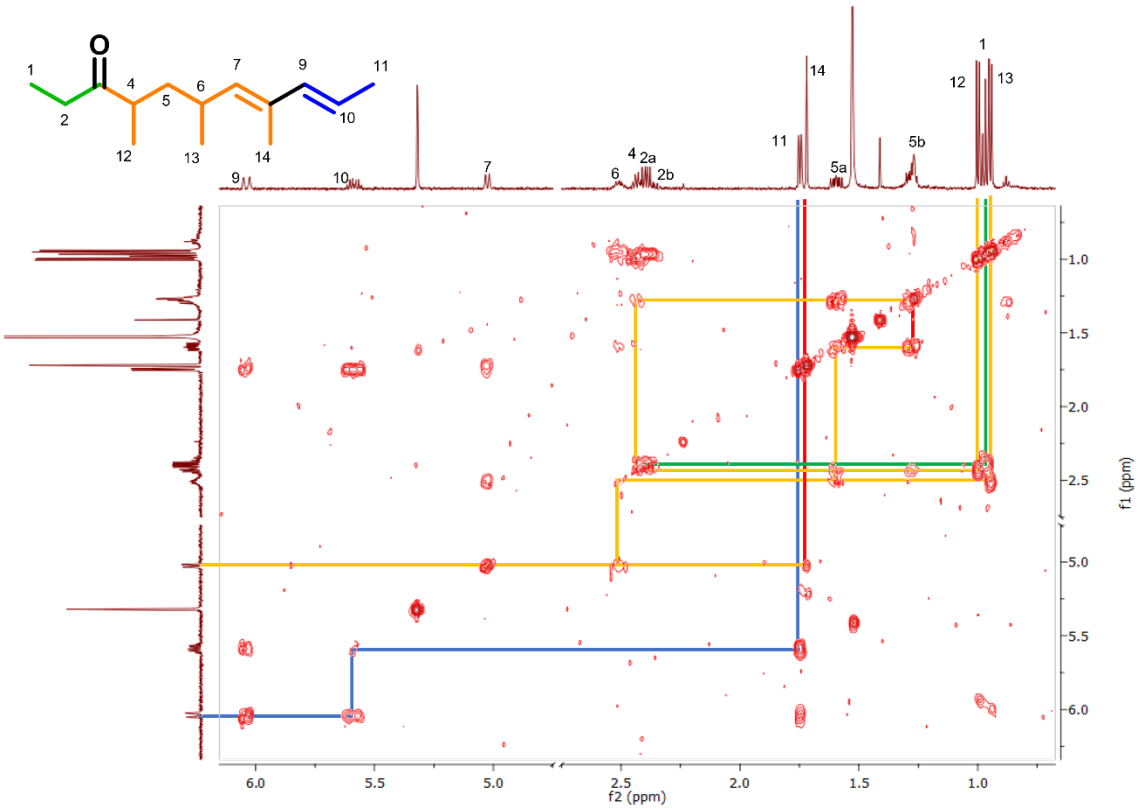

Figure 4.05 *^{1}H-^{1}H COSY NMR spectrum of the compound produced by Graphisurus fasciatus, showing three spin systems.*

Upon returning to the mass spectrum with a tentative structure in hand, the base peak at *m/z* 107 (possible C_8H_{11}) might be explained by cleavage of the C-5—C-6 bond producing an allylic cation, accompanied by loss of two protons.

The 4 stereochemical elements in the proposed structure indicate a total of 16 possible stereoisomers. However, one stereochemical element, the C-9 to C-10 double bond, was clearly shown to be *trans* from the vicinal ^{1}H-^{1}H coupling constant, reducing the remaining total to 8 candidate stereoisomers (**Figure 4.06**). That is, there were two chiral centers of unknown configuration, and the trisubstituted alkene which could have

either an (*E*)- or (*Z*)-configuration. Thus, the remaining structural uncertainties and stereochemistry were approached stepwise, as follows.

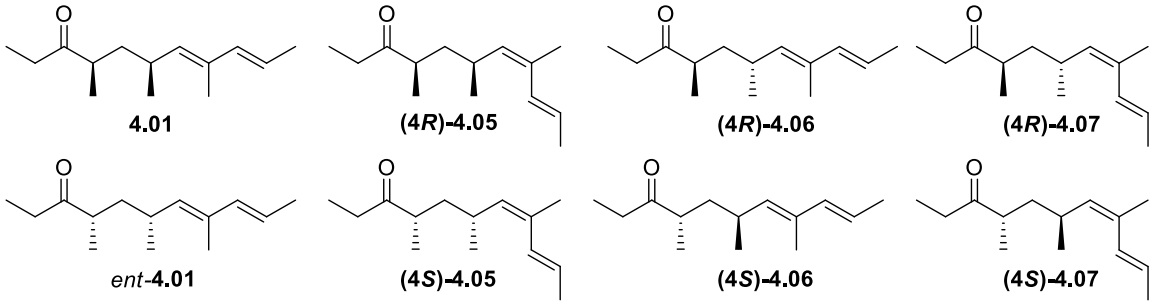

Figure 4.06 *Candidate structures for the likely aggregation-sex pheromone of Graphisurus fasciatus.*

4.1.2 Synthetic Strategy to Eliminate Candidates

A short synthesis to confirm the gross structure was initially proposed (**Scheme 4.01**). However, even if the gross structure was confirmed by the synthesis proposed in **Scheme 4.01A**, this synthesis would give us no information about the absolute stereochemistry and little information about the relative stereochemistry.

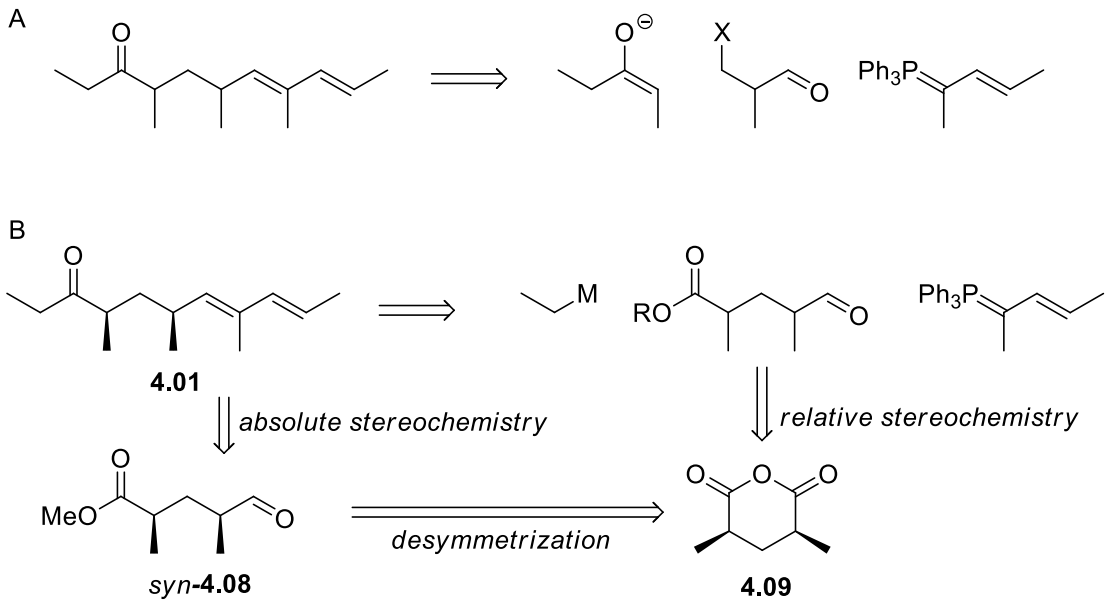

Scheme 4.01 *Synthetic strategy to confirm the tentative gross structure of the insect-produced compound: A) preliminary proposed synthesis to quickly confirm the gross structure; B) synthesis carried out to determine both gross structure and stereochemistry.*

Because the *E*/*Z*-selectivity of Wittig olefinations is well established,[14,15] I initially focused my attention on establishing the stereochemistry of the methyl branches. It was envisioned that use of intermediate *syn*-2,4-dimethylglutaric anhydride **4.09** (**Scheme 4.02**) to establish a known *syn*-dimethyl moiety in the major product would provide clues for determining the stereochemistry of each product among a mixture containing each candidate. Anhydride **4.09** was synthesized by modifications to literature procedures as follows. Deprotonation of diethyl methylmalonate (**4.10**) with NaOEt in ethanol and reaction with methyl methacrylate (**4.11**) produced a mixture of triesters **4.12**.[16] The triester mixture was hydrolyzed and decarboxylated by refluxing in concentrated HCl to produce diacid **4.13**,[17] which upon refluxing with acetyl chloride produced a mixture of the *syn*- and *anti*-anhydride isomers **4.14**.[18] Finally, isomerization of the mixture with 1,8-

diazobicyclo[5.4.0]undecane (DBU) and recrystallization produced *syn*-dimethylglutaric anhydride **4.09** in 97% diastereoisomeric purity. At this point, the synthetic route can diverge into an enantioselective pathway, using an enzyme to desymmetrize intermediate **4.09** (**Scheme 4.01B**, see below), providing a chiral monoester intermediate to aid in determining the absolute stereochemistry of the likely aggregation-sex pheromone.

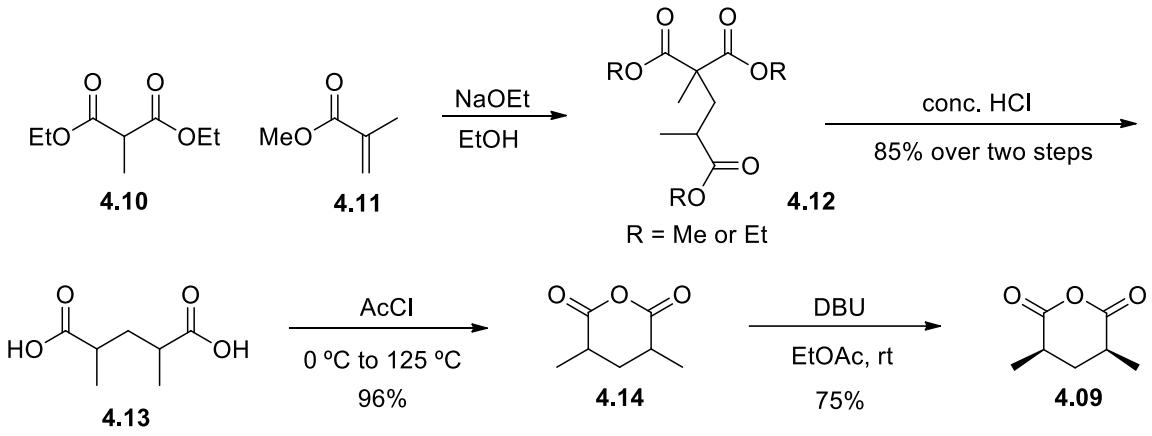

Scheme 4.02 *Synthesis of anhydride **4.09**, providing access to a 2,4-dimethyl moiety with known syn-configuration.*

4.2 First synthesis

My first racemic synthesis, outlined in **Scheme 4.03**, was based on two key disconnections from a central core derived from *syn*-dimethylglutaric anhydride, of the ethyl group adjacent to the ketone, and of the trisubstituted double bond. Thus, reduction of anhydride **4.09** with $LiAlH_4$ in ether at -60 ºC produced lactone *rac*-**4.15**,[19] followed by transesterification with methanol with an acid catalyst to produce hydroxyester *rac*-**4.16**.[20] Throughout these steps, the *syn*-dimethyl moiety was conserved (validated by NMR spectra), but when the hydroxyl group was oxidized to the corresponding aldehyde **4.08** using Swern oxidation conditions,[21] partial epimerization of the methyl group adjacent to

the aldehyde was observed, eroding the isomeric purity to an approximately 2:1 mixture of the *syn*:*anti*-dimethyl diastereomers. In the event, this intermediate was still valuable because it would still inform the relative stereochemistry of the two methyl groups in the components in the final product mixture because the two epimers were present in an easily distinguishable ratio.

It was expected that the Wittig olefination reaction would produce the (*E*)-trisubstituted alkene as the major product[14]. Therefore, if the stereochemistry of the dimethyl moiety had little to no effect on the olefination selectivity, the most abundant component in the product mixture would bear a *syn*-dimethyl moiety and an (*E*)-trisubstituted alkene (*rac*-**4.01**). Similarly, the least abundant component would bear an *anti*-dimethyl and (*Z*)-alkene (*rac*-**4.07**), whereas the two intermediate components would correspond to the remaining stereoisomers (*rac*-**4.05** and *rac*-**4.06**).

Conversion of (*E*)-3-penten-2-ol (**4.17**) to the phosphonium bromide salt (**4.19**) by bromination with PBr_3, then reaction with triphenylphosphine gave the phosphonium salt required for the Wittig olefination. Thus, reaction between **4.08** and **4.19**, with butyllithium as base, produced a complex mixture of isomers (*rac*-**4.20**) along with several analogs with molecular ions of *m/z* 196 (14 amu less than the desired *m/z* 210). Despite the unexpected presence of these analogs, the sequence was completed by conversion of the methyl esters **4.20** to the corresponding ethyl ketones through formation of the Weinreb amides[22] by treatment with methylmethoxylamine hydrochloride, followed by ethylmagesium bromide to produce the desired pheromone candidates with molecular weight 208, in an approximate ratio of 4:2:2:1, as part of a complex product mixture.

The *m/z* 196 analogs had apparently undergone the same transformation, as they now appeared as a mixture of *m/z* 194 analogs with mass fragmentation patterns reminiscent of their precursors, and the desired *m/z* 208 compounds. The source of these analogs, 14 amu (= 1 methylene group) less than the target compounds, is not clear. Specifically, the GC-MS trace of the aldehyde partner **4.08** was seemingly free of any analogs with molecular ions 14 amu less than **4.08**, and the NMR of the phosphonium salt used was seemingly devoid of any analogs missing a methylene unit. I did synthesize crotyltriphenylphosphonium bromide with the intention of reacting it with base and methyl iodide in an alternate route to **4.19**, but those samples were kept separate from the **4.19** sample produced from the secondary bromide **4.18**. In the enantioselective pathway below, the same outcome was observed, despite checking the purity of the phosphonium salt and aldehyde partners beforehand.

The GC retention time and mass spectrum of one component with *m/z* 208 were good matches for those of the insect-produced compound (see **Figure 4.07** below). This component of the product mixture was isolated in impure form by preparative GC, with the desired **4.01** as the major constituent (**Figure 4.07C**). The purity was sufficient to allow the full interpretation of the NMR spectrum, including confirmation of the stereochemistry of the trisubstituted double bond as (*E*). These data proved that the insect-produced compound contained a *syn*-dimethyl moiety and an (*E)*-trisubstituted alkene. Thus, the only remaining uncertainty was its absolute configuration.

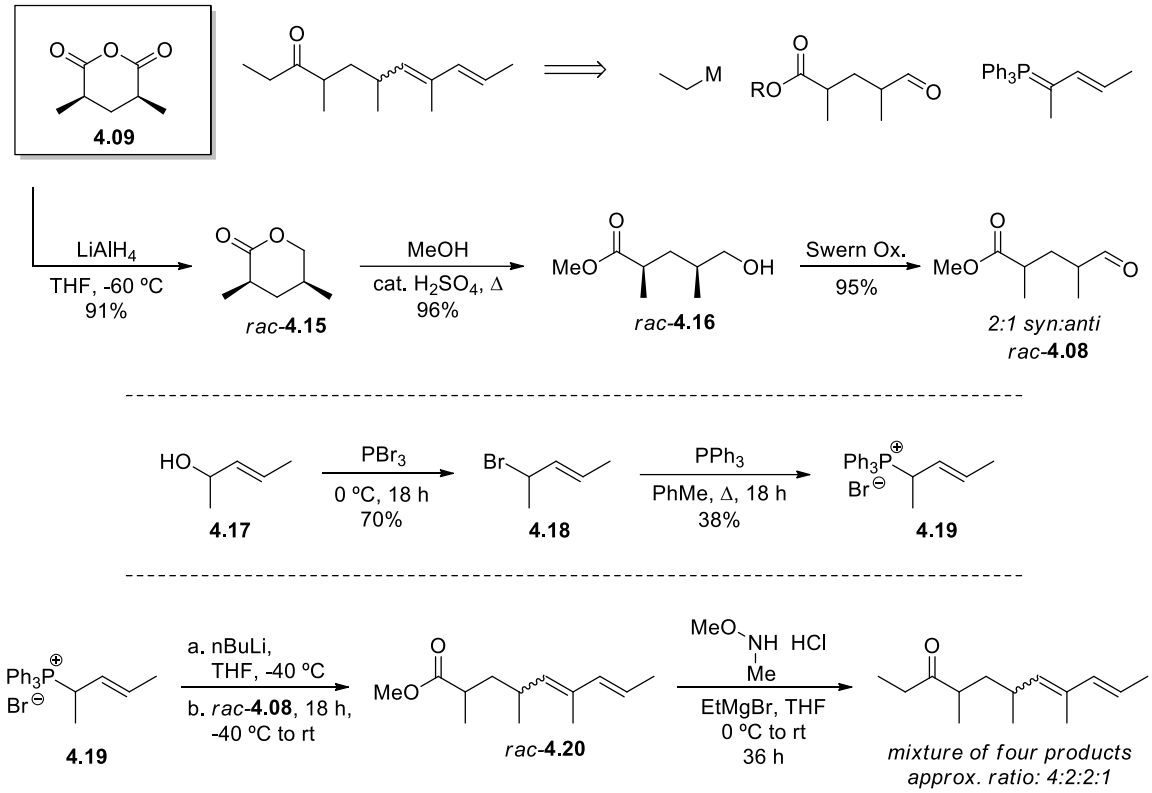

Scheme 4.03 *Diastereoselective synthesis toward the likely aggregation-sex pheromone of Graphisurus fasciatus.*

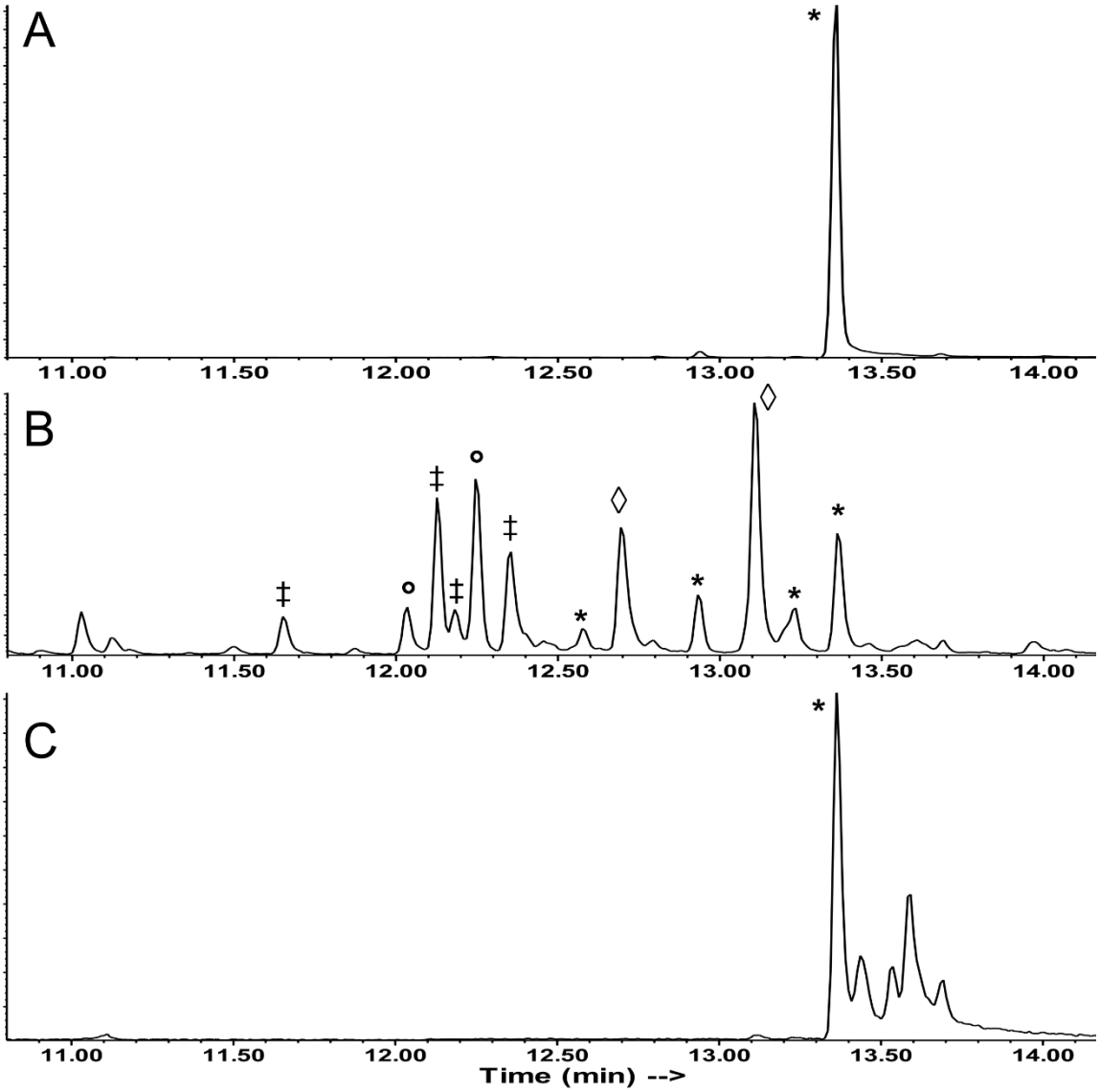

Figure 4.07 *EI-GC/MS chromatograms of: A) the purified insect produced compound; B) the crude product mixture; and C) the partially purified compound (preparative GC) that matched the insect-produced compound. Peaks marked with the same symbol had similar mass spectra. The target peaks with m/z 208 are marked with asterisks (*). Peaks marked with a double dagger (‡) had an apparent M^+ of m/z 194 and displayed similar fragmentation patterns to the m/z 208 peaks, indicating that they were homologs with one less methylene group. Unmarked peaks or peaks marked with a ° or ◊ bore little to no similarity to the insect produced compound.*

4.2.2 Relative and Absolute Stereochemistry

Modification of the synthetic route to include desymmetrization of the dimethyl ester derivative (**4.21**) of anhydride **4.09**, formed by treatment of the anhydride with methanol and acid catalyst, allowed us to identify the absolute configuration of the natural compound (**Scheme 4.04**). Thus, the enzyme α-chymotrypsin selectively hydrolyzed[23,24] the right side ester of dimethyl ester **4.21** (as drawn) producing hemiester **4.22** in approximately 92% ee. Selective reduction of the acid with borane, followed by oxidation of the resulting alcohol to the ester aldehyde coupling partner, and Wittig reaction as before produced an analogous complex product mixture, one component of which was the (4*R*,6*S*)-enantiomer, the retention times of which on both achiral (DB-5, DB-17) and chiral (Cyclodex B) GC stationary phases matched those of the insect-produced compound (**Figure 4.08D**). Furthermore, analysis of the racemate proved that the two enantiomers were resolved on the Cyclodex B column. This allowed me to unequivocally assign the insect-produced compound as the *syn*-(4*R*,6*S*)-enantiomer.

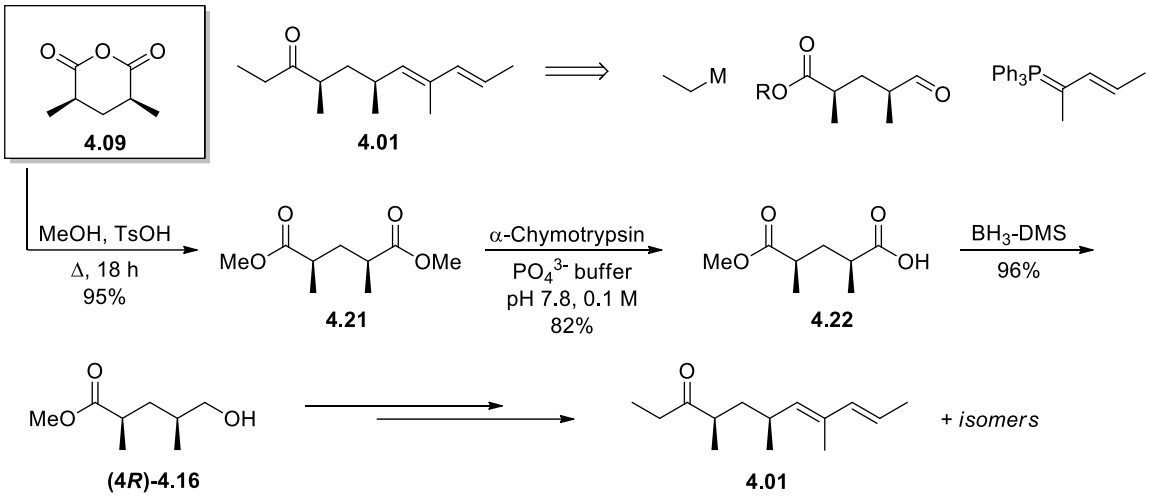

Scheme 4.04 *Synthetic route to an enantioenriched coupling partner for the Wittig olefination, featuring an enzyme-mediated desymmetrization.*

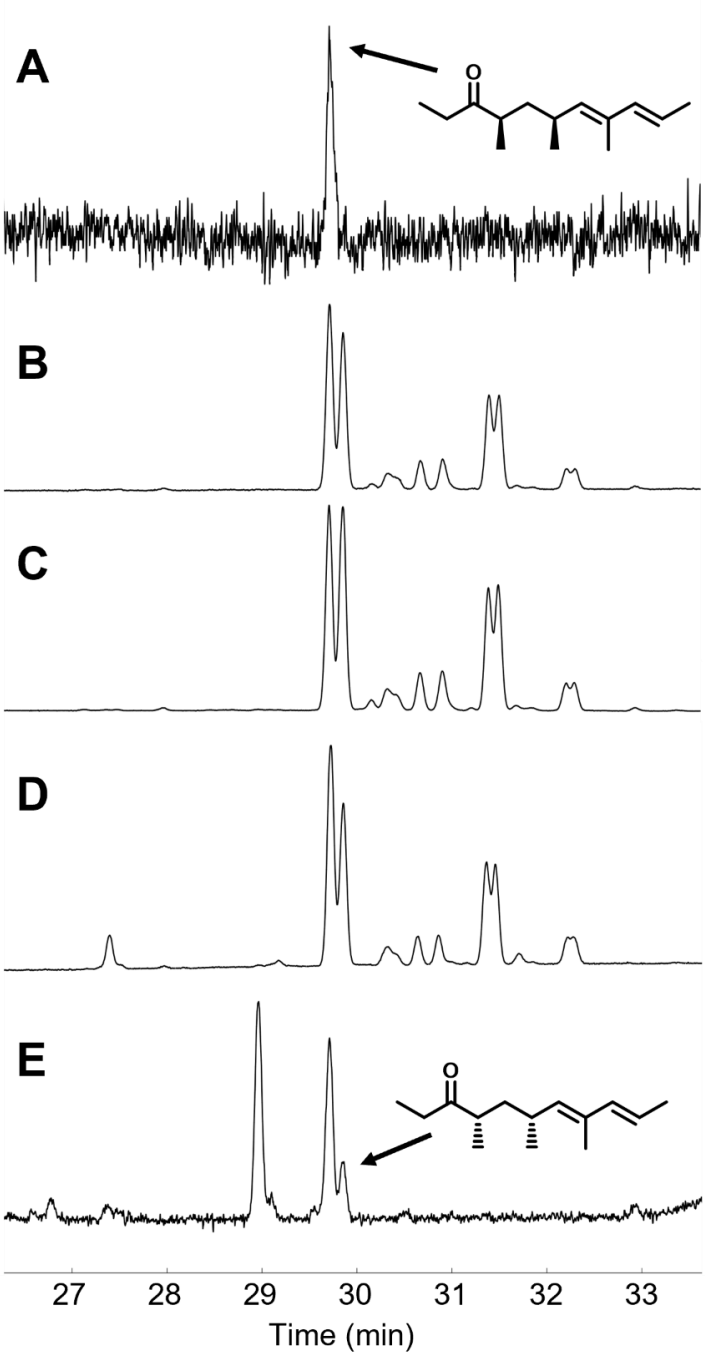

Figure 4.08 *A series of injections and co-injections of the insect-produced compound and synthetic standards revealed the absolute stereochemistry of the target compound: A) the insect-produced compound; B) co-injection of the racemic synthetic standard and insect-produced compound; C) racemic synthetic standard; D) co-injection of the racemic synthetic standard and the enantioenriched synthetic standard from* ***Scheme 4.04****; E) enantioenriched synthetic standard from* ***Scheme 4.08****.*

To verify the geometry of the trisubstituted diene and further confirm the identity of the insect-produced compound, the sample of racemic **4.01** partially purified by prep GC was subjected to NMR spectroscopy. A ^{1}H spectrum of the preparative GC sample contained the same peaks as were present in the ^{1}H spectrum of the insect-produced compound. Furthermore, the synthetic sample was large enough to be able to obtain a ^{1}H-^{1}H NOESY spectrum where two key pieces of information were obtained: (1) the presence of an NOE enhancement was observed between H-7 and H-9, and (2) there was no NOE enhancement between H-7 and H_3-14 (**Figure 4.09**). The NOE enhancement between H-7 and H-9 confirmed that the trisubstituted alkene had to be the (*E*)-configuration, because no enhancement would be expected for the corresponding (Z)-isomer. Conversely, an NOE enhancement between H-7 and H_3-14 would be expected if those groups were on the same side of the alkene, and such an enhancement was not seen.

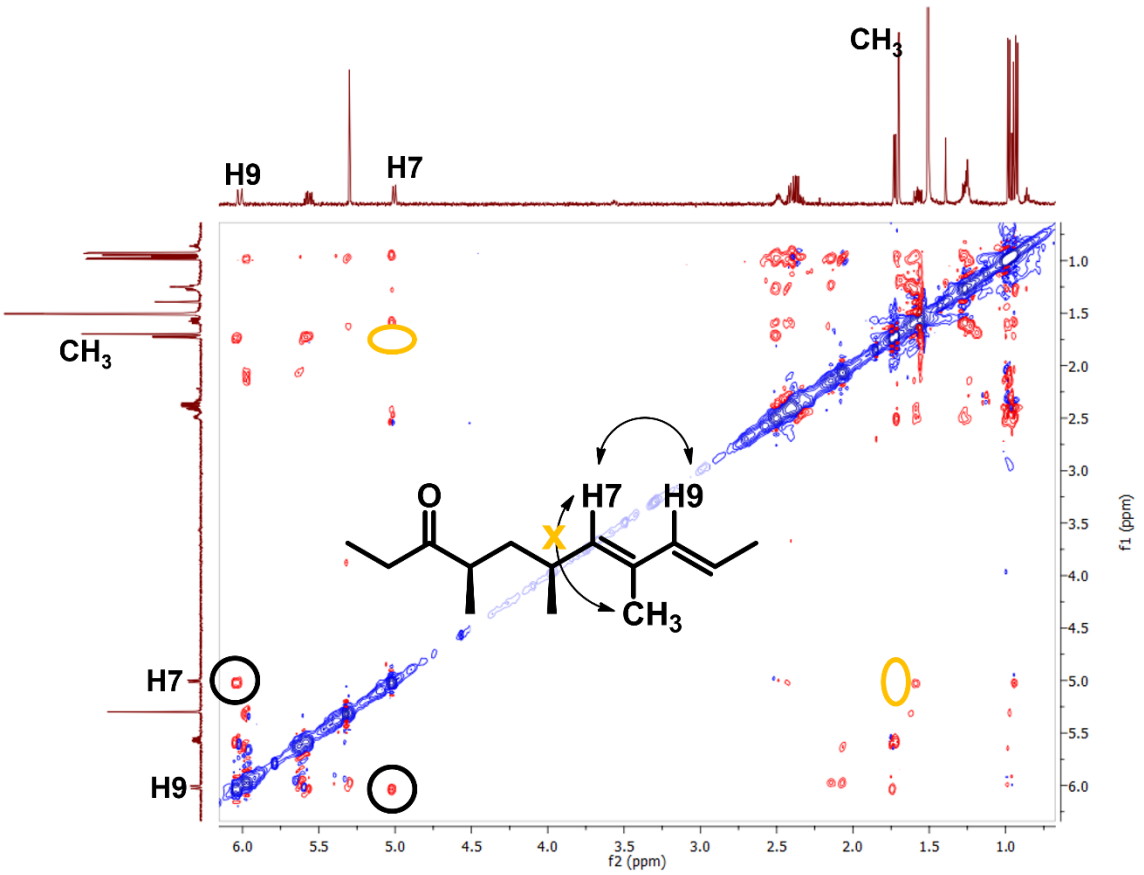

Figure 4.09 *^{1}H-^{1}H NOESY spectrum of the synthetic standard isolated by preparative GC, showing an NOE enhancement between H7 and H9, but not between H7 and the C14 methyl protons.*

In total, the data proved that the insect-produced compound was (4*R*,6*S*,7*E*,9*E*)-4,6,8-trimethylundeca-7,9-dien-3-one (**4.01, Figure 4.01**).

4.2.3 Pursuit of an Enantioselective, Scalable Synthetic Route

During the syntheses described above, significant problems were encountered with:

1. isolating the *syn*-dimethyl aldehyde **4.09** while minimizing epimerization,
2. synthesizing the secondary allylic triphenylphosphonium bromide salt, and
3. complications in the synthetic outcome of the Wittig coupling.

Specifically, these complications included: (1) low stereoselectivity in the Wittig olefination, (2) projected difficulty in separating the *syn*- and *anti*- diastereomers from each other, and (3) the presence of several homologs with molecular ions of *m/*z 194. Each of these factors individually, let alone combined, would make preparative scale liquid chromatographic purification of the desired product difficult if not impossible, and the overall yield would be minimal because so much of the crude product would consist of undesired byproducts. Consequently, I decided not to pursue this route for a preparative scale synthesis of the natural product.

4.2.4 Development of an Enantioselective Synthesis

The following disconnection (**Scheme 4.05**) was envisioned to be more suitable for an enantioselective synthesis.

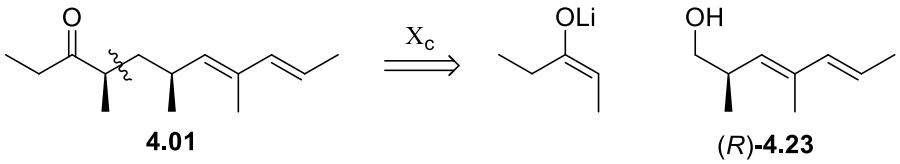

Scheme 4.05 *Retrosynthetic analysis of an enolate alkylation using a chiral auxiliary.*

Activation of dien-1-ol (*R*)-**4.23** by conversion to the iodide and use of a chiral auxiliary to induce chirality at the 4-position during enolate alkylation could furnish the desired pheromone candidate. Racemic dien-1-ol **4.23** was synthesized starting from ethyl acetate. Thus, reaction of ethyl acetate with an excess of propynylmagnesium bromide in THF (**Scheme 4.06**) gave diynol **4.24**. Reduction of diynol **4.24** with lithium aluminum hydride ($LiAlH_4$) formed a cyclic organoaluminum species[25] which upon hydrolysis produced an (*E*)-allylic alcohol.[26] A second reaction with $LiAlH_4$ afforded the (*E*,*E*)-dien-4-ol **4.25** stereospecifically. The dien-4-ol was then converted to stannyl ether **4.26.**

Lithium-tin exchange of the stannyl ether intermediate **4.26** resulted in a [2,3]-Wittig-Still rearrangement[27], producing dien-1-ol **4.23** as a single geometric isomer. Kinetic resolution of this β-branched primary alcohol with *Pseudomonas cepacia* lipase[28] then gave (*R*)-2-methylheptadienol, (*R*)-**4.23** in 91% ee. Straightforward conversion of this alcohol to an appropriate electrophile (e.g. the iodide analog (*R*)-**4.27**) then set the stage for an enantioselective alkylation to install the 3-pentanon-2-yl segment of the target molecule.

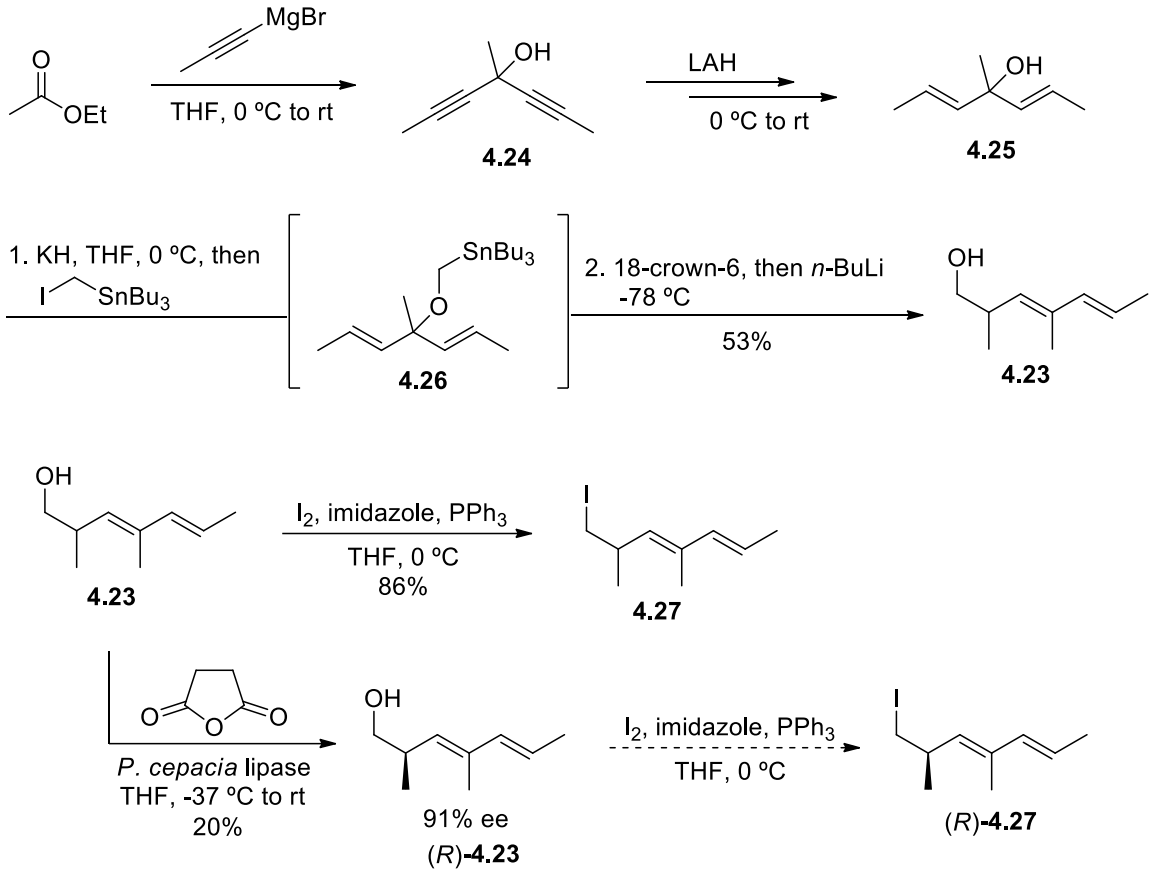

Scheme 4.06 *Synthetic route toward a suitable electrophile for enolate alkylation.*

In several experiments to probe the efficacy of different chiral auxiliaries for an enolate alkylation of iodide **4.27**, model reactions were run using a variety of alkyl electrophiles, monitoring the results by GC. Alkylation of benzyl and isopropyl Evans

oxazolidinones[29] with alkyl triflate and iodide model substrates met with little success (**Scheme 4.07**). I consistently encountered extensive decomposition of the chiral auxiliary, which led to the formation of the deacylated oxazolidinones via a ketene pathway.[30,31] As a result, alkylation of the free oxazolidinones was observed. Because I was not able to find conditions to prevent this decomposition, other chiral auxiliaries were explored.

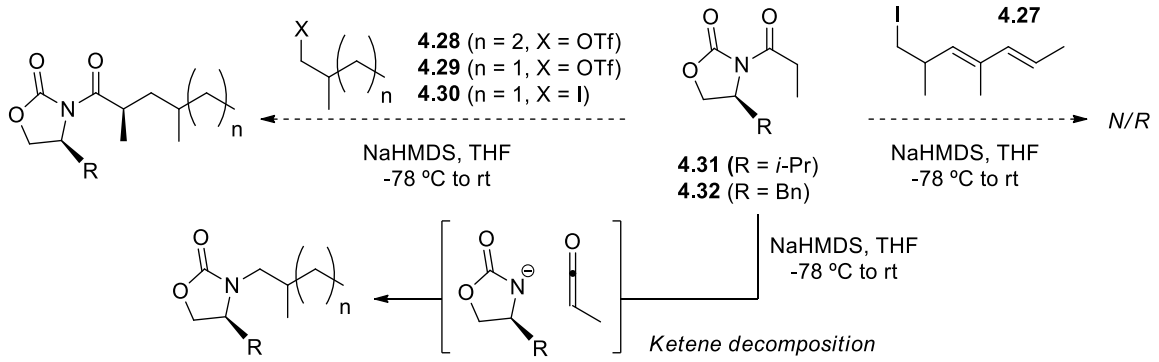

Scheme 4.07 *Unsuccessful attempts to alkylate Evans oxazolidinones with the crucial primary iodide **4.27** and several model substrates.*

Alkylation of a chiral *N*-amino cyclic carbamate (NCC) hydrazone **4.33** developed by the Coltart group[32–35] was successful when using a β-methyl branched alkyl iodide model substrate (**Scheme 4.08A**). This NCC hydrazone alkylation chemistry offered easier access to the 3-pentanon-2-yl moiety relative to Evans oxazolidinone alkylation chemistry, because the only step needed to complete the synthesis was a simple hydrolysis of the hydrazone product, with no anticipated epimerization. Many attempts were made to optimize the alkylation of NCC hydrazone **4.33** with the crucial iodide **4.27**, testing a wide set of reaction conditions (**Table 4.02**). However no set of conditions resulted in full consumption of iodide **4.27**, although in some cases, minor amounts of the desired product were obtained (**Scheme 4.08**). Forming a more reactive alkylation electrophile, such as the

triflate or mesylate analogs **4.38** and **4.39** respectively, proved to be problematic, resulting in extensive decomposition.

Table 4.02 *Efforts to optimize the conversion of iodide **4.27** to the desired product **4.34**.*

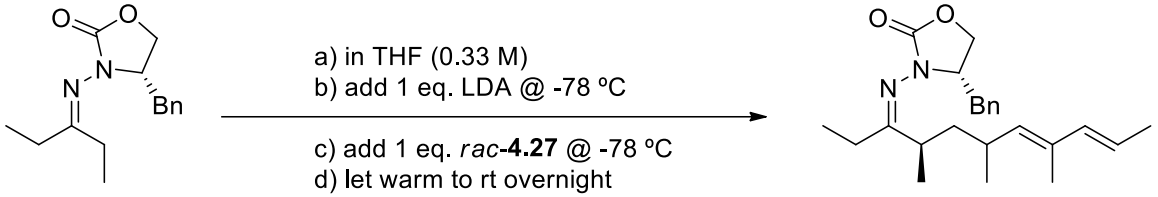

4.33 **4.34**

Expt #	Deviation from above conditions/ Notes	Form **4.34**? (Y/N)
K95a	n/a	N
K95b	Et_2O instead of THF	N
K95c	Et_2O instead of THF, warm to 0 ºC after b), then maintain at 0 ºC until d), ~25% conversion (by GC)	Y
K95d	Warm to 0 ºC after b) and maintain until d), ~40% conv.	Y
K95e	K95d conditions but NaHMDS instead of LDA, <5% conv.	Y
K95f	K95d conditions but 0.33 eq *rac*-**4.27**, K95d, ~40% conv.	Y
K95g	K95d conditions but NaHMDS instead of LDA, K95d	N
K95h	K95d conditions but 3 eq. *rac*-**4.27**, K95d, ~50% conv.	Y
K95i	K95d conditions but 1.5 eq LDA. ~50% conv.	Y
K95j	K95d conditions but Warm to -40 ºC after b) and maintain until d), 1.5 eq LDA	N
K95k	K95d conditions but add 1 eq. DMPU after b), 1.5 eq LDA	N
Several-month hiatus due to COVID-19 pandemic		
K95l	Repeat K95i	N
K95m	Repeat K95i, correcting for degraded titer of LDA	N
K95n	Repeat K95i, with freshly made LDA	N
K95o	Repeat K95i	N
K95p	Repeat K95i, let reach rt after b)	N
K95q	K95d conditions but 1.25 eq LDA, 0.5 eq *rac*-**4.27**	N
K95r	Repeat K95i, but with 2.5 eq *rac*-**4.27**	N

From the reactions that did produce some of the desired product, hydrolysis of the alkylated NCC hydrazone successfully produced the target enantiomer **4.01** in 74% ee. At this stage, my plan was to synthesize iodide (*R*)-**4.27**, conduct and purify future alkylation

reactions, recycle the unreacted starting material, and combine the alkylated NCC hydrazones for hydrolysis to the target compound. I also speculated that it might be possible to recrystallize the alkylated NCC hydrazone to increase the enantiomeric excess of the product, but in the event, recrystallization was not attempted for reasons described below.

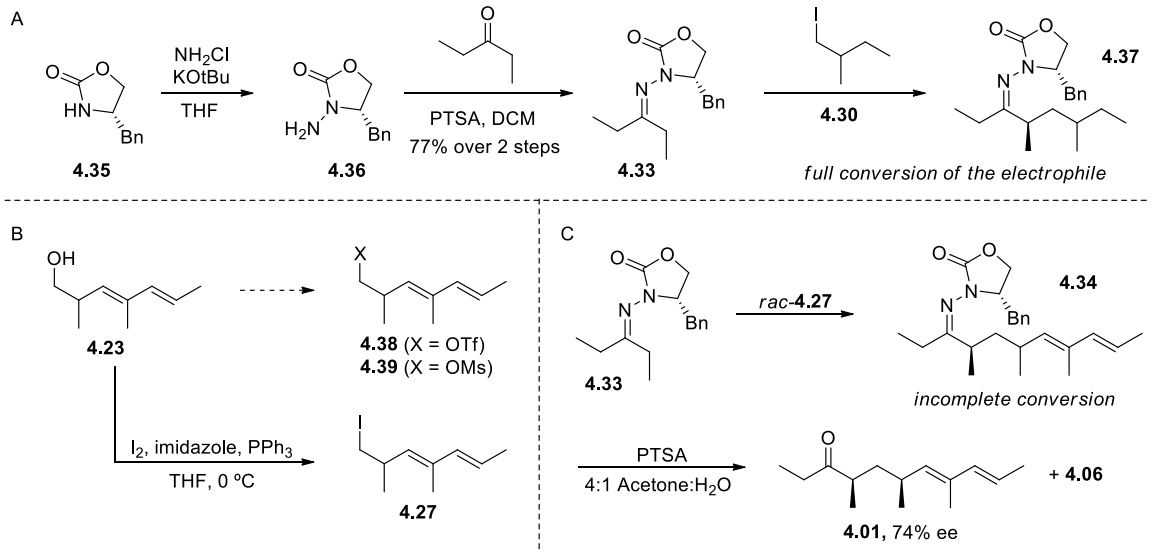

Scheme 4.08 *Attempted synthesis using an N-amino cyclic carbamate hydrazone for the enantioselective alkylation of a 3-pentanone derivative: A) synthesis of the chiral auxiliary and alkylation with model substrates; B) synthesis of electrophiles derived from dien-1-ol* ***4.23****; C) alkylation of the chiral auxiliary with the crucial dien-1-yl electrophile and subsequent hydrolysis.*

Returning to this reaction after a several-month hiatus, a number of attempts to reproduce the alkylation of the NCC hydrazone were unsuccessful (**Table 4.02**). Re-optimization with model substrate **4.30** led to slightly different conditions (1.5 eq of iodide **4.30**, and use of triphenylmethane as an indicator for formation of the aza-enolate). Applying this new set of NCC hydrazone alkylation conditions with use of **4.27** followed by hydrolysis to the ketone yielded a completely new product, with an apparent molecular

ion of *m/z* 240, 32 amu greater than the expected *m/z* 208. Suspicions that the NCC hydrazone starting material might have degraded over time were dispelled by NMR and GC-MS analyses of the hydrazone.

This byproduct was analyzed by high resolution mass spectrometry and confirmed the molecular weight to be 240 amu, as the $[M+H]^+$ was found to be 241.1454 amu, which could correspond to the molecular formulae (amu): $C_{14}H_{17}N_4$ (241.1453), $C_{16}H_{19}NO$ (241.1467), $C_{13}H_{21}O_4$ (241.1440), and $C_{11}H_{19}N_3O_3$ (241.1426). EI-GC/MS analysis of this unexpected product indicated several similarities with the target compound, including mass fragments of *m/z* 109 and 122 (compared to 107 and 122 of the insect produced compound, **Figure 4.03**), and NMR signals representing what appeared to be the same spin systems (**Figure 4.10**, compared to **Figure 4.05**). Several peaks in the ^1H NMR spectrum were shifted downfield, suggesting a heteroatom connecting the spin systems, however no molecular formulae seemed plausible given this spectral data. I have not yet been able to fully identify this unexpected byproduct, despite consultation with the Coltart group about possible side reactions.

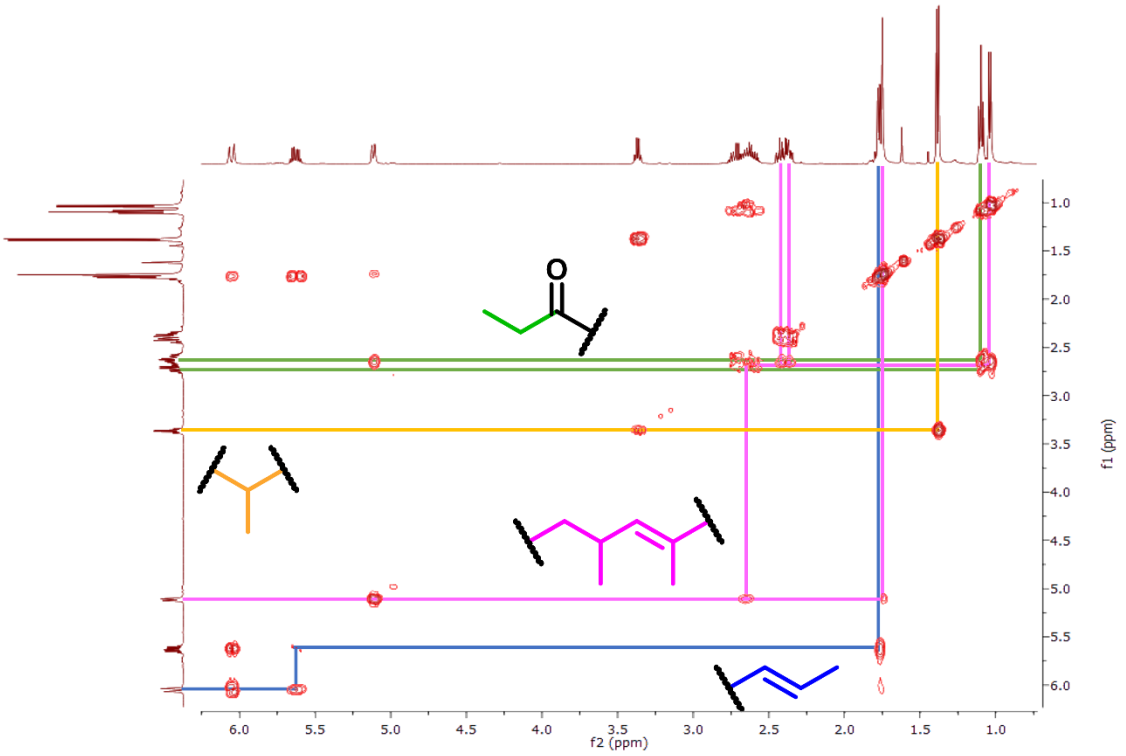

Figure 4.10 *^{1}H-^{1}H COSY NMR spectrum for the unexpected product showing spin systems similar to the insect-produced compound.*

Because I was not able to shift the selectivity back to the desired alkylation pathway, and because the yields had been poor and variable in the earlier instances in which the alkylation did appear to go correctly, I shelved the NCC hydrazone synthetic route in favor of the more established alkylation of pseudoephedrine-based Myers' auxiliary.[36–39]

4.2.5 Recent Developments in the Enantioselective Synthesis of 4.01

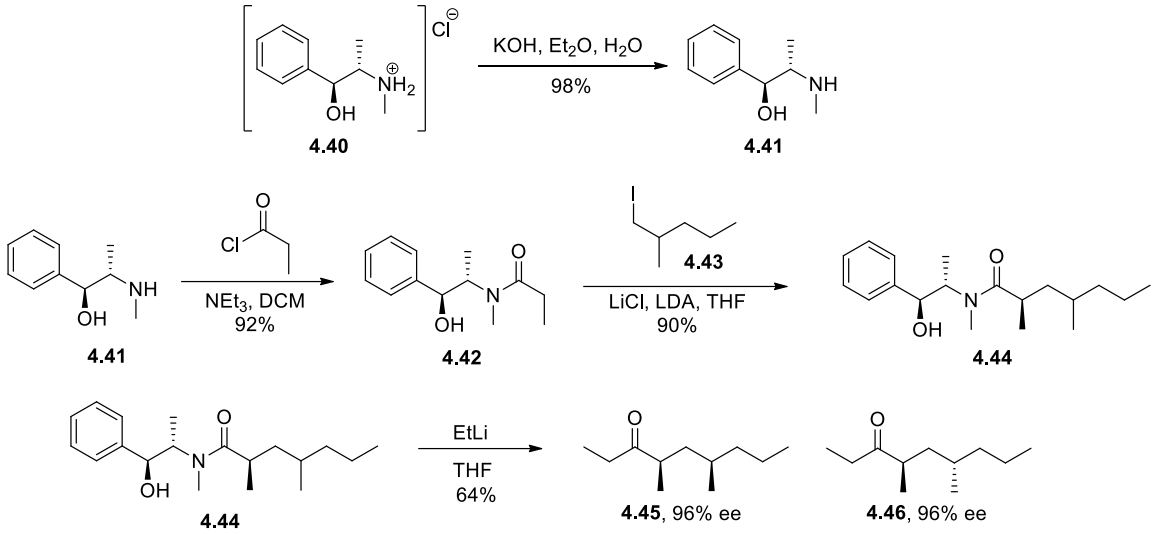

Scheme 4.09 *Model reactions towards the synthesis of **4.01** via use of Myers' auxiliary **4.42**.*

Synthesis of the pseudoephedrine-based Myers' auxiliary was facile (**Scheme 4.09**). Neutralization of the hydrochloride salt followed by acylation with propionyl chloride and recrystallization produced the auxiliary. The alkylation was optimized using iodide **4.43** as a model substrate and insight from previous literature reports.[36–39] Aside from insight from the literature, especially the call for rigorously dried LiCl, success was only achieved when using an excess of the enolate form of **4.42** and heating **4.42** and LiCl with a heat gun under vacuum, then backfilling with argon. This heating and backfill process was repeated three times, melting the auxiliary over the course of this reaction set up. Preliminary optimizations were conducted on a 0.25 mmol scale (relative to **4.43**) then scaled up to 1.3 mmol, producing **4.44** in 90% yield. Conversion of a sample of this alkylated auxiliary to the ethyl ketone produced two diastereomers, which when separated on GC with a chiral stationary phase, displayed enantiomeric excesses of 96%.

4.3 Conclusions

Efforts to synthesize **4.01** stereoselectively and on a larger scale with Myers' alkylation chemistry are currently underway. Presently, very low conversion but very high enantioselectivity are observed, though it has not been calculated due to difficulties fully resolving the enantiomers (see Supporting Information **4.6.41**). Assuming the enantioselective synthesis can be completed, the suspected ecological role of this compound in mediating aggregation-sex behavior for *Graphisurus fasciatus* will be tested in field trials. During the pursuit of the target molecule, a species of longhorn beetle in Brazil, *Eutrypanus dorsalis* (subfamily Lamiinae), also was found to produce the same compound. In particular, the compound from *E. dorsalis* had the same mass spectrum, and GC retention times on both chiral and achiral GC stationary phases as the compound from *G. fasciatus*, proving that the two species produce the identical compound. Although not congeners, both species are in the same tribe (Acanthocinini), and the presence of **4.01** in extracts of males of both species provides another example of conservation of pheromone structures among related cerambycid species. Because species in two genera have been shown to produce **4.01**, it seems likely that, despite continental differences in geographic origin, other species will be shown to produce **4.01**. Thus, a synthetic route toward **4.01** will be useful in determining the extent to which this compound may be shared among species within the tribe, in the Americas and possibly worldwide.

4.4 Methods

All solvents were Optima grade (Fisher Scientific, Pittsburgh PA, USA) unless otherwise noted. Anhydrous diethyl ether stabilized with BHT was purchased from Fisher Scientific. Solutions of crude reaction products were dried over anhydrous Na_2SO_4 and concentrated by rotary evaporation under partial vacuum unless otherwise noted. Vacuum flash chromatography and flash column chromatography were carried out on silica gel (230–400 mesh; Fisher Scientific). TLC analyses were conducted on aluminum-backed sheets of analytical silica gel 60 F_{254} (Merck, Darmstadt, Germany), and compounds were visualized by spraying with 10% phosphomolybdic acid in ethanol and heating. Yields are reported as isolated yields of chromatographically pure products unless otherwise noted. Mass spectra were obtained with an HP 6890 GC (Hewlett-Packard, now Agilent, Santa Clara CA, USA) equipped with a DB-17 column (30 m × 0.25 mm × 0.25 μ film; J&W Scientific, Folsom CA, USA) coupled to an HP 5973 mass selective detector, in EI mode (70 eV) with helium carrier gas. Purity was assessed by gas chromatography (unless otherwise noted) with an HP 5890 GC equipped with a DB-5 column (30 m × 0.25 mm × 0.25 μm film). Enantiomeric purity was assessed by gas chromatography with an HP 5890 GC equipped with a chiral stationary phase β-cyclodextrin column (Cyclodex-B, 30 m × 0.25 mm × 0.25 μm film + 2 m × 0.25 mm ID deactivated fused silica; J&W Scientific). NMR spectra were recorded as $CDCl_3$ solutions on either a Bruker Avance 500 or Bruker NEO 400 spectrometer (unless otherwise noted). Chemical shifts are reported in ppm relative to $CDCl_3$ (^1H 7.26 ppm; ^{13}C 77.0 ppm).

4.4.1 Acquisition of Insect-Produced Sample

Methylene chloride extracts of headspace volatiles collected from male *Graphisurus fasciatus* were obtained from Professor Lawrence Hanks, Dept. of Entomology, University of Illinois, Urbana-Champaign. The extracts were analyzed by GC-MS, and the two extracts that contained the largest amounts of the unknown compound were combined and concentrated down to ~10 ul in a conical-bottomed vial under a gentle stream of nitrogen. The whole sample was then injected splitless onto a DB-5 25 m x 0.53 mm ID Megabore GC column, over about 30 sec, after which the temperature program was started (50ºC/1 min, then 10 ºC/min to 250 ºC, hold 20 min), with the effluent split ~ 30:1 between the collection port and an FID detector. Injector and detector temperatures were 250 ºC, and the heated outlet was 200 ºC. Three fractions were taken from 5-15.9 min, then 15.9-18 min containing the desired compound, and 18-30 min. Fractions were collected in dry ice cooled glass capillaries, and the collected material was rinsed from the capillaries with a minimal volume of 99.96% deuterated CD_2Cl_2, then transferred to a 1 mm OD microbore NMR tube, for NMR analysis. NMR spectra were recorded on a Bruker NEO 600 spectrometer fitted with a microbore probe. Chemical shifts are reported in ppm relative to CD_2Cl_2 (^{1}H 5.30 ppm).

4.4.2 Racemic Synthesis of the Insect-Produced Compound via Key Wittig Olefination Step

Synthesis of Triesters 4.12

The following procedure was adapted from Paquette and Boulet.[16]

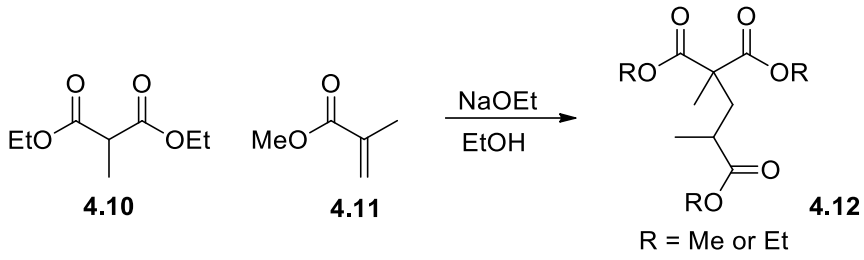

A dry flask was charged with dimethyl methylmalonate (33.4 g, 192 mmol), methyl methacrylate (21.2 g, 212 mmol), and absolute ethanol (40 mL). In a separate vessel, a solution of sodium ethoxide was prepared by portionwise addition of sodium metal (1.4 g) to ethanol (40 mL) cooled to 0 ºC and under argon. This mixture was stirred for 1 h at 0 ºC, warmed to room temperature, then added to the first flask over 30 min. The contents were stirred overnight at room temperature before adding glacial acetic acid (1.5 mL). The mixture was diluted with water (75 mL) and diethyl ether (80 mL). The layers were separated, and the aqueous layer was extracted with additional diethyl ether (2x40 mL). The combined organic layers were washed with brine, dried, and concentrated under reduced pressure to yield 51.63 g (approx. quant. yield) of a mixture of methyl/ethyl triesters **4.12**. This mixture was carried on to the next step without further purification.

Decarboxylation of triesters 4.12 to diacid 4.13

The following procedure was adapted from Lautens and Bouchain.[17]

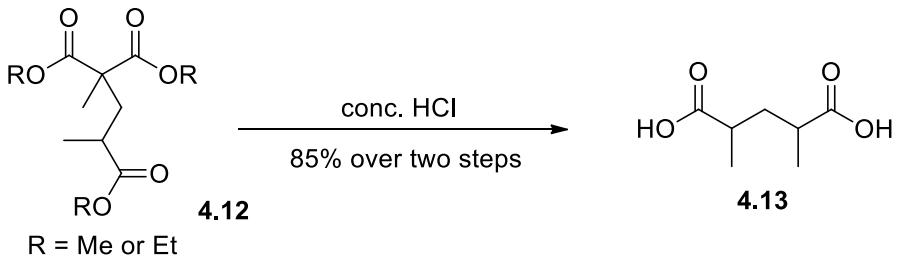

A flask was charged with a mixture of triesters **4.12** (44.5 g, ~177 mmol) then cooled to 0 ºC. Concentrated HCl (100 mL) was added to the flask, and the reaction was heated to 140 ºC and stirred overnight. Upon cooling to room temperature, white crystals precipitated out. The precipitate was isolated by vacuum filtration. More product was obtained by cooling the filtrate in a freezer (~-23 ºC) overnight and collecting the precipitate by vacuum filtration. In total, 24.06 g (85%) of the diacid **4.13** *syn*- and *anti*- diastereomers were obtained. ^{1}H NMR (400 MHz, $CDCl_3$, * = *syn*-diastereomer) δ 2.78 – 2.64 (m, 2H), 2.54 (dqd, *J* = 14.1, 7.0, 3.1 Hz, 2H)*, 2.11 (dt, *J* = 14.0, 11.5 Hz, 1H)*, 1.99 (dd, *J* = 6.3, 5.6 Hz, 2H), 1.49 (dt, *J* = 14.1, 3.1 Hz, 1H)*, 1.26 – 1.16 (m, 12H). ^{13}C NMR (101 MHz, $CDCl_3$) δ 183.19, 182.70, 39.37, 38.30, 36.57, 35.74, 18.47, 16.40.

Synthesis of *syn*-2,4-dimethylglutaric anhydride 4.09

The following procedure was adapted from Saicic.[18]

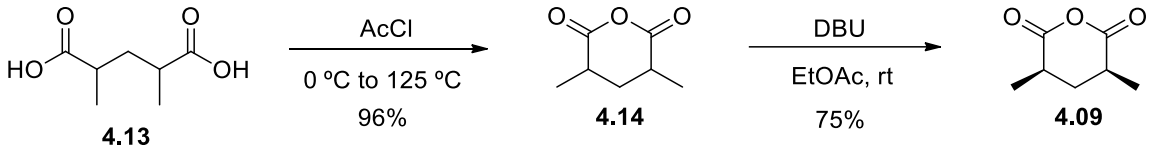

A dry flask was charged with diacid **4.13** (7.22 g, 45.1 mmol) and acetyl chloride (18.4 mL, 257 mmol). The reaction was stirred for 20 h at room temp. The excess acetyl chloride was distilled off under reduced pressure. The residue was diluted 2-fold with ethyl acetate, then DBU (1 drop) was added to the solution. The contents were stirred for 30 min at room temp, then left in a freezer (~-23 ºC) overnight. Crystals had formed which were isolated by vacuum filtration. The crystals were rinsed with cold EtOAc and the filtrate was concentrated under reduced pressure. No additional DBU was added and the recrystallization was repeated to eventually yield **4.09** (6.134 g, 96%, 97% isomerically

pure). ^{1}H NMR (400 MHz, $CDCl_3$) δ 2.81 – 2.63 (m, 2H), 2.06 (dt, *J* = 13.6, 5.3 Hz, 1H), 1.67 – 1.49 (m, 1H), 1.38 (t, *J* = 5.8 Hz, 3H). ^{13}C NMR (101 MHz, $CDCl_3$) δ 169.98, 37.00, 33.16, 15.93. EI-GC/MS *m/z* (%): 98 (13), 70 (13), 56 (100), 41 (9).

Reduction of anhydride 4.09 to lactone 4.15

The following procedure was adapted from Schregenberger and Seebach.[19] Initially, the reaction was run at -78 ºC not knowing that the reaction would not proceed until warmed to -60 ºC. The following account details excessive additions of lithium aluminum hydride which would likely be unnecessary had the reaction be warmed to -60 ºC.

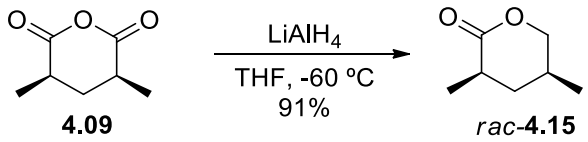

4.09 *rac*-**4.15**

A dry flask flushed with Ar was charged with lithium aluminum hydride (0.481 g, 12.7 mmol) and freshly distilled THF (60 mL), then cooled to -78 ºC. The anhydride **4.09** (2.97 g, 20.9 mmol) was added in portions over 5 min. Over the next 2 d, additional portions of lithium aluminum hydride were added: 160 mg, 400 mg, 490 mg. The reaction was then warmed to -60 ºC and maintained at that temperature, at which point the lactone product began to be observed. Upon completion, the reaction was quenched with 6 M HCl then stirred for 15 min while the reaction was warmed to rt. The contents were diluted with water and extracted with ether. The organic layer was washed with brine, dried, and concentrated. The crude product was purified by vacuum flash chromatography (loaded with hexanes, then eluted with diethyl ether) to yield 2.449 g (91%) of lactone *rac*-**4.15**. ^{1}H NMR (400 MHz, $CDCl_3$) δ 4.25 (ddd, *J* = 11.1, 4.8, 2.2 Hz, 1H), 3.85 – 3.78 (m, 1H),

2.53 – 2.40 (m, 1H), 2.13 – 1.95 (m, 2H), 1.21 – 1.19 (d, J = 7.0 Hz, 3H), 1.17 (m, 1H), 0.92 (d, J = 6.6 Hz, 3H). ^{13}C NMR (126 MHz, $CDCl_3$) δ 174.61, 74.94, 36.76, 35.35, 28.61, 17.34, 16.97. EI-GC/MS *m/z* (%): *anti*-**4.15**: 128 (M^+, 22), 98 (6), 70 (10), 69 (66), 56 (100), 42 (37). *syn*-**4.15**: 128 (M^+, 21), 98 (6), 69 (58), 56 (100), 42 (38).

Esterification of lactone 4.15 to hydroxyester 4.16

The following procedure was adapted from Huckstep and Taylor.[20] NMR identification of the *syn*-[40] and *anti*-[41] stereoisomers was facilitated by previous literature reports.

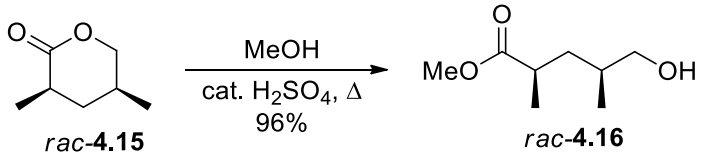

rac-**4.15** *rac*-**4.16**

A solution of lactone **4.15** (2.337 g, 18.2 mmol) and MeOH (47 mL) was treated with conc. H_2SO_4 (3 drops) and refluxed overnight, then cooled with an ice/salt bath and solid $NaHCO_3$ (1 g) was added. The contents were stirred for 10 min, then filtered, and the filtrate was concentrated under vacuum. To prevent the hydroxyester from recyclizing, this material was used without further purification, and was taken up in dichloromethane (DCM, 15 mL) for the next step. Quick ^{1}H-NMR and GC-MS identification of the mixture of isomers was performed based on the following data. ^{1}H NMR (400 MHz, $CDCl_3$) *anti*-**4.16**: δ 3.667 (s, 3H), 1.17 (d, J = 7.0 Hz, 3H), 0.91 (d, J = 6.7 Hz, 3H). *syn*-**4.16**: δ 3.674 (s, 3H), 1.18 (d, J = 7.0 Hz, 3H), 0.94 (d, J = 6.7 Hz, 3H). EI-GC/MS *m/z* (%): *anti*-**4.16**: 142 (4), 129 (23), 111 (6), 101 (22), 88 (100), 83 (46), 73 (22), 69 (38), 59 (29), 55 (29),

41 (23). *syn*-**4.16**: 142 (2), 129 (16), 111 (7), 101 (20), 88 (100), 83 (42), 73 (19), 69 (30), 59 (25), 55 (27).

Representative oxidation of hydroxyester 4.16 to aldehyde 4.08

The following procedure was adapted from Hoffmann et al.[21]

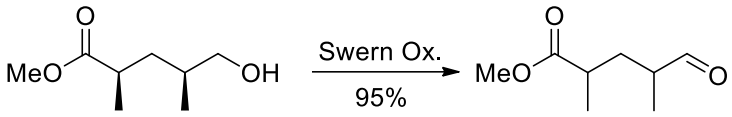

rac-**4.16** *2:1 syn:anti* *rac*-**4.08**

A dry flask flushed with Ar containing a solution of oxalyl chloride (2.15 mL, 25.2 mmol, 1.4 eq) in DCM (45 mL) was cooled to -78 ºC. A solution of dimethylsulfoxide (1.93 mL, 27 mmol, 1.5 eq) in DCM (2.5 mL) was added dropwise. The contents were stirred for 30 min, then the previously prepared solution of **4.16** was added dropwise over 1 h. The contents were stirred for an additional 30 min before adding triethylamine (12.3 mL, 90 mmol, 5 eq). The reaction was warmed to rt, and diluted sequentially with 27 mL water, 9 mL diethyl ether, and 45 mL pentane. The organic layer was washed with brine (25 mL), dried, and concentrated. The crude material was purified by vacuum flash chromatography (30% Et_2O/pentanes) to yield aldehyde **4.08** (1.41 g, 50%). The identity of the product was verified on the basis[41] of the aldehyde HCO and CH_3O- peaks in the ^{1}H-NMR (400 MHz, $CDCl_3$) δ 9.62 (*anti*-**4.08**; d, *J* = 1.6 Hz, 1H), 9.59 (*syn*-**4.08**; d, *J* = 1.8 Hz, 1H); and mass spectral data. EI-GC/MS *m/z* (%): *anti*-**4.08**: 127 (18), 126 (20), 101 (13), 98 (10), 88 (100), 73 (12), 69 (21), 59 (20), 57 (25), 56 (27), 43 (28). *syn*-**4.08**: 127 (19), 126 (18), 101 (13), 98 (10), 88 (100), 73 (11), 69 (20), 59 (20), 57 (26), 56 (25), 43 (28).

Bromination of 3-penten-2-ol

The following procedure was adapted from Zhang et al.[42]

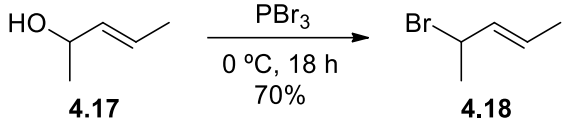

A dry flask flushed with Ar containing a solution of (*E*)-3-penten-2-ol (5.0 g, 58 mmol) in diethyl ether (60 mL) was cooled to 0 ºC. Phosphorus tribromide (10 g, 37 mmol) was added dropwise over 30 min and the mixture was stirred for 3 h at 10 ºC then slowly warmed to rt overnight. The reaction contents were poured onto ice (80 g) then transferred to a separatory funnel. The contents were washed sequentially with water, sat. aq. $NaHCO_3$, and brine, and the organic layer was dried and concentrated. The bromide product was purified by Kugelrohr distillation (approx. bp 50 ºC, 60 mm Hg,) yielding 6.01 g (70%) of **4.18**. ^{1}H NMR (400 MHz, $CDCl_3$) δ 5.78 – 5.65 (m, 2H), 4.70 (p, J = 6.8 Hz, 1H), 1.77 (d, J = 6.7 Hz 3H), 1.71 (d, J = 5.0 Hz, 3H). ^{13}C NMR (101 MHz, $CDCl_3$) δ 134.31, 127.23, 50.43, 26.21, 17.41. EI-GC/MS *m/z* (%): 150 (M^+ (^{81}Br), <1%), 148 (M^+ (^{79}Br), <1%), 135 (<1%), 133 (<1%), 69 (100), 53 (13), 41 (69).

Formation of phosphonium salt Wittig olefination partner 4.19

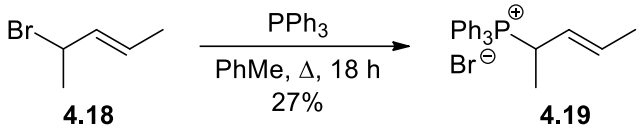

A dry flask was charged with bromide **4.18** (6.00 g, 40.27 mmol), triphenylphosphine (10.56 g, 40.27 mmol), and dry toluene (45 mL), then flushed with Ar and refluxed overnight under Ar. The following day, the reaction was allowed to cool,

producing a glassy amorphous solid. The supernatant was decanted and then the flask was subjected to Kugelrohr distillation. Upon heating the flask to 110 ºC under a high vacuum (0.1 mm Hg), the amorphous solid began to solidify into a translucent pale-yellow mass. This material (4.49 g, 10.9 mmol, 27%) was collected and used without further purification. ^{1}H NMR (400 MHz, $CDCl_3$) δ 8.06 – 7.10 (m, 15H), 6.43 – 6.30 (m, 1H), 6.20 (m, 1H), 5.28 – 5.11 (m, 1H), 1.66 – 1.59 (m, 3H), 1.44 (dd, *J* = 19.1, 6.9 Hz, 3H). Partial ^{13}C NMR (101 MHz, $CDCl_3$) δ 121.96, 117.96 (d, *J* = 82.9 Hz), 30.52 (d, *J* = 44.4 Hz), 18.41, 15.03.

Wittig olefination of partners 4.19 and 4.08

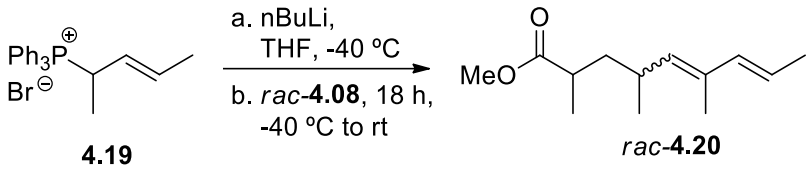

4.19 *rac*-**4.20**

A dry flask flushed with Ar was charged with the phosphonium salt **4.19** (2.704 g, 6.57 mmol) and THF (60 mL) then cooled to -40 ºC. A solution of *n*-BuLi (3.69 mL, 5.91 mmol, 1.6 M in THF) was added dropwise over 30 min, and the solution progressively turned vivid orange. The reaction was stirred for 2 h maintaining this temperature as the mixture turned blood red. Then, a solution of aldehyde **4.08** (421 mg, 2.66 mmol) in THF (5 mL) was added over 1 h. The reaction was stirred overnight and allowed to warm to room temperature, eventually turning cloudy and pale orange in color. The reaction was quenched with sat. aq. NH_4Cl and extracted with hexanes (3x70 mL). The organic layer was washed with brine, then dried and concentrated. The crude oil was taken up in hexanes for vacuum flash chromatography (4% EtOAc/Hex), producing approximately 300 mg of a mixture containing the ethyl esters **4.20**. The success of the reaction was determined by

EI-GC/MS *m/z* (%): (*E*,*E*)-*syn*-**4.20**: 210 (M^+, 32), 179 (5), 163 (5), 151 (7), 139 (4), 135 (10), 123 (20), 109 (100), 107 (65), 91 (13), 88 (17), 81 (18), 79 (16), 77 (11), 67 (30), 55 (11).

Synthesis and Alkylation of Weinreb Amide Analogs of 4.20

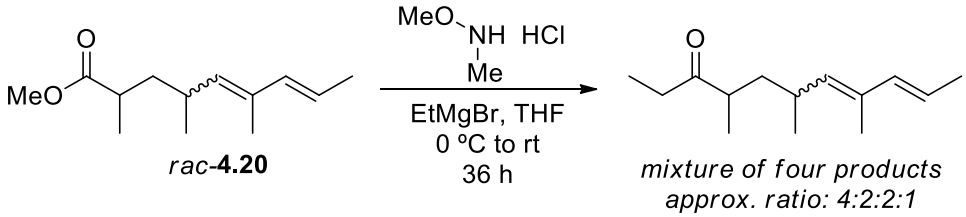

A dry flask was charged with THF (20 mL), *N*,*O*-dimethylhydroxylamine hydrochloride (146 mg, 1.5 mmol), and the fractions of the Wittig olefination product mixture containing methyl esters **4.20** (<1 mmol), then cooled to 0 ºC. A solution of ethylmagnesium bromide (10 mL, 10 mmol, 1 M in THF) was added dropwise over 1 h, monitoring for the formation of the ketone by GC. Additional batches of EtMgBr (6.5 mmol) were added over several days, monitoring the progress of the reaction until no further change was observed. Saturated aqueous NH_4Cl (2.8 mL) was then added, the mixture diluted with pentanes (40 mL), and the layers were separated. The organic layer was washed with brine, dried, and concentrated. The resulting oil was purified by vacuum flash chromatography (2.5% EtOAc/Hex). The fractions containing the target compound **4.01** were combined and partially purified by preparative GC on an HP 5890 GC equipped with a DB-5 column (25 m × 0.53 mm × 5 µm film, Agilent, Santa Clara CA, USA), collecting fractions in dry ice cooled capillaries. Runs were conducted splitless with a head pressure of 9 psi and with a temperature program starting at 100 ºC rising by 3 ºC/min to 200 ºC, then rising by 20 ºC/min to 250 ºC, hold for 20 min. Material eluting from about

23.40 min to 24.00 min which contained the desired product was rinsed from the collection capillary with CD_2Cl_2 for NMR analysis. Though the preparative GC fraction contained additional chemical species, the major constituent provided an excellent match to the retention time and mass spectrum, and ^{1}H-NMR compared to that of the insect-produced compound: ^{1}H NMR (600 MHz, CD_2Cl_2) δ 5.95 (d, *J* = 14.2 Hz, 1H), 5.56 (m, 1H), 5.00 (d, *J* = 9.9 Hz, 1H), 2.52 – 2.44 (m, 2H), 2.44 – 2.31 (m, 2H), 1.73 (d, *J* = 6.5 Hz, 3H), 1.70 (s, 3H), 1.63 – 1.54 (m, 1H), 1.28 – 1.19 (m, 1H), 1.01 – 0.89 (m, 9H). EI-GC/MS *m/z* (%): 208 (9), 151 (2), 122 (24), 107 (100), 91 (7), 79 (6), 67 (9), 57 (7).

4.4.3 Enantioselective Modifications of the Racemic Synthesis of the Insect-Produced Compound

Esterification of Anhydride 4.09

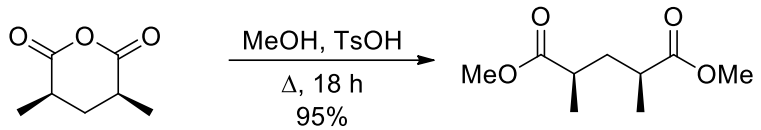

4.09 **4.21**

A dry flask was charged with *syn*-**4.09** (4.06 g, 28.6 mmol), anhydrous MeOH (89 mL), and PTSA (407 mg, 2.1 mmol) and heated to reflux overnight. The methanol then was removed by rotary evaporation, the residue was diluted in diethyl ether, washed with sat. aq. $NaHCO_3$ then brine, dried, and concentrated to yield 5.13 g (95%) of pure dimethyl ester **4.21**. ^{1}H NMR (400 MHz, $CDCl_3$) δ 3.67 (s, 6H), 2.55 – 2.44 (m, 2H), 2.14 – 2.06 (dt, *J* = 13.8, 7.8 Hz, 1H), 1.47 (dt, *J* = 13.8, 6.8 Hz, 1H), 1.16 (t, *J* = 7.4 Hz, 6H). ^{13}C NMR (101 MHz, $CDCl_3$) δ 176.55, 51.64, 37.28, 17.26. EI-GC/MS *m/z* (%): 157 (54), 129

(47), 128 (100), 113 (39), 101 (29), 97 (10), 88 (43), 73 (32), 69 (67), 59 (40), 56 (23), 41 (21).

Desymmetrization of Diester 4.21 with α-Chymotrypsin

The following procedure was adapted from Mohr et al.[24] and Aldrich et al.[23]

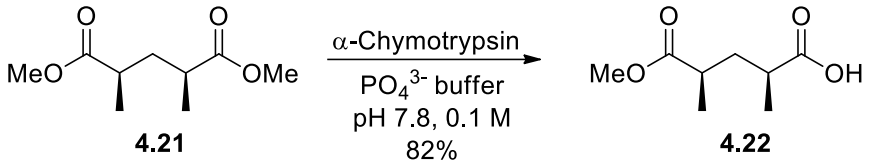

A flask was charged with dimethyl ester **4.21** (4.64 g, 24.7 mmol), aqueous phosphate buffer (0.1 M, pH 7.8, 150 mL), and α-chymotrypsin (900 mg, MilliporeSigma, St. Louis, Missouri, USA). The pH of the reaction was stabilized around pH 7.7 over a period of 8 d with a pH sensitive power relay connected to a syringe pump set to dispense a solution of 1 M NaOH into the reaction vessel. When all the starting material had been consumed, the reaction was acidified with conc. HCl to pH 2.1, and the aqueous layer was extracted with diethyl ether (3x100 mL). The combined organic layer was concentrated under reduced pressure and residual methanol was removed by Kugelrohr distillation, leaving 3.535 g (82%) of the hemiester **4.22** which was used without further purification. ^{1}H NMR (400 MHz, $CDCl_3$) δ 3.67 (s, 3H), 2.61 – 2.46 (m, 2H), 2.18 – 2.07 (m, 1H), 1.49 (dt, J = 13.8, 6.8 Hz, 1H), 1.22 (d, J = 7.0 Hz, 3H), 1.19 (d, J = 7.0 Hz, 3H). ^{13}C NMR (101 MHz, $CDCl_3$) δ 181.63, 176.52, 51.68, 37.23, 37.11, 36.92, 17.23, 17.14. EI-GC/MS *m/z* (%):156 (3), 143 (29), 142 (15), 128 (52), 114 (55), 101 (34), 97 (12), 88 (41), 73 (13), 69 (100), 69 (39), 56 (50), 45 (43), 41 (46).

Selective Reduction of Hemiester 4.22 with Borane-Dimethyl Sulfide Complex

The following procedure was adapted from Hoffmann et al.[40]

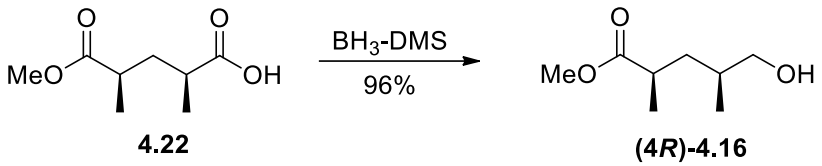

4.22 **(4*R*)-4.16**

A dry flask flushed with Ar was charged with the hemiester **4.22** (3.1 g, 17.8 mmol) and anhydrous diethyl ether (30 mL), then cooled to 0 ºC. Borane-dimethyl sulfide complex (2.2 mL, 23.2 mmol) was added dropwise over 40 min during which gas was initially produced. The reaction was stirred at this temperature for 1 h, then diluted slowly with water (20 mL) and stirred until no further gas evolution was observed. The mixture was extracted with diethyl ether (4x15 mL), washed with brine, dried over anh. Na_2SO_4, and concentrated under vacuum, yielding 2.747 g (96%) of the hydroxyester. This product was quickly taken up in CH_2Cl_2 (30 mL) to prevent lactonization and used without further purification. ^{1}H NMR (400 MHz, $CDCl_3$) δ 3.67 (s, 3H), 3.53 – 3.37 (m, 2H), 2.62 – 2.49 (m, 1H), 1.83 (ddd, J = 13.9, 9.6, 5.4 Hz, 1H), 1.59 (m, 1H), 1.23 – 1.11 (m, 4H), 0.94 (d, J = 6.7 Hz, 3H). ^{13}C NMR (101 MHz, $CDCl_3$) δ 177.51, 67.86, 51.62, 37.45, 37.38, 34.05, 18.30, 15.23. EI-GC/MS *m/z* (%): 142 (3), 129 (16), 111 (6), 101 (19), 88 (100), 83 (40), 73 (18), 69 (29), 59 (22), 55 (25).

4.4.4 Formation of Crucial Iodide 4.27 for Key Enolate Alkylation Step

Alkynylation of Ethyl Acetate

The following procedure was adapted from Shi et al.[26]

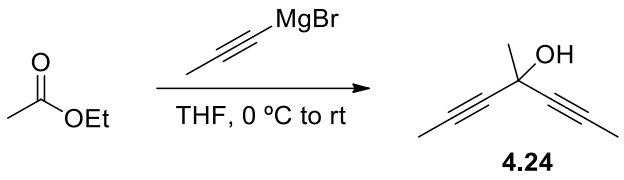

4.24

A dry flask flushed with Ar was cooled to 0 ºC and charged with a solution of propynylmagnesium bromide (800 mL, 400 mmol, 0.5 M in THF) by cannula. Ethyl acetate (15.8 mL, 162 mmol) was added dropwise over 2 h, maintaining the temperature for the duration of the addition. The reaction was allowed to warm slowly to room temperature overnight. The reaction contents then were poured into ice-chilled sat. aq. NH_4Cl (400 mL). The aqueous layer was extracted with diethyl ether (2x150 mL), then the combined organic layer was washed with brine, dried, and concentrated. The residue was taken up in pentanes (200 mL) and washed with brine (2x100 mL), then dried and concentrated again, producing a solution of the diyne **4.24** contaminated with THF. ^{1}H NMR (500 MHz, $CDCl_3$) δ 1.85 (s, 3H), 1.70 (s, 3H). ^{13}C NMR (126 MHz, $CDCl_3$) δ 81.15, 78.58, 60.04, 32.32, 3.56. EI-GC/MS *m/z* (%): 122 (M^+, 1), 121 (7), 107 (100), 79 (11), 77 (21), 67 (28), 63 (7), 51 (8), 43 (18).

Reduction of Diynol 4.24 with Lithium Aluminum Hydride

The following transformation was accomplished over two steps, based on Shi et al.[26]

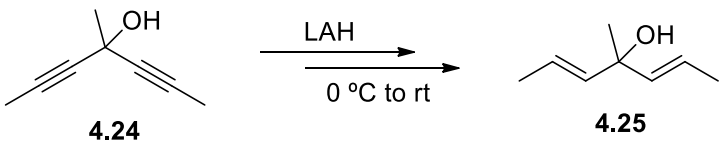

4.24 **4.25**

A dry flask flushed with Ar was charged with dry THF (475 mL), cooled to 0ºC, and $LiAlH_4$ (10 g, 264 mmol) was added in portions. A solution of the diynol **4.24** (16.69

g, 137 mmol) in THF (40 mL) then was added dropwise over 90 min at room temperature. When the reaction had reached full conversion, the reaction was quenched by the sequential addition of water (10.52 mL), 20% NaOH (7.89 mL), and water (36.82 mL), followed by stirring for 1 h.[43] The resulting slurry was filtered, the filter cake was rinsed with ether, and the combined filtrate was concentrated, yielding 16.7 g (135 mmol, 99%) of partially reduced material.

Another dry flask flushed with Ar was charged with $LiAlH_4$ (10 g, 264 mmol) and dry THF (450 mL). A solution of the enynol (16.7 g) in THF (40 mL) was added to the flask over 1 h at room temperature. The next morning, when some starting material was still present, an additional portion of $LiAlH_4$ (1 g, 26.4 mmol) was added and the contents stirred for 6 h at which point the reaction had reached completion. The reaction was quenched and worked up as described above, with the sequential addition of water (11.75 mL), 20% NaOH (8.81 mL), and water (41.1 mL), and stirring. The slurry was filtered, the filter cake was rinsed with ether, and the combined filtrate was concentrated under reduced pressure yielding a biphasic concentrate. The mixture was taken up in pentanes (200 mL), washed with brine (2x100 mL), dried, and concentrated again, yielding 13.4 g (79%) of the (*E,E*)-dien-4-ol **4.25** which was used without further purifcation. ^{1}H NMR (400 MHz, $CDCl_3$) δ 5.70 – 5.52 (m, 4H), 1.69 (dd, J = 6.0, 1.1 Hz, 6H), 1.32 (s, 3H). ^{13}C NMR (101 MHz, $CDCl_3$) δ 137.31, 123.11, 72.50, 28.20, 17.62. EI-GC/MS *m/z* (%): 126 (M^+, 5), 111 (87), 97 (20), 93 (24), 91 (23), 85 (33), 83 (46), 77 (25), 72 (19), 69 (29), 67 (37), 55 (63), 43 (100), 41 (40).

[2,3]-Wittig-Still Rearrangement of dien-4-ol 4.25

The following procedure was adapted from Millar et al.[27]

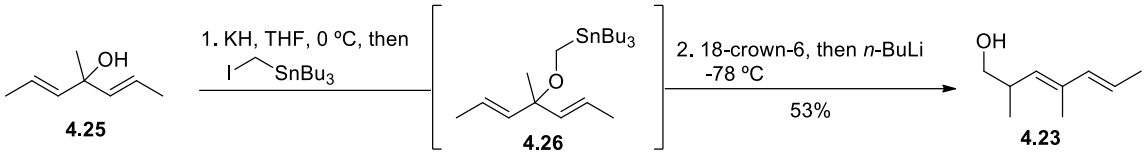

A dry flask flushed with Ar was charged with 30% potassium hydride suspended in mineral oil (2 g, 15 mmol). The KH suspension was rinsed with pentanes (3x20 mL), removing the supernatant after each aliquot. The flask was cooled to 0 ºC, then dry THF (100 mL) was added slowly. A solution of (*E*,*E*)-dien-4-ol **4.25** (1.059 g, 6 mmol) in THF (12 mL) was added dropwise over 30 min. The reaction was warmed to rt then stirred for 30 min. 18-Crown-6 (1.35 g, 5.11 mmol) was added in portions over 1 min and the reaction stirred for 15 min. Then, tributyl(iodomethyl)stannane (2 mL, 8 mmol) was added dropwise over 30 min, and the mixture was cooled to -78 ºC. A solution of *n*-BuLi (9 mL, 8 mmol, 2.2 M in hexanes) was added dropwise over 30 min. The reaction was complete in 5 min, and was quenched with sat. aq. NH_4Cl (4 mL) followed by slow warming to rt. The mixture was diluted with half saturated brine (100 mL) and the aqueous layer was extracted with hexanes (2x50 mL). The combined organic layers were washed with brine, dried, and concentrated, then taken up in hexanes for vacuum flash chromatography (5-10% EtOAc/Hex) yielding dien-1-ol **4.23** (441 mg, 53%). ^{1}H NMR (500 MHz, $CDCl_3$) δ 6.08 (d, *J* = 15.0 Hz, 1H), 5.71 – 5.58 (m, 1H), 5.11 (d, *J* = 9.5 Hz, 1H), 3.50 (dd, *J* = 10.4, 5.9 Hz, 1H), 3.37 (dd, *J* = 10.4, 8.0 Hz, 1H), 2.74 (m, 1H), 1.78 (d, *J* = 0.8 Hz, 3H), 1.77 (dd, *J* = 7.0, 0.9 Hz , 3H), 0.96 (d, *J* = 6.7 Hz, 3H). ^{13}C NMR (126 MHz, $CDCl_3$) δ 135.71,

135.52, 131.96, 123.37, 67.84, 35.51, 18.16, 16.96, 12.92. EI-GC/MS *m/z* (%): 140 (M^+, 29), 125 (1), 109 (100), 91 (9), 81 (17), 67 (46), 55 (14), 41 (13).

Lipase Kinetic Resolution of dien-1-ol 4.23

The following transformation was based on the report from Wang et al.[28]

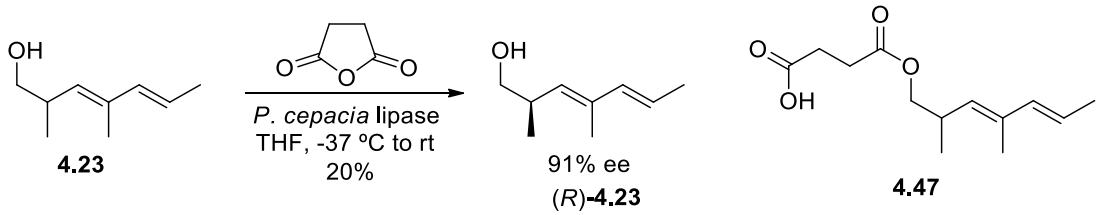

A flask was charged with **4.23** (2.1 g, 15 mmol), THF (15 mL), *Pseudomonas cepacia* lipase (300 mg, MilliporeSigma, St. Louis, Missouri, USA), and succinic anhydride (750 mg, 7.50 mmol), then cooled to -37 ºC. The reaction was stirred and allowed to reach room temperature overnight. Due to quarantine requirements imposed by the COVID-19 pandemic, the stirring was stopped at 54 h, sealed, and stored at -23 ºC for about three months. Analysis of the products on a Cyclodex B GC column revealed a 66% ee of the free alcohol. An additional batch of succinic anhydride (75 mg, 0.75 mmol) was added but no further reaction was observed. The lipase was filtered off via a celite pad, and the pad was rinsed with THF (2 mL). A fresh batch of *P. cepacia* lipase (300 mg) was added to the flask though no further reaction was observed overnight. Over the next 3 d, a batch of succinic anhydride (100 mg, 1.0 mmol) was added each day eventually reaching a 91% ee of the free alcohol. The reaction contents were diluted with hexanes (50 mL) and the organic layer was washed with a solution of Na_2CO_3 (1 M, 30 mL). The aqueous layer was extracted with hexanes (40 mL), then the combined organic layers were washed with brine (2x30 mL), dried, and concentrated producing a crude oil enriched in (*R*)-**4.23**.

The aqueous layer was made basic with NaOH (5 g) and stirred to hydrolyze the succinate **4.47**. The free alcohol enriched in (*S*)-**4.23** was subjected to the same kinetic resolution with THF (15 mL), *P. cepacia* lipase (300 mg), and succinic anhydride (500 mg, 5.00 mmol). Succinic anhydride was added at the following time points: 200 mg at 3 d, 100 mg at 4 d. On day 5, the reaction was worked up as described above.

The combined portions enriched in (*R*)-**4.23** were purified by Kugelrohr distillation (approx. bp 56 ºC, 0.1 mm Hg), yielding 536 mg of (*R*)-**4.23** (26%, 91% ee).

Iodination of dien-1-ol 4.23

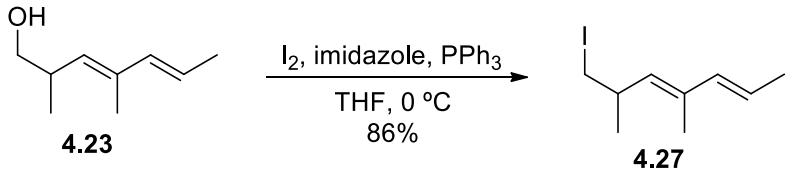

A dry flask flushed with Ar was charged with dien-1-ol **4.23** (100 mg, 0.71 mmol), triphenylphosphine (278 mg, 1.06 mmol), imidazole (71 mg, 1.06 mmol), and freshly distilled THF (7 mL). The reaction vessel was sealed and partially wrapped in foil to block entry of light and cooled to 0 ºC. A single batch of iodine (278 mg, 1.09 mmol) was added swiftly and the reaction vessel was resealed and completely wrapped in foil, and stirred at 0ºC. After 1.5 h when the reaction was complete, concentrated aqueous $Na_2S_2O_3$ (5 mL) was added swiftly, keeping the contents dark until the excess iodine was quenched. The reaction contents were diluted with hexanes (20 mL) and brine (5 mL), the aqueous phase was extracted with hexanes (10 mL), and the combined organic layers were washed with brine, dried, and concentrated. The concentrate was taken up in pentanes (10 mL) and filtered through a short plug of silica gel before being concentrated under vacuum to yield

166 mg of **4.27** (86%), which was stored in the dark in a freezer (~-23 ºC) until used. ^{1}H NMR (500 MHz, $CDCl_3$) δ 6.06 (dd, *J* = 15.5, 0.9 Hz, 1H), 5.65 (dq, *J* = 15.3, 6.6 Hz, 1H), 5.11 (d, *J* = 9.1 Hz, 1H), 3.13 (dd, *J* = 9.4, 6.0 Hz, 1H), 3.06 (dd, *J* = 9.4, 7.3 Hz, 1H), 2.78 – 2.68 (m, 1H), 1.77 (dd, *J* = 6.7, 1.2 Hz, 3H), 1.75 (d, *J* = 1.0 Hz, 3H), 1.10 (d, *J* = 6.6 Hz, 3H). ^{13}C NMR (126 MHz, $CDCl_3$) δ 135.47, 134.34, 132.80, 123.80, 34.99, 21.45, 18.24, 14.91, 12.91. EI-GC/MS *m/z* (%): 250 (M^+, 12), 123 (100), 109 (7), 93 (20), 81 (49), 67 (19), 55 (14), 41 (16).

4.4.5 Previous Studies for the Key Enantioselective Enolate Alkylation

Representative Procedure for Evans Alkylation

The following procedure was adapted from Decicco and Grover.[44]

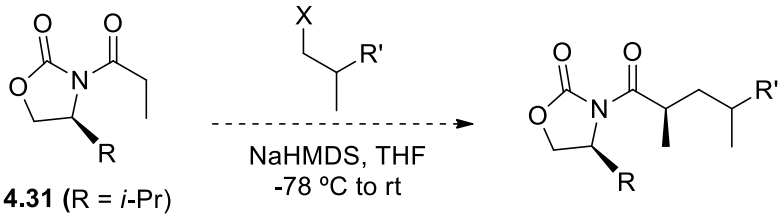

4.31 (R = *i*-Pr)
4.32 (R = Bn)

A dry flask flushed with Ar was charged with THF (3 mL) and a solution of NaHMDS (325 µL, 0.65 mmol, 2M in THF), and cooled to -78 ºC. A solution of the oxazolidinone (130 mL) in THF (1 mL) was added dropwise over 5 min, rinsing the syringe with THF (0.5 mL). The reaction was stirred for 1 h at this temperature. A solution of the alkyl electrophile (0.5 eq.) in THF (1 mL) was added over 20 min. The reaction was stirred and allowed to warm to room temperature overnight before being quenched with sat. aq. NH_4Cl (3 mL). The mixture was diluted with brine (3 mL) and extracted with a 1:1 mixture

of hexanes:ethyl acetate (6 mL). The organic layer was washed with brine, dried, and concentrated.

Preparation of Benzyl NCC Hydrazone

A solution of monochloramine and the NCC hydrazones were prepared according to Huynh et al.[32,33]

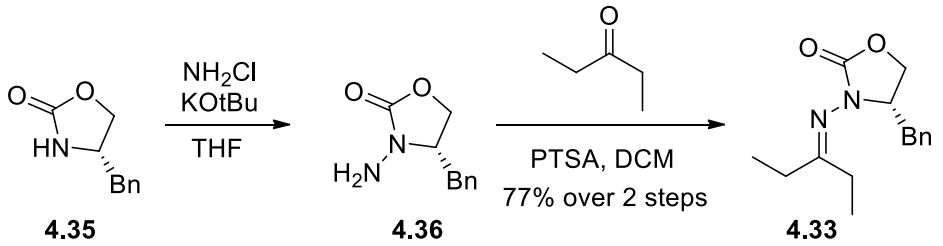

Monochloramine (NH_2Cl) was synthesized by the addition of NH_4OH (5.86 mL) to NH_4Cl (3.75 g) in Et_2O (46 mL) at -10 ºC, then a solution of sodium hypochlorite pentahydrate (14.25 g) in water (15 mL) was added dropwise over 30 min, and the mixture was stirred for an additional 15 min at -10 ºC. The layers were separated and the organic layer was washed with brine. This organic layer was dried over anhydrous $CaCl_2$ at around -20 ºC for at least 1 h, producing a solution of NH_2Cl (0.21 M). The aqueous layer was extracted with Et_2O (50 mL), then this organic layer was washed with brine and dried over anhydrous $CaCl_2$ at around -20 ºC for at least 1 h, producing a second solution of NH_2Cl (0.17 M).

The concentration of NH_2Cl in Et_2O was estimated by titration using a starch-iodide test.[33,45] Thus, a solution of starch indicator was prepared by boiling water (10 mL) containing potato starch (1 g) for 5 min. A second flask was charged with an aqueous solution of KI (1 mL, 0.5 M) and a measured volume of NH_2Cl in Et_2O. The mixture was

titrated by dropwise addition of an aqueous solution of $Na_2S_2O_3$ (0.1 M) until the solution turned pale-yellow in color. Add a drop of the starch indicator solution to form a deep indigo colored solution, and titrate until a clear endpoint is reached. The mmol of NH_2Cl added is equal to half the mmol of $Na_2S_2O_3$ added.

A dry flask flushed with Ar was charged with (*S*)-4-benzyl-2-oxazolidinone (1.0 g, 5.6 mmol) and THF (60 mL). Potassium *tert*-butoxide (1.91 g, 16.8 mmol) was added in portions over 10 min, and then stirred for 3.5 h. A solution of NH_2Cl in ether (~0.24 M) was added over 10 min, and the resulting mixture was stirred for 1.5 h at room temperature. The excess NH_2Cl was quenched with $Na_2S_2O_3$ (50 mL) and the layers were separated. The organic layer was washed with brine, dried, and concentrated, and the crude product was used in the next step without further purification.

The flask containing the crude *N*-amino-oxazolidinone was charged with 3-pentanone (15 mL), CH_2Cl_2 (25 mL), and *p*-toluenesulfonic acid (225 mg), and stirred at room temperature until the reaction reached completion. Excess 3-pentanone was removed by Kugelrohr distillation, and the residue was purified by vacuum flash chromatography (25% EtOAc/Hex), yielding 898 mg (77%) of the benzyl NCC hydrazone. ^{1}H NMR (500 MHz, $CDCl_3$) δ 7.35 – 7.13 (m, 5H), 4.34 (ddd, J = 16.6, 8.7, 4.3 Hz, 1H), 4.28 (t, J = 8.0 Hz, 1H), 4.06 (t, J = 8.7 Hz, 1H), 3.14 (dd, J = 13.6, 4.2 Hz, 1H), 2.78 – 2.72 (m, 1H), 2.53 – 2.36 (m, 4H), 1.16 (m, 6H). ^{13}C NMR (126 MHz, $CDCl_3$) δ 182.04, 154.89, 135.61, 129.06, 128.67, 126.98, 66.59, 60.71, 38.37, 28.69, 25.32, 10.84, 10.40. EI-GC/MS *m/z* (%): 260 (M^+,31), 231 (1), 169 (74), 117 (46), 91 (24), 84 (45), 56 (100).

Representative Alkylation of NCC Hydrazones

The following alkylation reaction was adapted from Huynh et al.[32]

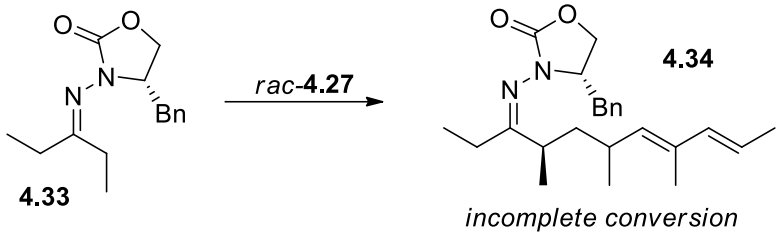

A dry flask flushed with Ar was charged with the benzyl NCC hydrazone (26 mg, 0.1 mmol) and freshly distilled THF (300 uL), then cooled to -78 ºC. A solution of LDA (75 µL, 0.15 mmol, 2 M in THF/heptane/ethylbenzene) was added, then the reaction was stirred for 1 h at 0 ºC. Freshly prepared iodide **4.27** (25 mg, 0.1 mmol) in THF (100 uL) was added to the reaction and stirred for 1 h at this temperature. The ice-water bath was removed and the mixture was stirred overnight. The reaction was quenched with sat. aq. NH_4Cl, diluted with ethyl acetate, the organic layer was washed with brine, then dried and concentrated. The concentrate was suspended in hexanes and purified by vacuum flash chromatography (5%-20% EtOAc/Hex), yielding 20 mg of a mixture of compounds containing the desired alkylated NCC hydrazone.

A 1 mg aliquot of this mixture was hydrolyzed by addition of 4:1 acetone:water (200 uL) and a substoichiometric amount of PTSA. After the reaction had reached completion, solid $NaHCO_3$ was added and the mixture was stirred for 30 min. The mixture was diluted with hexanes, and the organic layer was washed with brine, dried, and concentrated. The crude product was purified by vacuum flash chromatography (2.5-5% EtOAc/Hex) and kept as a dilute solution for GC analysis on chiral and achiral stationary phase columns.

4.4.6 Current Synthetic Route for the Enantioselective Enolate Alkylation using Myers' Pseudoephedrine Chiral Auxiliary

Recovery of (1*S*,2*S*)-(+)-pseudoephedrine free base

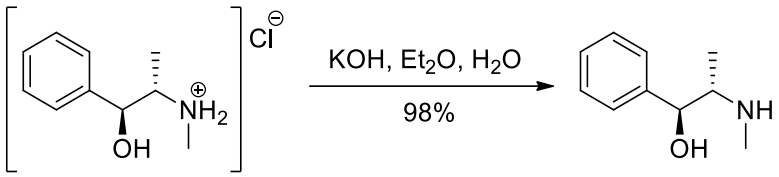

4.40 **4.41**

A flask was charged with (1*S*,2*S*)-(+)-pseudoephedrine hydrochloride salt (24.41 g, 121 mmol), diethyl ether (244 mL), and water (98 mL). Potassium hydroxide (7.5 g, 133 mmol) was added in portions over 10 min and the reaction mixture was stirred overnight. A solution of Na_2CO_3 (10% w/w, 100 mL) and ethyl acetate (200 mL) were added. The organic layer was washed with brine (2x100 mL), dried, and partially concentrated. The biphasic residue was dissolved in the minimum amount of hot EtOAc, and the product was allowed to precipitate upon cooling to room temperature. The crystalline product was isolated by vacuum filtration and washed with room temperature Et_2O. The filtrate was partially concentrated and this recrystallization procedure was repeated twice, combining all crops of recrystallized product. Finally, residual solvent was removed under high vacuum to yield (1*S*,2*S*)-(+)-pseudoephedrine (19.57 g, 98%). ^{1}H NMR (500 MHz, $CDCl_3$) δ 7.39 – 7.26 (m, 5H), 4.14 (dd, *J* = 24.6, 7.8 Hz, 1H), 2.60 (dq, *J* = 12.8, 6.4 Hz, 1H), 2.45 (s, 3H), 0.94 (d, *J* = 6.4 Hz, 3H). ^{13}C NMR (126 MHz, $CDCl_3$) δ 142.62, 128.21, 127.55, 127.01, 77.54, 61.19, 33.42, 15.34.

Acylation of (1*S*,2*S*)-(+)-pseudoephedrine

The following synthetic procedure was adapted from Ghosh and Anderson,[46] and recrystallization conditions from Myers et al.[36]

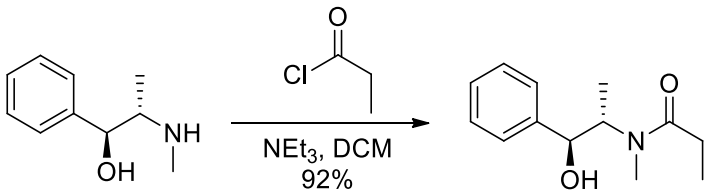

4.41 **4.42**

A dry flask flushed with Ar was charged with CH_2Cl_2 (440 mL), (1*S*,2*S*)-(+)-pseudoephedrine (36.9 g, 223 mmol), and triethylamine (37.4 mL, 268 mmol). The reaction was cooled to 0 ºC, propionyl chloride (20.3 mL, 235 mmol) was added over 20 min, then the mixture was stirred for 1 h allowing the reaction to reach room temperature. The reaction was quenched by the slow addition of water (75 mL), then diluted with diethyl ether (470 mL). The organic layer was washed sequentially with sat. aq $NaHCO_3$ (2x375 mL), HCl (1M, 375 mL), and brine (300 mL). The organic layer was dried and concentrated to yield a white solid which was recrystallized from hot toluene, with the product precipitating upon cooling to room temperature then to 4 ºC in a refrigerator. The crystals were separated by vacuum filtration, washing the filter cake with room temperature hexanes. The filtrate was concentrated and this recrystallization was repeated twice, combining all crops of the recrystallized product. After removal of residual volatiles by high vacuum, the white crystalline propionyl Myers' auxiliary **4.42** (45.67 g, 92%) was isolated as a mixture of rotamers. ^{1}H NMR (approx. 3:1 rotamer ratio, * denotes distinguishable minor rotamer peaks, 500 MHz, $CDCl_3$) δ 7.40 – 7.23 (m, 5+5H), 4.57 (t,

J = 7.8 Hz, 1H), 4.44 (br s, 1H), 4.36* (br s, 1H), 4.04 – 3.93* (m, 1H), 2.92* (s, 3H), 2.80 (s, 3H), 2.55 – 2.48* (m, 1H), 2.43 – 2.36* (m, 1H), 2.37 – 2.23 (m, 2H), 1.15* (t, *J* = 7.4 Hz, 1H), 1.13 – 1.06 (m, 6H), 0.97* (d, *J* = 6.8 Hz, 3H). ^{13}C NMR (approx. 3:1 rotamer ratio, * denotes distinguishable minor rotamer peaks, 126 MHz, $CDCl_3$) δ 176.22, 174.95*, 142.45, 141.12*, 128.68, 128.34, 127.61, 126.89, 126.35, 76.63, 75.44*, 58.67*, 58.23, 32.73*, 27.56, 26.83, 26.66, 15.23*, 14.45, 9.57*, 9.17.

Representative Myers' Alkylation Procedure

The following procedure was adapted from Myers et al.[36]

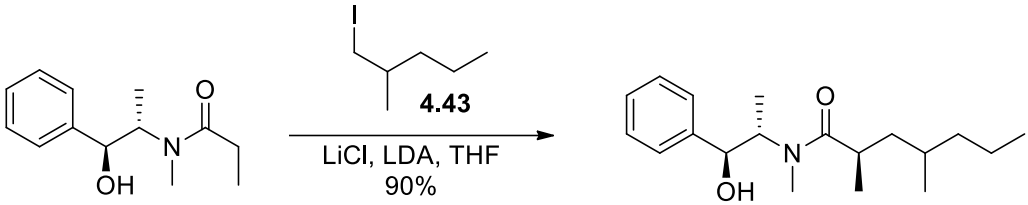

A dry flask flushed with Ar was charged with **4.42** (1.15 g, 5.2 mmol) and anhydrous LiCl (1.49 g, 35.1 mmol). The flask was stirred, and heated with a heat gun under house vacuum, melting the auxiliary in the process. The hot flask was then backfilled with Ar. This heat and backfill process was repeated twice. After cooling to room temp, the contents were partially dissolved in THF (20.8 mL) before being cooled to -78 ºC. A solution of LDA (2M, 5.2 mL, 10.4 mmol) was added dropwise over 30 min, and the reaction was stirred for 1 h at -78 ºC, 30 min at 0 ºC, and finally 5 min at 23 ºC. The mixture was then cooled to 0 ºC, and a solution of iodide **4.43** (276 mg, 1.3 mmol) in THF (2.5 mL) was added dropwise over 5 min. The reaction was stirred overnight and allowed to reach room temperature. The following morning, the reaction was quenched with sat. aq. NH_4Cl

(15 mL), then diluted with water (15 mL) and brine (30 mL). The mixture was extracted with ethyl acetate (4x15 mL), then the combined organic layer was washed with brine (30 mL), dried, and concentrated. The crude product mixture was purified by vacuum flash chromatography (40% EtOAc) yielding alkylated Myers' auxiliary **4.44** (359 mg, 90%). Partial identification of this intermediate was facilitated by changes in retention time on an achiral column and several NMR signals of the complex mixture of rotamers and diastereomers: ^{1}H NMR (* = minor rotamer) 400 MHz, $CDCl_3$) δ 2.90* (s, 3H), 2.85 (s, 3H). ^{13}C NMR (* = minor rotamer) 101 MHz, $CDCl_3$) δ 179.37, 179.10, 178.13*, 177.80*, 142.54, 141.30*, 76.38, 75.19, 75.10.

Ethylation of Myers' Alkylation Product to the Ethyl Ketone Derivative

The following procedure was adapted from Myers et al.[36] A large excess of EtLi was added in error; the intended amount added would have been 2.1 equivalents.

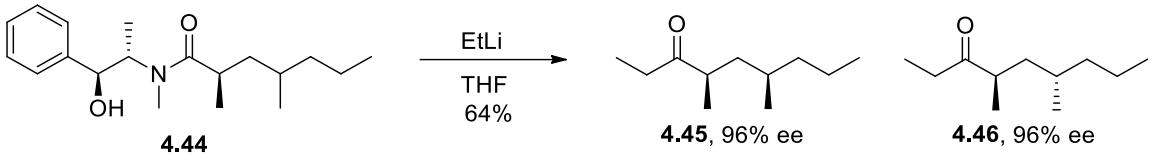

4.44 **4.45**, 96% ee **4.46**, 96% ee

A dry flask flushed with Ar was charged with the alkylated Myers' auxiliary product **4.44** (60 mg, ~0.2 mmol) and THF (2.5 mL) before being cooled to -78 ºC. A solution of ethyllithium (0.5 M in benzene:cyclohexane, 8.2 mL, 4.1 mmol) was added dropwise over 20 min, then the reaction was warmed to 0 ºC and stirred at this temperature for 5 min. The excess ethyllithium was quenched with diisopropylamine (273 µL), stirred for 15 min, and then the reaction was diluted with 10% acetic acid in diethyl ether (2.5 mL). The mixture was diluted further with EtOAc (10 mL) and the organic layer was

washed with sat. aq. $NaHCO_3$ (15 mL). The combined aqueous layer was extracted with EtOAc (10 mL), and then the combined organic layer was washed with a 1:1 mixture of sat. aq. $NaHCO_3$ and brine (12 mL, total), dried, and concentrated under vacuum. The crude oil was purified by flash chromatography (2.5% EtOAc/Hexanes), yielding **4.45** and **4.46** (21 mg, 64%) as an approx. 1:1 mixture of diastereomers. ^{1}H NMR (400 MHz, $CDCl_3$) δ 2.69 – 2.56 (m, 1H), 2.52 – 2.35 (m, 2H), 1.70 – 1.64 (m, 1H), 1.45 – 1.18 (m, 6H), 1.07 – 0.99 (m, 7H), 0.89 – 0.81 (m, 7H). ^{13}C NMR (101 MHz, $CDCl_3$) δ 215.67, 43.83, 43.78, 40.78, 40.28, 39.62, 39.21, 34.13, 34.01, 30.43, 30.19, 19.97, 19.86, 19.79, 19.36, 17.37, 16.27, 14.27, 7.85, 7.78. Both diastereomers exhibited the same fragmentation. EI-GC/MS *m/z* (%): 141 (2), 127 (1), 123 (1), 113 (3), 99 (7), 86 (100), 71 (37), 57 (86), 43 (26).

4.5 References

(1) Paine, T.; Hoddle, M. *The Asian Long-Horned Beetle, Anoplophora glabripennis*. https://cisr.ucr.edu/invasive-species/asian-long-horned-beetle (accessed 2022-06-17).

(2) Garonna, A. P. *Aromia bungii (red necked longicorn)*. https://www.cabi.org/isc/datasheet/118984 (accessed 2022-06-17).

(3) Paine, T. D.; Millar, J. G.; Hanks, L. M.; Gould, J.; Wang, Q.; Daane, K.; Dahlsten, D. L.; McPherson, E. G. Cost-Benefit Analysis for Biological Control Programs That Target Insects Pests of Eucalypts in Urban Landscapes of California. *J Econ Entomol* **2015**, *2015* (6), 1–8. https://doi.org/10.1093/JEE/TOV224.

(4) Seybold, S. J.; Bentz, B. J.; Fettig, C. J.; Lundquist, J. E.; Progar, R. A.; Gillette, N. E. Management of Western North American Bark Beetles with Semiochemicals. *Ann Rev Entomol* **2018**, *63* (1), 407–432. https://doi.org/10.1146/annurev-ento-020117-043339.

(5) Cui, G. Z.; Zhu, J. J. Pheromone-Based Pest Management in China: Past, Present, and Future Prospects. *J Chem Ecol* **2016**, *42* (7), 557–570. https://doi.org/10.1007/s10886-016-0731-x.

(6) Norin, T. Semiochemicals for Insect Pest Management. *Pure Appl Chem* **2007**, *79* (12), 2129–2136. https://doi.org/10.1351/pac200779122129.

(7) Tumlinson, J. H.; Klein, M. G.; Doolittle, R. E.; Ladd, T. L.; Proveaux, A. T. Identification of the Female Japanese Beetle Sex Pheromone: Inhibition of Male Response by an Enantiomer. *Science* **1977**, *197* (4305), 789–792. https://doi.org/10.1126/SCIENCE.197.4305.789.

(8) Lacey, E. S.; Moreira, J. A.; Millar, J. G.; Ray, A. M.; Hanks, L. M. Male-Produced Aggregation Pheromone of the Cerambycid Beetle *Neoclytus mucronatus* m*ucronatus*. *Entomol Exp Appl* **2007**, *122* (2), 171–179. https://doi.org/10.1111/J.1570-7458.2006.00508.X.

(9) Reddy, G. V. P.; Fettköther, R.; Noldt, U.; Dettner, K. Capture of Female *Hylotrupes bajulus* as Influenced by Trap Type and Pheromone Blend. *J Chem Ecol* **2005**, *31* (9), 2169–2177. https://doi.org/10.1007/S10886-005-6083-6/TABLES/4.

(10) Lacey, E. S.; Moreira, J. A.; Millar, J. G.; Hanks, L. M. A Male-Produced Aggregation Pheromone Blend Consisting of Alkanediols, Terpenoids, and an Aromatic Alcohol from the Cerambycid Beetle *Megacyllene caryae*. *J Chem Ecol* **2008**, *34* (3), 408–417. https://doi.org/10.1007/S10886-008-9425-3/FIGURES/3.

(11) Hanks, L. M.; Millar, J. G. Sex and Aggregation-Sex Pheromones of Cerambycid Beetles: Basic Science and Practical Applications. *J Chem Ecol* **2016**, *42* (7), 631–654. https://doi.org/10.1007/S10886-016-0733-8.

(12) Millar, J. G.; Hanks, L. M. Chemical Ecology of Cerambycids. In *Cerambycidae of the world: biology and pest management*; Wang, Q., Ed.; CRC Press/ Taylor & Francis Group: Boca Raton, 2017; pp 161–208.

(13) Žunič Kosi, A.; Zou, Y.; Hoskovec, M.; Vrezec, A.; Stritih, N.; Millar, J. G. Novel, Male-Produced Aggregation Pheromone of the Cerambycid Beetle *Rosalia alpina*, a Priority Species of European Conservation Concern. *PLoS ONE* **2017**, *12* (8), e0183279. https://doi.org/10.1371/JOURNAL.PONE.0183279.

(14) Tröger, A.; van Beek, T. A.; Huigens, M. E.; Silva, I. M. M. S.; Posthumus, M. A.; Francke, W. Structure Elucidation of Female-Specific Volatiles Released by the Parasitoid Wasp *Trichogramma turkestanica* (Hymenoptera: Trichogrammatidae). *Beilstein J Org Chem* **2014**, *10*, 767–773. https://doi.org/10.3762/bjoc.10.72.

(15) Tamura, R.; Saegusa, K.; Kakihana, M.; Oda, D. *Stereoselective E and Z Olefin Formation by Wittig Olefination of Aldehydes with Allylic Phosphorus Ylides. Stereochemistry*; 1988; Vol. 53.

(16) Paquette, L. A.; Boulet, S. L. Toward a Total Synthesis of Okilactomycin. 1. A Direct, Enantiocontrolled Route to the Western Sector. *Synthesis* **2002**, *2002* (07), 888–894. https://doi.org/10.1055/s-2002-28510.

(17) Lautens, Mark.; Bouchain, Gilliane. (SI) Total Synthesis of Ionomycin Using Ring Opening Strategies. *Org Lett* **2002**, *4* (11), 1879–1882.

(18) Saicic, R. N. Improved Procedure for the Preparation of Cis-2,4-Dimethylglutaranhydride. *Synthetic Comm* **2006**, *36* (17), 2559–2562. https://doi.org/10.1080/00397910600781497.

(19) Schregenberger, C.; Seebach, D. Totalsynthese Des Makrodiolids (+)-Conglobatin. *Liebigs Ann Chem* **1986**, *1986* (12), 2081–2103. https://doi.org/10.1002/jlac.198619861204.

(20) Huckstep, M.; Taylor, R. J. K. A Convenient Method of Preparing the Leukotriene Precursor Methyl 5-Oxopentanoate. *Synthesis* **1982**, *1982* (10), 881–882. https://doi.org/10.1055/s-1982-29988.

(21) Hoffmann, R. W.; Ditrich, K.; Köster, G.; Stürmer, R. Stereoselective Synthesis of Alcohols, XXXI: Stereoselective C-C Bond Formation Using Chiral Z-Pentenylboronates. *Chem Ber* **1989**, *122* (9), 1783–1789. https://doi.org/10.1002/cber.19891220926.

(22) Prosser, A. R.; Liotta, D. C. One-Pot Transformation of Esters to Analytically Pure Ketones: Methodology and Application in Process Development. *Tetrahedron Lett* **2015**, *56* (23), 3005–3007. https://doi.org/10.1016/J.TETLET.2014.10.024.

(23) Aldrich, C. C.; Beck, B. J.; Fecik, R. A.; Sherman, D. H. Biochemical Investigation of Pikromycin Biosynthesis Employing Native Penta-and Hexaketide Chain Elongation Intermediates. *J Am Chem Soc* **2005**. https://doi.org/10.1021/ja042592h.

(24) Mohr, P.; Waespe-Sarcevic, N.; Tamm, C.; Gawronska, K.; Gawronski, J. K. A Study of Stereoselective Hydrolysis of Symmetrical Diesters with Pig Liver Esterase. *Helv Chim Acta* **1983**, *66* (8), 2501–2511. https://doi.org/10.1002/hlca.19830660815.

(25) Grant, B.; Djerassi, C. The Mechanism of Hydride Reduction of 1-Alkyn-3-Ols. *J Org Chem* **1974**, *39* (7), 968–970. https://doi.org/10.1021/JO00921A024/ASSET/JO00921A024.FP.PNG_V03.

(26) Shi, X.; Webster, F. X.; Meinwald, J. Syntheses of the Female Sex Pheromones of Matsucoccus Pine Scales Using the [2,3]-Wittig Rearrangement of a Bisallylic Tertiary Ether. *Tetrahedron* **1995**, *51* (38), 10433–10442. https://doi.org/10.1016/0040-4020(95)00622-F.

(27) Millar, J. G.; Moreira, J. A.; McElfresh, J. S.; Daane, K. M.; Freund, A. S. Sex Pheromone of the Longtailed Mealybug: A New Class of Monoterpene Structure. *Org Lett* **2009**, *11* (12), 2683–2685. https://doi.org/10.1021/OL802164V/SUPPL_FILE/OL802164V_SI_002.PDF.

(28) Wang, Y.; Wang, R.; Li, Q.; Zhang, Z.; Feng, Y. Kinetic Resolution of Rac-Alkyl Alcohols via Lipase-Catalyzed Enantioselective Acylation Using Succinic Anhydride as Acylating Agent. *J Mol Catal B- Enzym* **2009**, *56* (2–3), 142–145. https://doi.org/10.1016/J.MOLCATB.2008.02.002.

(29) Evans, D. A.; Ennis, M. D.; Mathre, D. J. Asymmetric Alkylation Reactions of Chiral Imide Enolates. A Practical Approach to the Enantioselective Synthesis of α-Substituted Carboxylic Acid Derivatives. *J Am Chem Soc* **1982**, *104* (6), 1737–1739. https://doi.org/10.1021/JA00370A050/ASSET/JA00370A050.FP.PNG_V03.

(30) Evans, D. A.; Ennis, M. D.; Mathre, D. J. Asymmetric Alkylation Reactions of Chiral Imide Enolates. A Practical Approach to the Enantioselective Synthesis of α-Substituted Carboxylic Acid Derivatives. *J Am Chem Soc* **1982**, *104* (6), 1737–1739. https://doi.org/10.1021/JA00370A050/ASSET/JA00370A050.FP.PNG_V03.

(31) Arvanitis, E.; Ernst, H.; Ludwig, A. A.; Robinson, A. J.; Wyatt, P. B. Enantioselective Synthesis of 2-Substituted 3-Aminopropanoic Acid (β-Alanine) Derivatives Which Are β-Analogues of Aromatic Amino Acids. *J Chem Soc, Perk T 1* **1998**, No. 3, 521–528. https://doi.org/10.1039/A706163C.

(32) Huynh, U.; McDonald, S. L.; Lim, D.; Uddin, Md. N.; Wengryniuk, S. E.; Dey, S.; Coltart, D. M. Formation, Alkylation, and Hydrolysis of Chiral Nonracemic N-Amino Cyclic Carbamate Hydrazones: An Approach to the Enantioselective α-Alkylation of Ketones. *J Org Chem* **2018**, *83* (21), 12951–12964. https://doi.org/10.1021/acs.joc.8b00655.

(33) Huynh, U.; Uddin, Md. N.; Wengryniuk, S. E.; McDonald, S. L.; Coltart, D. M. A Simple and Efficient Approach to the N-Amination of Oxazolidinones Using Monochloroamine. *Tetrahedron Lett* **2016**, *57* (43), 4799–4802. https://doi.org/10.1016/J.TETLET.2016.09.034.

(34) Huynh, U.; Uddin, Md. N.; Wengryniuk, S. E.; McDonald, S. L.; Coltart, D. M. On the Regioselectivity and Diastereoselectivity of ACC Hydrazone Alkylation. *Tetrahedron* **2017**, *73* (5), 432–436. https://doi.org/10.1016/J.TET.2016.11.064.

(35) Uddin, M. N.; Tarsis, E. M.; Wu, C.-H.; Wu, J. I.; Coltart, D. M. A Mismatch-Free Strategy for the Diastereoselective α,α-Bisalkylation of Chiral Nonracemic Methyl Ketones Scheme 1. Diastereomerically Matched Asymmetric α,α-Bisalkylation of an ACC Hydrazone Derived from a Chiral Nonracemic Methyl Ketone. *Organic Letters* **2018**, *20*, 59. https://doi.org/10.1021/acs.orglett.8b01146.

(36) Myers, A. G.; Yang, B. H.; Chen, H.; McKinstry, L.; Kopecky, D. J.; Gleason, J. L. Pseudoephedrine as a Practical Chiral Auxiliary for the Synthesis of Highly Enantiomerically Enriched Carboxylic Acids, Alcohols, Aldehydes, and Ketones. *J Am Chem Soc* **1997**. https://doi.org/10.1021/JA970402F.

(37) Mortison, J. D.; Kittendorf, J. D.; Sherman, D. H. Synthesis and Biochemical Analysis of Complex Chain-Elongation Intermediates for Interrogation of Molecular Specificity in the Erythromycin and Pikromycin Polyketide Synthases. *J Am Chem Soc* **2009**, *131* (43), 15784–15793. https://doi.org/10.1021/ja9060596.

(38) Vamsee Krishna, C.; Bhonde, V. R.; Devendar, A.; Maitra, S.; Mukkanti, K.; Iqbal, J. A Cross Metathesis Strategy for the Synthesis of Highly Functionalized Conjugated Cyanodienes: Synthesis of the C3–C17 Framework of (−)-Borrelidin. *Tetrahedron Lett* **2008**, *49* (12), 2013–2017. https://doi.org/10.1016/J.TETLET.2008.01.055.

(39) Reyes, E.; Ruiz, N.; Vicario, J.; Badía, D.; Carrillo, L. Stereoselective Total Synthesis of (-)-β-Conhydrine and (+)-α-Conhydrine. *Synthesis* **2011**, *2011* (03), 443–450. https://doi.org/10.1055/s-0030-1258390.

(40) Hoffmann, R. W.; Schopfer, U.; Müller, G.; Brandl, T. Synthesis of a Conformationally Flexible -Hairpin Mimetic. *Helv Chim Acta* **2002**, *85* (12), 4424–4441. https://doi.org/10.1002/hlca.200290020.

(41) Skepper, C. K.; Quach, T.; Molinski, T. F. Total Synthesis of Enigmazole A from Cinachyrella Enigmatica. Bidirectional Bond Constructions with an Ambident 2,4-Disubstituted Oxazole Synthon. *J Am Chem Soc* **2010**, *132* (30), 10286–10292. https://doi.org/10.1021/ja1016975.

(42) Zhang, Z.; Zhang, J.; Tan, J.; Wang, Z. A Facile Access to Pyrroles from Amino Acids via an Aza-Wacker Cyclization. *J Org Chem* **2008**, *73* (13), 5180–5182. https://doi.org/10.1021/jo800433b.

(43) Fieser LF, F. M. Reagents for Organic Synthesis; John Wiley & Sons: New York, 1967; pp 581–595.

(44) Decicco, C. P.; Grover, P. Total Asymmetric Synthesis of the Potent Immunosuppressive Marine Natural Product Microcolin A. *J Org Chem* **1996**, *61* (10), 3534–3541. https://doi.org/10.1021/JO952123L/SUPPL_FILE/JO3534.PDF.

(45) Harp, D. L. *Current Technology of Chlorine Analysis for Water and Wastewater*. https://stpnq.com/wp-content/uploads/2014/08/Chlorine-Analysis-EN.pdf (accessed 2022-07-07).

(46) Ghosh, A. K.; Anderson, D. D. Enantioselective Total Synthesis of Pladienolide B: A Potent Spliceosome Inhibitor. *Org Lett* **2012**, *14* (18), 4730–4733. https://doi.org/10.1021/OL301886G/SUPPL_FILE/OL301886G_SI_001.PDF.

4.6 Supporting Information

4.6.1 ^{1}H NMR for *Graphisurus fasciatus* produced compound (CD_2Cl_2, 600 MHz, 298 K)

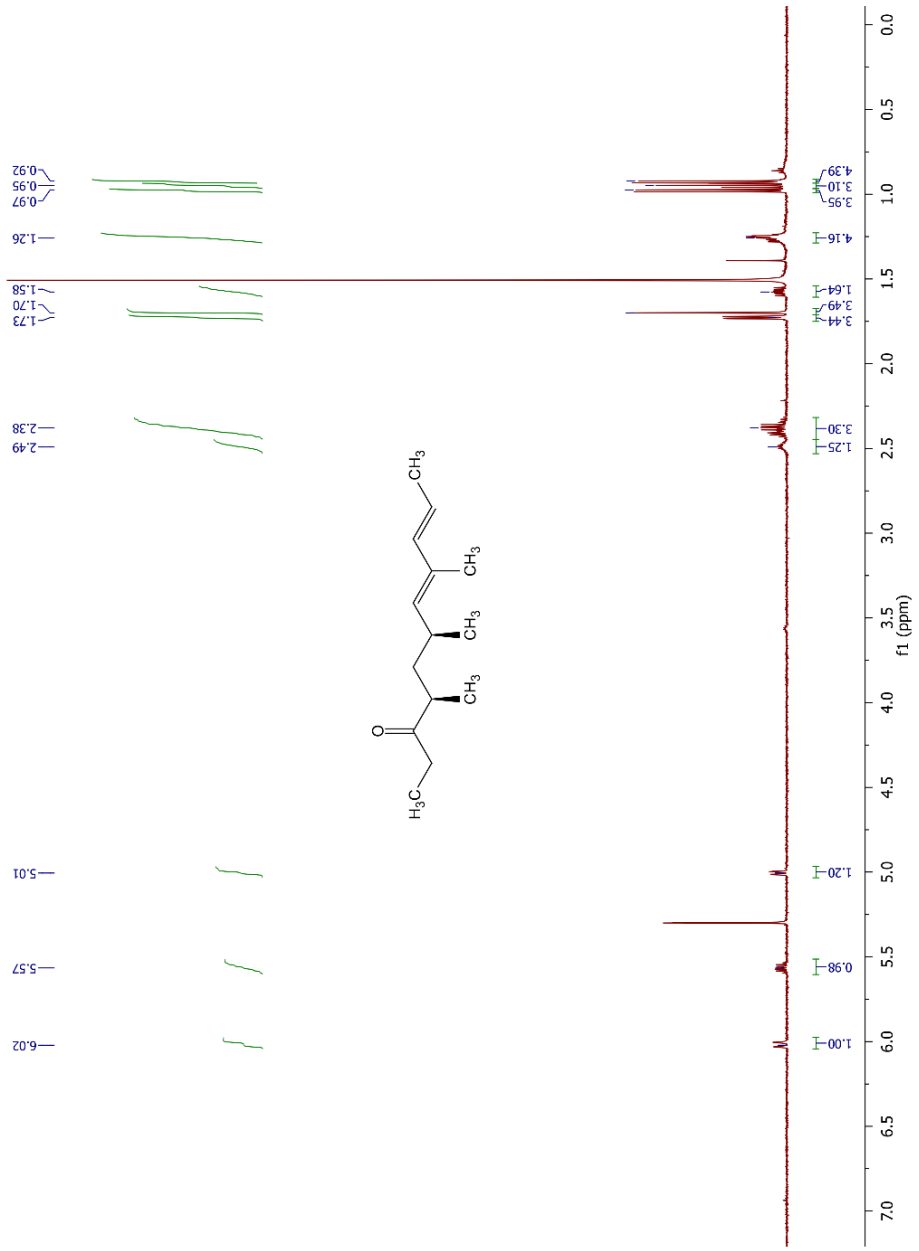

4.6.2 ^{1}H-^{1}H COSY NMR for *Graphisurus fasciatus* produced compound (CD_2Cl_2, 600 MHz, 298 K)

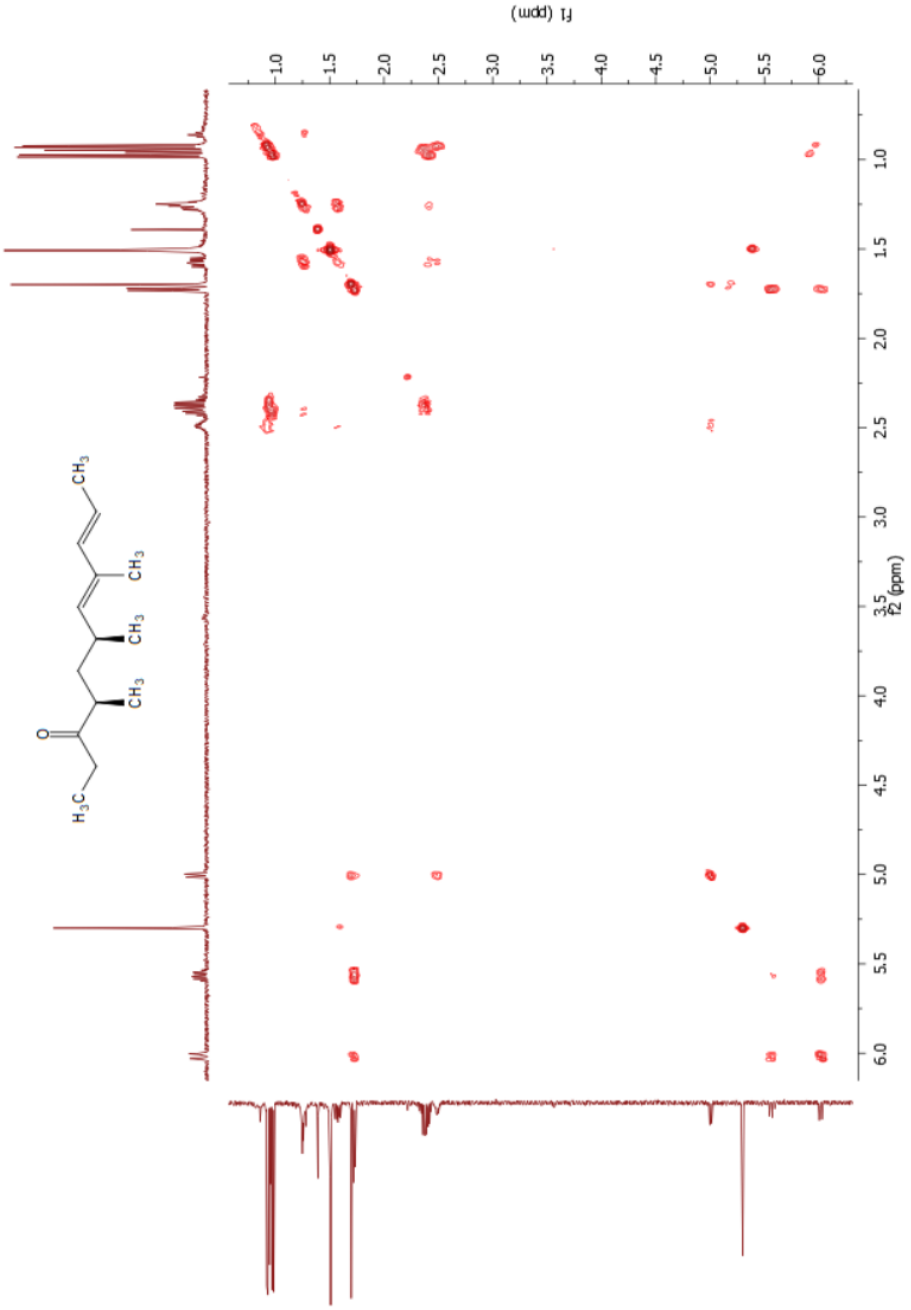

4.6.3 ^{1}H NMR of diacid 4.13 ($CDCl_3$, 400 MHz, 298 K)

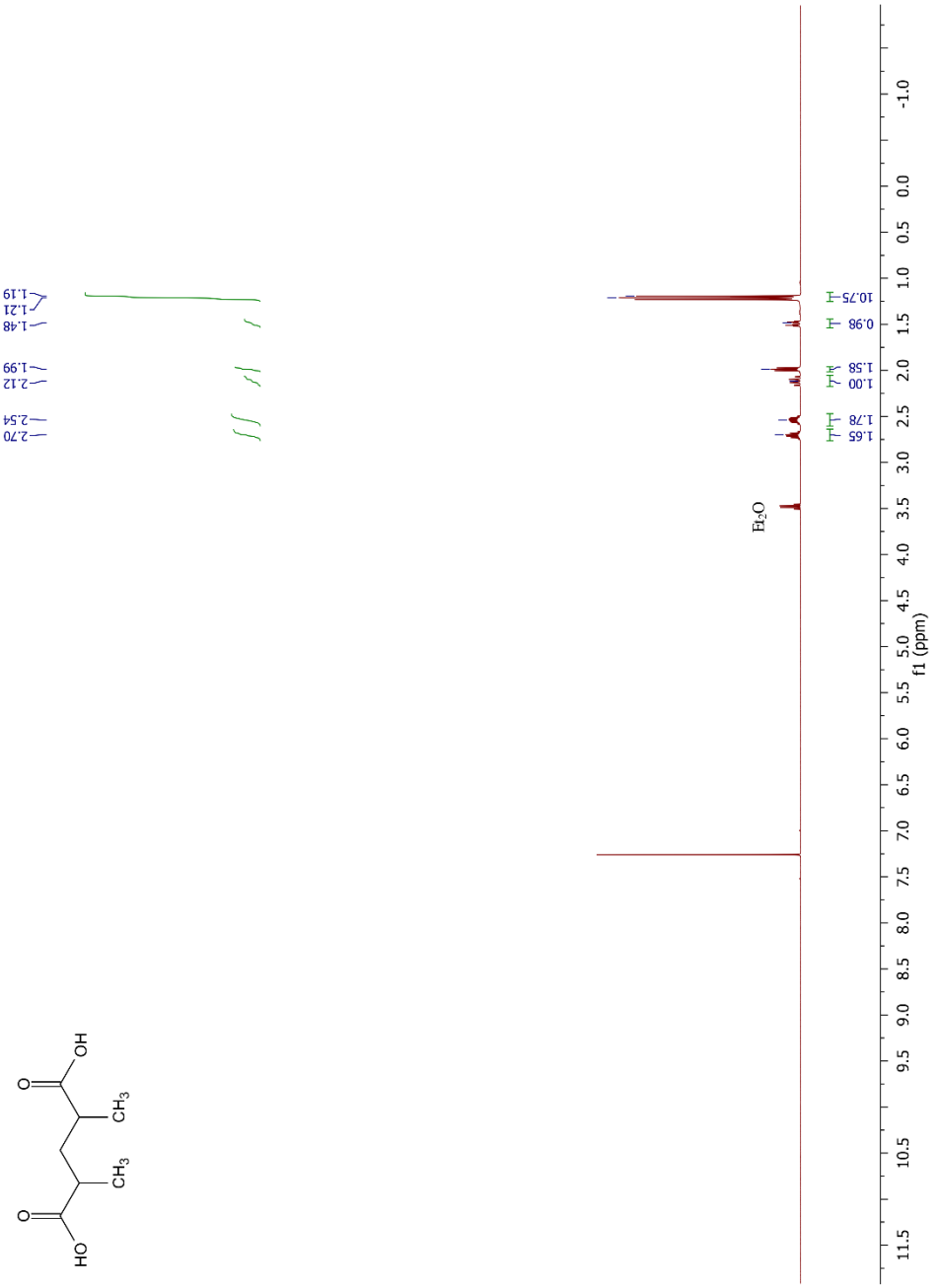

4.6.4 ^{13}C NMR of diacid 4.13 ($CDCl_3$, 101 MHz, 298 K)

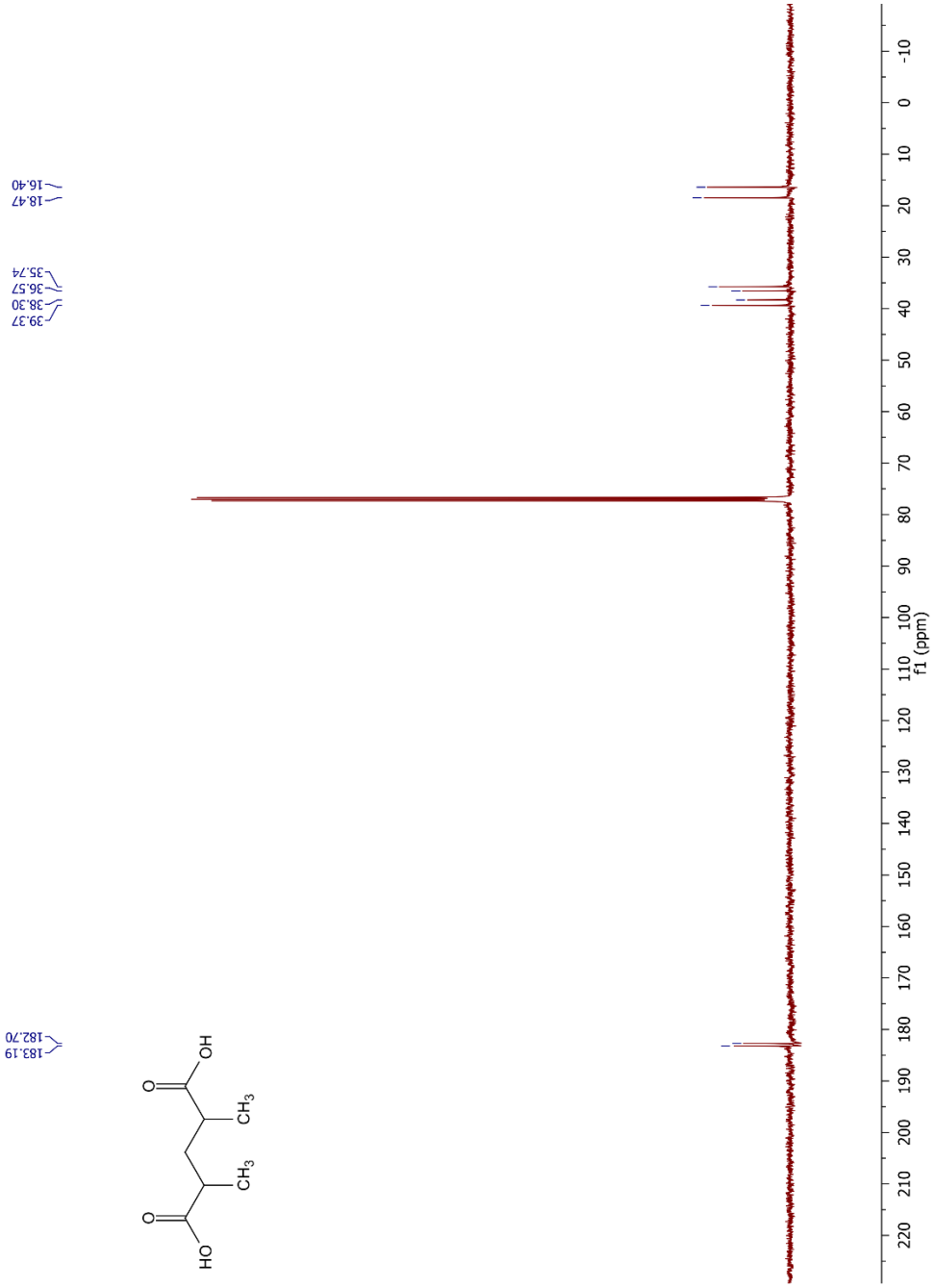

4.6.5 ^{1}H NMR of *syn*-dimethyl anhydride 4.09 ($CDCl_3$, 400 MHz, 298 K)

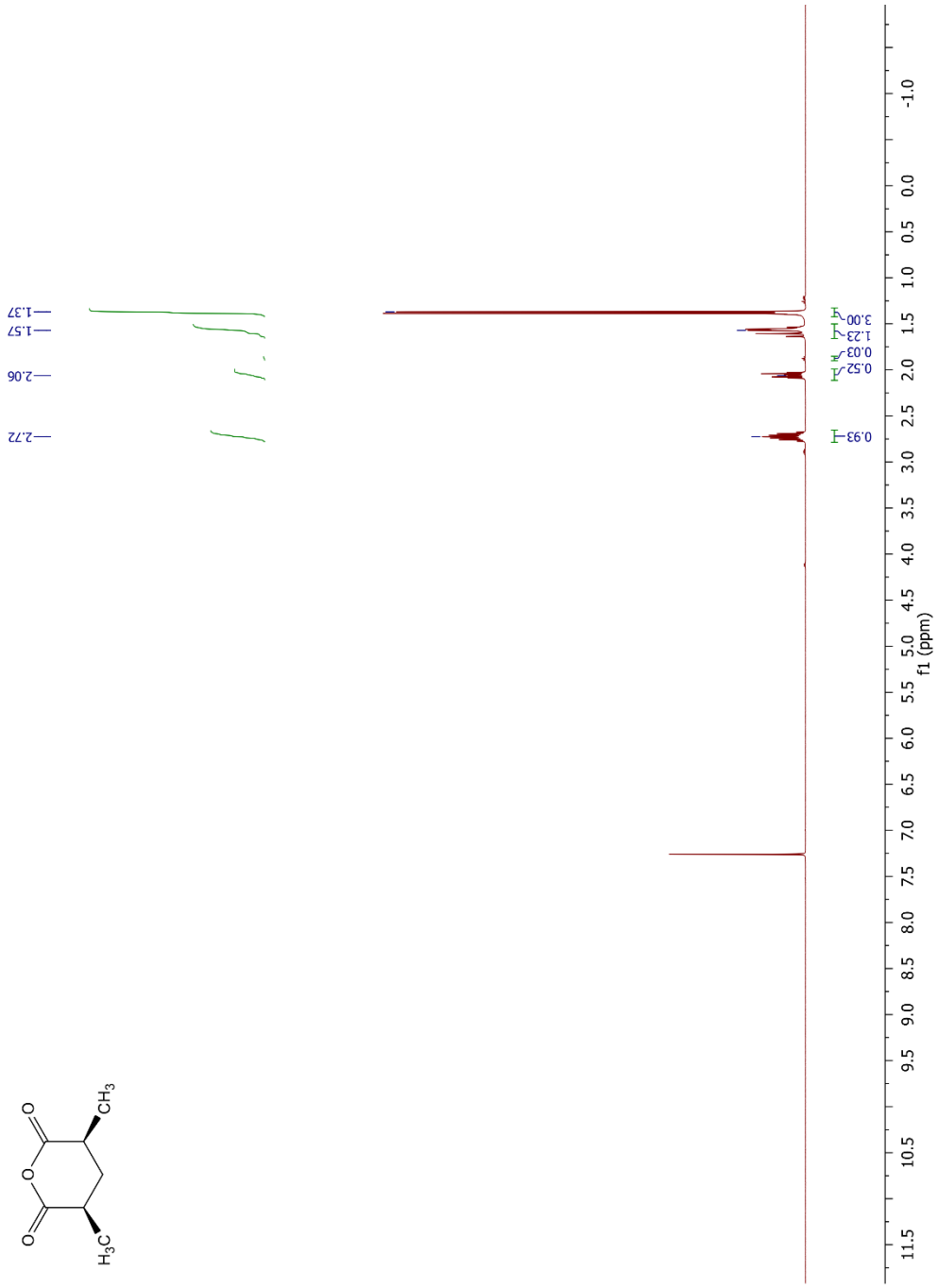

4.6.6 ^{13}C NMR of *syn*-dimethyl anhydride 4.09 ($CDCl_3$, 101 MHz, 298 K)

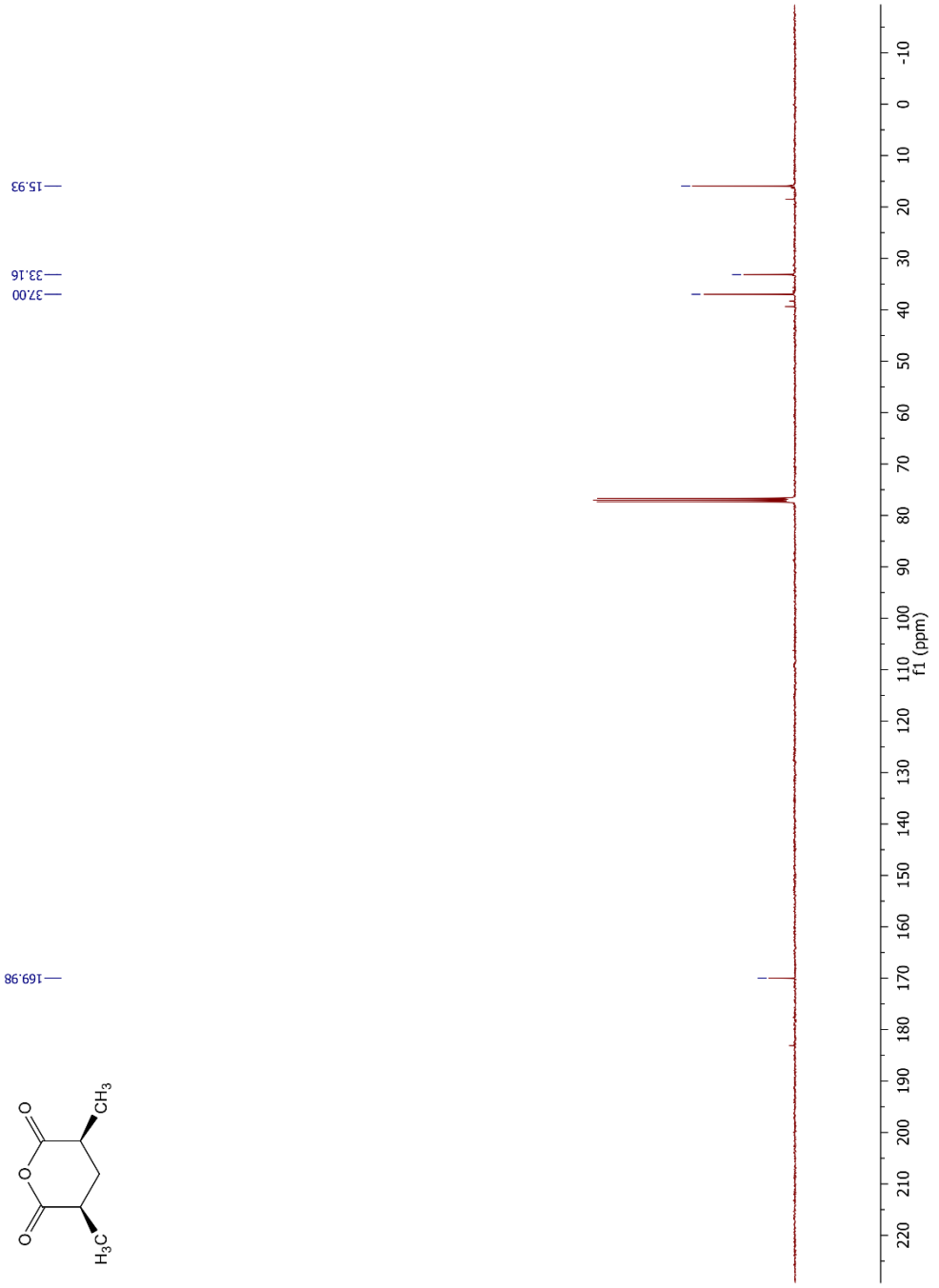

4.6.7 ^{1}H NMR of lactone 4.15 ($CDCl_3$, 500 MHz, 294 K)

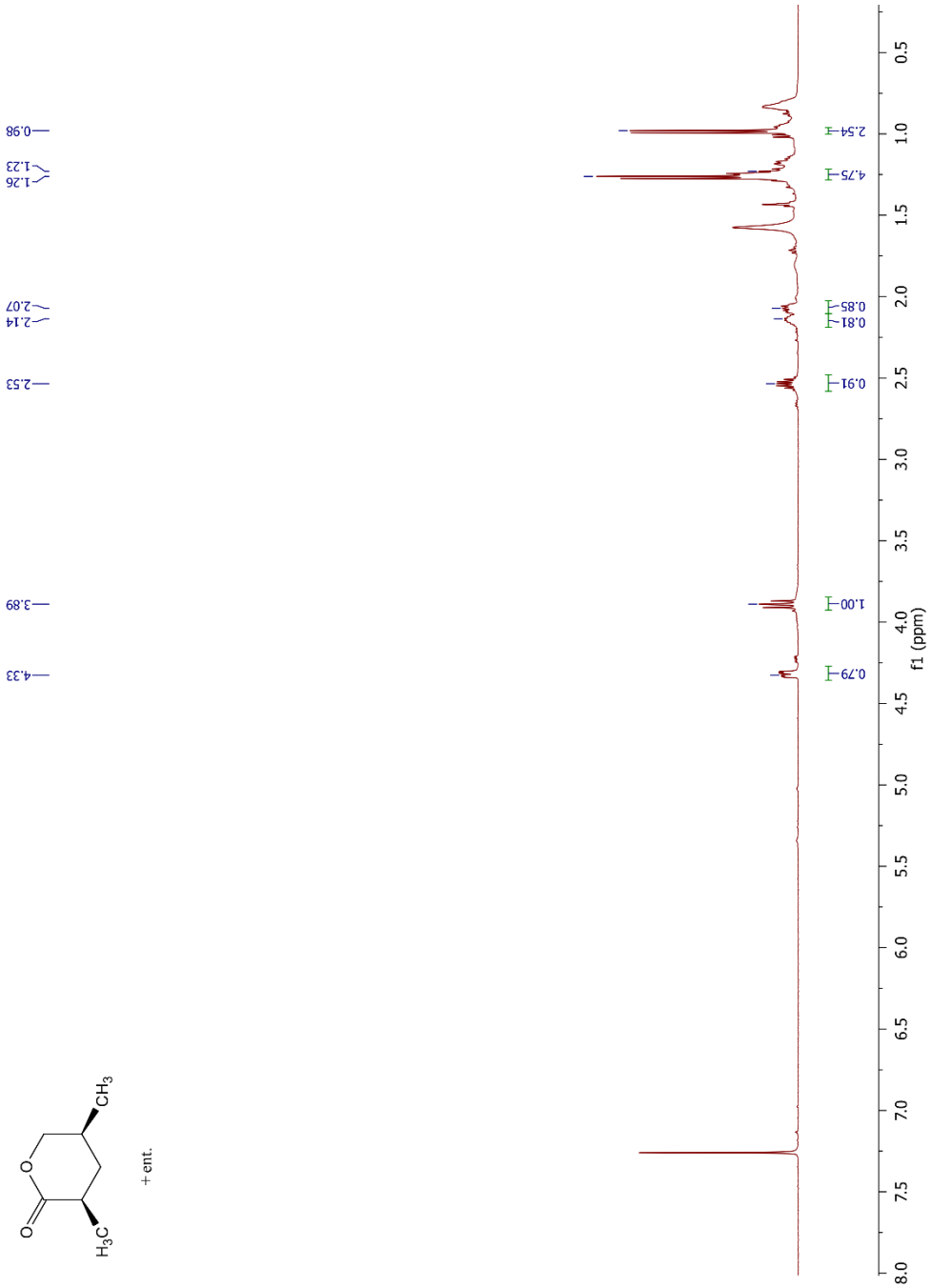

4.6.8 ^{13}C NMR of lactone 4.15 ($CDCl_3$, 500 MHz, 294 K)

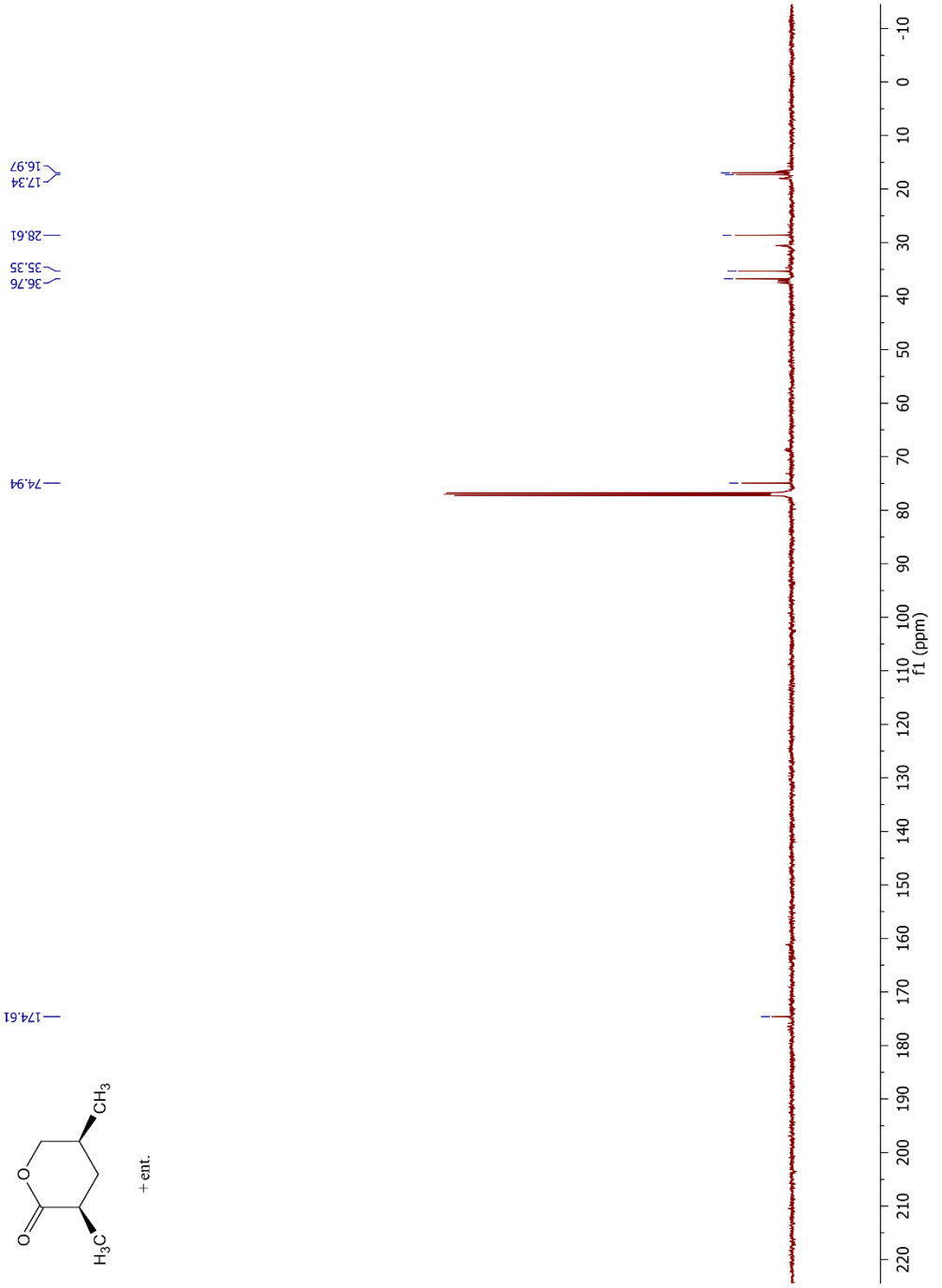

4.6.9 ^{1}H NMR of *syn*-dimethylhydroxy ester 4.16 ($CDCl_3$, 400 MHz, 298 K)

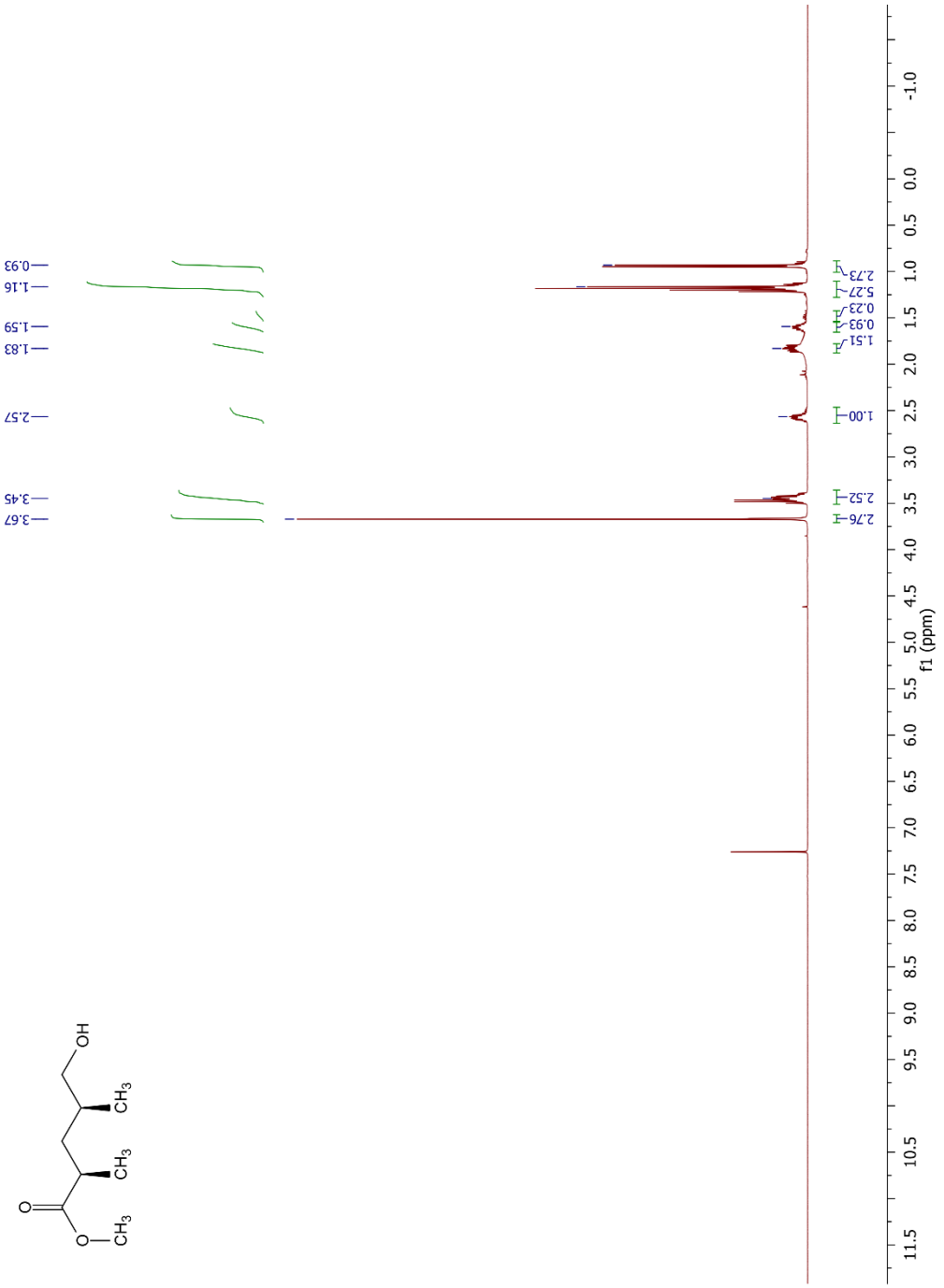

4.6.10 ^{13}C NMR of *syn*-dimethylhydroxy ester 4.16 ($CDCl_3$, 101 MHz, 298 K)

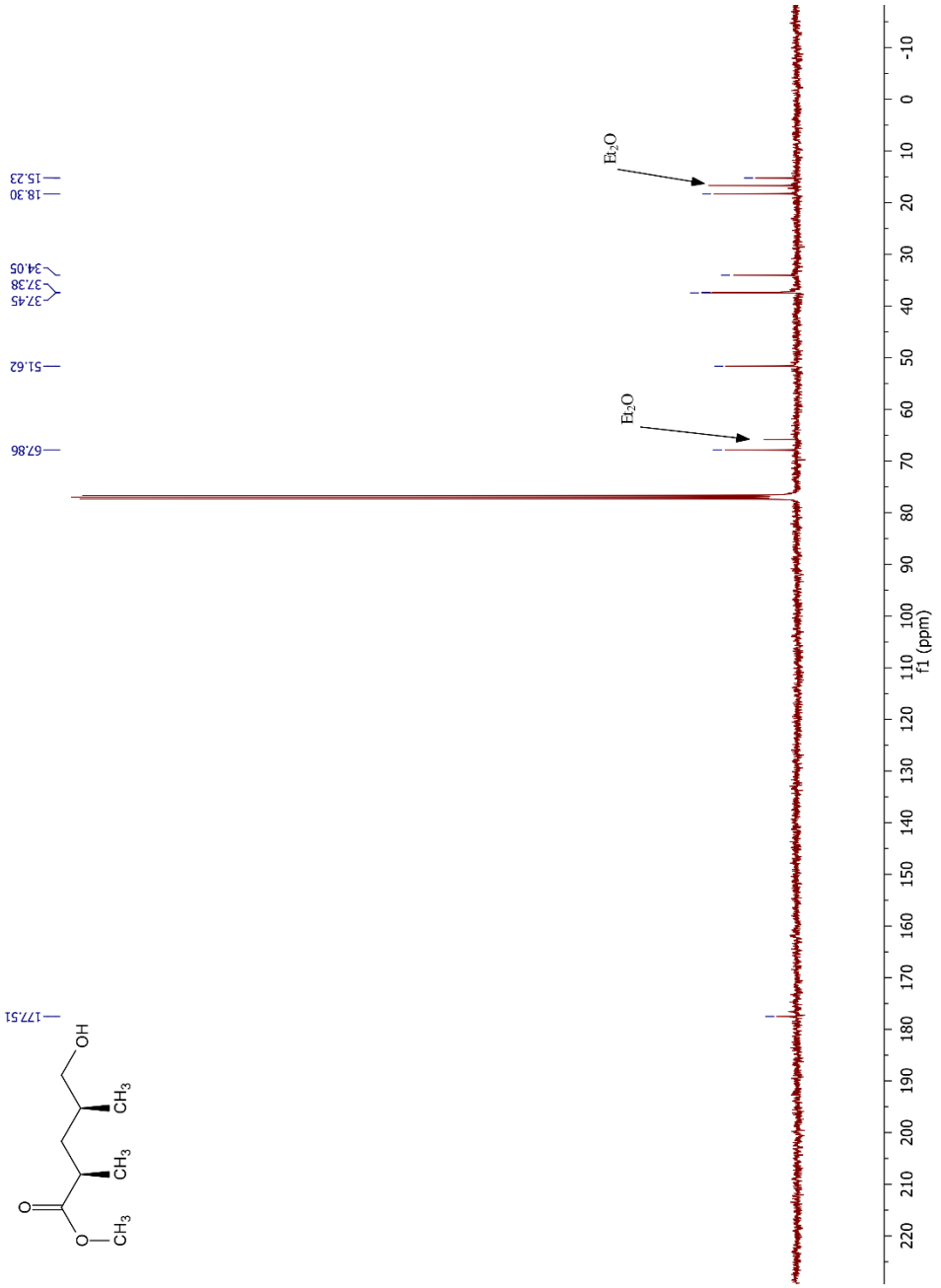

4.6.11 ^{1}H NMR of *syn*- & *anti*-4.08 ($CDCl_3$, 400 MHz, 298 K)

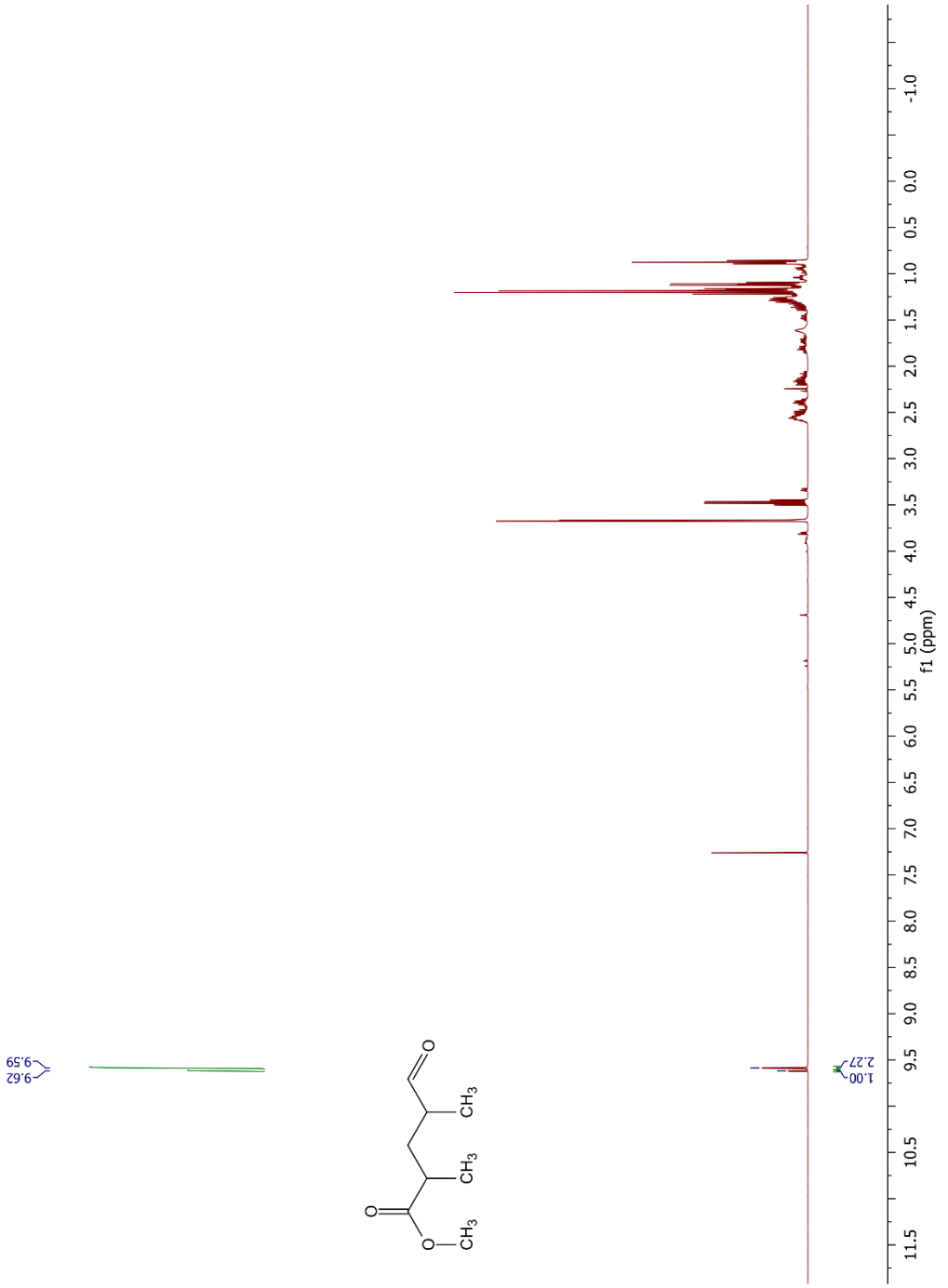

4.6.12 ^{13}C NMR of *syn*- & *anti*-4.08 ($CDCl_3$, 400 MHz, 298 K)

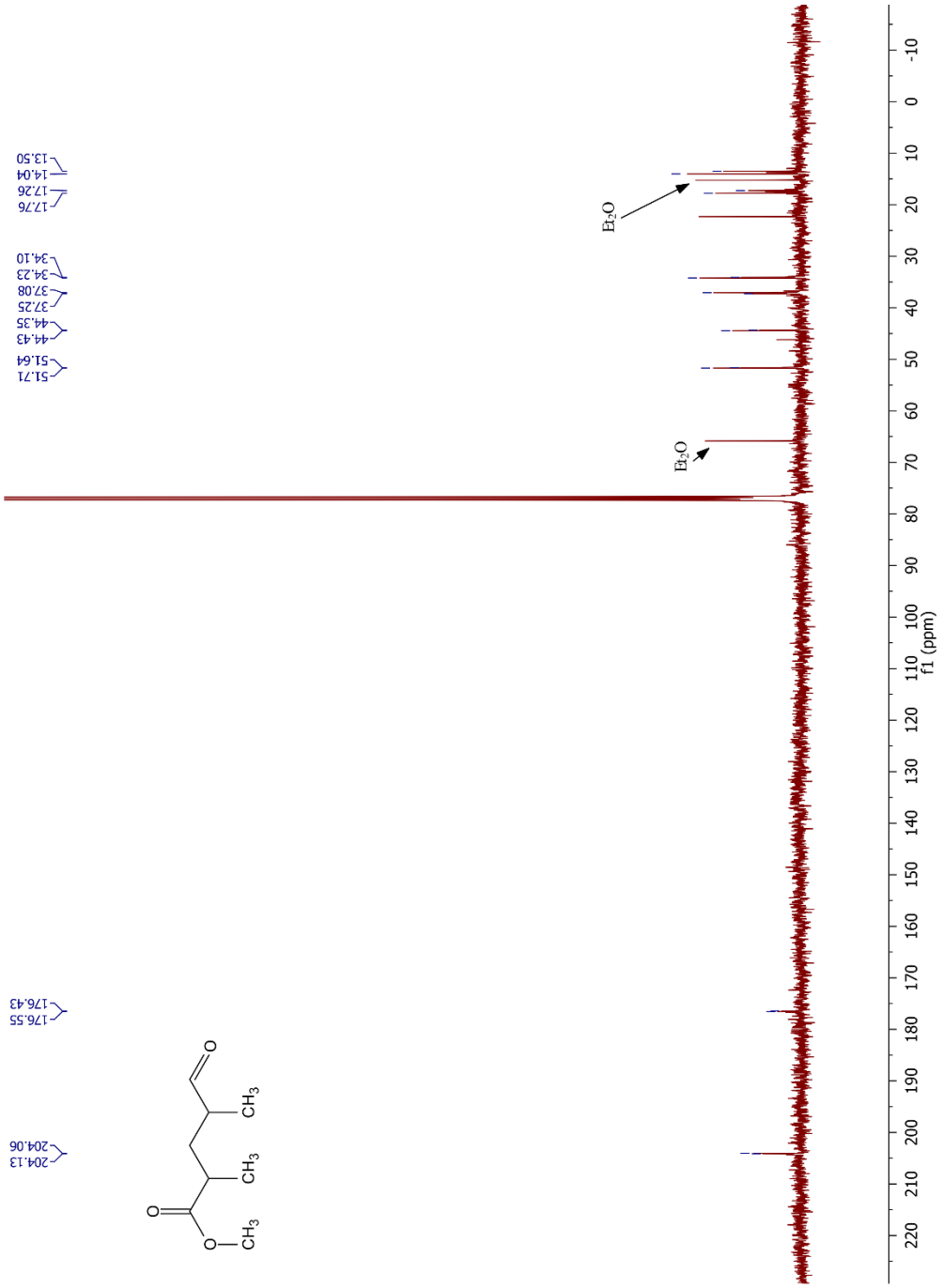

4.6.13 ^{1}H NMR of (*E*)-2-bromo-3-pentene ($CDCl_3$, 400 MHz, 298 K)

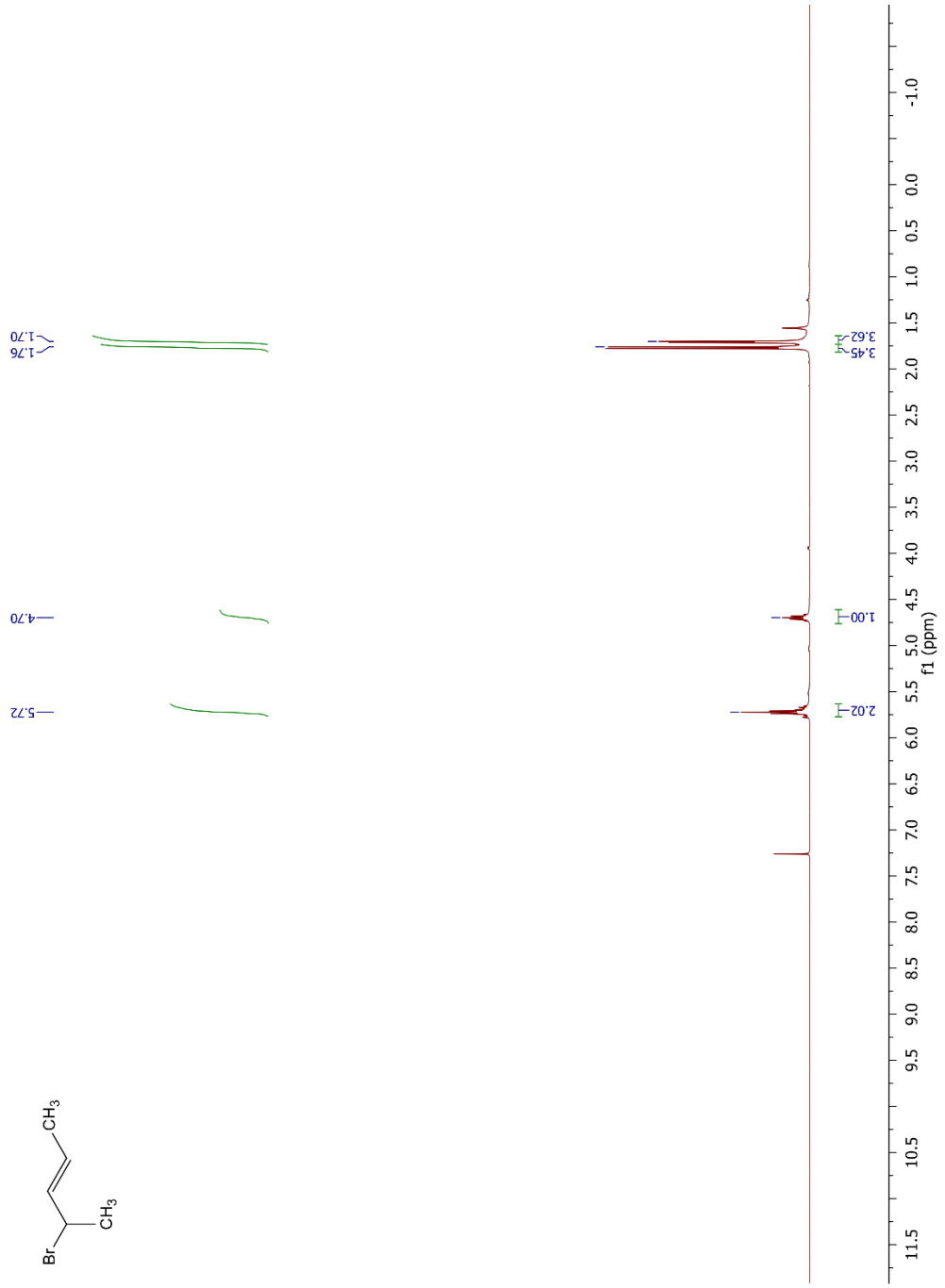

4.6.14 ^{13}C NMR of (*E*)-2-bromo-3-pentene ($CDCl_3$, 101 MHz, 298 K)

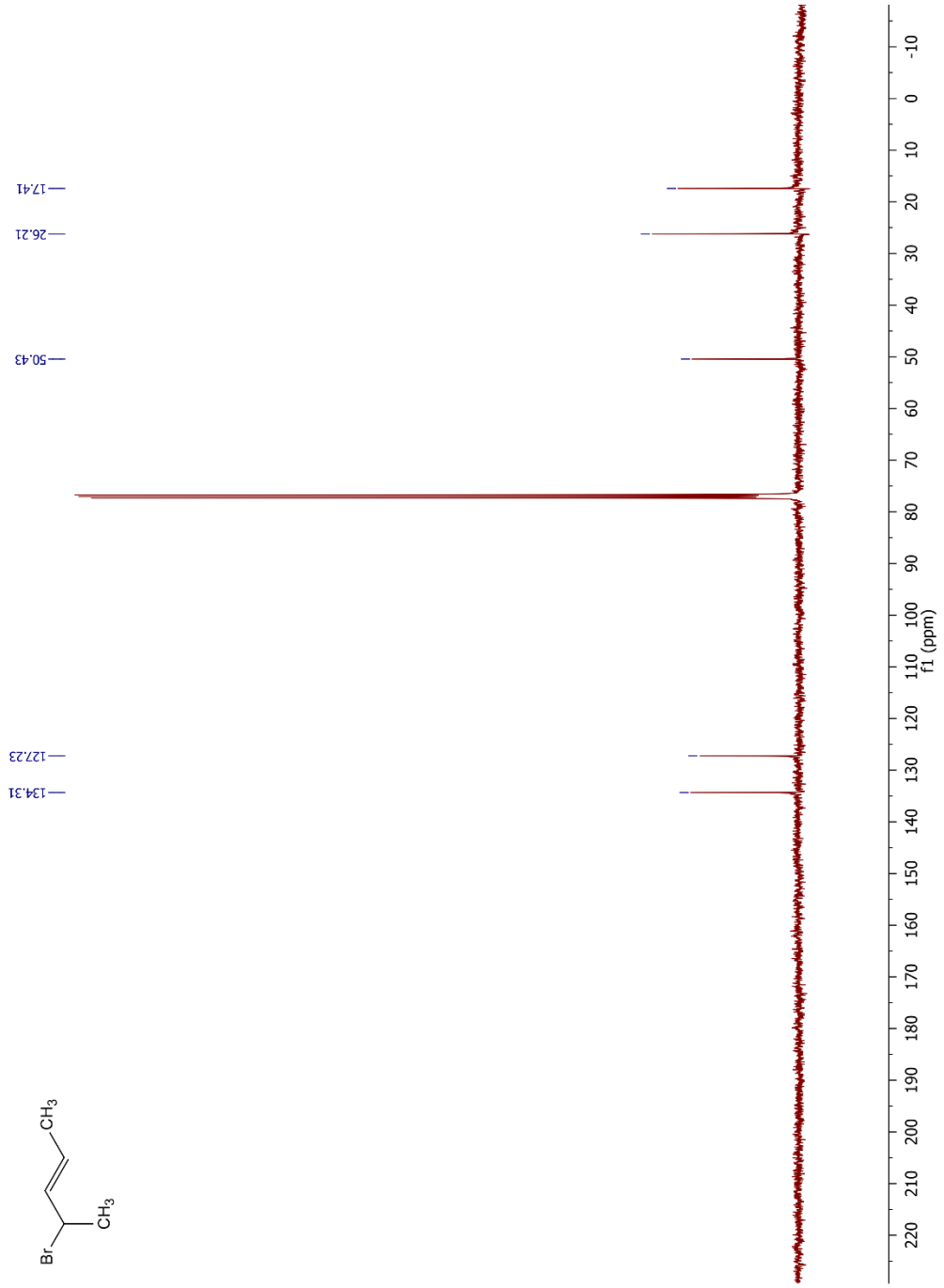

4.6.15 ^{1}H NMR of (*E*)-pent-3-en-2-yltriphenylphosphonium bromide ($CDCl_3$, 400 MHz, 298 K)

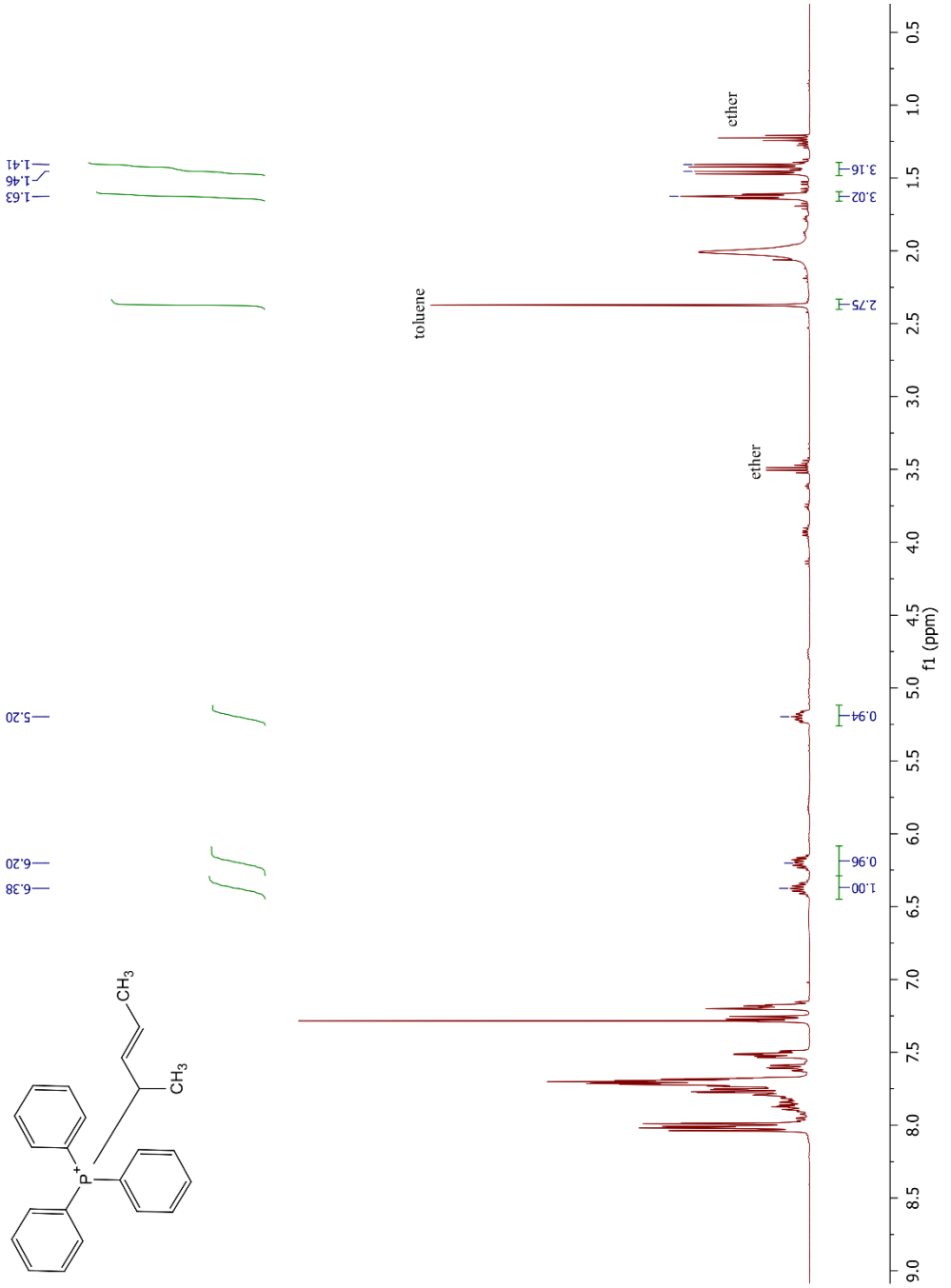

4.6.16 ^{13}C NMR of (*E*)-pent-3-en-2-yltriphenylphosphonium bromide ($CDCl_3$, 101 MHz, 298 K)

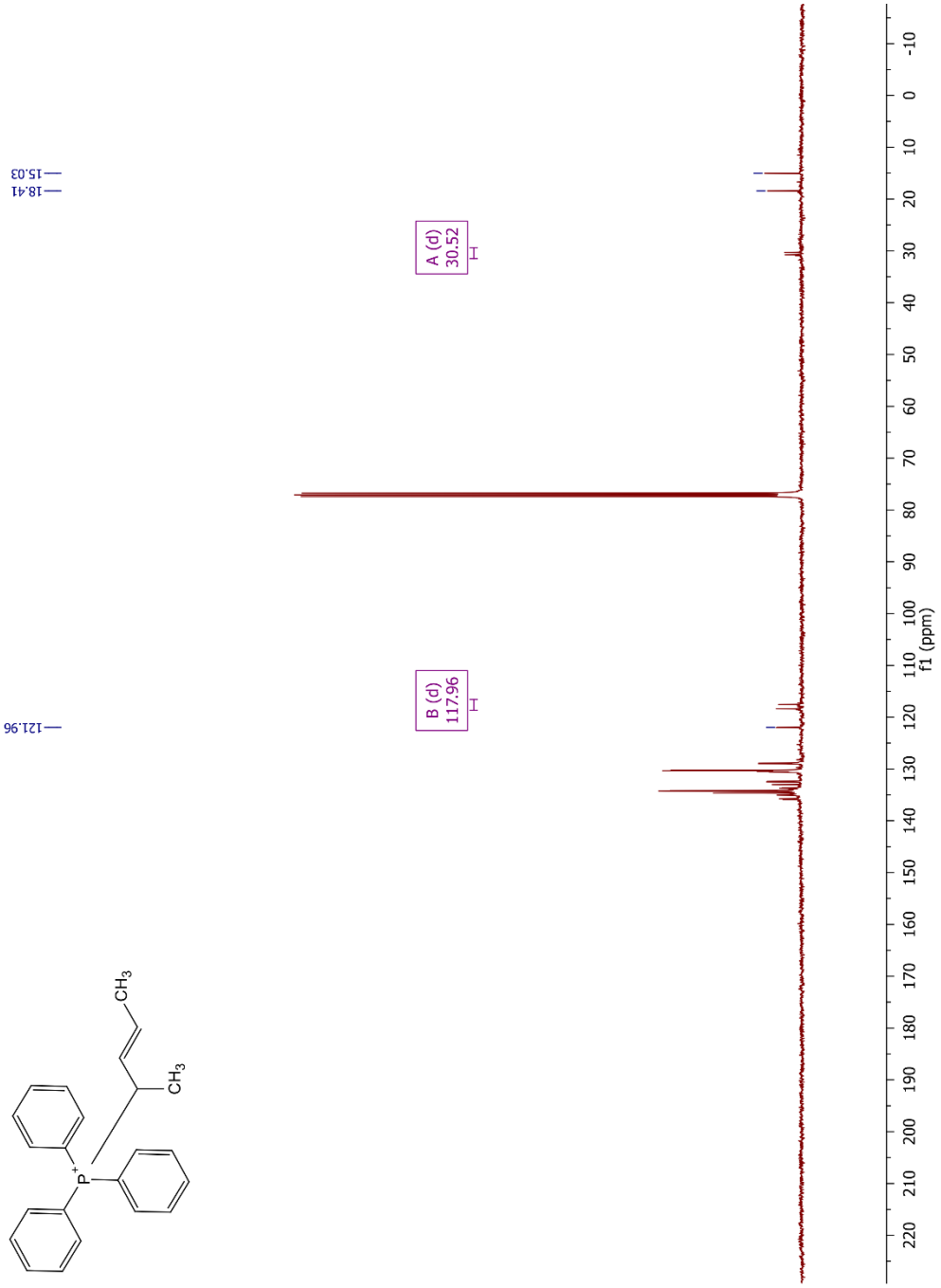

4.6.17 ^{1}H NMR of synthetic *rac*-4.01, isolated by prep GC (CD_2Cl_2, 600 MHz, 296 K)

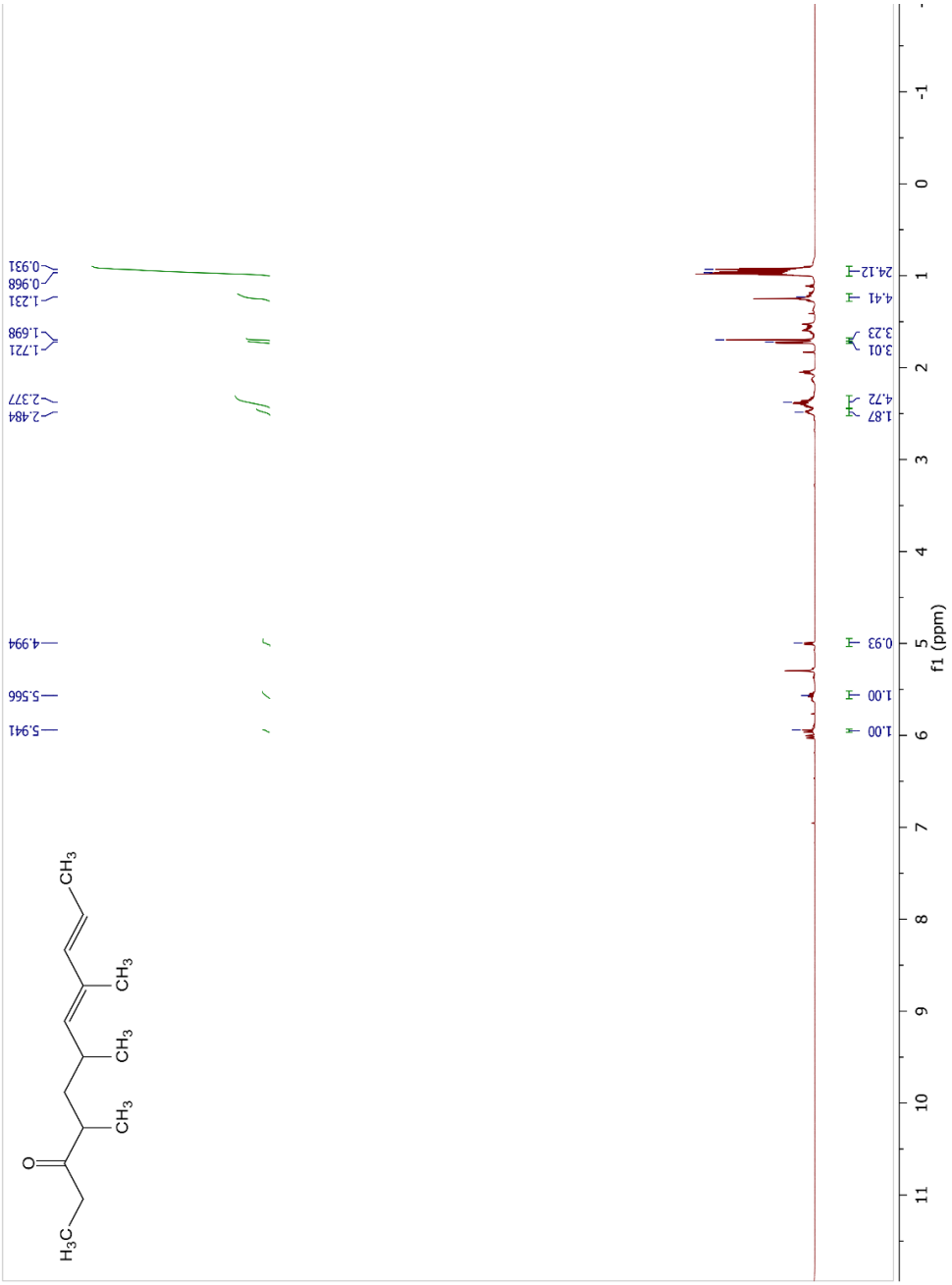

4.6.18 ^{1}H-^{1}H NOESY NMR of synthetic *rac*-4.01, isolated by prep GC (CD_2Cl_2, 600 MHz, 296 K, mixing time = 0.8 s)

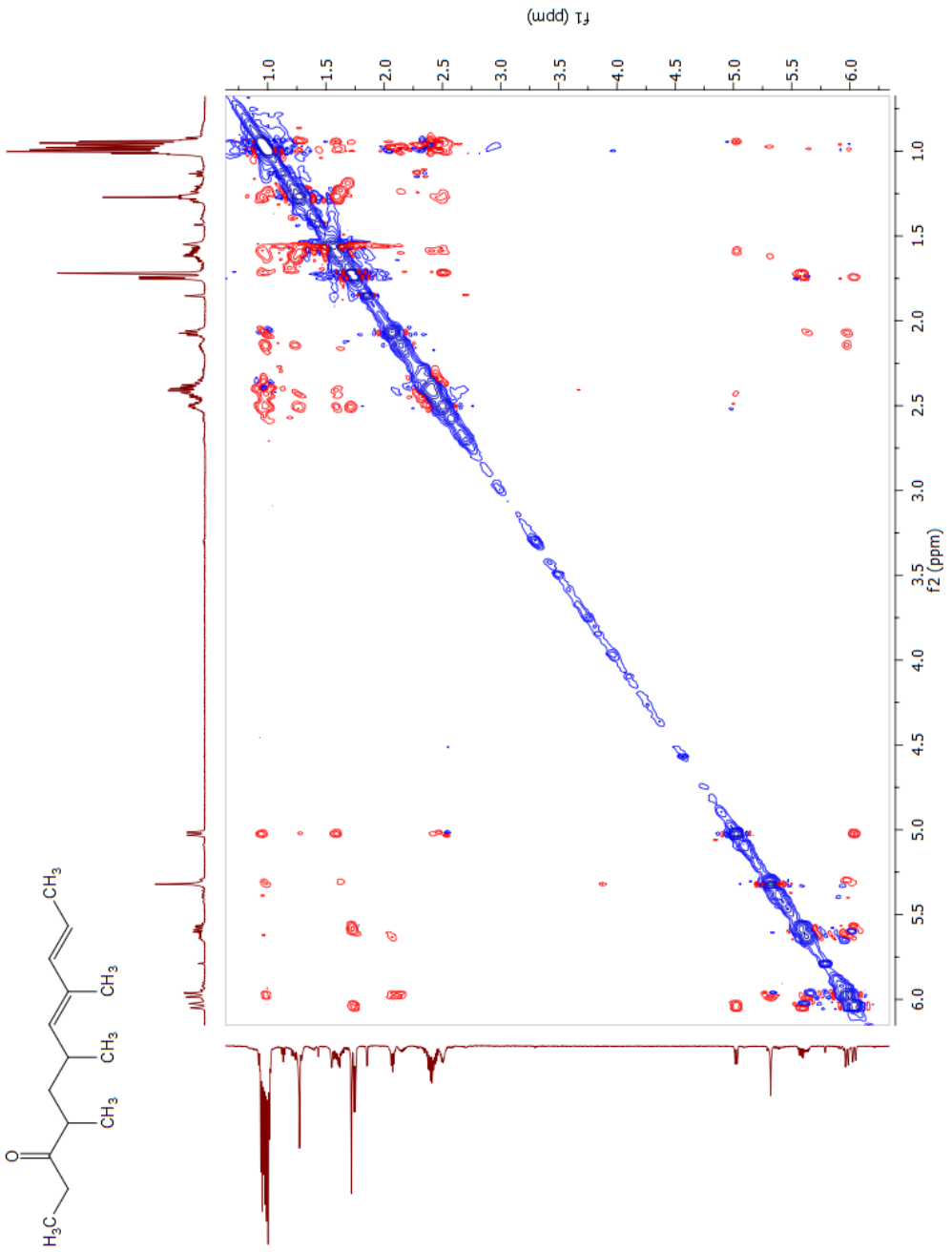

4.6.19 ^{1}H NMR of dimethyl ester 4.21 ($CDCl_3$, 400 MHz, 298 K)

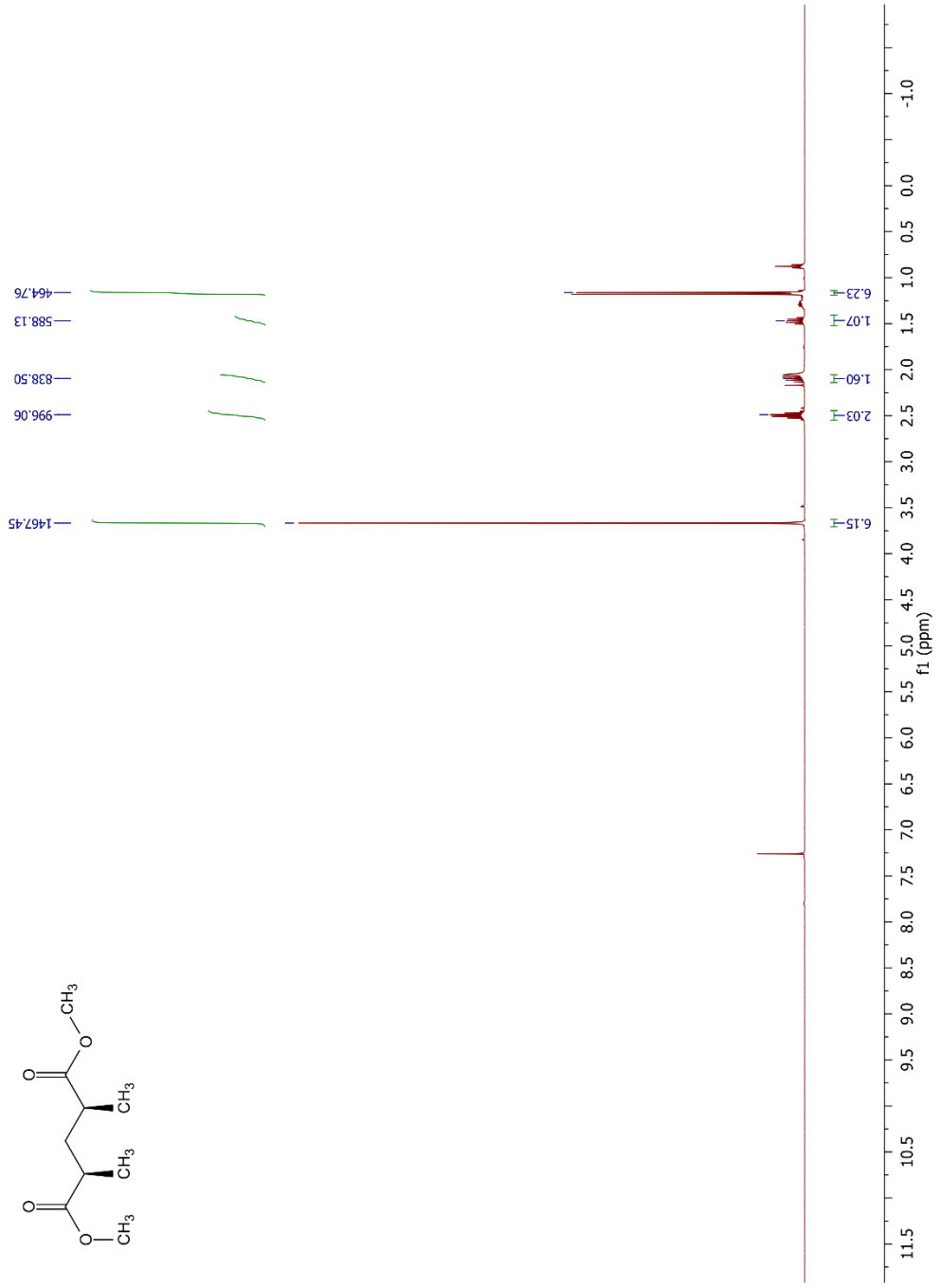

4.6.20 ^{13}C NMR of dimethyl ester 4.21 ($CDCl_3$, 101 MHz, 298 K)

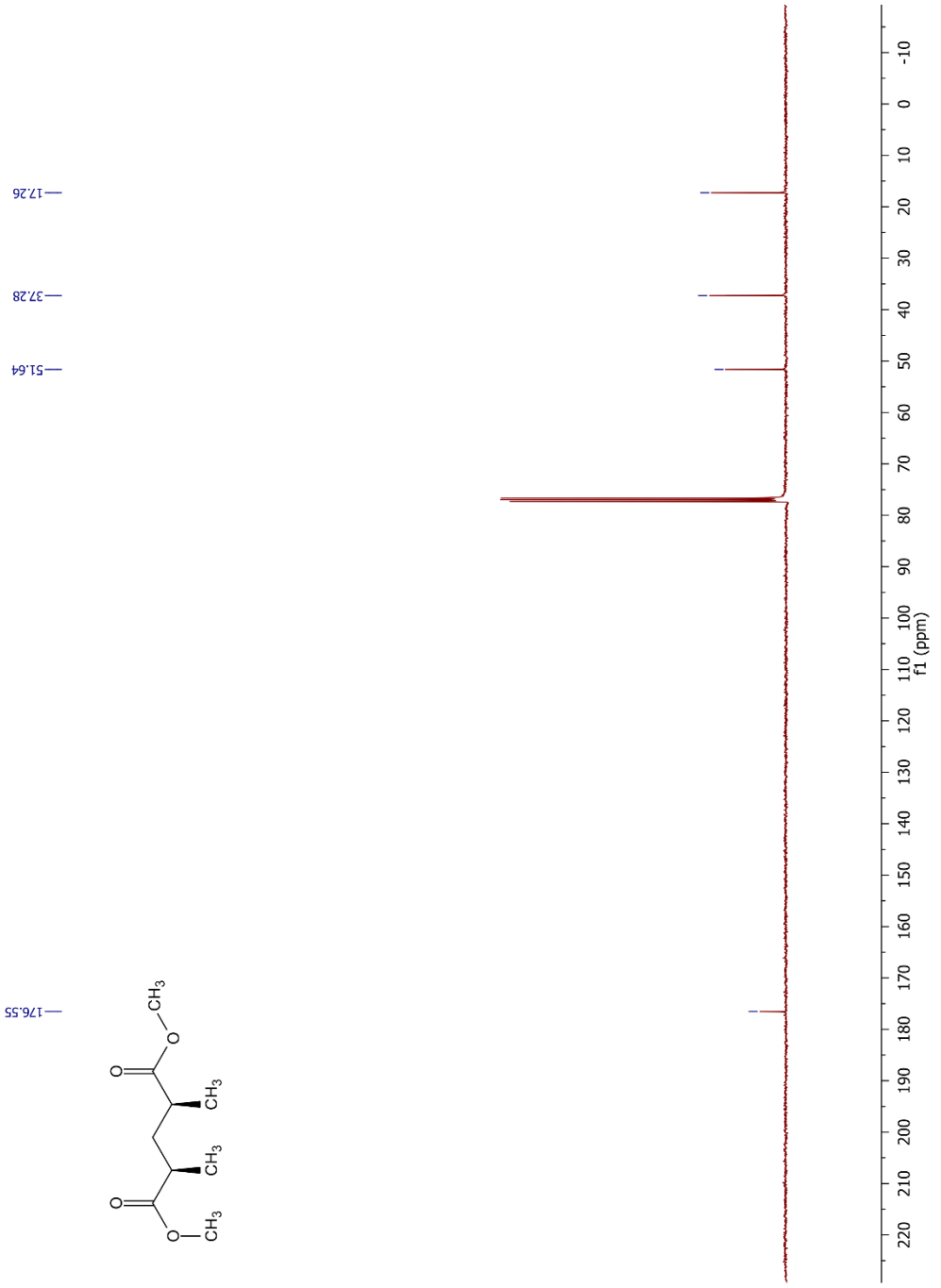

4.6.21 ^{1}H NMR of hemiester 4.22 ($CDCl_3$, 400 MHz, 298 K)

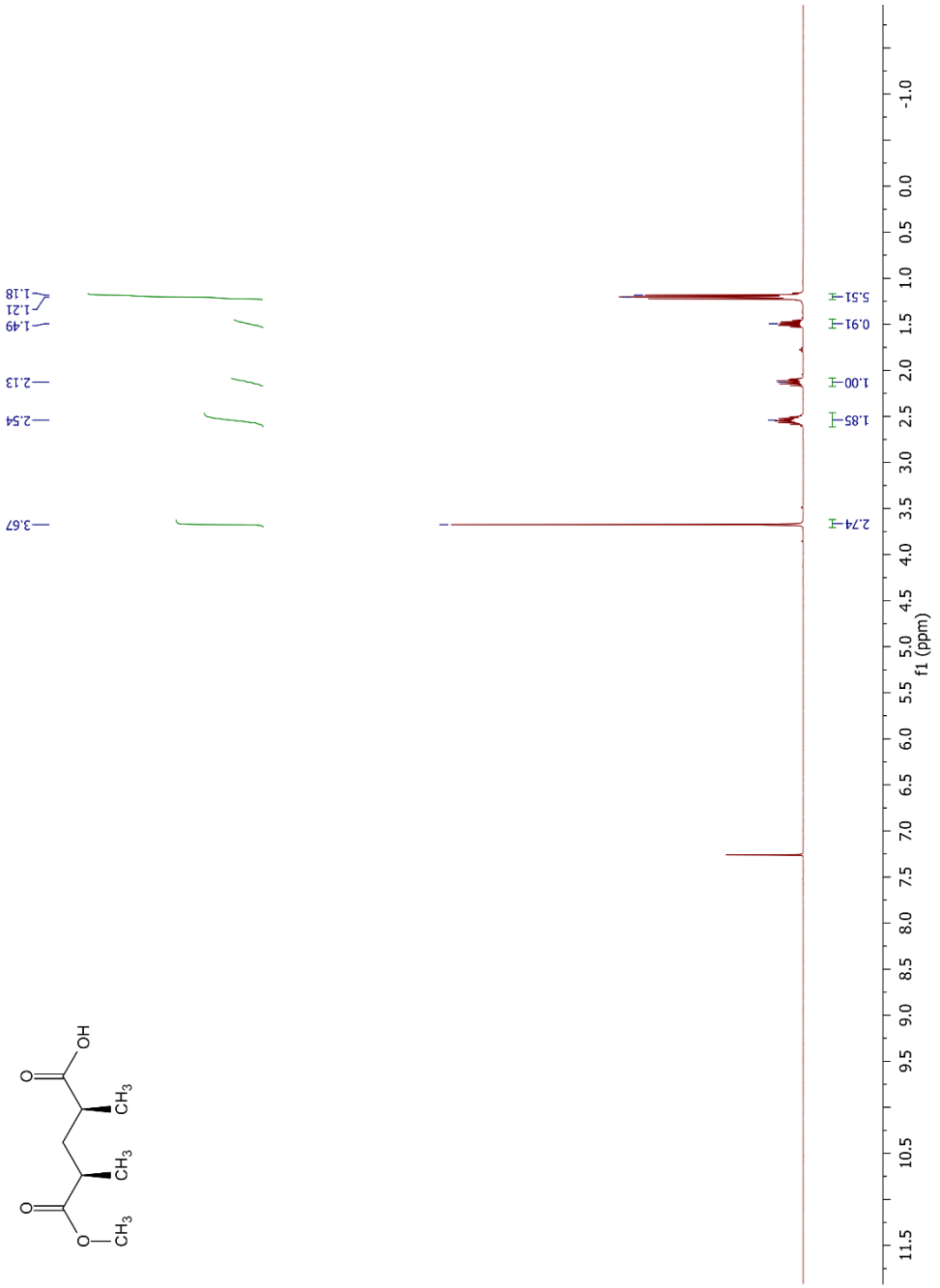

4.6.22 ^{13}C NMR of hemiester 4.22 ($CDCl_3$, 101 MHz, 298 K)

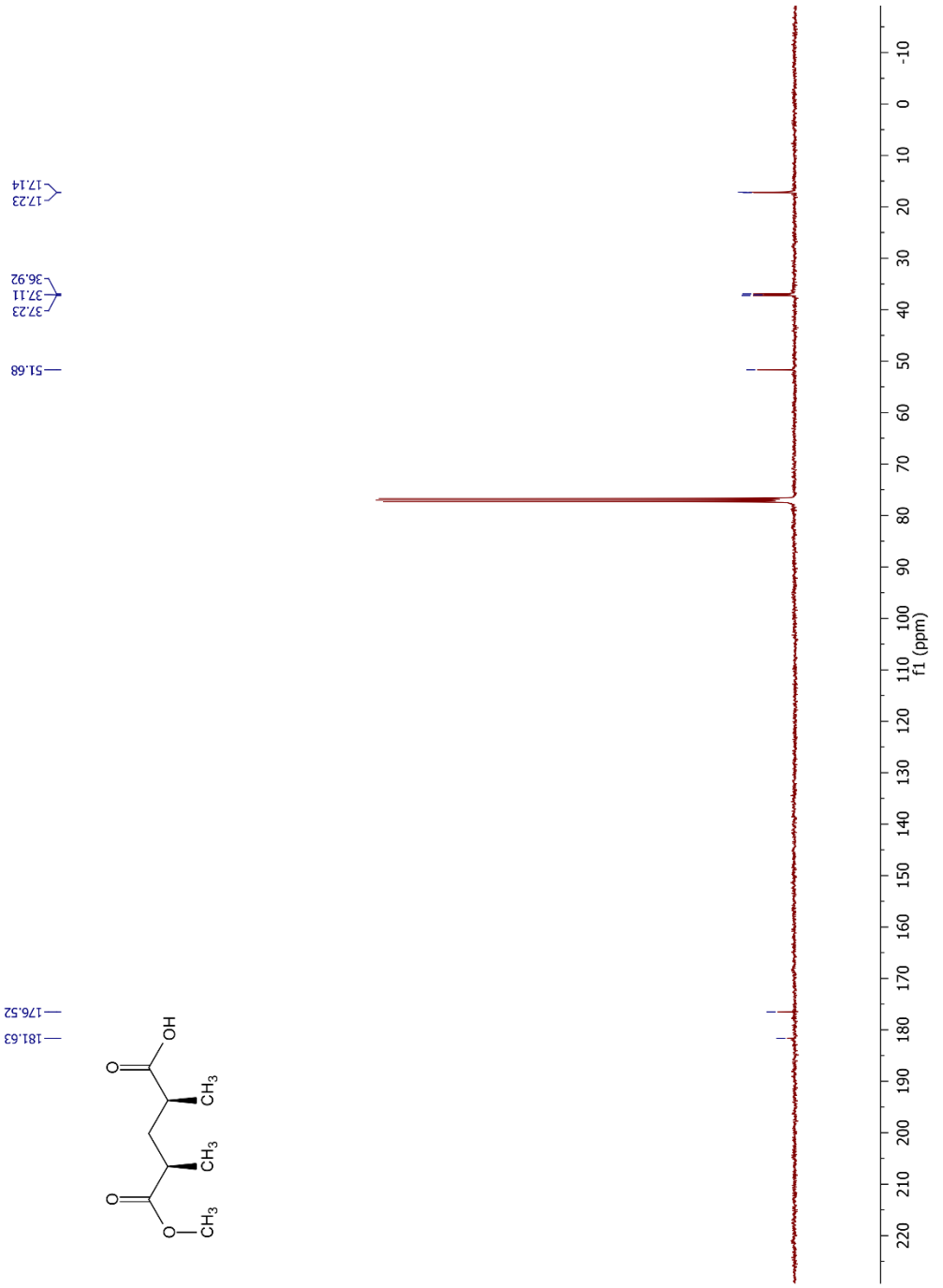

4.6.23 ^{1}H NMR of diynol 4.24 ($CDCl_3$, 500 MHz, 294 K)

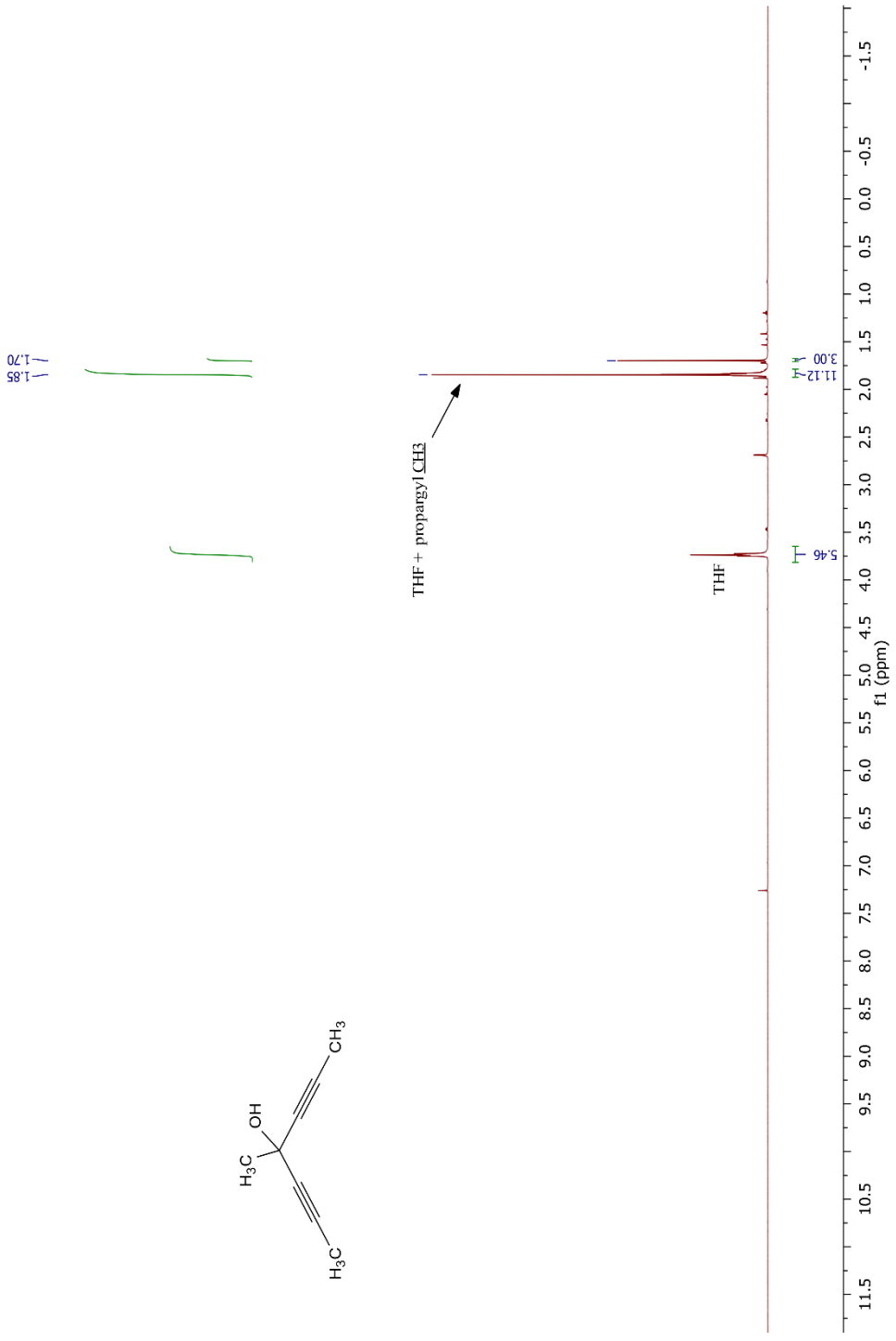

4.6.24 ^{13}C NMR of diynol 4.24 ($CDCl_3$, 126 MHz, 294 K)

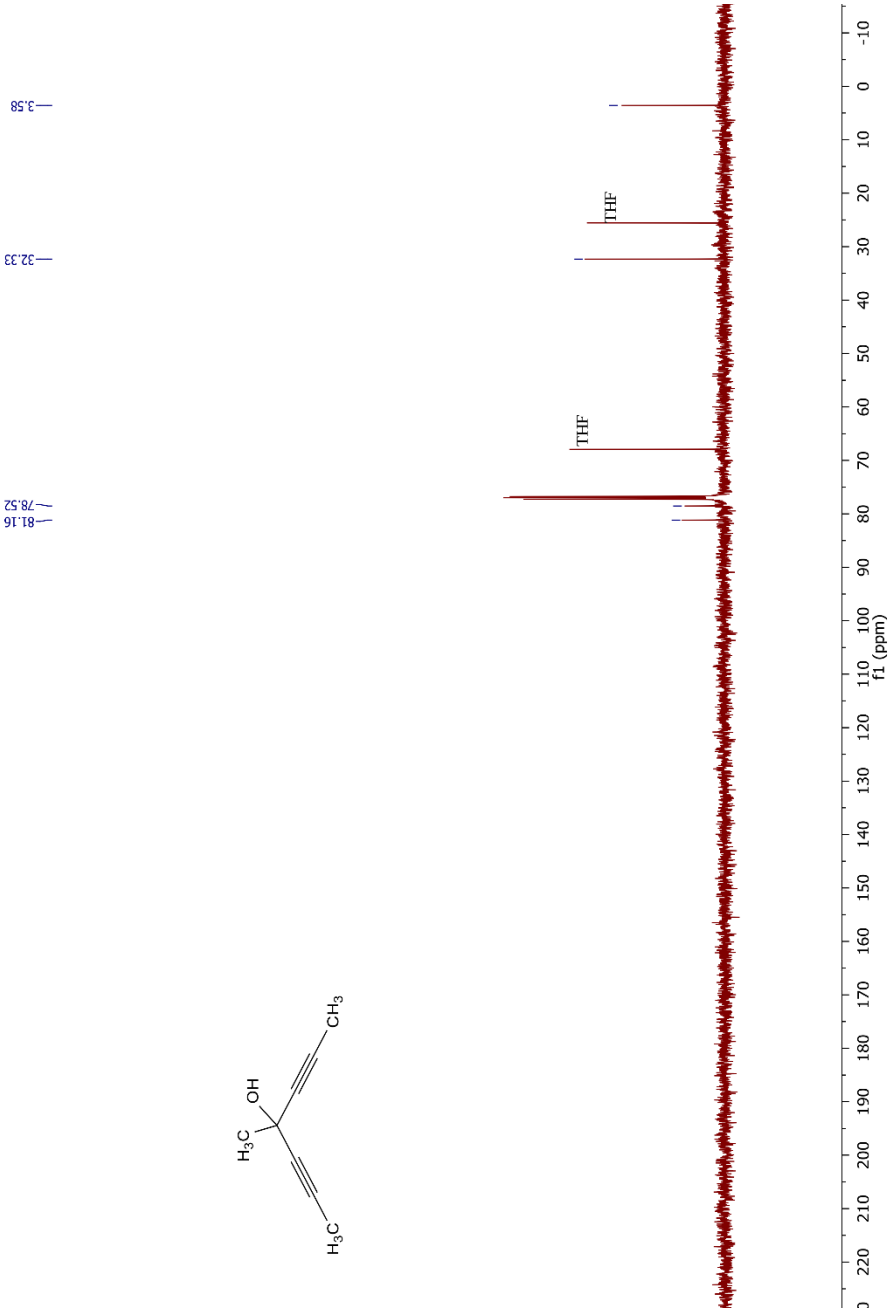

4.6.25 ^{1}H NMR of (*E*,*E*)-dien-4-ol 4.25 ($CDCl_3$, 400 MHz, 297 K)

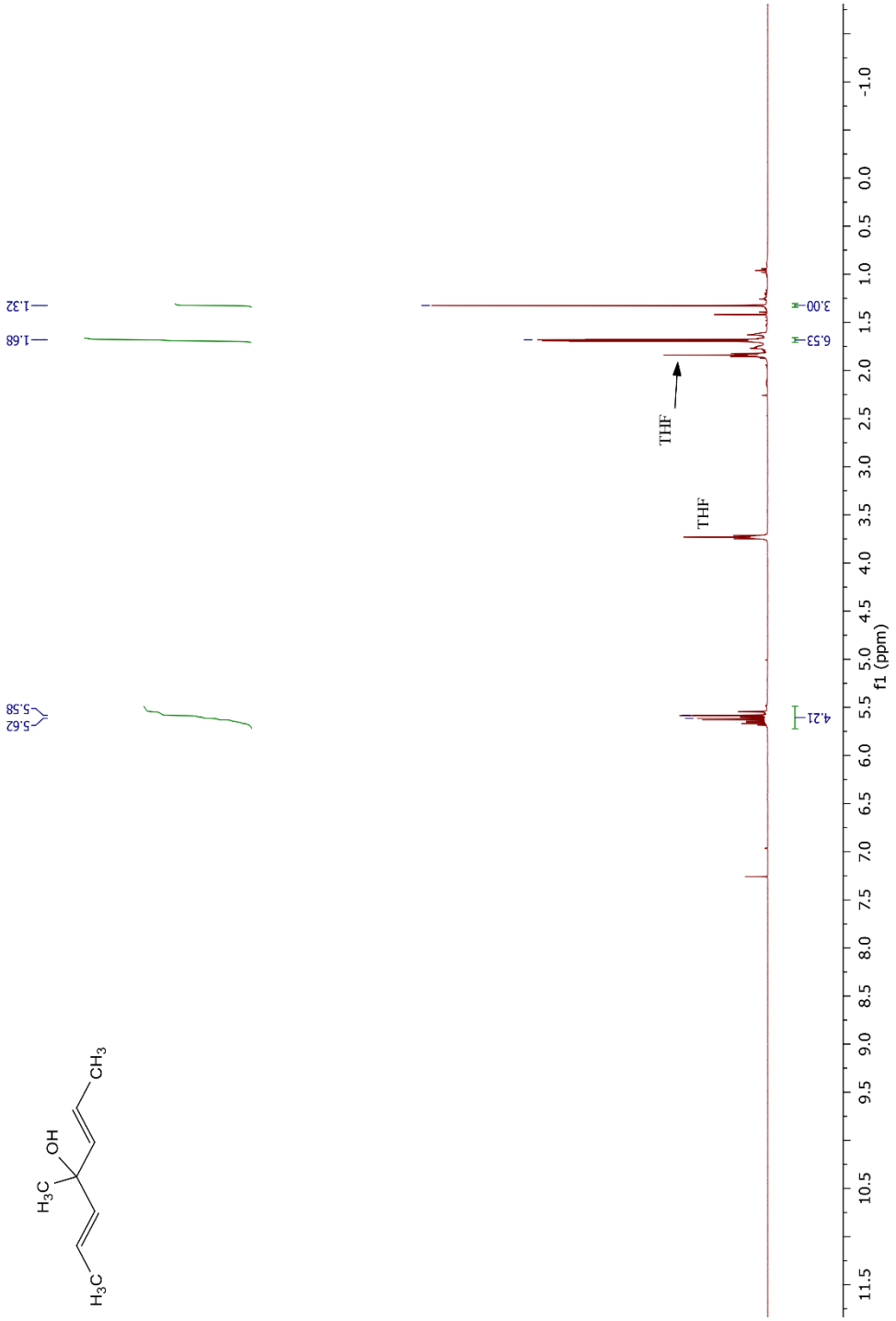

4.6.26 ^{13}C NMR of (*E*,*E*)-dien-4-ol 4.25 ($CDCl_3$, 101 MHz, 297 K)

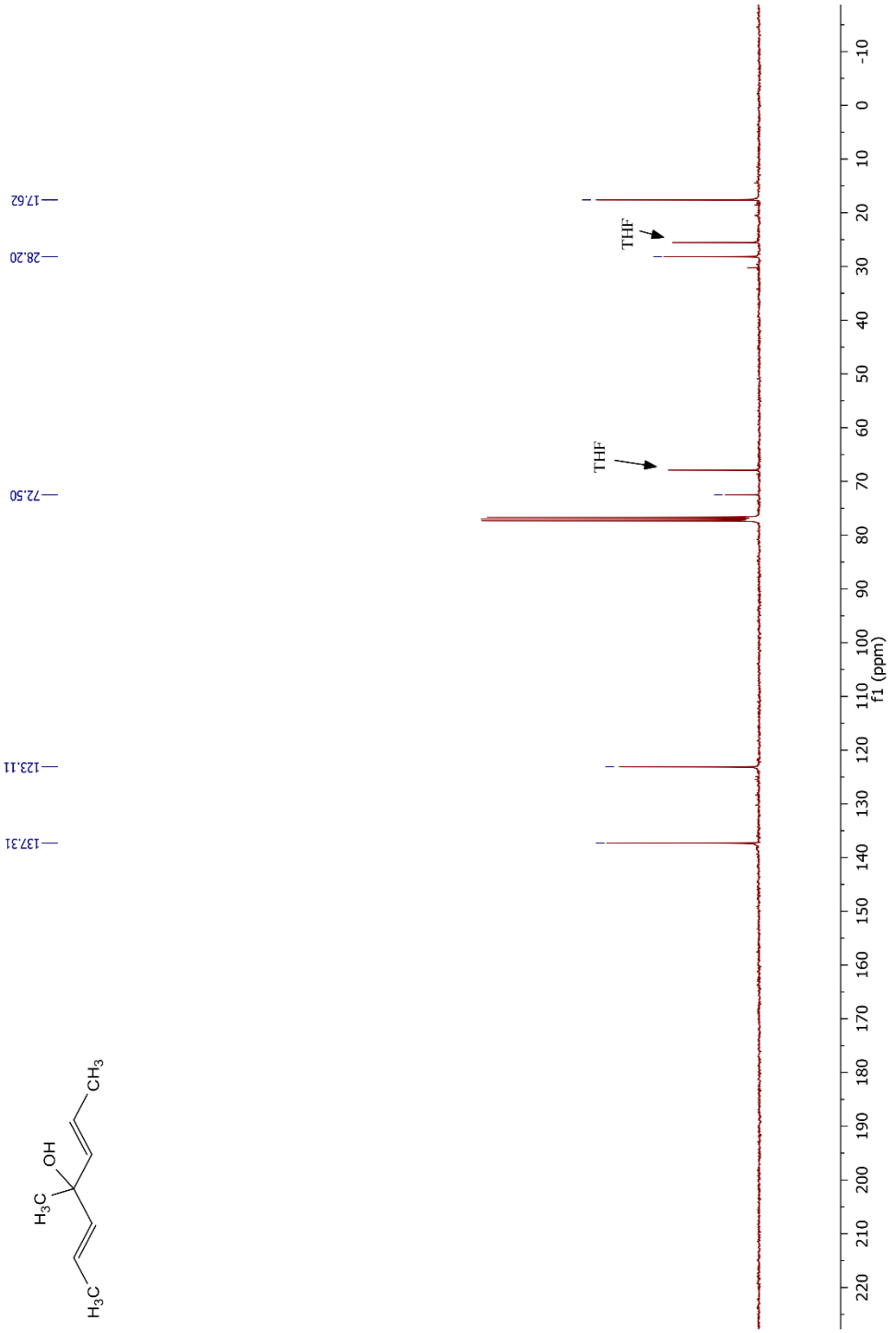

4.6.26 ^{1}H NMR of (*E*,*E*)-dien-1-ol 4.23 ($CDCl_3$, 500 MHz, 294 K)

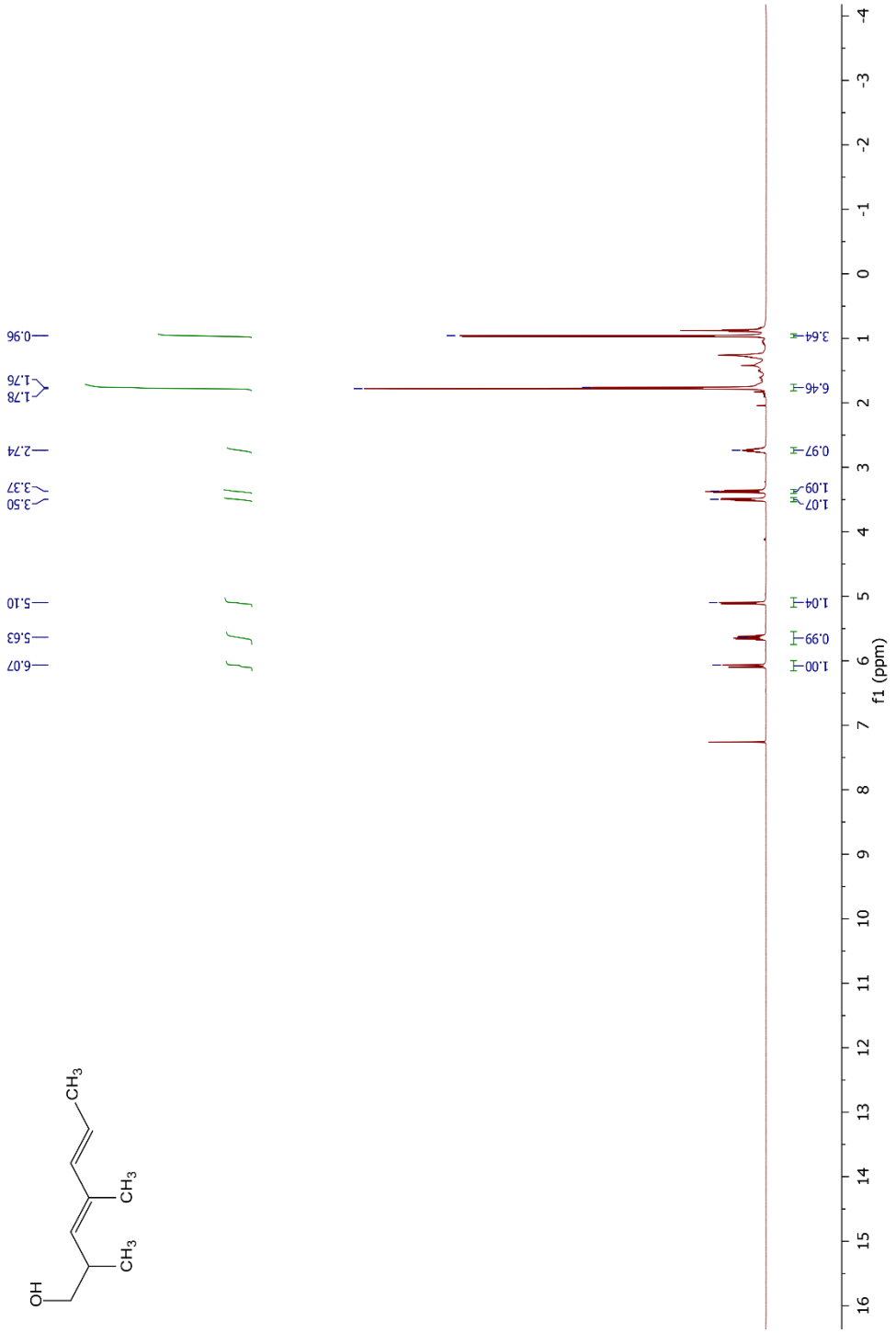

4.6.27 ^{13}C NMR of (*E*,*E*)-dien-1-ol 4.23 ($CDCl_3$, 126 MHz, 294 K)

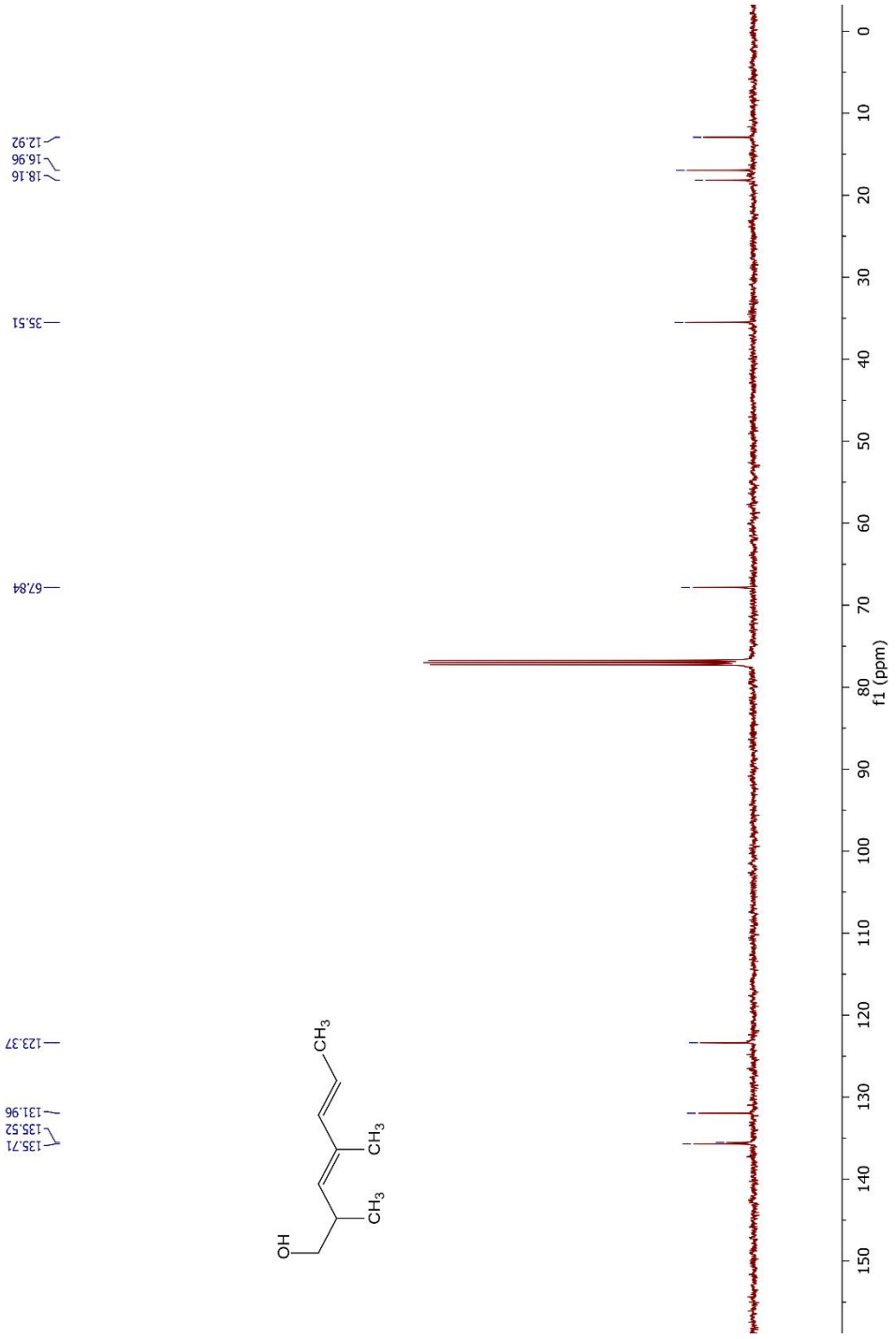

4.6.28 ^{1}H NMR of iodide 4.27 ($CDCl_3$, 500 MHz, 296 K)

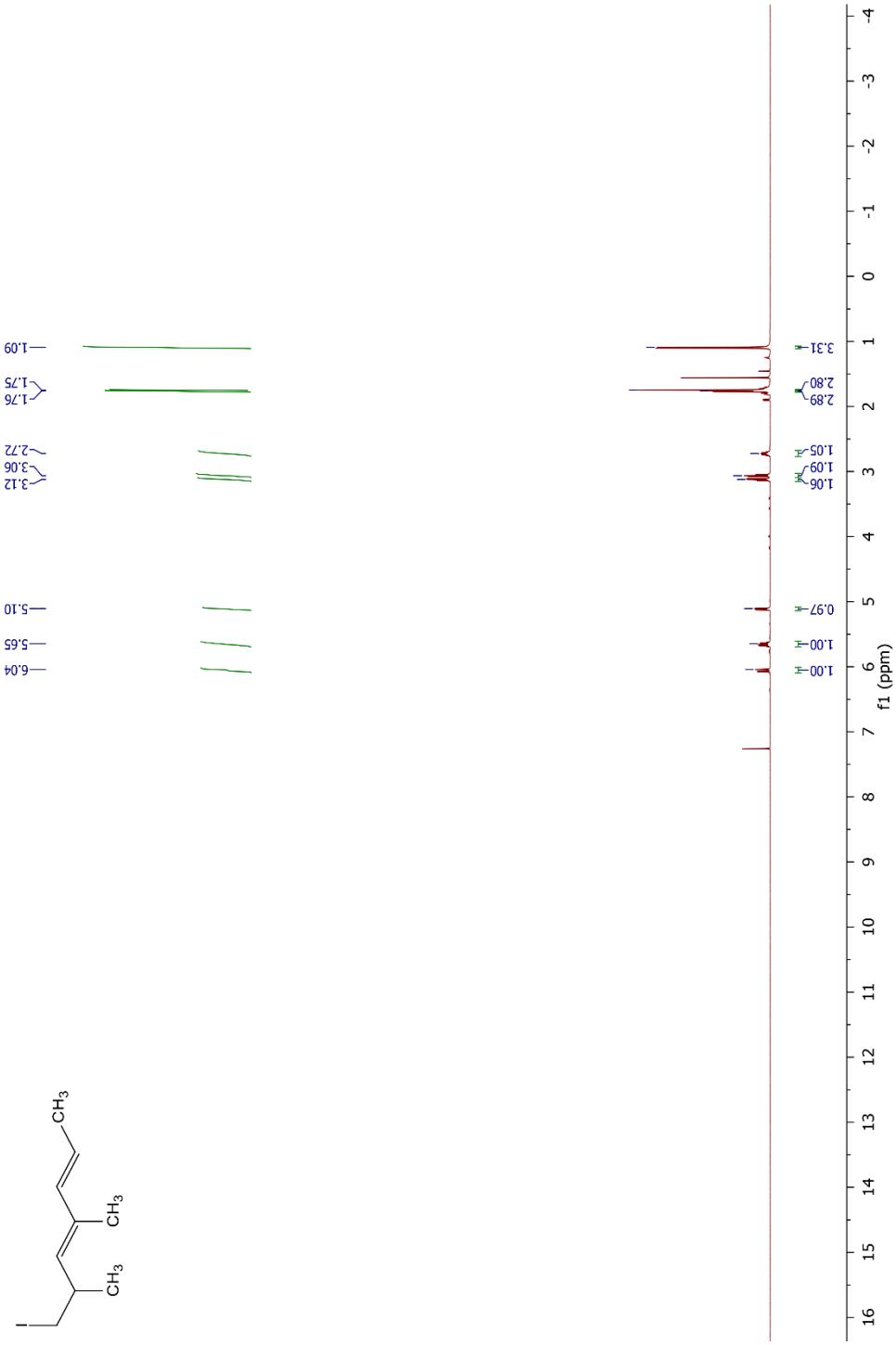

4.6.29 ^{13}C NMR of iodide 4.27 ($CDCl_3$, 126 MHz, 296 K)

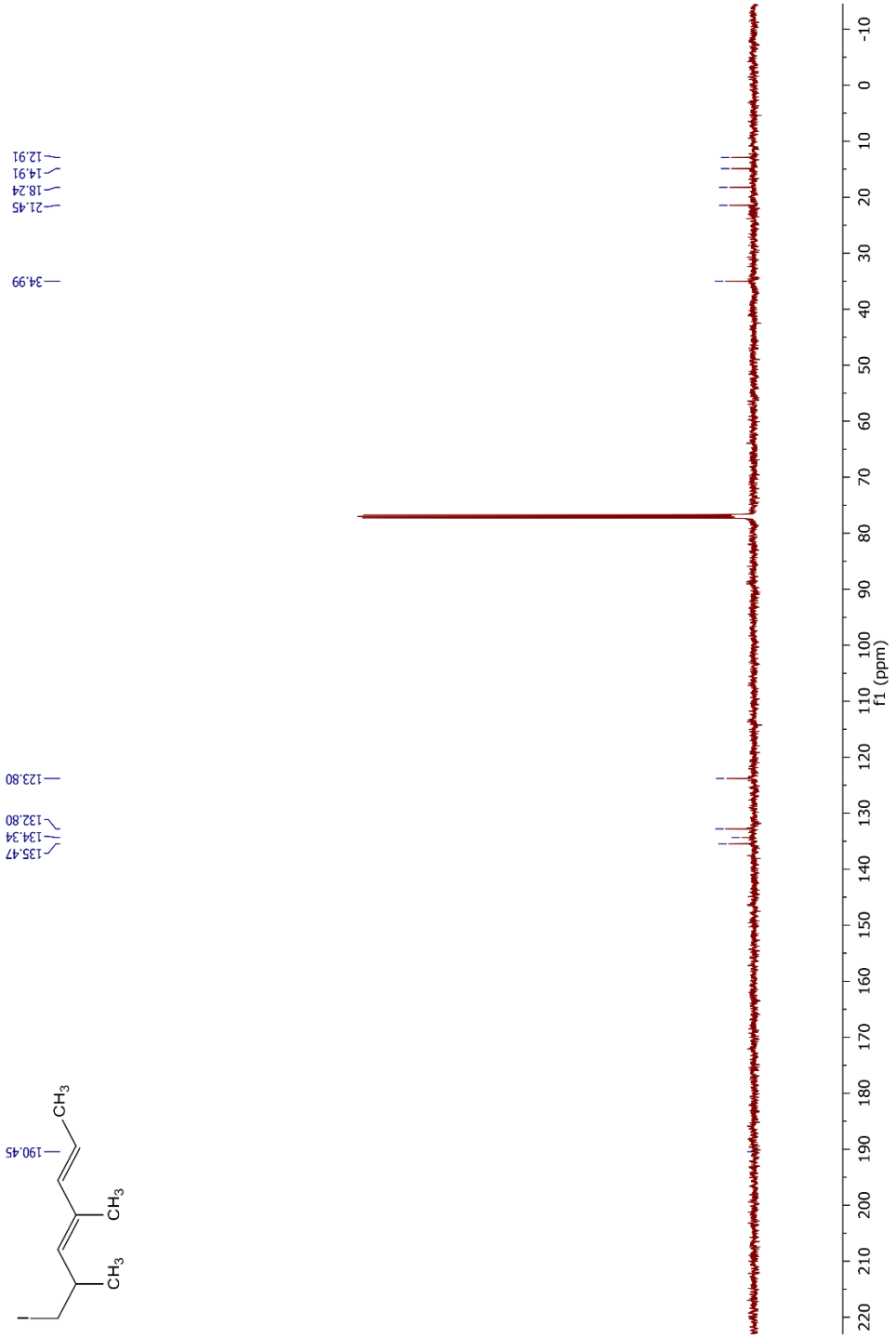

4.6.30 ^{1}H NMR of Benzyl NCC hydrazone 4.33 ($CDCl_3$, 500 MHz, 294 K)

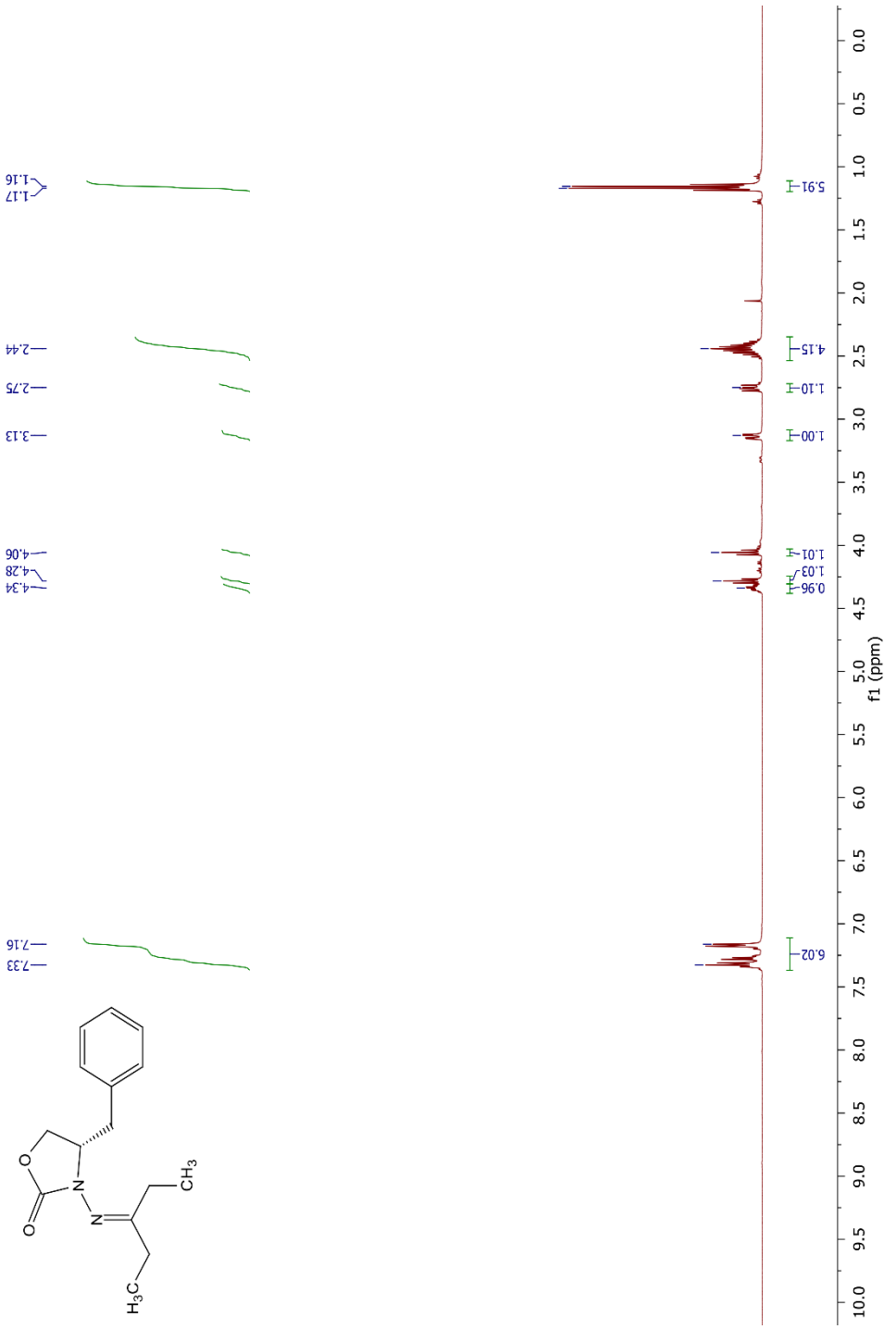

4.6.31 ^{13}C NMR of Benzyl NCC hydrazone 4.33 ($CDCl_3$, 126 MHz, 294 K)

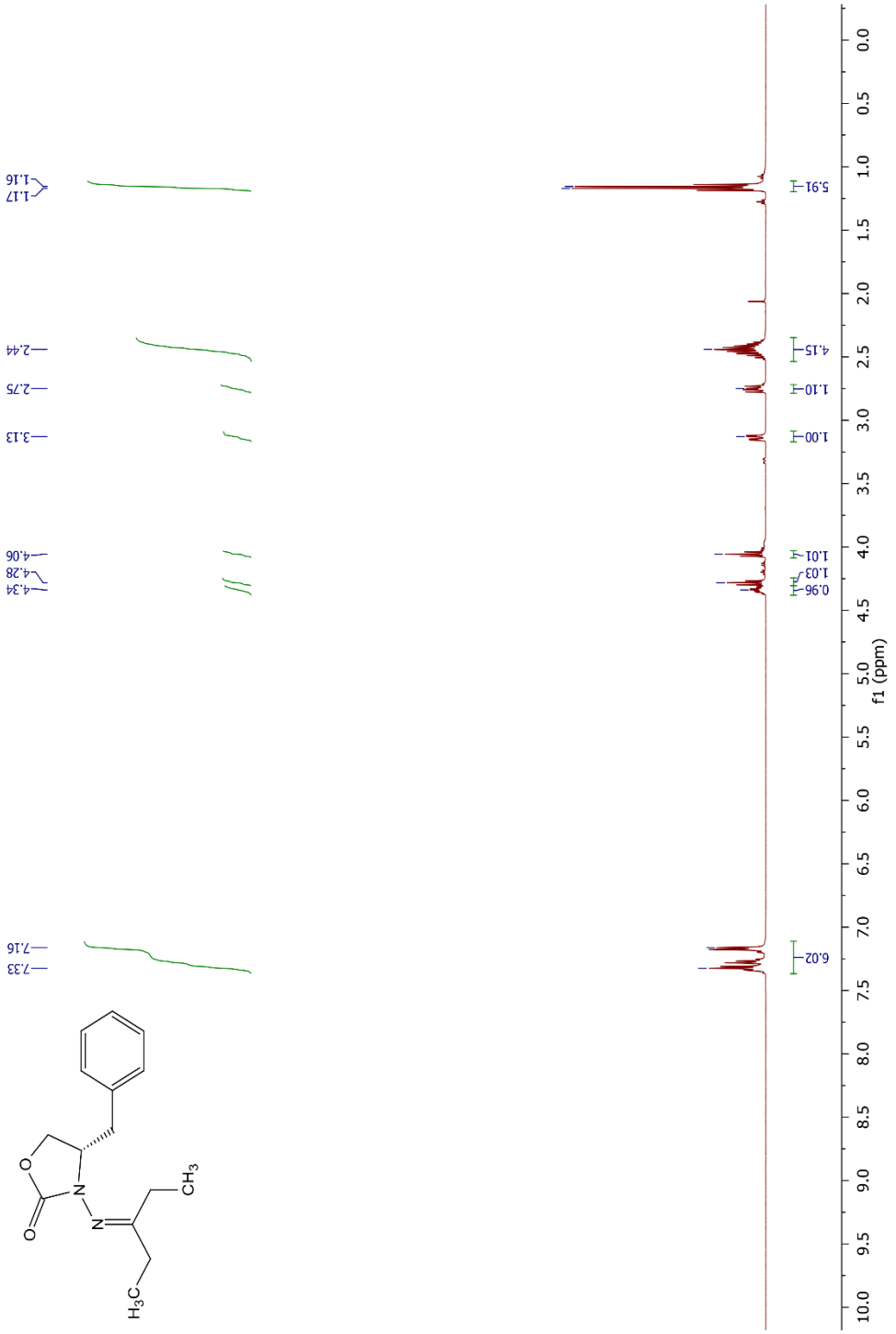

4.6.32 ^{1}H NMR of (1*S*,2*S*)-(+)-pseudoephedrine ($CDCl_3$, 500 MHz, 294 K)

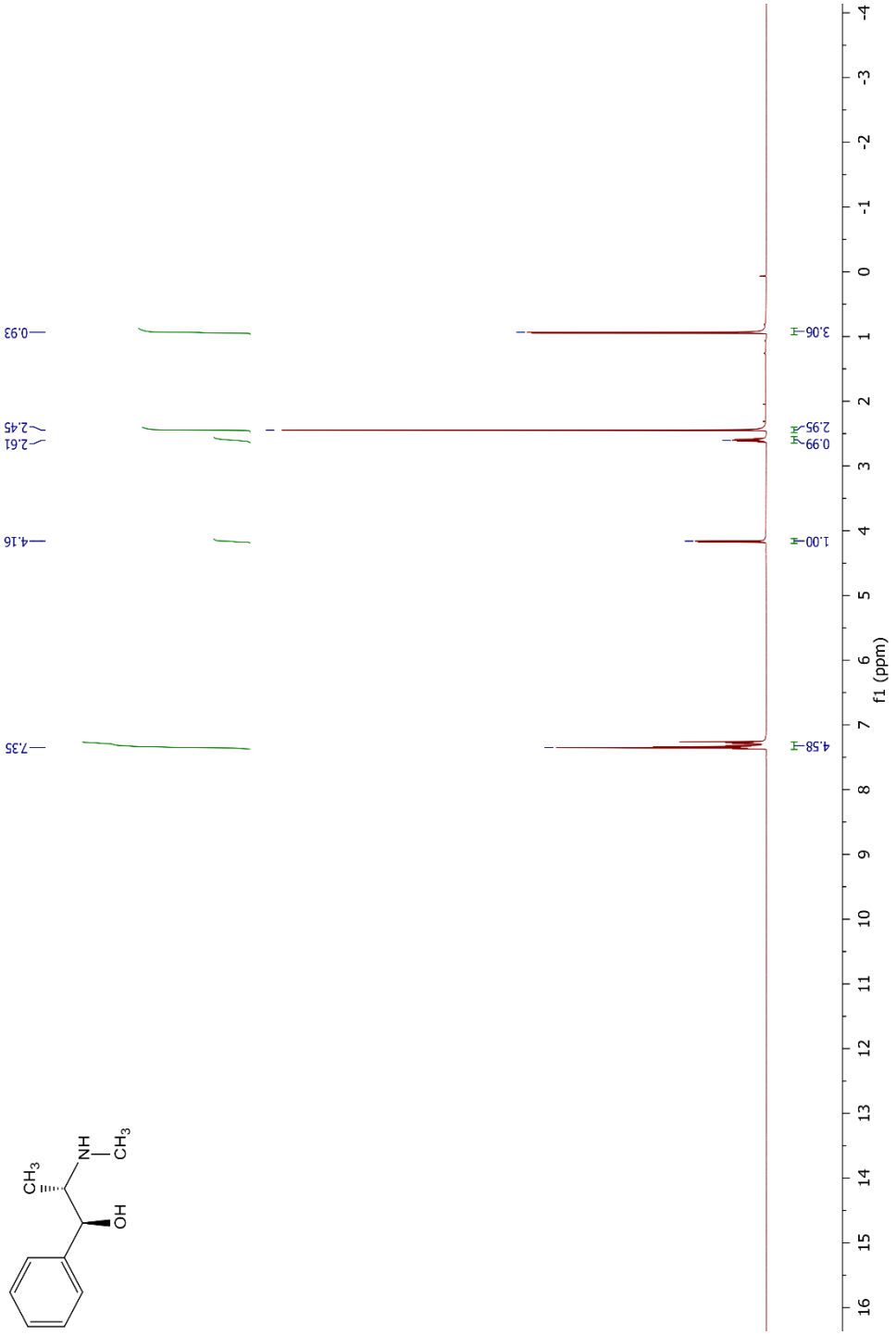

4.6.33 ^{13}C NMR of (1*S*,2*S*)-(+)-pseudoephedrine ($CDCl_3$, 126 MHz, 294 K)

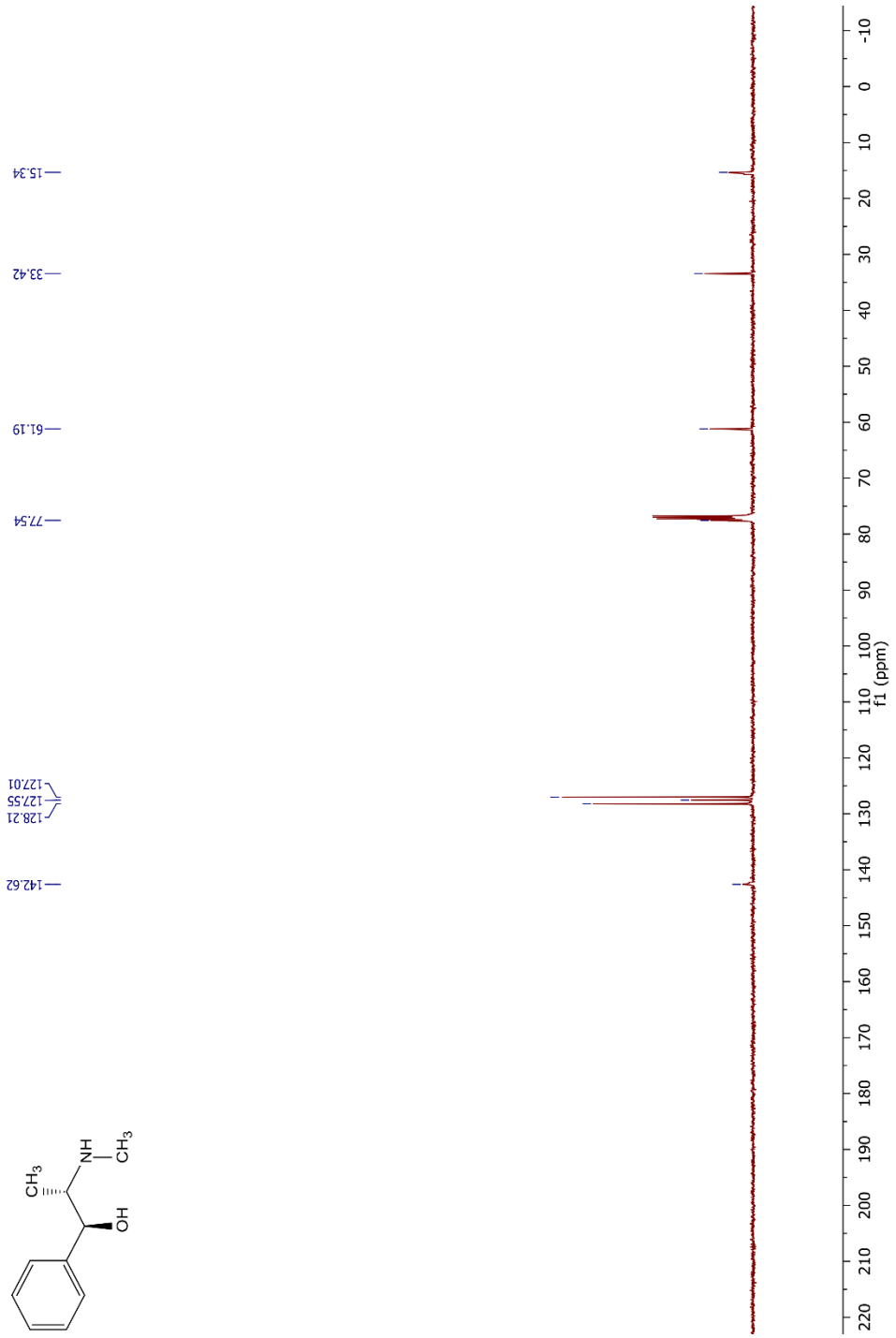

4.6.34 ^{1}H NMR of Myers auxiliary *N*-propionyl (1*S*,2*S*)-(+)-pseudoephedrine ($CDCl_3$, 500 MHz, 294 K)

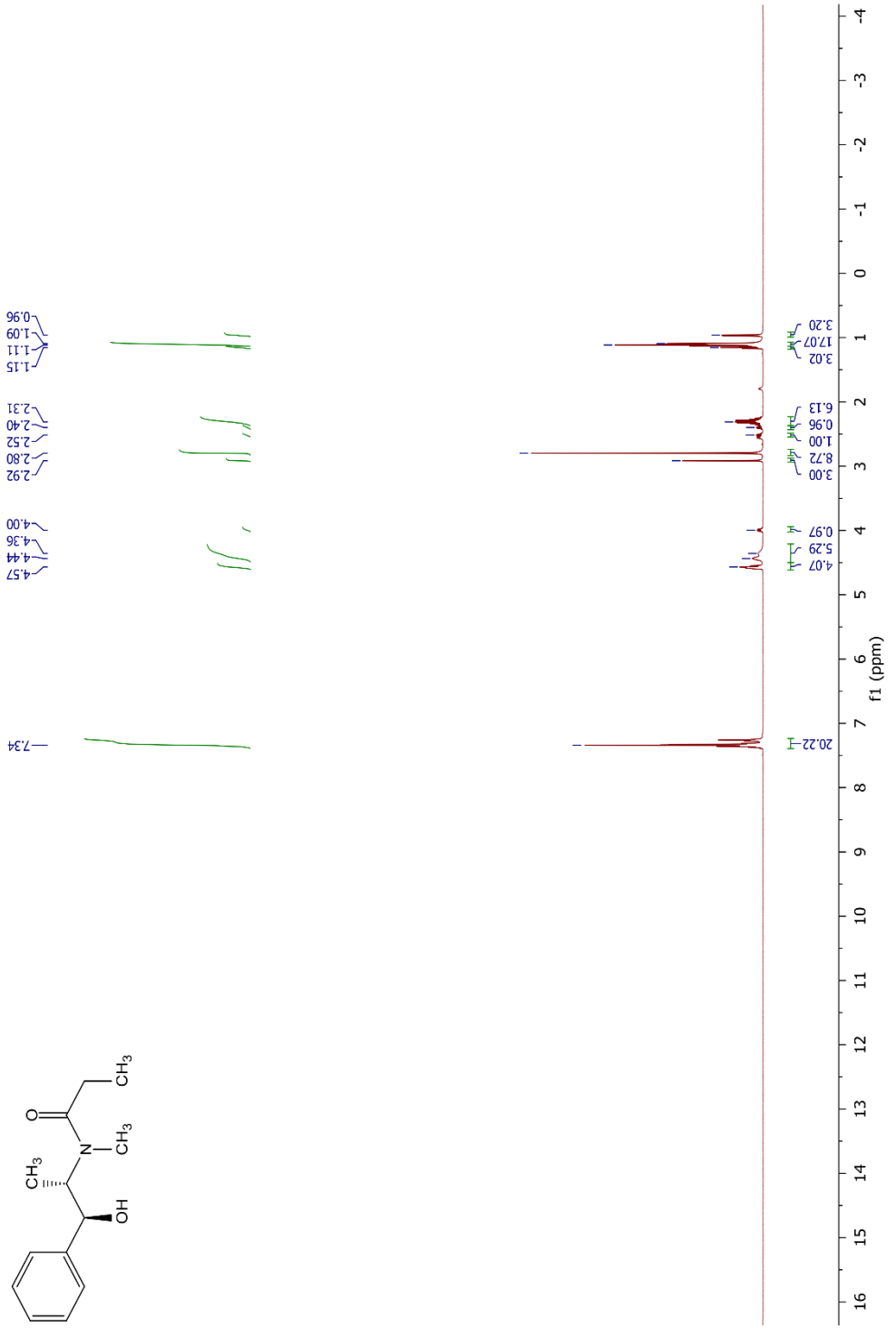

4.6.35 ^{13}C NMR of Myers auxiliary *N*-propionyl (1*S*,2*S*)-(+)-pseudoephedrine ($CDCl_3$, 126 MHz, 294 K)

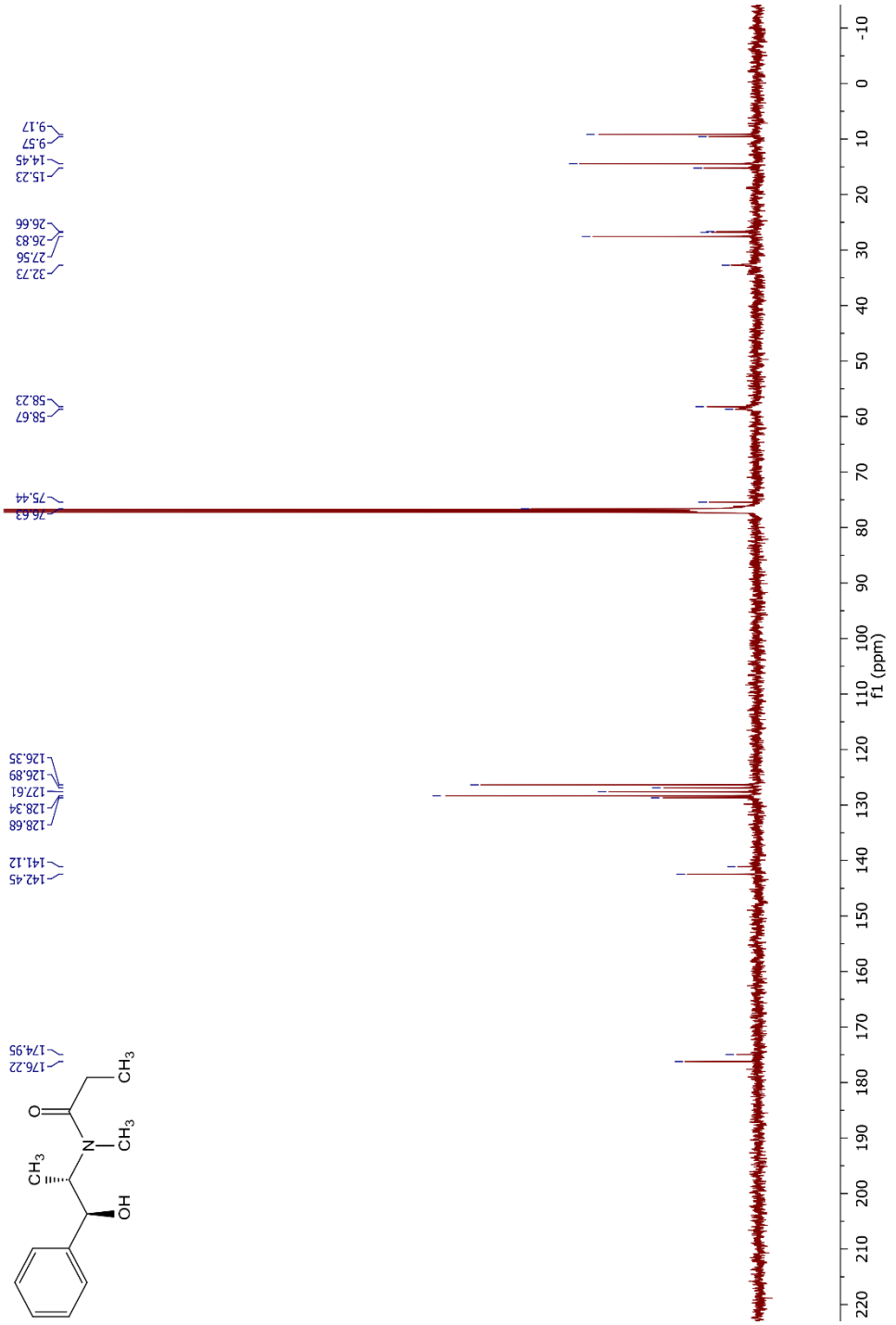

4.6.37 ^{1}H NMR of alkylated Myers auxiliary ($CDCl_3$, 400 MHz, 297 K)

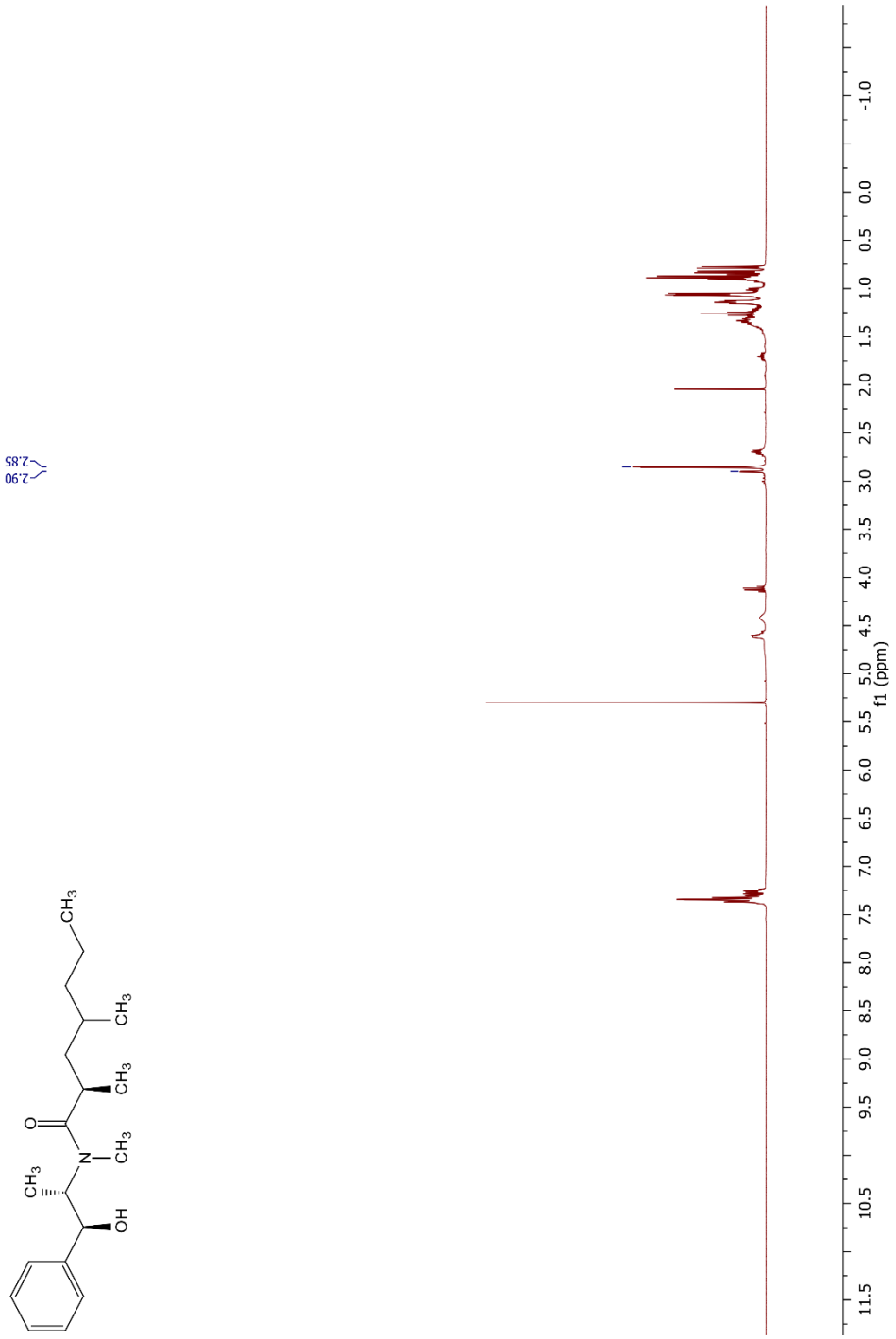

4.6.38 ^{13}C NMR of alkylated Myers auxiliary ($CDCl_3$, 101 MHz, 297 K)

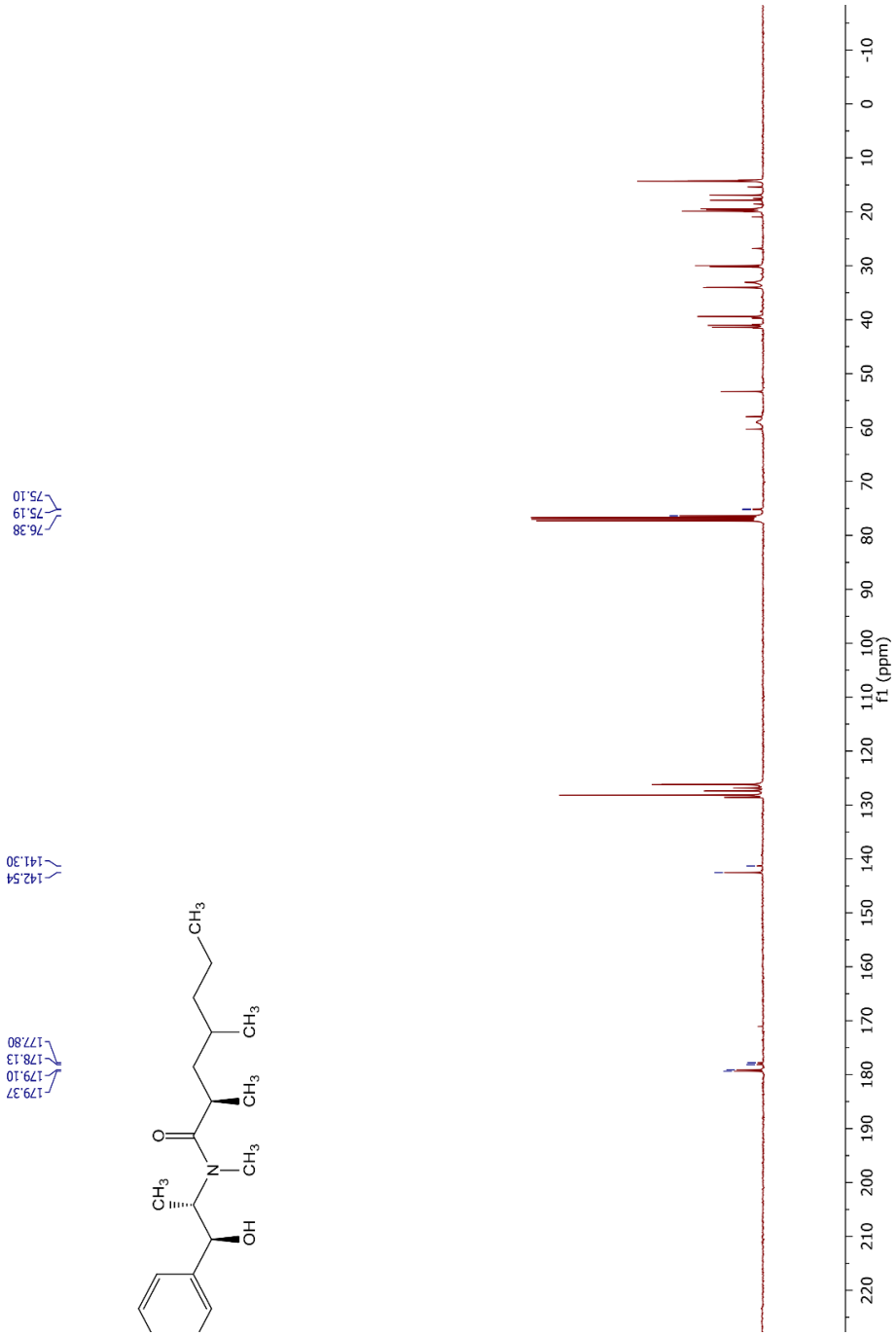

4.6.39 ^{1}H NMR of ketones 4.45 and 4.46 ($CDCl_3$, 400 MHz, 297 K)

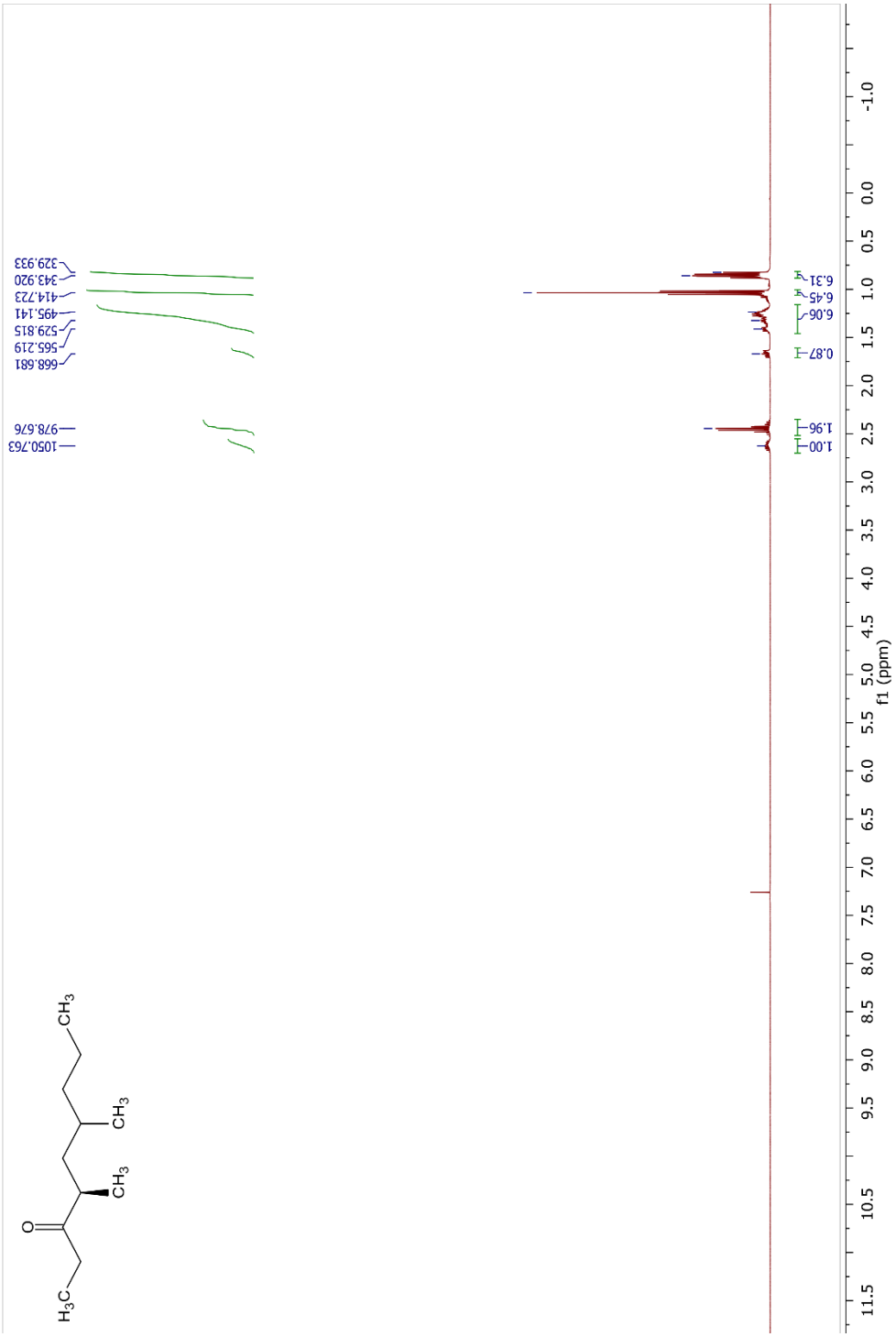

4.6.40 ^{13}C NMR of ketones 4.45 and 4.46 ($CDCl_3$, 101 MHz, 297 K)

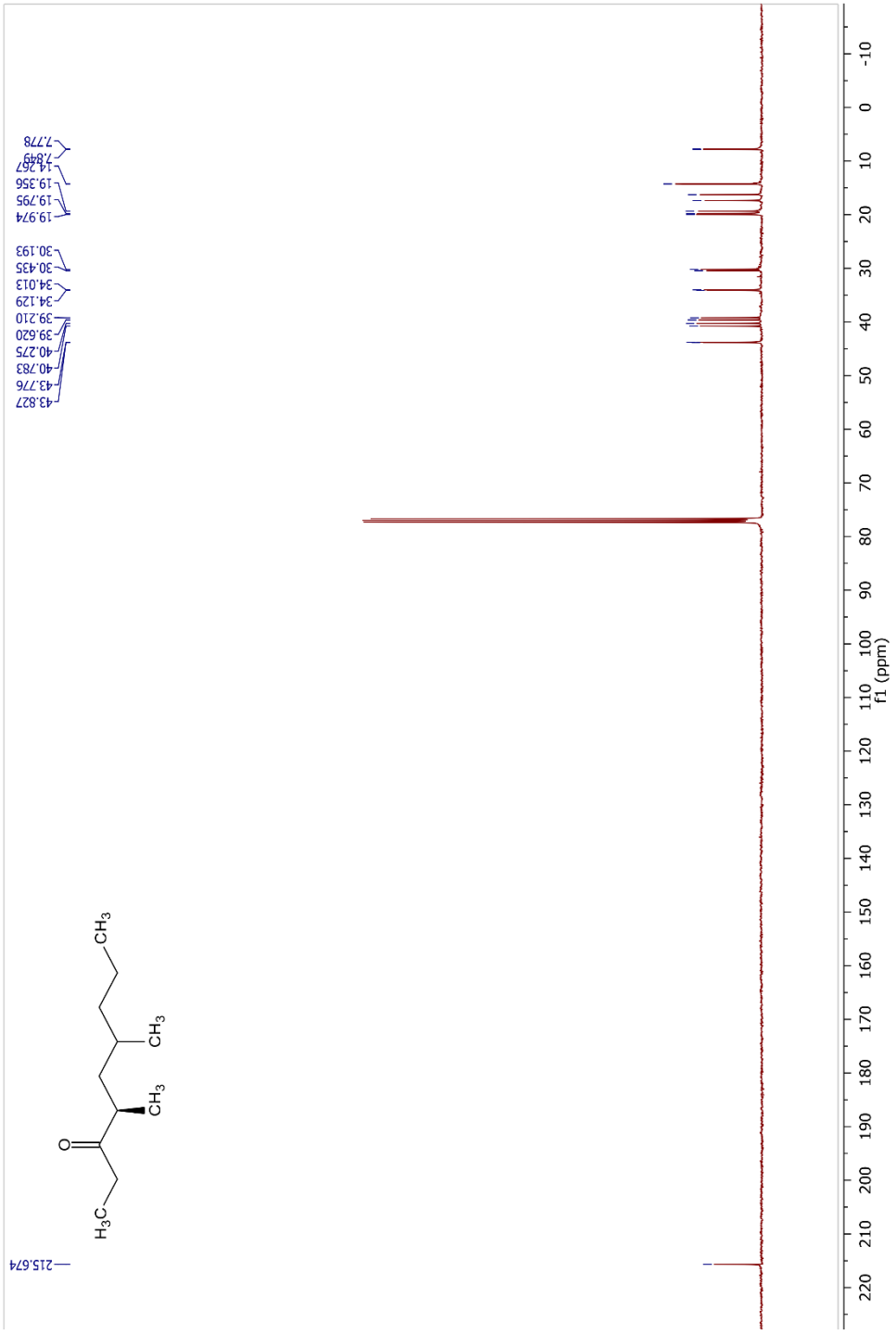

4.6.41 Enantioselectivity of Myers Alkylation with Iodide 4.27 and Subsequent Ethylation

Top chiral GC chromatogram displays product **4.01** formed by Myers alkylation with the crucial iodide **4.27** and subsequent ethylation with EtLi. *Ent*-**4.01** elutes as a right-side shoulder peak. Bottom chromatogram displays a co-injection of the previous with the racemate of candidate structures formed from **Scheme 4.03**.

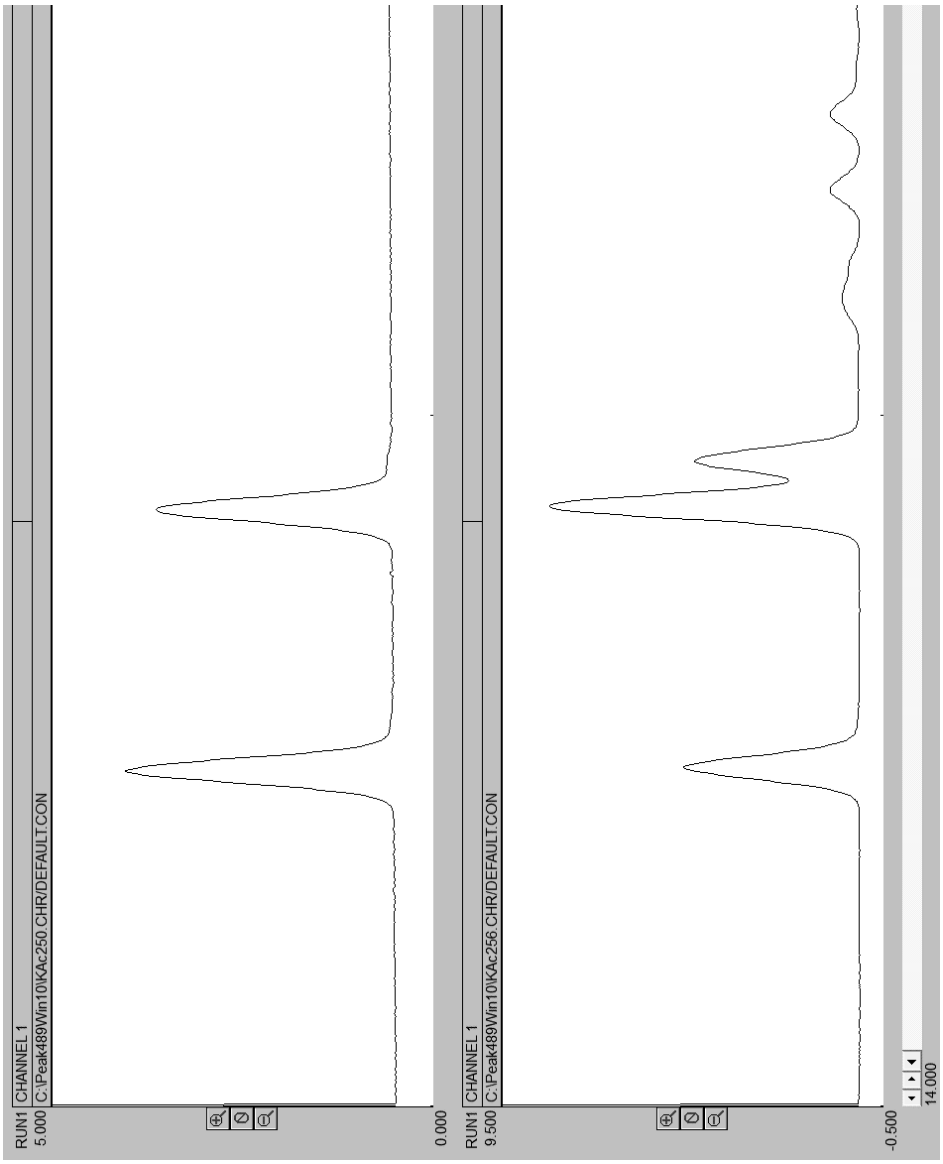

4.6.42 Desymmetrization by α-Chymotrypsin and Synthesis of Candidates by Scheme 4.04

Top chiral GC chromatogram displays **4.01** formed by enantioselective synthesis, outlined in **Scheme 4.04**. Bottom chromatogram displays a co-injection of the previous with the racemate of the candidate structures formed in **Scheme 4.03**.

Chapter 5 – Identification and Synthesis of *p*-Mentha-1,3-dien-9-ol, an Aggregation-Sex Pheromone Shared by Two Longhorn Beetle Species Native to Different Continents

ABSTRACT

Longhorn beetles (Coleoptera: Cerambycidae) constitute a diverse family of environmentally and economically important insects. They contribute to ecosystem health by initiating the decomposition of woody plants, but may also be destructive forest pests and vectors of pathogens. Semiochemicals can be exploited in the detection and monitoring of cerambycids and similarly cryptic animals. In recent years as more pheromones have been identified from these beetles, patterns in the function and structure of these compounds have been revealed. Here, I describe the identification and synthesis of the aggregation-sex pheromones of the Eurasian longhorn beetle *Aromia moschata moschata* (subfamily Cerambycinae; tribe Callichromatini) and the North American longhorn beetle *Holopleura marginata* (Cerambycinae; Holopleurini). Both species were shown to use *p*-mentha-1,3-dien-9-ol as a pheromonal attractant, which also attracted the cerambycid *Xestoleptura crassipes* (Lepturinae; Lepturini) in field experiments in California. This pheromone provides another example of the conservation of structures in cerambycid pheromones and represents a novel class of semiochemicals within these tribes.

5.1 Introduction

Longhorn beetles (Coleoptera: Cerambycidae) are mainly xylophagous insects, developing in living or dead wood of numerous trees and shrubs, and thus assisting in the natural recycling of woody biomass. Due to their taxonomic diversity (>36,000 described taxa), global distribution, and association with woody plants, cerambycids are economically and biologically important insects.[1–3] It is now known that many longhorn beetle species produce long-distance sex or aggregation-sex pheromones to facilitate mate finding.[4] Because many species are cryptic and difficult to monitor, which can be compounded by annual flight periods of only a few weeks, monitoring populations with traps baited with synthetic pheromone lures is an effective methodology for quantitative studies of both pest species,[5–7] and non-pest species of concern for environmental management.[8–10] Recent research has substantially enlarged the database of identified compounds that serve as pheromones in a number of cerambycid species and subfamilies.[11] Nevertheless, to date, fewer than one percent of all cerambycids have been studied in terms of their pheromone chemistry.

As part of ongoing efforts to explore the chemical space occupied by cerambycid pheromones and extend the applications of pheromone-based monitoring of these insects, the pheromone chemistry of two non-pest species, the musk beetle *Aromia moschata moschata* (L.), native to Europe and Central Asia, and *Holopleura marginata* LeConte, native to western North America, were examined. Both species are members of the subfamily Cerambycinae, in the tribes Callichromatini and Holopleurini, respectively.[12,13] *Aromia m. moschata* is well known for the musky scent produced by adults of both sexes,

consisting of the monoterpenoids rose oxide and iridodial that are presumed to be defensive secretions,[14] but neither species has been studied previously with respect to their use of attractant pheromones.

Here, male beetles of *A. m. moschata* and *H. marginata* were both found to emit the unstable monoterpene alcohol *p*-mentha-1,3-dien-9-ol, not previously known as a cerambycid pheromone component. Synthetic *p*-mentha-1,3-dien-9-ol, combined with a stabilizer, was significantly attractive to both species in field bioassays in Sweden and California, respectively. Because both sexes were attracted, the novel compound functions as an aggregation-sex pheromone. We discuss the potential to use the newly identified pheromone in an applied context during field studies of *A. m. moschata* and *H. marginata*, and also discuss the need for further bioassays of this compound in other countries and continents. These bioassays will assess how prevalent this particular structure, and more generally other analogues with the same 1-isopropyl-4-methylcyclohexane structural motif, may be as pheromone components among the Cerambycidae.

5.2 Results

The headspace volatiles of *H. marginata* were dominated by two compounds (ratio 100:75±31, n = 6) with apparent molecular ions at *m/z* 152 and 150 respectively, for possible molecular formulae of $C_{10}H_{16}O$ and $C_{10}H_{14}O$, respectively. There were no good matches for either compound in the NIST 14 mass spectral database, so the compounds were identified by interpretation of their spectra in combination with biosynthetic considerations.

The mass spectrum of the compound with a molecular ion of *m/z* 150 exhibited limited fragmentation, which, along with an ion at *m/z* 91, suggested a methyl-substituted benzene ring with an additional substituent (**Figure 5.01A**). The base peak at *m/z* 119, from a possible loss of 31 amu (= CH_2OH), suggested the presence of a primary alcohol. Furthermore, the 119 ion was 28 mass units larger than the *m/z* 91 ion, indicating that the CH_2OH group had likely been cleaved from a methyl-substituted benzene with an additional alkyl substitution consisting of either $-CH_2CH_2CH_2OH$ or $-CH(CH_3)CH_2OH$. The latter seemed more likely given the base peak at *m/z* 119 because the secondary benzylic ion resulting from loss of the CH_2OH group would be stabilized by resonance, whereas the corresponding ion from the isomer with an unbranched alkyl chain would not. Furthermore, from biosynthetic considerations, numerous monoterpenoids are characterized by a six-membered ring with methyl and isopropyl groups at the 1 and 4 positions, respectively, and so the unknown of *m/z* 150 was tentatively identified as 2-(4-methylphenyl)-1-propanol (= *p*-cymen-9-ol, **5.01**). The tentative identification was confirmed by synthesis of an authentic standard from the corresponding acid, 2-(4-methylphenyl)propanoic acid **5.02**.

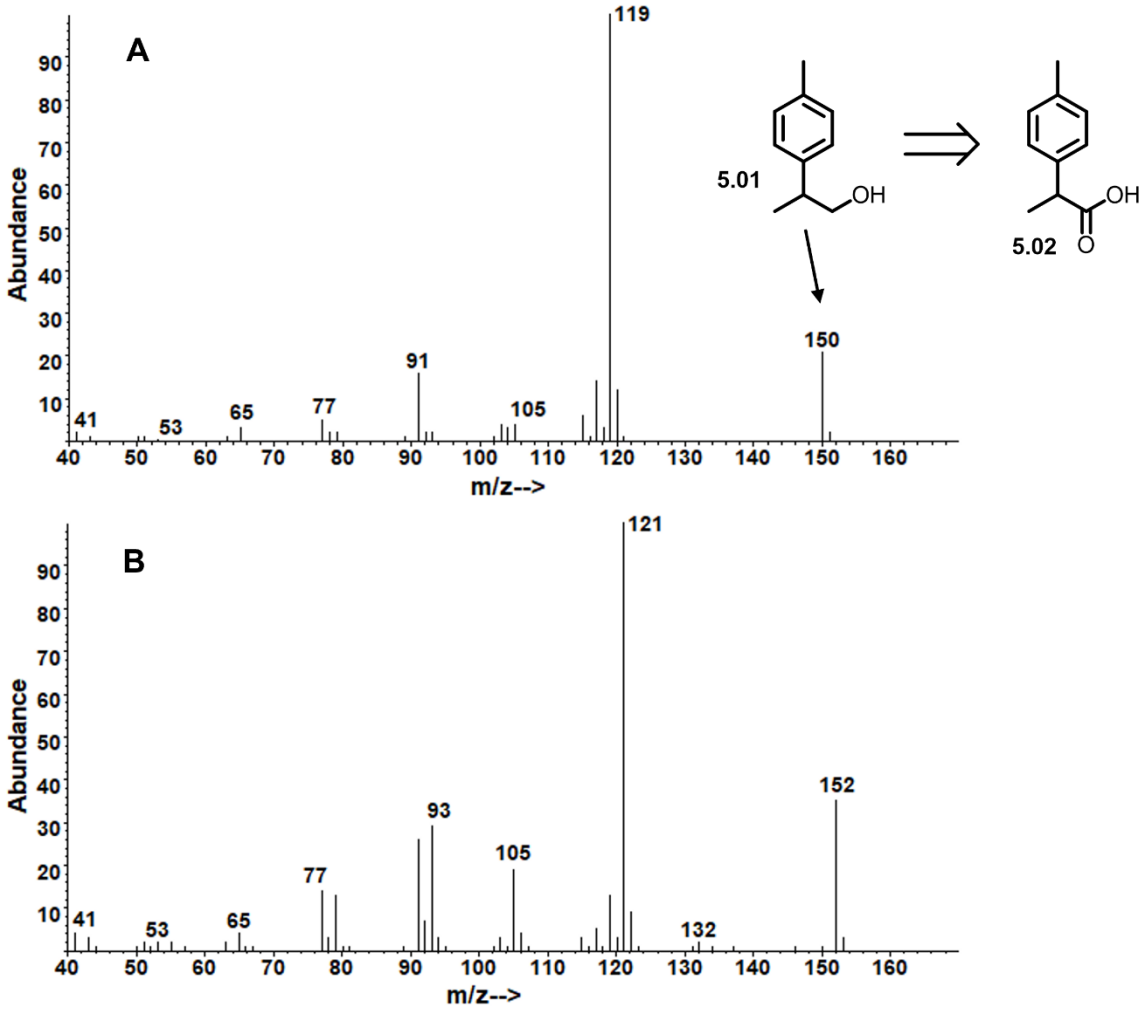

Figure 5.01 *GC-MS spectra for: A) unknown of m/z 150, identified as p-cymen-9-ol* ***5.01****, synthesized from 2-(4-methylphenyl)propanoic acid* ***5.02****, and; B) unknown of m/z 152, identified to be p-mentha-1,3-dien-9-ol (see below).*

It seemed probable that the second compound, with molecular weight 152, was a diene analog of *p*-cymen-9-ol because the mass spectrum exhibited several fragment ions analogous to those in the spectrum of **Figure 5.01A**. Thus, the base peak at *m/z* 121 suggested loss of CH_2OH to form a stabilized allylic carbocation, and the fragment at *m/z* 93 was tentatively identified as a methylated cyclohexadiene resulting from cleavage of

the alkyl group. There were five possible structures with two double bonds in the ring (three conjugated and two unconjugated, **5.03**-**5.07** in **Figure 5.02**). Of these, a search of Chemical Abstracts revealed that structures **5.05** and **5.06** were apparently unknown. Thus, we first focused our attention on structures **5.03**, **5.04**, and **5.07**.

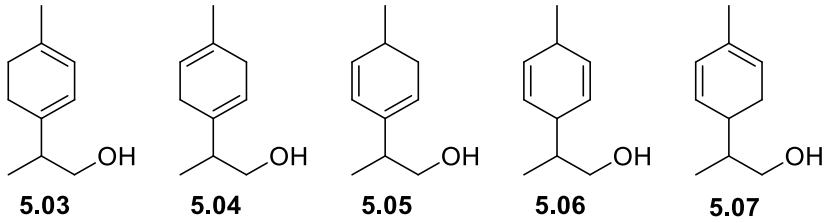

Figure 5.02 *Candidate structures for the unknown compound of m/z 152 produced by A. m. moschata and H. marginata.*

5.2.1 Synthesis of Candidate Structures

Compound **5.07** was previously synthesized by Rönn et al.[15] from carvone (**5.08, Scheme 5.01**). Commercially available (*R*)-carvone was converted to the tosylhydrazone **5.09**, then by a Shapiro reaction,[16] converted to triene **5.10**. Selective hydroboration-oxidation of the volatile triene with 9-borabicyclo[3.3.1]-nonane (9-BBN) afforded a mixture with diastereomers of candidate **5.07**, the aromatic analog **5.01**, and an unidentified impurity with a molecular ion of *m/z* 154 (for spectral information, see section 2.6.11 of the Supporting Information). However, the EI mass spectra and retention time (the two diastereomers were observed to co-elute) of the synthetic diastereomers of compound **5.07** did not match those of the insect-produced sample eliminating **5.07** as a possibility.

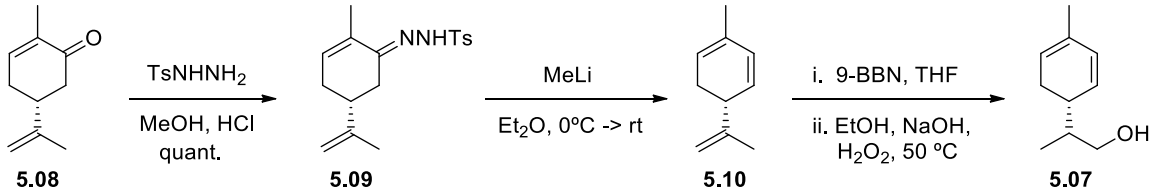

Scheme 5.01 *Synthesis of **5.07** from (R)-carvone **5.08**.*

In pursuit of compounds **5.03** and **5.04**, we were pleased to find that dienol **5.04** was readily available by Birch reduction[17] of its aromatic analog **5.01** (**Scheme 5.02**)**,** which in turn was readily available by $LiAlH_4$ reduction of commercially available 2-(4-methylphenyl)propanoic acid. Unfortunately, the mass spectrum and retention time of the nonconjugated **5.04** did not match those of the insect-produced compound. However, base-catalyzed isomerization of **5.04** gave **5.03**, the retention time and mass spectrum of which were an excellent match for the insect-produced compound, confirming the structure of the unknown as **5.01,** the conjugated cyclohexadienol *p*-mentha-1,3-dien-9-ol.

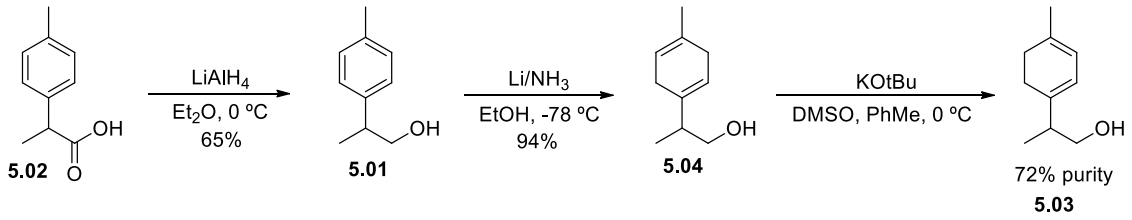

Scheme 5.02 *Synthesis of conjugated dienol **5.03** by Birch reduction of aromatic alcohol **5.01** followed by base-catalyzed isomerization of unconjugated **5.04** into conjugation.*

5.2.2 Scale-up of the Synthesis of Candidate Pheromone 5.03

Base-catalyzed isomerization of **5.04** yielded compound **5.03** contaminated with the aromatic analog **5.01** and an unidentified impurity with a molecular ion of *m/z* 154. To obtain higher-purity material for field testing, the mixture was treated with a powerful

Diels-Alder dienophile, 4-phenyl-1,2,4-triazoline-3,5-dione (PTAD, **5.13**, **Scheme 5.03**). The resulting adduct **5.11** was easily separated from the two impurities by column chromatography, and subsequently reverted to compound **5.03** with potassium hydroxide in ethanol. Finally, purification of this material by column chromatography produced two batches of material sufficiently pure (>99% and 92%, by GC) for field testing. As the cyclohexadiene core of compound **5.03** is susceptible to oxidation to the arene, samples of compound **5.03** were stored as solutions in hexanes with an antioxidant, butylated hydroxytoluene (5% wt.).

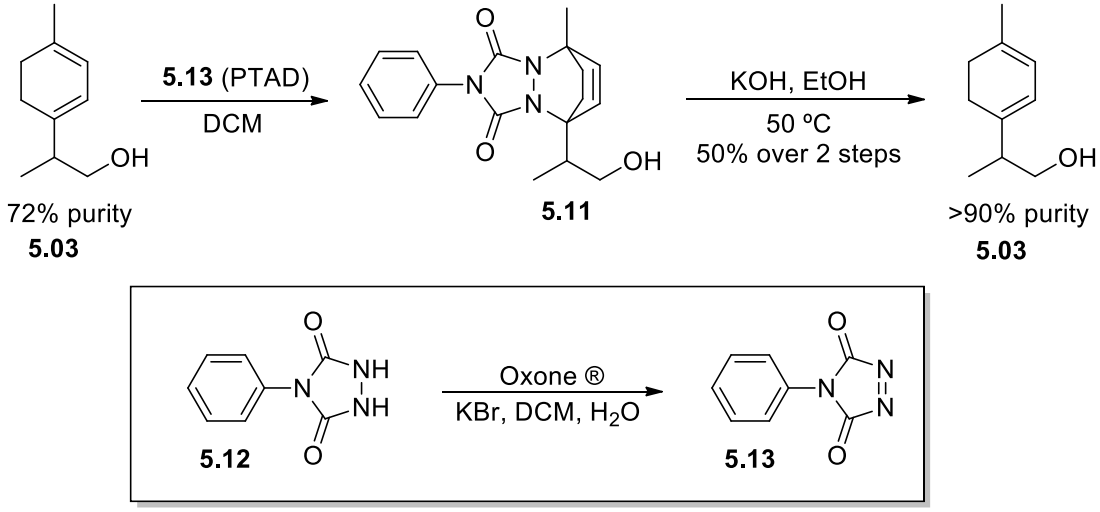

Scheme 5.03 *Chemoselective purification of the base-catalyzed isomerization product mixture by reversible formation of a Diels-Alder adduct with the dienophile PTAD.*

5.2.3 Attraction of Cerambycids to Synthetized Racemic Dienol 5.03

In Sweden, a total of 76 *A. m. moschata* were captured in a field trial. The species was significantly attracted to *p*-mentha-1,3-dien-9-ol **5.03** compared to the solvent control (**Figure 5.03A**, Friedman's test: $Q_{1,3}$=30.5, $P < 0.001$). Traps with lures of *p*-mentha-1,3-dien-9-ol captured a total of 75 individuals, of which 51% were female and 49% were male

(38 females, and 37 males). A single male beetle was caught in one of the control traps (0.05 ± 0.05 beetles/trap). Three individuals of another cerambycid species, *Leptura quadrifasciata* ssp. *Quadrifasciata* L., were captured in traps baited with *p*-mentha-1,3-dien-9-ol.

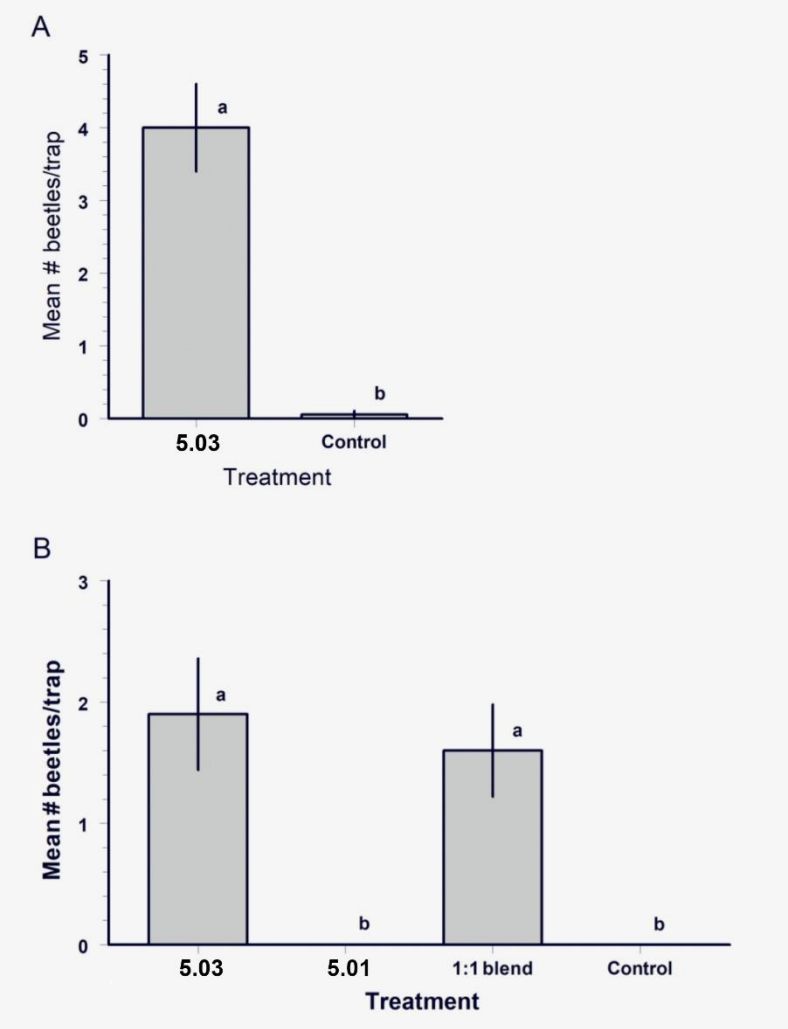

Figure 5.03 *Mean (± SD) number of adult female and male beetles caught in panel traps baited with **5.03** and/or **5.01** for the species: A) A. m. moschata in southern Sweden, and; B) H. marginata in northern California, USA. Bars with different letters are significantly different (REGWQ test, P < 0.05).*

During the field bioassay in California, traps captured a total of 592 cerambycid beetles of 39 species of five subfamilies. Of species that were represented by at least 10 specimens, only two species showed significant differences between treatment means, the target species *H. marginata* and *Xestoleptura crassipes* (LeConte) of the subfamily Lepturinae. A total of 42 adults of *H. marginata* were captured (36F:6M), and the beetles were similarly attracted to **5.03** alone and to the 1:1 blend with **5.01** (**Figure 5.03B**; $Q_{3,36}$=25.6, $P < 0.001$). *p*-Cymen-9-ol **5.01** was not significantly attractive as a single component, nor did it appear to influence attraction to **5.03**.

The lepturine *X. crassipes* was equally attracted to traps baited with *p*-mentha-1,3-dien-9-ol and the blend of *p*-mentha-1,3-dien-9-ol with *p*-cymen-9-ol with both sexes being attracted (sex ratio of all trapped beetles, 20M:5F).

5.3 Discussion

The consistent and sex-specific presence of *p*-mentha-1,3-dien-9-ol in headspace extracts of males of *A. m. moschata* and *H. marginata,* and the significant attraction of both sexes to synthetic racemic *p*-mentha-1,3-dien-9-ol demonstrates that this compound functions as an aggregation-sex pheromone for both species. Because individuals of *A. moschata* and *H. marginata* were significantly attracted to the racemic material, bioassays with enantioenriched material were not explored. The absolute stereochemistry of the insect-produced *p*-mentha-1,3-dien-9-ol has not been determined for either species. If needed, enantioenriched material could be obtained and the absolute stereochemistry determined through a lipase-mediated kinetic resolution[18] of the racemate, using trends of enantiodifferentiation to determine the absolute stereochemistry of the favored and

disfavored enantiomer. Alternatively, chiral auxiliaries could be employed, for example to enantioselectively methylate the α-position of imidate **5.15**, producing an enantioenriched sample of the aromatic starting material as accomplished by Shvartsbart and Smith.[17]

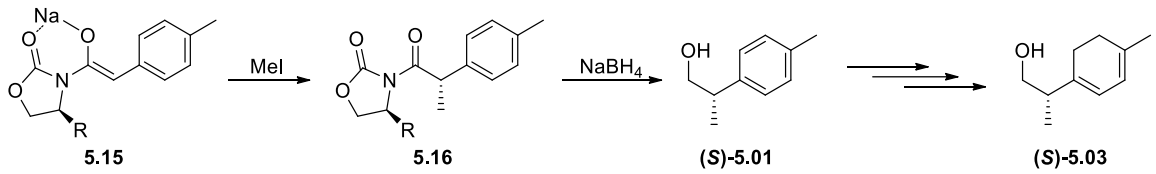

5.15 **5.16** **(*S*)-5.01** **(*S*)-5.03**

Scheme 5.04 *Synthesis by Shvartsbart and Smith*[17] *providing access to enantiomers of* ***5.03****.*

In preliminary field trials where lures were loaded with dienol **5.03** without a stabilizer such as BHT (butylated hydroxytoluene), few beetles were attracted, likely due to the rapid atmospheric oxidation of the dienol to the aromatic analog **5.01** under field conditions. Similarly, it is likely that the aromatic analog **5.01** detected in the insect extracts is the result of degradation during collection of headspace volatiles from the beetles.

Recently, Collignon et al.[19] reported an isomeric compound, *p*-mentha-1,3-dien-8-ol, as a pheromone component of at least one (but possibly two) North American species in the subfamily Cerambycinae and tribe Oemini, *Paranoplium gracile*. These two compounds share the same carbon skeleton and conjugated diene placement but have different placements of the hydroxyl group. This same carbon skeleton is also featured in the pheromone components of two *Megacyllene* (subfamily: Cerambycinae) species in the tribe Clytini, those components including α-terpineol and limonene.[20,21] The three species mentioned above, in addition to *H. marginata,* are native to the Nearctic ecozone.

The fact that *p*-mentha-1,3-dien-9-ol is used as a pheromone component by the two geographically isolated species *A. moschata* and *H. marginata* suggests that the

semiochemistry of these insects is highly conserved, or less likely, that the two species have independently converged to use the same compound as a pheromone. Despite *H. marginata* being the only member of its tribe (Holopleurini), the tribes Callichromatini, Oemini, and Clytini altogether comprise ~400 genera and occur in all biogeographic regions of the world.[22] Therefore, this compound or analogs with the same basic structural motif could be used to screen for pheromonal attractants for other species in different geographical regions and habitats, to assess how widespread these compounds may be as pheromone components for the subfamily Cerambycinae. In previous tests of this screening strategy[23,24] using another conserved pheromone motif, 3-hydroxyalkan-2-ones and the analogous diols, a wide variety of cerambycids were attracted, on all six habitable continents.

Significant numbers of the lepturine species *X.* crassipes were attracted during the field trials in California. To date, all known examples of sex pheromones within this subfamily are female-produced and attract only males[4], so it is unlikely that *p*-mentha-1,3-dien-9-ol is a sex pheromone for *X. crassipes*. However, adults of *X. crassipes* are flower feeders[2,25] and the attraction to *p*-mentha-1,3-dien-9-ol suggests that the dienol could be a floral volatile or a mimic of a floral odor. To the best of our knowledge, *p*-mentha-1,3-dien-9-ol has not been conclusively identified from any natural source other than the beetles described here, but given the instability of the compound, it may have been missed in analyses of various plants.

Pheromone-based monitoring systems represent a potential game-changer for monitoring both invasive pest insect species, and the distribution and abundance of rare or

elusive insects.[26] For example, for the invasive cerambycid species *Aromia bungii*, an important economic pest of pome and stone fruit trees, detection methods were limited to manual inspection of tree trunks, which is labor-intensive and unreliable because larvae are buried deep within the wood.[27] Recently, the pheromone for this species was identified and shown to attract both sexes, making it a standardized and valuable tool for detecting the presence of *A. bungii* in countries where it has invaded and successfully established.[7] Similarly, *p*-mentha-1,3-dien-9-ol has considerable potential as a practical tool to study the range and seasonal dynamics of *A. moschata* and *H. marginata* under field conditions. Monitoring of either species with pheromone traps could not only be useful for biological studies of these beetles, but also as an indirect method to monitor and quantify ecosystem health, for example, the abundance of the large, old willow trees that *A. moschata* use as hosts, at the local and landscape levels, by using the presence and abundance of *A. moschata* as a proxy. Old willow trees in particular are important ecological resources not only for saproxylic taxa, but also for many generalist and specialist pollinators active in spring. A similar pheromone-based monitoring system for multiple non-pest cerambycids, including threatened species, is already available for species associated with recently dead oak wood in Northern Europe.[8] Thus, the pheromone of *A. moschata* could be part of a parallel system for species dependent on willow. Similarly, in the case of the poorly known *H. marginata*, pheromone-based surveys could be a useful tool to determine the abundance and distribution of this rarely observed species, and to begin studies of its environmental requirements.

5.4 Methods

5.4.1 Isolation of Insect-Produced Compound

Volatile compounds emitted by adults of *A. m. moschata* and *H. marginata* were sampled using headspace collections.

Adults of *A. m. moschata* were reared from branches and stems of goat willow (*Salix caprea* L.) cut from several large, mature willow trees at various locations within Ecopark Hornsö, southern Sweden (approximate center coordinates of the park, WGS 84: DD 57.0120 N, 16.0897 E). Many of the trees showed evidence of recent feeding by larvae of *A. m. moschata*, with fresh galleries and emergence holes. In total, ~0.25 m^3 of wood (diameter ~10-15 cm) was collected in mid-December 2015. In mid-January 2016, the logs were cut into ~50 cm-long pieces that were placed in transparent plastic boxes with part of the lid replaced with a fine plastic mesh for ventilation. The boxes were stored in a greenhouse at the SLU campus (daily mean temperature ~15 °C), and checked at least once per day for emerged insects. Logs were periodically misted with water to prevent desiccation.

Adults of *A. m. moschata* began to emerge after seven weeks and continued to emerge for nearly a week, yielding a total of four males and five females (sex determined by antennal length relative to body length, longer in males).[28] The adult beetles were caged separately by sex in smaller plastic containers with lids partially covered by plastic mesh for ventilation. Pieces of paper, smeared with honey water, were added to the containers to provide nourishment, and replaced every two to three days. While adults were continuing

to emerge, and in between headspace collections (see below), the containers were kept in a refrigerator at 8 °C to prolong longevity.

Headspace collections were obtained from three males and three females of *A. m. moschata*.[29] Beetles were held in 1 L gas washing bottles (Lenz Laborglas Gmbh, Wertheim, Germany), with an empty bottle used as a system control. To reduce the risk of aggression between same-sex individuals, strips of metal mesh were added to the bottles to allow beetles to distribute themselves. Ambient air was pulled through the glass bottles with a pump (model PM 10879 NMP 03, KNF Neuberger, Freiburg, Germany) at 0.2 L min^{-1}. A volatiles trap consisting of a bed of Porapak Q^{TM} adsorbent (25 mg, mesh size 50–80, Supelco/Sigma-Aldrich, Munich, Germany), enclosed in polytetrafluoroethylene (PTFE) tubing was placed in line between each glass bottle and the pump. A second Porapak Q^{TM} trap was connected to the bottle inlet to purify the incoming air. Headspace collections were performed from ~10 AM–4 PM, and lasted for ~5–6 h. In total, four headspace collections were performed, each resulting in one extract of volatiles from males, females, and the control. Collectors were eluted immediately after each headspace collection with 300 µL of hexane, and reconditioned with 3 × 300 µL of hexane followed by 3 × 300 µL of acetone before reuse. Extracts of volatiles were stored at −18 °C until analysis.

Adults of *H. marginata* used for collection of headspace odors were reared from infested branches of Douglas fir collected on 29 March 2013 at Nelson Ravine in Tehama Co., California (Highway 32 near mile 32.48; 39.98111, -121.63889, 955 m). The rearing chamber was a plastic 19 L bucket with a mesh-covered hole in the lid for ventilation, held

in an unheated garage to simulate seasonal temperatures. Five adults of *H. marginata* emerged from the wood from 13–26 March 2015. Although the flight period for this species is May–July (Linsley, 1962), adults can be reared outside the normal emergence period. The beetles were removed from the rearing chamber before they could mate and placed individually into glass vials.

Analogous headspace extracts were prepared from *H. marginata*,[30] using beetles shipped by overnight courier to UC Riverside.[30] Individual beetles were placed in separate 0.5 L wide-mouth screw-cap canning jars whose metal lids were modified with Teflon circles fitted with Swagelok bulkhead unions (Swagelok, Solon OH, USA) to connect inlet and outlet tubing. Each jar contained a vial of 10% sugar water provided for nutrition. Each jar was flushed with air (charcoal-filtered, 500 mL/min), and headspace odors were trapped on activated charcoal collectors made of 10 cm-long glass tubes (0.5 cm ID) with a 1 cm-long bed of activated charcoal (50-200 mesh; Fisher Scientific, Pittsburgh, PA, USA) secured by glass wool plugs. A collector was attached to the outlet bulkhead union of each aeration chamber. Collectors were changed every 24 h, and the trapped volatiles were collected by elution of the collectors with dichloromethane (0.5 mL).

Extracts of *H. marginata* were analyzed by GC-MS at UC Riverside, with an Agilent 7820A GC coupled to a 5977E mass selective detector (Agilent, Santa Clara CA, USA). Samples were run in splitless mode on an HP-5 column (30 m × 0.25 mm i.d. × 0.25 μm film; Agilent) using helium as carrier gas, at a linear velocity of 37 cm/sec. The GC oven was programmed from 40 °C/1 min, 10 °C/min to 280 °C, hold for 10 min. Spectra were taken with electron impact ionization (70 eV). The transfer line, GC inlet, ion source,

and quadrupole temperatures were 280, 250, 150, and 200 ºC respectively. Extracts of *A. m. moschata* shipped from Sweden were analyzed under the same conditions.

5.4.2 General Synthesis Conditions

Reactions were conducted in oven-dried glassware, and all solvents were Optima grade (Fisher Scientific, Pittsburgh PA, USA) unless otherwise noted. Anhydrous diethyl ether stabilized with BHT was purchased from Fisher Scientific, and absolute ethanol from Koptec (King of Prussia, PA, USA). Solutions of worked-up products were dried over anhydrous Na_2SO_4, and concentrated by rotary evaporation under partial vacuum. Vacuum flash chromatography was carried out on silica gel (230–400 mesh; Fisher Scientific). TLC analyses were conducted on aluminum-backed sheets of analytical silica gel 60 F_{254} (Merck, Darmstadt, Germany), and compounds were visualized by spraying with 10% phosphomolybdic acid in ethanol and heating. Yields are reported as isolated yields of chromatographically pure products unless otherwise noted. Mass spectra were obtained with an HP 6890 GC (Hewlett-Packard, now Agilent, Santa Clara CA, USA) equipped with a DB-17 column (30 m × 0.25 mm × 0.25 μ film) coupled to an HP 5973 mass selective detector, in EI mode (70 eV) with helium carrier gas. Purity was assessed by gas chromatography (unless otherwise noted) with an HP 5890 GC with a flame ionization detector, and equipped with a DB-5 column (30 m × 0.25 mm × 0.25 μ film). NMR spectra were recorded as $CDCl_3$ solutions on either a Bruker Avance 500 or Bruker NEO 400 spectrometer. Chemical shifts are reported in ppm relative to $CDCl_3$ (^{1}H 7.26 ppm; ^{13}C 77.0 ppm).

5.4.3 Synthesis of the Tosylhydrazone of (*R*)-Carvone

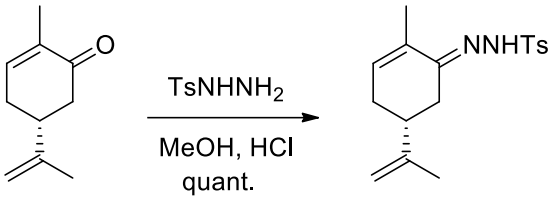

5.08 **5.09**

A 500 mL flask was charged with tosylhydrazine (9.31 g, 50.0 mmol, 1 eq.) and MeOH (50 mL). Concentrated HCl (0.5 mL) was added to the flask, then (*R*)-carvone **5.08** (7.51 g, 50.0 mmol, 1 eq) was added, and the reaction mixture was stirred for 10 min as a cream-colored precipitate formed. The flask was placed in a refrigerator (4 °C) overnight. The precipitate was collected by vacuum filtration, rinsed with cold methanol and water, and dried under vacuum yielding **5.09** (15.9 g, quant.) as a cream-colored powder. ^{1}H NMR (400 MHz, $CDCl_3$) δ 7.88 (d, *J* = 8.0 Hz, 2H), 7.76 (bs, 1H), 7.30 (d, *J* = 8.0 Hz, 2H), 6.09 – 6.03 (m, 1H), 4.75 (m, 1H), 4.70 (s, 1H), 2.64 (dd, *J* = 15.9, 4.1 Hz, 1H), 2.42 (s, 3H), 2.40 – 2.28 (m, 1H), 2.23 (dt, *J* = 10.5, 4.7 Hz, 1H), 2.07 – 1.98 (m, 1H), 1.93 (dd, *J* = 15.9, 12.7 Hz, 1H), 1.80 – 1.76 (s, 3H), 1.70 (s, 3H). ^{13}C NMR (101 MHz, $CDCl_3$) δ 154.79, 147.06, 143.94, 135.14, 133.51, 132.40, 129.31, 128.19, 110.31, 40.31, 29.90, 29.07, 21.57, 20.59, 17.58.

5.4.4 Shapiro Reaction of the Tosylhydrazone of (*R*)-Carvone

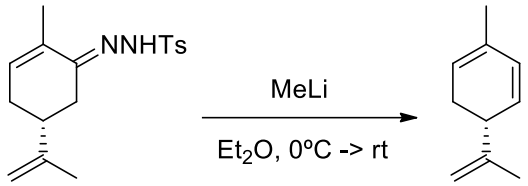

5.09 **5.10**

The tosylhydrazone of (*R*)-carvone **5.09** (4.77 g, 15 mmol) was dissolved in diethyl ether (20 mL) and the solution was cooled to 0 °C. A 1.6 M solution of methyllithium in diethyl ether (28.13 mL, 45 mmol, 3 eq.) was added dropwise over 30 min and the reaction was stirred for 30 additional min at 0 °C, acquiring a bright red-orange color. The reaction was further stirred at room temperature for 3 h, then quenched by slow addition of water (35 mL). The reaction mixture was extracted with pentanes (2 x 30 mL) and the combined organic layer was washed with water (2 x 30 mL) and brine (30 mL), and dried. Due to the volatile nature of triene **5.10**, the organic layer was partially concentrated under reduced pressure (~400 mm Hg, 35 °C), then taken up in dry THF (10 mL) without purification. EI-GC/MS *m/z* (%): 134 (74), 119 (100), 105 (31), 91 (99), 79 (18), 77 (31), 65 (11), 51 (7), 41 (12).

5.4.5 Hydroboration/Oxidation of Triene 5.10

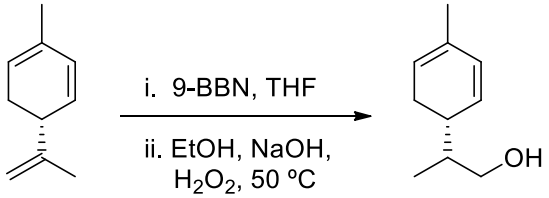

5.10 **5.07**

A 3-neck flask containing a solution of triene **5.10** (~2 g, ~15 mmol) from the previous step in dry THF was flushed with Ar and diluted with dry THF (10 mL). A 0.5 M

solution of 9-borabicyclo[3.3.1]nonane in THF (33.3 mL, 16.7 mmol, ~1.11 eq.) was added, and the mixture was stirred for 21 h. Ethanol (18.75 mL) and aqueous NaOH (6 M, 6.25 mL) were added, then 30% H_2O_2 (12.50 mL) was added dropwise over 1.5 h. The reaction was heated to 50 °C for 3 h. The resulting mixture was concentrated under reduced pressure, diluted with diethyl ether (40 mL), washed with saturated aqueous $NaHCO_3$ (40 mL), dried, then concentrated by rotary evaporation. The resulting crude oil was first purified by vacuum flash chromatography (7:3 pentane:diethyl ether), then by Kugelrohr distillation (approx. bp 75 °C, 1.1 mm Hg) yielding 1.067 g (47%, over two steps) of a clear, colorless oil containing diastereomers of pheromone candidate **5.07**, the aromatic analog **5.01**, and an unidentified impurity with a molecular ion of *m/z* 154. **5.07** EI-GC/MS *m/z* (%): 152 (12), 121 (13), 119 (12), 105 (18), 94 (45), 93 (100), 92 (88), 91 (79), 79 (14), 77 (42), 65 (7).

5.4.6 Reduction of 2-(4-Methylphenyl)propanoic Acid, the Acid Analog of *p*-cymen-9-ol

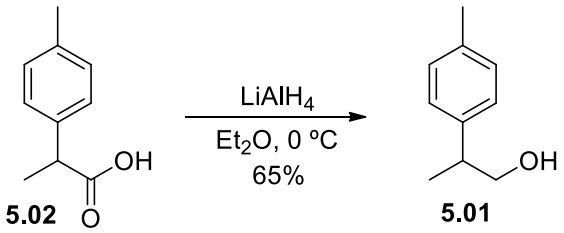

A dry 1 L 3-neck flask under Ar was charged with anhydrous ether (400 mL), cooled in an ice-bath, and $LiAlH_4$ (5.933 g, 156 mmol) was added in portions with vigorous stirring. A solution of 2-(4-methylphenyl)propanoic acid **5.02** (23.86 g, 145.3 mmol; Combi-Blocks, San Diego CA, USA) in Et_2O (100 mL) was added dropwise over 80 min.

The mixture was stirred for 2.5 h, then quenched[31] by sequential dropwise addition of water (6.24 ml), 20% aqueous NaOH (4.68 ml), and water (21.84 ml). The resulting slurry was stirred 30 min, then filtered, rinsing the solids with ether, and the filtrate was dried and concentrated. The residue was purified by Kugelrohr distillation (approx. bp 85 °C, 1 mm Hg) to yield 14.2 g (65%) of alcohol **5.01** as a colorless oil. ^{1}H NMR (500 MHz, $CDCl_3$) δ 7.14 (s, 4H), 3.68 (d, *J* = 7.3 Hz, 2H), 2.98 – 2.85 (m, 1H), 2.34 (s, 3H), 1.26 (d, *J* = 7.0 Hz, 3H). ^{13}C NMR (126 MHz, $CDCl_3$) δ 140.51, 136.20, 129.32, 127.32, 68.73, 41.99, 20.98, 17.63 ppm. EI-GC/MS *m/z* (%): 150 (36), 120 (22), 119 (100), 117 (25), 115 (10), 91 (31), 77 (10).

5.4.7 Birch Reduction of *p*-Cymen-9-ol

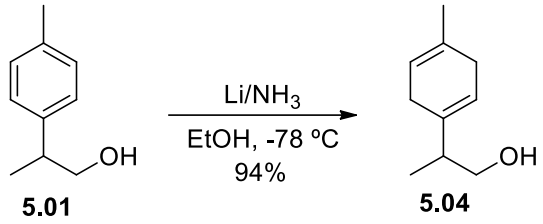

5.01 **5.04**

Gaseous anhydrous ammonia was piped into a dry 3-neck flask flushed with Ar and cooled to -78 °C, equipped with a dry ice/acetone cold finger condenser, until about 400 mL of liquid NH_3 had collected. A solution of alcohol **5.01** (14 g, 93.3 mmol) in absolute EtOH (90 mL) was added dropwise over 30 min. Lithium wire (3.3 g, 476 mmol) was then added in approximately 0.75 g portions until the solution turned a cobalt-blue color. The reaction was stirred at -78 °C for several hours, adding more pieces of lithium as the blue color dissipated. After the reaction was complete (monitored by GC), the mixture was quenched at -78 °C by slow addition of EtOH (50 mL), followed by dropwise addition of saturated aqueous NH_4Cl (100 mL) over 30 min. A vent tube leading to the back of the

fume hood was attached to one of the flask necks, the cooling bath was removed, and the mixture was stirred and allowed to warm to room temperature overnight, during which time the bulk of the ammonia evaporated.

The following morning, more saturated aqueous NH_4Cl (70 mL) was added and the mixture was stirred for 15 min, followed by addition of EtOAc (100 mL). The two phases were separated, and the aqueous layer was extracted with EtOAc (2 × 50 mL). The combined organic layers were washed with brine (2 × 120 mL), dried, and concentrated. The resulting crude material was purified by Kugelrohr distillation (approx. bp 80 °C, 0.05 mm Hg) to yield 13.2 g (composition: 84% **5.04**, 12% **5.01**) of a pale-yellow oil. The major peaks in the NMR spectrum of this mixture matched those in a previously reported[17] spectrum of pure **5.04**. ^{1}H NMR (500 MHz, $CDCl_3$) δ 5.55 (s, 1H), 5.41 (s, 1H), 3.49 – 3.45 (m, 2H), 2.63 – 2.57 (m, 4H), 2.37 – 2.31 (m, 1H), 1.65 (s, 3H), 1.00 (d, J = 7.0 Hz, 3H). ^{13}C NMR (101 MHz, $CDCl_3$) δ 135.70, 131.24, 120.55, 118.36, 65.26, 43.01, 31.52, 26.95, 22.88, 15.28 ppm. EI-GC/MS (**5.03**) *m/z* (%): 152 (28), 122 (11), 121 (100), 119 (14), 105 (29), 93 (39), 92 (22), 91 (47), 79 (16), 77 (21).

5.4.8 Isomerization of the Unconjugated Cyclohexadienol

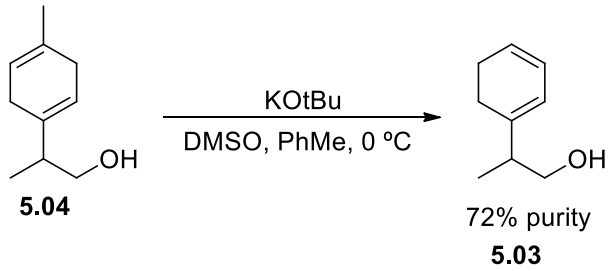

5.04 72% purity **5.03**

A dry flask flushed with Ar was charged with dry DMSO (80 mL), and potassium *tert*-butoxide (20 g, 178 mmol) was added in portions with stirring. The mixture was stirred

for 30 min and then cooled to 0 °C. A solution of **5.04** (13.4 g, 88.2 mmol) in dry toluene (50 mL) was added over a few minutes, and the resulting mixture was stirred at 0 °C for 1 h, warmed to room temperature, then stirred at room temperature for 2 h. When there was no further change in the mixture of products (monitored by GC), the reaction was cooled to 0 °C, and carefully quenched with sat. aq. NH_4Cl. The mixture was extracted with EtOAc (2x50 mL), washed with brine, dried, and concentrated. The crude material was purified by Kugelrohr distillation (approx. bp 75 °C, 0.7 mm Hg) to yield 13.3 g of a 72:17:11 mixture of **5.03**:**5.02**:an unknown byproduct (M^+=154).

5.4.9 Formation of the Diels-Alder Adduct with 4-Phenyl-1,2,4-triazoline-3,5-dione (PTAD)

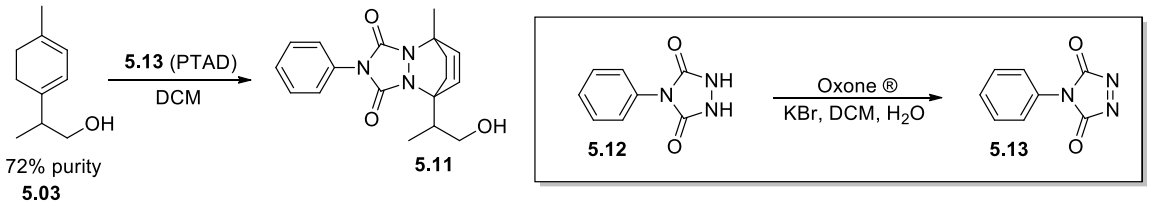

PTAD **5.13** was prepared from 4-phenylurazole **5.12** as described by Zolfigol et al.[32] Thus, a round-bottomed flask was charged with 4-phenylurazole **5.12** (14 g, 79 mmol), dichloromethane (80 mL), potassium bromide (1.904 g, 16 mmol), and Oxone® (98.4 g, 160 mmol), and vigorously stirred. Water (6 drops) was added, and the mixture was stirred for 1 h. The solid residue was separated by vacuum filtration and the filter cake was rinsed with dichloromethane. The deep, fuchsia-colored filtrate containing PTAD **5.13** was used directly.

Impure **5.03** (6.04 g) was dissolved in dichloromethane (60 mL), and the solution of freshly prepared PTAD **5.13** was added to the reaction flask in small portions until a

slight pink color persisted. The dichloromethane was removed by rotary evaporation, and the residue was dissolved in 20% ethyl acetate in hexanes and loaded onto a silica gel column. The column was eluted sequentially with 20% ethyl acetate in hexanes to elute the less polar impurities, then with 66% ethyl acetate in hexanes. The fractions containing the PTAD adduct were concentrated, yielding 10.38 g of viscous orange-brown oil, which was used directly in the next step without further purification.

5.4.10 Release of *p*-Mentha-1,3-dien-9-ol from the PTAD Adduct

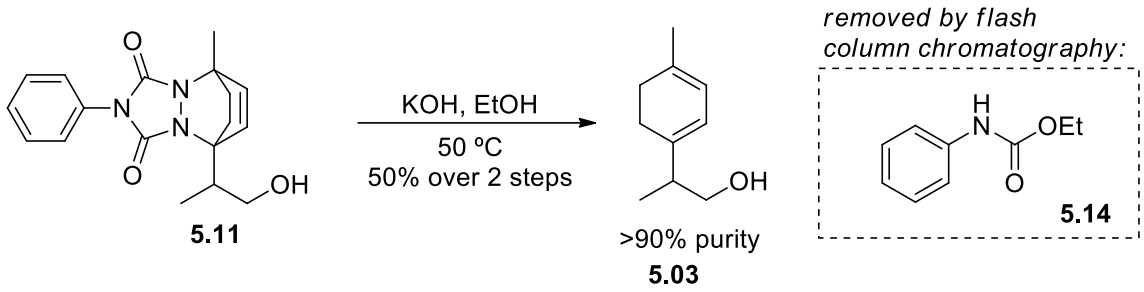

A mixture of crude **5.11** (3.8 g), EtOH (40 mL), and KOH (9.5 g) was stirred vigorously and heated to 50 °C, monitoring the reaction progress by TLC. As the reaction progressed, the color of the cloudy mixture turned from orange-brown to pale-yellow, and additional portions of KOH (total additional added: 3.6 g) were added periodically. After 6 h, the reaction was cooled to room temperature, and stirred overnight. The following morning, the reaction was complete. The mixture was diluted with water (200 mL), and extracted with Et_2O (5 x 60 mL), and the combined organic phases were washed with brine (2 x 100 mL), dried, and concentrated to yield 1.82 g of crude product as a 55:45 ratio of **5.03**:**5.14**. The desired compound **5.03** was purified by flash chromatography (55:45 Et_2O:hexanes, Rf **5.03** = 0.38, Rf **5.14** = 0.62) to yield 0.43 g of >99% purity (GC) **5.03** and 0.50 g of 92% purity (GC). The purified sample of **5.03** was stored as a dilute solution

in hexanes with about 5% BHT/**5.03** by weight. ^{1}H NMR (400 MHz, $CDCl_3$) δ 5.69 (s, 1H), 5.63 (s, 1H), 3.49 (d, J = 5.6 Hz, 2H), 2.44 – 2.32 (m, 1H), 2.11 (s, 4H), 1.77 (s, 3H), 1.02 (d, J = 6.9 Hz, 3H). ^{13}C NMR (101 MHz, $CDCl_3$) δ 136.62, 134.58, 120.89, 119.09, 65.48, 43.06, 28.74, 24.20, 22.89, 15.17 ppm. EI-GC/MS *m/z* (%): 152 (34), 121 (100), 105 (17), 93 (30), 91 (23), 79 (14), 77 (13).

5.4.11 Field Bioassays

Adults of *A. m. moschata* were trapped with custom-built, cross-vane, flight-intercept traps with an underhanging funnel protruding into a collecting jar, and a top cover for rain protection (detailed description in Molander et al.).[8] The traps were wired to steel reinforcing bars that were driven partway into the ground, with the central part of the trap hanging at ~1.5 m above ground. The cross-vane panels, and the inside of the funnel, were coated with Fluon® (polytetrafluoroethylene dispersion, 60 wt % in H_2O, Sigma-Aldrich, St. Louis, Missouri, USA, further diluted 1:1 with water) just before trap deployment, to increase trapping efficiency.[33] Propylene glycol (~0.25 L per trap) was used as a killing and preservative agent in the collecting jars.

Traps were deployed with twenty spatial replicates dispersed in two areas directly west (13 replicates) and east (seven replicates) of Lake Krankesjön in southern Sweden in 2018 (approximate center coordinates, WGS 84: DD 55.6996 N, 13.4765 E). Willows (*Salix* spp.) are common in this area and often grow in open, or semi-open, sun-exposed conditions along the edges of wetlands and grasslands where adults of *A. m. moschata* can sometimes be observed on flowering herbs.[34] The replicates were mainly situated in sun-exposed locations along woodland fringes, or within glades, typically in the vicinity of

willow trees and bushes, sometimes with evidence of recent activity by *A. m. moschata* larvae.

The replicates were on average spaced ~200 m apart (range 30 – 568 m, mean 182 ± 28 m). Each replicate consisted of one trap with a lure of *p*-mentha-1,3-dien-9-ol and one control trap (neat solvent). Within the replicates, the two traps were deployed ~10 m apart, and the lure treatment was assigned at random.

Lures consisted of Grippie ® zip-lock polyethylene bags (6.5 × 5.5 cm × 40 μm, Grippie Light Nr-02, b.n.t. Scandinavia AB, Arlöv, Sweden) with 50 mg racemic *p*-mentha-1,3-dien-9-ol and 2.5 mg of butylated hydroxytoluene stabilizer, dissolved in 0.5 ml of isopropanol. The control consisted of 0.5 ml of isopropanol alone. The bag was attached with metal wire (without piercing the bag) to the central (south-facing) part of the trap, just below the top cover. Traps were deployed from 11–30 July, 2018, with the 19 d trapping period covering the main peak of flight activity for *A. m. moschata* in this area of Sweden.[34,35]

All longhorn beetles were counted and identified to species using the key by Ehnström and Holmer.[36] The trapped cerambycids were preserved in 70% ethanol and stored at the Department of Plant Protection Biology, SLU Alnarp Campus. Voucher specimens will be transferred to the public entomological collections in the Biological Museum, Lund University, Sweden.

Attraction of *H. marginata* to synthesized candidate pheromone was tested with a field bioassay conducted during 2018 at four sites in northern California chosen for the presence of the host species and accessibility, as follows: 1) Slaughterhouse Ravine,

Magalia, Butte Co. (39.83861, -121.61694, 730 m elevation), trapping period 21 April – 27 July. Site dominated by black oak (*Quercus kelloggii* Newb.), with incense cedar (*Calocedrus decurrens* Torr.), Ponderosa pine (*Pinus ponderosa* Douglas ex. C. Lawson) and Douglas fir. 2) Rattlesnake Creek at Forest Road 27N12, ~2.8 km N Colby Mt., Tehama Co. (40.17205, -121.51889, 1322 m), trapping period 22 April – 12 August. Site dominated by Douglas fir, Ponderosa pine, big leaf maple (*Acer macrophyllum* Pursch), canyon live oak (*Quercus chrysolepis* Liebm.), and white fir. 3) Junction Forest Roads 27N06 and 27N12Y, ~2.7 km NW Colby Mt., Tehama Co. (40.16209, -121.54632, 1245 m), 6 May – 12 August. Site dominated by Douglas fir, black oak, Ponderosa pine, and big leaf maple. 4) Whispering Pines Pet Clinic property, Magalia, Butte Co. (39.84055, -121.59600, 767 m), 11 May – 19 July.

In field bioassays with *H. marginata*, black plastic cross-vane traps coated with Fluon® (Alpha Scents, Inc., West Linn, OR, USA) were used. Trap collection buckets were partly filled with propylene glycol as a killing agent and preservative. Traps were hung from tree branches at all four sites at heights of 3–5 m to prevent tampering by bears and other wildlife. Lures consisted of 5 × 7.5 cm low density polyethylene resealable baggies each with a cotton dental wick loaded with solutions of test compounds in isopropanol as described above. At each site four traps were deployed (~10 m apart), one baited with *p*-mentha-1,3-dien-9-ol as a single component, *p*-cymen-9-ol as a single component, a 1:1 blend of the two, and a control lure (neat isopropanol). Traps were serviced at intervals of ~1 week and fresh lures were deployed every other week. Trap servicing included transferring insect catches into 70% ethanol, recharging propylene

glycol, and cleaning dust and debris from the traps. Voucher specimens were deposited into the collection of the UC Riverside Entomology Museum.

5.4.12 Statistical Analysis

Differences among treatment means in numbers of adult beetles captured were tested separately for all species represented by at least 10 specimens with the nonparametric Friedman's test (PROC FREQ, option CMH; SAS Institute 2011), with replicates defined by number of traps per treatment within transects and collection date. Replicates that contained no specimens in any treatment of the beetle species in question (e.g., due to inclement weather) were dropped from analyses. Pairs of treatments were compared using the REGWQ test (controlling experiment wise error rates; SAS Institute 2011), and were protected (i.e., assuming a significant overall Friedman's test).

5.5 References

(1) Haack, R. A. Cerambycid Pests in Forests and Urban Trees. In *Cerambycidae of the World: Biology and Pest Management*; Wang, Q., Ed.; CRC Press/ Taylor & Francis Group: Boca Raton, 2017; pp 351–407.

(2) Linsley, E. G. Ecology of Cerambycidae. *Ann Rev Entomol* **1959**, *4*, 99–138.

(3) Nearns, E. H. Systematics of Longhorned Beetles (Insecta: Coleoptera: Cerambycidae). PhD Dissertation, University of New Mexico, 2013.

(4) Hanks, L. M.; Millar, J. G. Sex and Aggregation-Sex Pheromones of Cerambycid Beetles: Basic Science and Practical Applications. *J Chem Ecol* **2016**, *42* (7), 631–654. https://doi.org/10.1007/S10886-016-0733-8.

(5) Rassati, D.; Toffolo, E. P.; Battisti, A.; Faccoli, M. Monitoring of the Pine Sawyer Beetle *Monochamus galloprovincialis* by Pheromone Traps in Italy. *Phytoparasitica* **2012**, *40* (4), 329–336. https://doi.org/10.1007/S12600-012-0233-5/TABLES/2.

(6) Sweeney, J. D.; Silk, P. J.; Gutowski, J. M.; Wu, J.; Lemay, M. A.; Mayo, P. D.; Magee, D. I. Effect of Chirality, Release Rate, and Host Volatiles on Response of *Tetropium fuscum* (F.), *Tetropium cinnamopterum* Kirby, and *Tetropium castaneum* (L.) to the Aggregation Pheromone, Fuscumol. *J Chem Ecol* **2010**, *36* (12), 1309–1321. https://doi.org/10.1007/S10886-010-9876-1/TABLES/3.

(7) Xu, T.; Yasui, H.; Teale, S. A.; Fujiwara-Tsujii, N.; Wickham, J. D.; Fukaya, M.; Hansen, L.; Kiriyama, S.; Hao, D.; Nakano, A.; Zhang, L.; Watanabe, T.; Tokoro, M.; Millar, J. G. Identification of a Male-Produced Sex-Aggregation Pheromone for a Highly Invasive Cerambycid Beetle, *Aromia bungii*. *Sci Rep-UK* **2017**, *7* (1), 1–7. https://doi.org/10.1038/s41598-017-07520-1.

(8) Molander, M. A Pheromone-Based Toolbox of Longhorn Beetles (Cerambycidae) for Monitoring Biodiversity in Ephemeral Deadwood Substrates of Oak. PhD Dissertation, Swedish University of Agricultural Sciences, 2019.

(9) Ray, A. M.; Arnold, R. A.; Swift, I.; Schapker, P. A.; McCann, S.; Marshall, C. J.; McElfresh, J. S.; Millar, J. G. (R)-Desmolactone Is a Sex Pheromone or Sex Attractant for the Endangered Valley Elderberry Longhorn Beetle *Desmocerus californicus dimorphus* and Several Congeners (Cerambycidae: Lepturinae). *PLoS ONE* **2014**, *9* (12), e115498. https://doi.org/10.1371/JOURNAL.PONE.0115498.

(10) Žunič Kosi, A.; Zou, Y.; Hoskovec, M.; Vrezec, A.; Stritih, N.; Millar, J. G. Novel, Male-Produced Aggregation Pheromone of the Cerambycid Beetle *Rosalia alpina*,

a Priority Species of European Conservation Concern. *PLoS ONE* **2017**, *12* (8), e0183279. https://doi.org/10.1371/JOURNAL.PONE.0183279.

(11) Millar, J. G.; Hanks, L. M. Chemical Ecology of Cerambycids. In *Cerambycidae of the world: biology and pest management*; Wang, Q., Ed.; CRC Press/ Taylor & Francis Group: Boca Raton, 2017; pp 161–208.

(12) Danilevsky, M. *Catalogue of Palaearctic Cerambycoidea*.

(13) Monné, M.; Hovore, F. *Checklist of the Cerambycidae (Coleoptera) of the Western Hemisphere*; BioQuip: Rancho Dominguez.

(14) Vidari, G.; de Bernardi, M.; Pavan, M.; Ragozzino, L. Rose Oxide and Iridodial from *Aromia moschata* L. (Coleoptera : Cerambycidae). *Tetrahedron Lett* **1973**, *14* (41), 4065–4068. https://doi.org/10.1016/S0040-4039(01)87113-6.

(15) Rönn, M.; Andersson, P. G.; Bäckvall, J.-E. Enantiocontrolled Formal Total Synthesis of Paeonilactone A and B from (S)-(+)-Carvone. *Acta Chem Scand* **1998**, *1998* (52), 524–527.

(16) Shapiro, R. H.; Heath, M. J. Tosylhydrazones. V. Reaction of Tosylhydrazones with Alkyllithium Reagents. A New Olefin Synthesis. *J Am Chem Soc* **1967**, *89* (22), 5734–5735. https://doi.org/10.1021/JA00998A601/ASSET/JA00998A601.FP.PNG_V03.

(17) Shvartsbart, A.; Smith, A. B. The Daphniphyllum Alkaloids: Total Synthesis of (-)-Calyciphylline N. *J Am Chem Soc* **2015**, *137* (10), 3510–3519. https://doi.org/10.1021/JA503899T/SUPPL_FILE/JA503899T_SI_003.CIF.

(18) Wang, Y.; Wang, R.; Li, Q.; Zhang, Z.; Feng, Y. Kinetic Resolution of Rac-Alkyl Alcohols via Lipase-Catalyzed Enantioselective Acylation Using Succinic Anhydride as Acylating Agent. *J Mol Catal B-Enzym* **2009**, *56* (2–3), 142–145. https://doi.org/10.1016/J.MOLCATB.2008.02.002.

(19) Collignon, R. M.; Halloran, S.; Serrano, J. M.; McElfresh, J. S.; Millar, J. G. An Unstable Monoterpene Alcohol as a Pheromone Component of the Longhorned Beetle *Paranoplium gracile* (Coleoptera: Cerambycidae). *J Chem Ecol* **2019**, *45* (4), 339–347. https://doi.org/10.1007/S10886-019-01063-7/FIGURES/3.

(20) Lacey, E. S.; Moreira, J. A.; Millar, J. G.; Hanks, L. M. A Male-Produced Aggregation Pheromone Blend Consisting of Alkanediols, Terpenoids, and an Aromatic Alcohol from the Cerambycid Beetle *Megacyllene caryae*. *J Chem Ecol* **2008**, *34* (3), 408–417. https://doi.org/10.1007/S10886-008-9425-3/FIGURES/3.

(21) Mitchell, R. F.; Ray, A. M.; Hanks, L. M.; Millar, J. G. The Common Natural Products (S)-α-Terpineol and (E)-2-Hexenol Are Important Pheromone Components of *Megacyllene antennata* (Coleoptera: Cerambycidae). *Environ Entomol* **2018**, *47* (6), 1547–1552. https://doi.org/10.1093/EE/NVY126.

(22) Monné, M. L.; Monné, M. A.; Wang, Q. General Morphology Classification, and Biology of Cerambycidae. In *Cerambycidae of the world: biology and pest management*; Wang, Q., Ed.; CRC Press/Taylor & Francis Group: Boca Raton, 2017; pp 1–70.

(23) Bobadoye, B.; Torto, B.; Fombong, A.; Zou, Y.; Adlbauer, K.; Hanks, L. M.; Millar, J. G. Evidence of Aggregation–Sex Pheromone Use by Longhorned Beetles (Coleoptera: Cerambycidae) Species Native to Africa. *Environ Entomol* **2019**, *48* (1), 189–192. https://doi.org/10.1093/EE/NVY164.

(24) Hanks, L. M.; Millar, J. G. Field Bioassays of Cerambycid Pheromones Reveal Widespread Parsimony of Pheromone Structures, Enhancement by Host Plant Volatiles, and Antagonism by Components from Heterospecifics. *Chemoecology* **2013**, *23* (1), 21–44. https://doi.org/10.1007/S00049-012-0116-8/TABLES/6.

(25) Frost, S. W. A Preliminary Study of North American Insects Associated with Elderberry Flowers. *The Florida Entomologist* **1979**, *62* (4), 341–355. https://doi.org/10.2307/3493991.

(26) Larsson, M. C. Pheromones and Other Semiochemicals for Monitoring Rare and Endangered Species. *J Chem Ecol 2016 42:9* **2016**, *42* (9), 853–868. https://doi.org/10.1007/S10886-016-0753-4.

(27) European and Mediterranean Plant Protection Organization. *Pest Risk Analysis for Aromia bungii*; Paris, 2014.

(28) Bilý, S.; Mehl, O. *Longhorn Beetles (Coleoptera, Cerambycidae) of Fennoscandia and Denmark*; E.J. Brill/Scandinavian Science Press Ltd.: Leiden - New York - København, 1989.

(29) Molander, M. A.; Larsson, M. C. Identification of the Aggregation-Sex Pheromone of the Cerambycid Beetle *Phymatodes pusillus* Ssp. *pusillus* and Evidence of a Synergistic Effect from a Heterospecific Pheromone Component. *J Chem Ecol* **2018**, *44* (11), 987–998. https://doi.org/10.1007/S10886-018-1008-3/FIGURES/5.

(30) Millar, J. G.; Richards, A. B.; Halloran, S.; Zou, Y.; Boyd, E. A.; Quigley, K. N.; Hanks, L. M. Pheromone Identification by Proxy Identification of Aggregation-Sex Pheromones of North American Cerambycid Beetles as a Strategy to Identify Pheromones of Invasive Asian Congeners. *J Pest Sci* **2019**, *92* (1), 213–220. https://doi.org/10.1007/S10340-018-0962-4/FIGURES/2.

(31) Fieser LF, F. M. Reagents for Organic Synthesis; John Wiley & Sons: New York, 1967; pp 581–595.

(32) Zolfigol, M. A.; Bagherzadeh, M.; Mallakpour, S.; Chehardoli, G.; Ghorbani-Choghamarani, A.; Koukabi, N.; Dehghanian, M.; Doroudgar, M. The First Report on the Catalytic Oxidation of Urazoles to Their Corresponding Triazolinediones via in Situ Catalytic Generation of Br+ Using Periodic Acid or Oxone®/KBr System. *J Mol Catal A-Chem* **2007**, *270* (1–2), 219–224. https://doi.org/10.1016/J.MOLCATA.2007.02.003.

(33) Graham, E. E.; Poland, T. M. Efficacy of Fluon Conditioning for Capturing Cerambycid Beetles in Different Trap Designs and Persistence on Panel Traps Over Time. *J Econ Entomol* **2012**, *105* (2), 395–401. https://doi.org/10.1603/EC11432.

(34) Anonymous. *List of records of Aromia moschata 2000-2017*. Swedish Species Observation System. https://www.artportalen.se/ (accessed 2022-07-11).

(35) Lindhe, A.; Jeppsson, T.; Ehnström, B. Longhorn Beetles in Sweden - Changes in Distribution and Abundance over the Last Two Hundred Years. *Entomologisk Tidskrift* **2010**, *131*, 241–508.

(36) Ehnström, B.; Holmer, M. *Nationalnyckeln till Sveriges Flora Och Fauna. Skalbaggar: Långhorningar: Coleoptera: Cerambycidae*; Swedish Species Information Centre.: Uppsala, 2007.

(37) Serra, S.; Nobile, I. Chemoenzymatic Preparation of the P-Menth-1,5-Dien-9-Ol Stereoisomers and Their Use in the Enantiospecific Synthesis of Natural p-Menthane Monoterpenes. *Tetrahedron: Asymmetr* **2011**, *22* (13), 1455–1463. https://doi.org/10.1016/J.TETASY.2011.07.014.

5.6 Supporting Information

5.6.1 ^{1}H NMR of the tosylhydrazone of (*R*)-carvone 5.09 ($CDCl_3$, 400 MHz, 297 K)

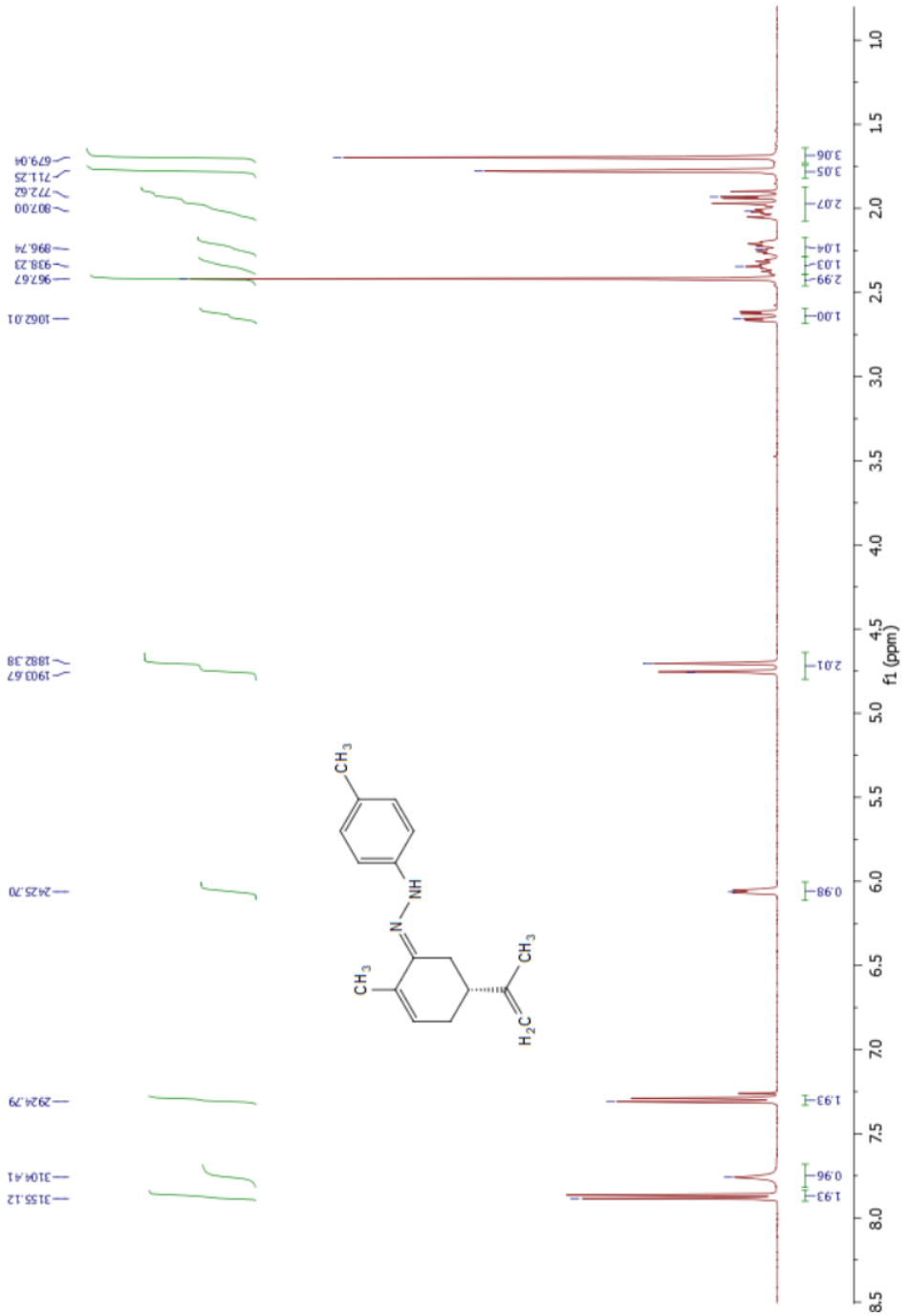

5.6.2 ^{13}C NMR of the tosylhydrazone of (*R*)-carvone 5.09 ($CDCl_3$, 101 MHz, 297 K)

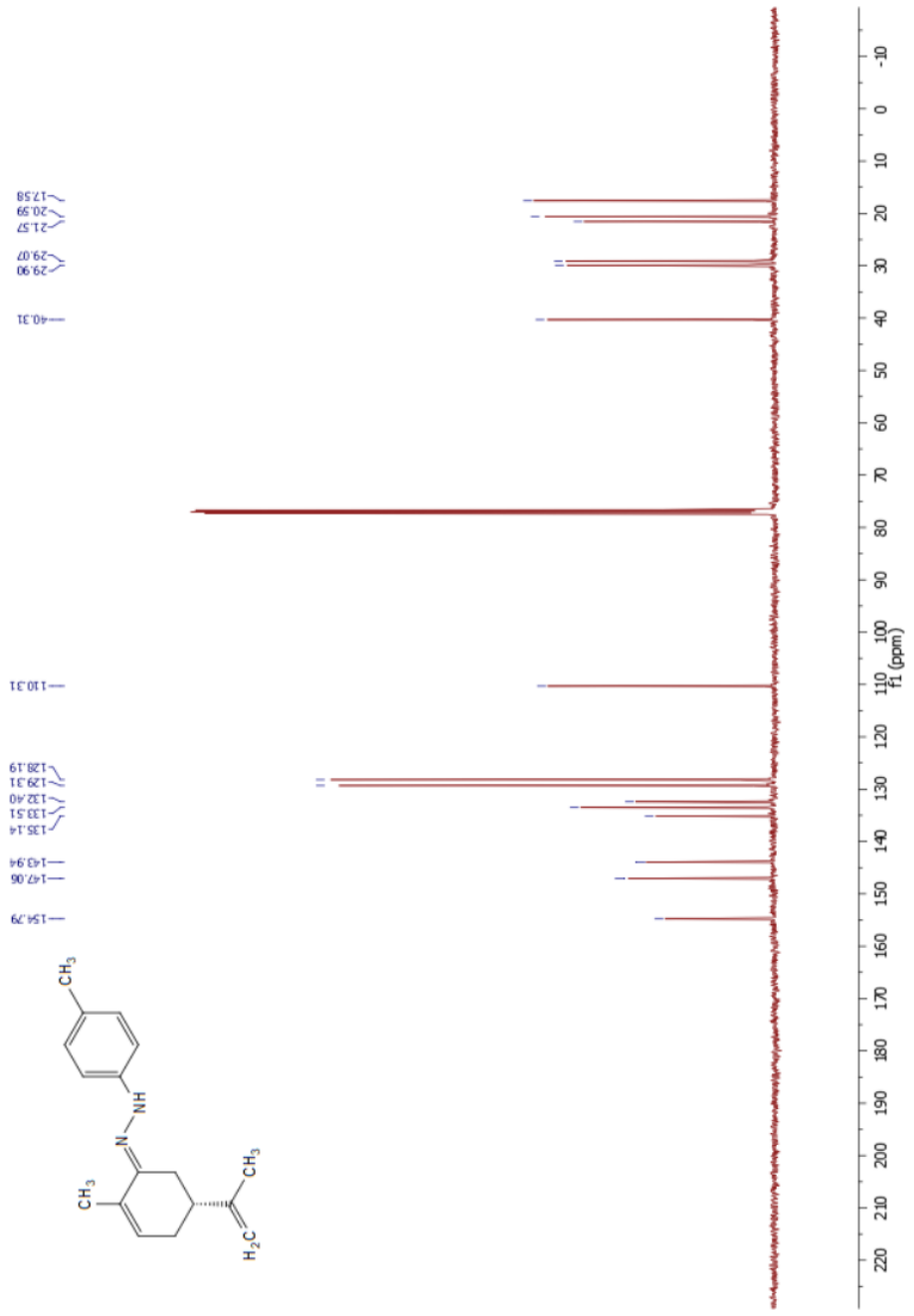

5.6.3 ^{1}H NMR of product mixture containing diastereomers of 2-(4-methylcyclohexa-2,4-dien-1-yl)propan-1-ol 5.07 ($CDCl_3$, 400 MHz, 297 K)

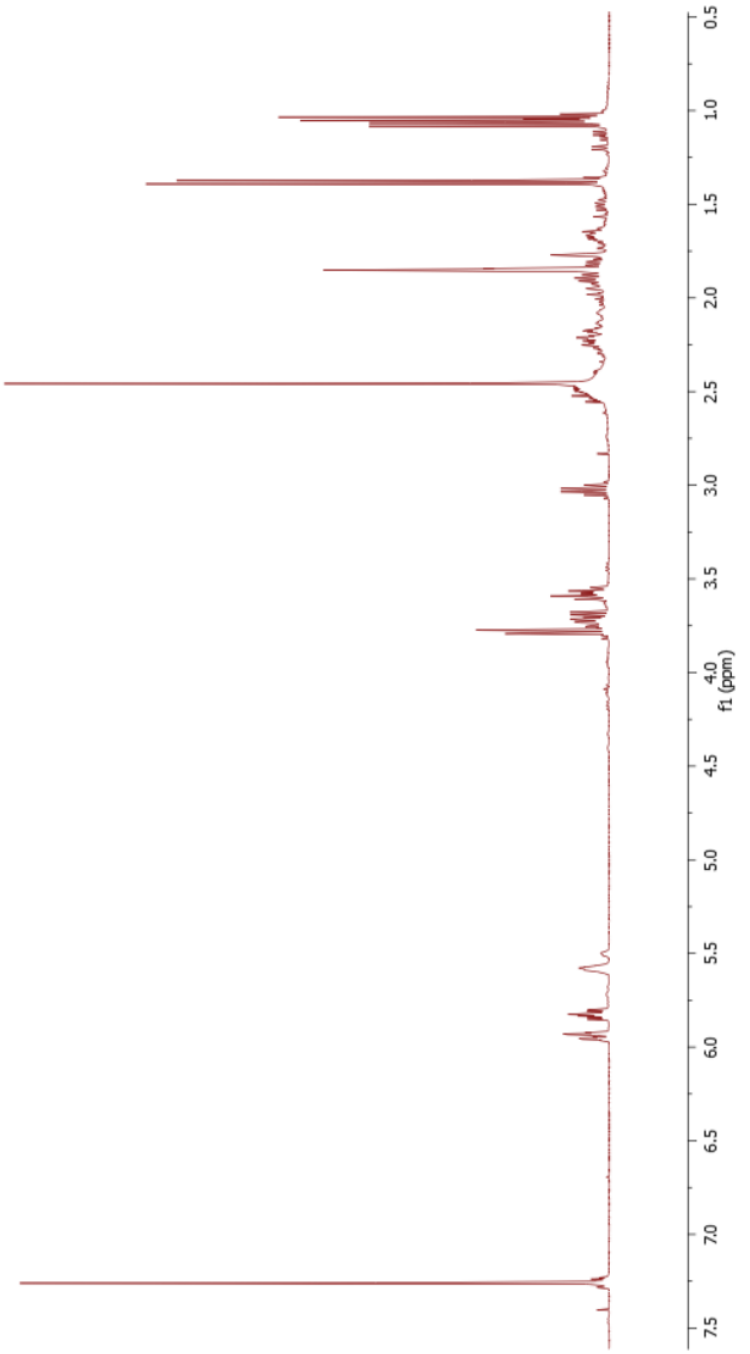

5.6.4 ^{13}C NMR of product mixture containing diastereomers of 2-(4-methylcyclohexa-2,4-dien-1-yl)propan-1-ol 5.07 ($CDCl_3$, 101 MHz, 297 K)

The spectrum included points to two peaks that likely correspond to each of the diastereomers (δ 65.66 & 65.53) and the aromatic analog **5.01** (δ 68.52) on the basis of chemical shift[37] and peak intensity.

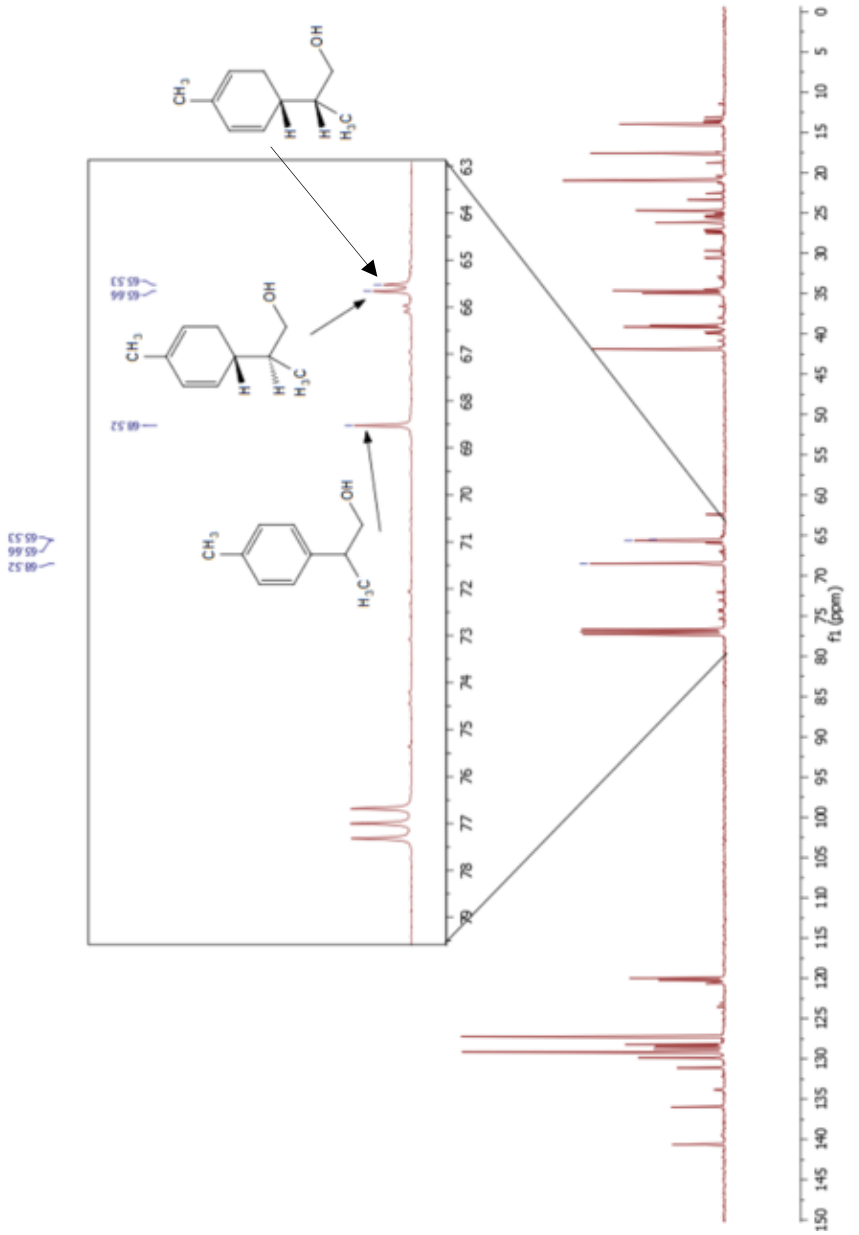

5.6.5 ^{1}H NMR of *p*-cymen-9-ol 5.01 ($CDCl_3$, 500 MHz, 294 K)

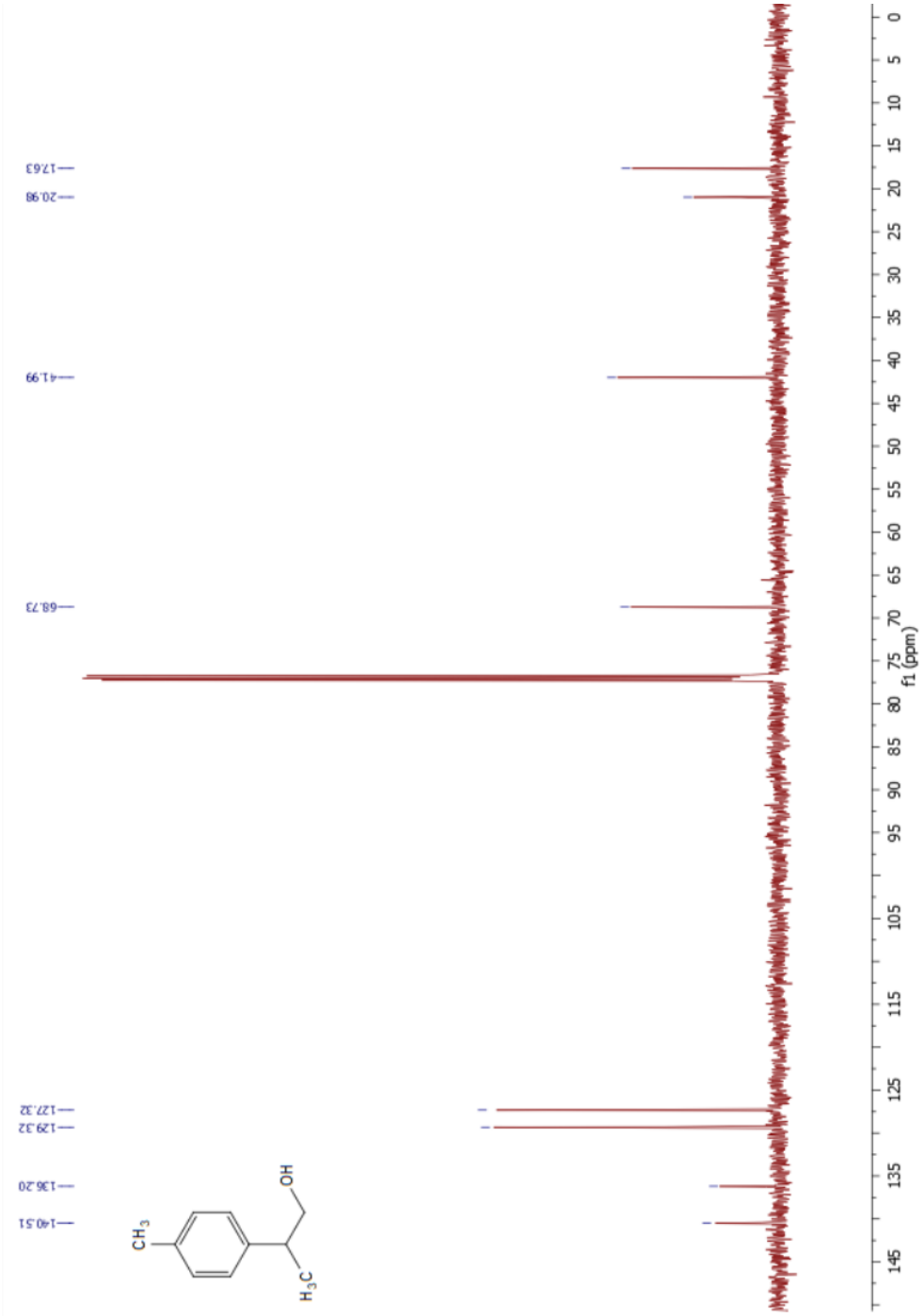

5.6.6 ^{13}C NMR of *p*-cymen-9-ol 5.01 ($CDCl_3$, 126 MHz, 295 K)

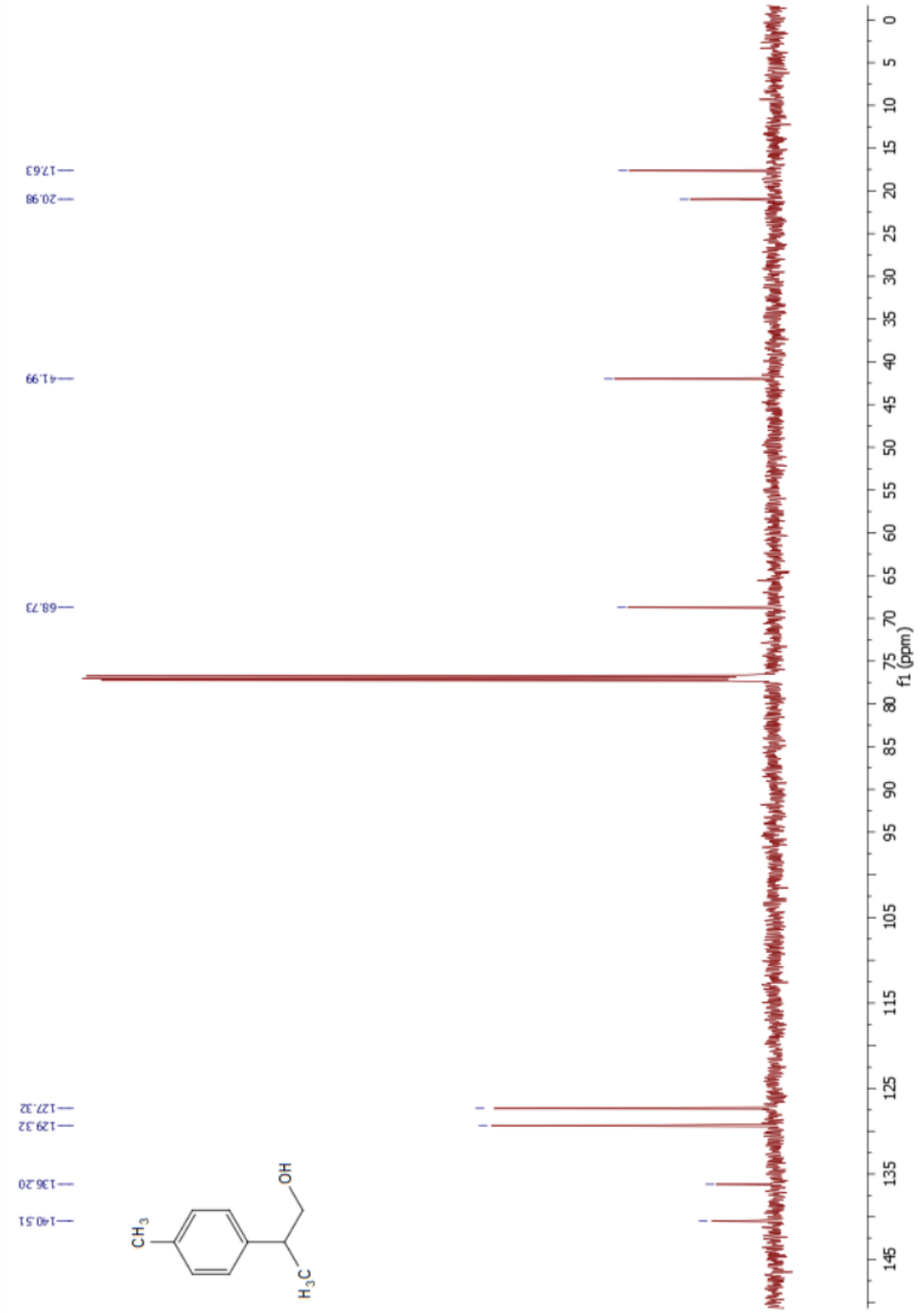

5.6.7 ^{1}H NMR of *p*-mentha-1,3-dien-9-ol 5.03 ($CDCl_3$, 500 MHz, 293 K)

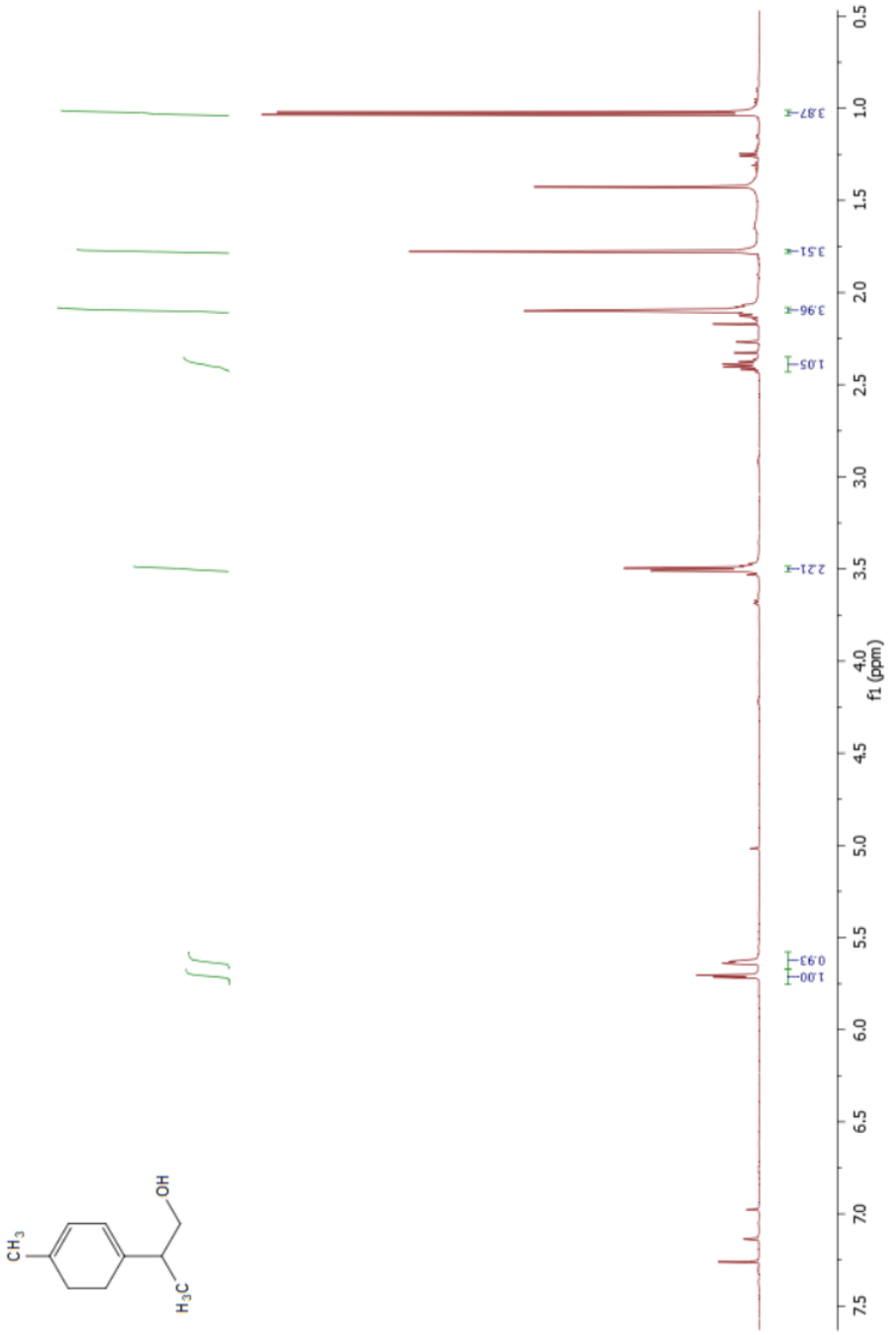

5.6.8 ^{13}C NMR of *p*-mentha-1,3-dien-9-ol 5.03 ($CDCl_3$, 126 MHz, 294 K)

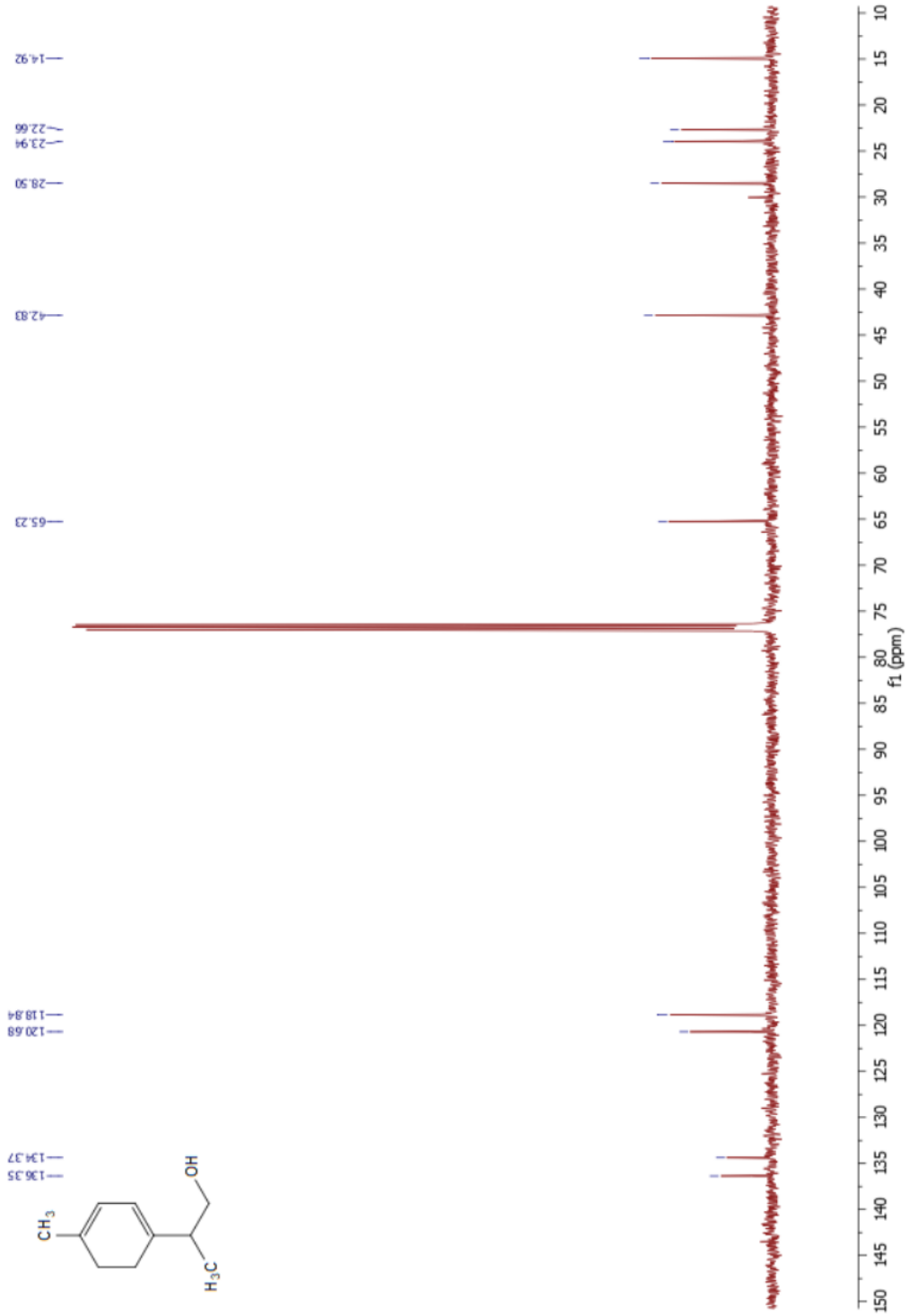

5.6.9 ^{1}H NMR of unconjugated diene 5.04 ($CDCl_3$, 500 MHz, 293 K)

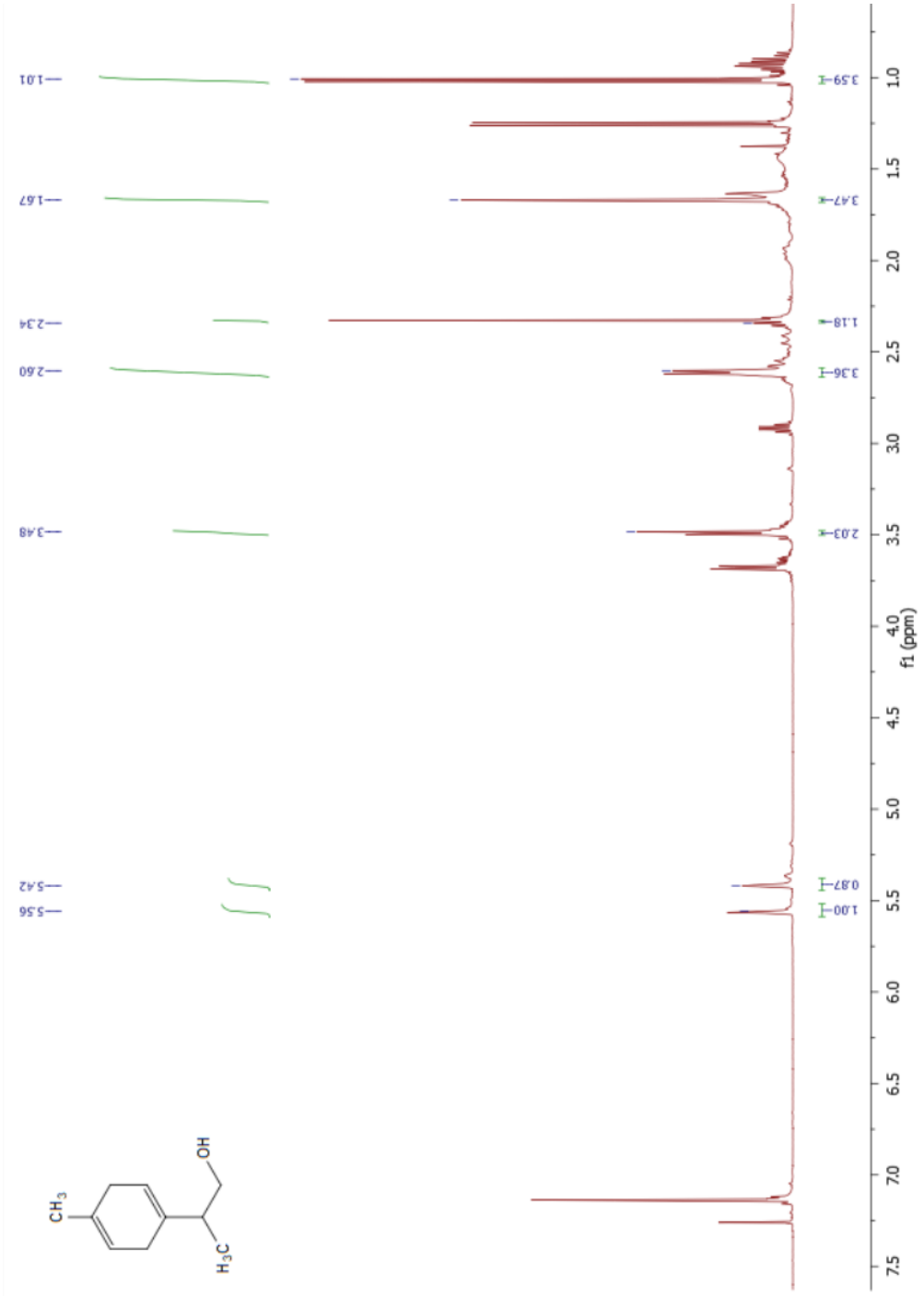

5.6.10 ^{13}C NMR of impure unconjugated diene 5.04 ($CDCl_3$, 101 MHz, 297 K)

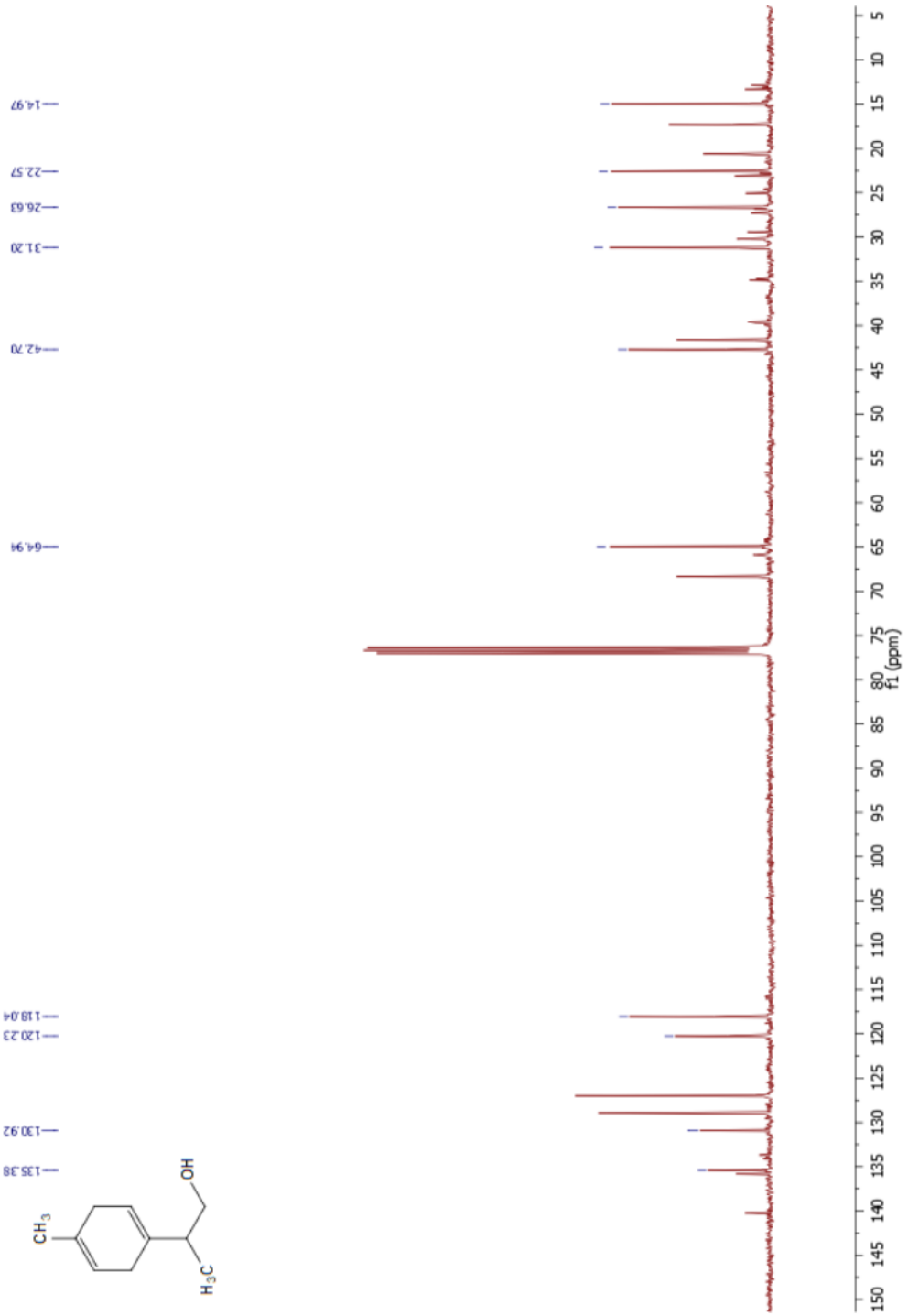

5.6.11 Mass Spectrum of the Unidentified Impurity with a Molecular Ion of *m/z* 154

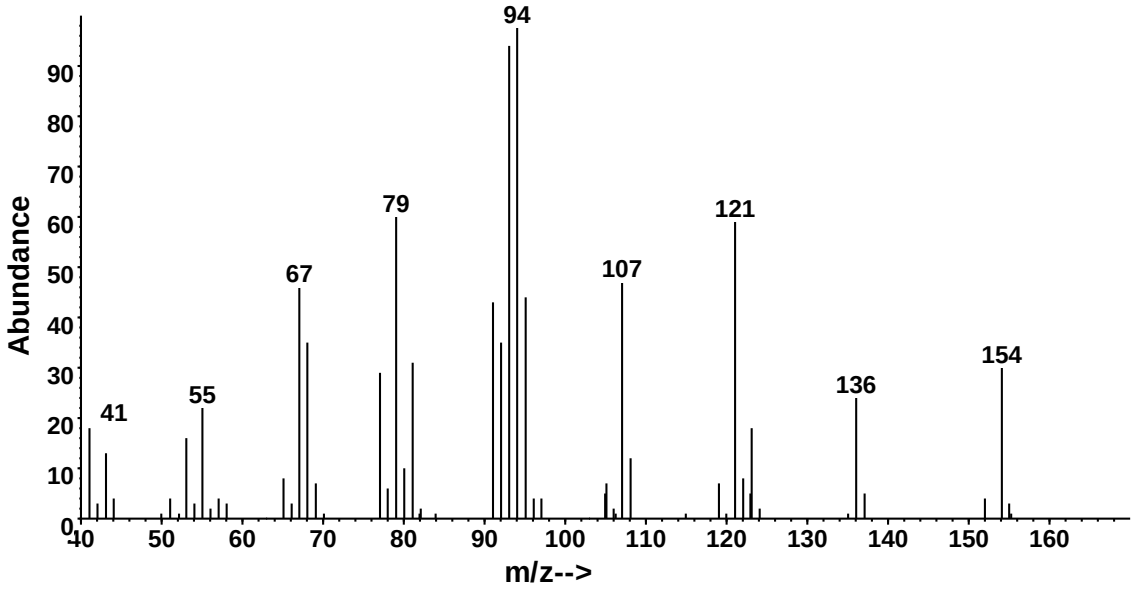

In separate syntheses of candidates **5.03** and **5.07**, an unidentified impurity with a molecular ion of *m/z* 154 was observed in each experiment. Both impurities shared near identical retention times and fragmentation patterns in their EI mass spectra. The impurity was tentatively identified as a *p*-menthen-9-ol with the position of the double bond unknown. This compound may have arisen through a disproportionation type reaction between two molecules of *p*-mentha-dien-9-ol, producing the oxidized aromatic *p*-cymen-9-ol and the reduced *p*-menthen-9-ol. EI-GC/MS *m/z* (%): 154 (34), 136 (23), 123 (29), 121 (63), 107 (47), 94 (100), 93 (79), 81 (34), 79 (51), 77 (21), 67 (46), 55 (25), 43 (14), 41 (17).

Chapter 6 – Conclusions

6.1 Conclusions

Pursuing the mysteries of chemical ecology allows us to uncover the mechanisms by which organisms communicate with other organisms and their environment. Through identification and synthesis, we begin to unlock the great potential represented by insect semiochemicals for integrated pest management strategies and conservation efforts.

The successful control of certain environmentally and economically important pests, as mentioned before, can be greatly assisted by our understanding and exploitation of semiochemistry. Pheromones played a crucial role in eradication of the boll weevil *Anthonomus gradis* (Coleoptera: Curculionidae) in the US,[1–3] significantly reduced the agricultural damage caused by the codling moth *Cydia pomonella* globally,[4,5] and suppressed the environmental damage and spread of the invasive spongy moth (formerly known as the gypsy moth) *Lymantria dispar*.[6] In contrast to broad spectrum pesticides, semiochemicals have high target organism specificity with minimal adverse effects on surrounding biota, are generally non-toxic, have large active spaces around point sources of pheromone, and rarely lead to development of resistance.[5]

Semiochemicals also find use in conservation efforts,[7] providing sensitive and standardized methods for the detection and monitoring of endangered or cryptic species, or bioindicators, that is, species that reveal information about ecosystem quality.[8] Examples of conservation efforts which have exploited semiochemistry include the identification[9] of the sex pheromone for the protected and emblematic moth *Graellsia isabellae* (though a more recent report using a non-semiochemistry approach for estimation of population suggests the moth is not endangered)[10] and the use of pheromone-based

trapping of the bioindicators *Elater ferrugineus* (Coleoptera: Elateridae) and *Osmoderma eremita* (Coleoptera: Scarabeaidae) that co-occur with rare and/or endangered species to assess populations in highly biodiverse environments.[8]

The main goals of this dissertation were to identify and where possible, synthesize semiochemicals that mediate insect behavior, two critical steps enabling integrated pest management and conservation efforts that exploit semiochemistry. The work presented here establishes the mechanism by which the invasive stink bug *Bagrada hilaris* locates its host, and the identities of aggregation-sex pheromones for several longhorn beetle species across multiple continents. Additionally, this work reports the first conclusive identification of a firefly pheromone, providing concrete evidence for the communication system of the subset of fireflies that lack their characteristic light communication.

The structural elucidation of brassicadiene was effected by a combined use of spectral analysis, microchemical tests, and computational chemistry.[11] A composite sample from an estimated 200 aerations of *Brassica oleracea* var. *botrytis* seedlings yielded approximately 200 μg of brassicadiene for NMR spectroscopy on a 700 MHz instrument, producing high quality spectra which enabled us to determine the structure and relative stereochemistry of the tricyclic diterpene hydrocarbon. I arrived at the gross structure of brassicadiene after detailed analysis of the spectra. After I had determined a tentative structure, Dr. Jocelyn Millar independently arrived at the same gross structure, giving us confidence that we had correctly identified the structure of brassicadiene. An optical rotation measurement of the authentic sample and DFT calculation of the specific rotation for each enantiomer of brassicadiene allowed us to identify the absolute configuration of

brassicadiene. Although direct control of the invasive stink bug *Bagrada hilaris* with the use of synthetic brassicadiene does not seem as though it could be cost-efficient given the complexity of the structure of brassicadiene, indirect control of *B. hilaris* could be possible by breeding of *Brassica* plants that do not produce brassicadiene. Due to the importance of brassicadiene, I would be excited to witness the first total synthesis of brassicadiene, or to see a varietal of a *Brassica* crop that has been altered by selective breeding or genetic engineering to lack the production of brassicadiene.

The identification of the winter firefly *Ellychnia corrusca* (syn. *Photinus corrusca*) pheromone constitutes the first conclusive verification of firefly (Coleoptera: Lampyridae) chemical communication. It has been generally regarded that fireflies lacking the characteristic light signals communicate with long-range and short-range chemical signals, on the basis of several bioassay studies,[12–16] but no study before ours has unambiguously identified a firefly pheromone. As part of a larger multidisciplinary study which is trying to elucidate evolutionary changes in mating signaling modes (specifically, lineages that have independently switched from light communication back to chemical communication), the identification of the winter firefly pheromone establishes a crucial piece to this puzzle. In light of chirality and mixtures of stereoisomers having unpredictable effects on insects' perception and behavioral responses, enantioenriched (85% and 92% ee) samples of (1*S*,3*S*,4*R*)-3-hydroxy-1,7,7-trimethylbicyclo[2.2.1]heptan-2-one were used in preliminary field experiments. In future bioassays and to ease synthesis of standards, it would be interesting to see if a mixture of the isomers, produced by reduction of (1*S*)-camphorquinone with sodium borohydride (paying no special attention to the difficult

chromatographic separation of the resulting isomers) elicits attraction similar to the more highly purified compound. We were fortunate because camphorquinone and both its enantiomers is commercially available and the desired pheromone can be produced from it in one step, but it would be useful to avoid having to do tedious chromatographic separation of the isomers.

In chapter 4, identification and synthesis of graphisurone, which was isolated from males of the North American longhorn beetle (Coleoptera: Cerambycidae) *Graphisurus fasciatus* and later identified from males of the South American longhorn beetle *Eutrypanus dorsalis*, illustrate recent trends observed in cerambycid semiochemistry. Research over the past two decades has discovered numerous examples of structural motifs being conserved among pheromones for different species of Cerambycidae.[17] Analysis of the insect-produced compound by GC/MS and microchemical tests generated target compounds for synthesis, culminating in the determination of the absolute stereochemistry of the likely aggregation-sex pheromones for *G. fasciatus* and *E. dorsalis*, which we have given the common name graphisurone. Many obstacles were encountered during this project, such as synthetic dead ends, compounded by the pandemic, but eventually producing graphisurone with high enantioselectivity and in gram scale could confirm its function in the biology of these insects. Enantioselective synthesis of graphisurone for use in field experiments is currently underway. Since *G. fasciatus* and *E. dorsalis* are from the same tribe (subfamily Lamiinae; tribe Acanthocinini) it is likely that members of other genera within the tribe also use graphisurone to communicate.

Lastly, chapter 5 is another example that further illustrates the trends towards conserved structures in cerambycid semiochemistry. This work successfully identified the aggregation-sex pheromone, *p*-mentha-1,3-dien-9-ol, for two species endemic to different continents: the North American longhorn beetle *Holopleura marginata* and the Eurasian longhorn beetle *Aromia moschata moschata*. The unstable monoterpene alcohol, when stabilized by butylated hydroxytoluene, provides a standardized method for the detection and monitoring of these two species of longhorn beetles. To our benefit, the beetles respond well to the racemate, facilitating production of material for field experiments. Similar to the previous chapter, the shared pheromone examined in this work suggests that other members of the Cerambycidae may also use *p*-mentha-1,3-dien-9-ol in chemical communication and could assist in further exploring the chemical space occupied by cerambycid semiochemistry. In future work, we can investigate whether scalemic mixtures or enantiopure samples of each stereoisomer influence capture rate or even attract different species. The latter could perhaps provide another interesting case of evolving species-specific pheromone channels between sympatric heterospecifics.

Chemical ecology and semiochemistry give us other options for pest control that generally leave a smaller environmental footprint compared to conventional, broad-spectrum insecticides. These fields of study can also illuminate the intricacies of our ever-evolving, natural world. Concerning cerambycid semiochemistry, there are many more species of longhorn beetles to be studied – fewer than one percent of longhorn beetles have been studied in terms of their pheromone chemistry.[17] I hope that through the study of semiochemicals and with the knowledge gained from this dissertation, we can combat and

prevent the establishment of invasive pests and unravel the mechanisms behind evolutionary changes in mating signaling modes.

6.2 References

(1) Mitchell, E. B.; Hardee, D. D. In-Field Traps: A New Concept in Survey and Suppression of Low Populations of Boll Weevils. *J Econ Entomol* **1974**, *67* (4), 506–508. https://doi.org/10.1093/JEE/67.4.506.

(2) Tumlinson, J. H.; Minyard, J. P.; Gueldner, R. C.; Hardee, D. D.; Thompson, A. C.; Hedin, P. A. Identification and Synthesis of the Four Compounds Comprising the Boll Weevil Sex Attractant. *J Org Chem* **1971**, *36* (18), 2616–2621. https://doi.org/10.1021/JO00817A012/SUPPL_FILE/JO00817A012_SI_001.PDF

(3) Hardee, D. D.; Graves, T. M.; McKibben, G. H.; Johnson, W. L.; Gueldner, R. C.; Olsen, C. M. A Slow-Release Formulation of Grandlure, the Synthetic Pheromone of the Boll Weevil. *J Econ Entomol* **1974**, *67* (1), 44–46. https://doi.org/10.1093/JEE/67.1.44.

(4) Witzgall, P.; Stelinski, L.; Gut, L.; Thomson, D. Codling Moth Management and Chemical Ecology. *Ann Rev Entomol* **2007**, *53*, 503–522. https://doi.org/10.1146/ANNUREV.ENTO.53.103106.093323.

(5) Rizvi, S. A. H.; George, J.; Reddy, G. V. P.; Zeng, X.; Guerrero, A. Latest Developments in Insect Sex Pheromone Research and Its Application in Agricultural Pest Management. *Insects* **2021**, *12* (6). https://doi.org/10.3390/INSECTS12060484.

(6) Lance, D. R.; Leonard, D. S.; Mastro, V. C.; Walters, M. L. Mating Disruption as a Suppression Tactic in Programs Targeting Regulated Lepidopteran Pests in US. *J Chem Ecol* **2016**, *42* (7), 590–605. https://doi.org/10.1007/S10886-016-0732-9/FIGURES/2.

(7) Larsson, M. C. Pheromones and Other Semiochemicals for Monitoring Rare and Endangered Species. *J Chem Ecol* **2016**, *42* (9), 853. https://doi.org/10.1007/S10886-016-0753-4.

(8) Andersson, K.; Bergman, K. O.; Andersson, F.; Hedenström, E.; Jansson, N.; Burman, J.; Winde, I.; Larsson, M. C.; Milberg, P. High-Accuracy Sampling of Saproxylic Diversity Indicators at Regional Scales with Pheromones: The Case of *Elater ferrugineus* (Coleoptera, Elateridae). *Biol Conserv* **2014**, *171*, 156–166. https://doi.org/10.1016/J.BIOCON.2014.01.007.

(9) Millar, J. G.; McElfresh, J. S.; Romero, C.; Vila, M.; Marí-Mena, N.; Lopez-Vaamonde, C. Identification of the Sex Pheromone of a Protected Species, the Spanish Moon Moth *Graellsia isabellae*. *J Chem Ecol* **2010**, *36* (9), 923–932. https://doi.org/10.1007/S10886-010-9831-1/FIGURES/2.

(10) Marí-Mena, N.; Naveira, H.; Lopez-Vaamonde, C.; Vila, M. Census and Contemporary Effective Population Size of Two Populations of the Protected Spanish Moon Moth (*Graellsia isabellae*). *Insect Conserv Diver* **2019**, *12* (2), 147–160. https://doi.org/10.1111/ICAD.12322.

(11) Arriola, K.; Guarino, S.; Schlawis, C.; Arif, M. A.; Colazza, S.; Peri, E.; Schulz, S.; Millar, J. G. Identification of Brassicadiene, a Diterpene Hydrocarbon Attractive to the Invasive Stink Bug *Bagrada hilaris*, from Volatiles of Cauliflower Seedlings, *Brassica oleracea* Var. *botrytis*. *Org Lett* **2020**, *22* (8), 2972–2975. https://doi.org/10.1021/ACS.ORGLETT.0C00707/SUPPL_FILE/OL0C00707_SI_001.PDF.

(12) Lloyd, J. E. Chemical Communication in Fireflies. *Environ Entomol* **1972**, *1* (2), 265–266. https://doi.org/10.1093/EE/1.2.265.

(13) Ohba, N. Flash Communication Systems of Japanese Fireflies. *Integr Comp Biol* **2004**, *44* (3), 225–233. https://doi.org/10.1093/ICB/44.3.225.

(14) de Cock, R.; Matthysen, E. Sexual Communication by Pheromones in a Firefly, *Phosphaenus hemipterus* (Coleoptera: Lampyridae). *Anim Behav* **2005**, *70* (4), 807–818. https://doi.org/10.1016/J.ANBEHAV.2005.01.011.

(15) Ming, Q. L.; Lewis, S. M. Mate Recognition and Sex Differences in Cuticular Hydrocarbons of the Diurnal Firefly *Ellychnia corrusca* (Coleoptera: Lampyridae). *Ann Entomol Soc Am* **2010**, *103* (1), 128–133. https://doi.org/10.1603/008.103.0116.

(16) McDermott, F. A. The Taxonomy of the Lampyridae (Coleoptera). *T Am Entomol Soc* **1964**, *90* (1), 1–72.

(17) Millar, J. G.; Hanks, L. M. Chemical Ecology of Cerambycids. In *Cerambycidae of the world: biology and pest management*; Wang, Q., Ed.; CRC Press/ Taylor & Francis Group: Boca Raton, 2017; pp 161–208.